INFORMATION TO USERS

This manuscript has been reproduced from the microfilm master. UMI films the text directly from the original or copy submitted. Thus, some thesis and dissertation copies are in typewriter face, while others may be from any type of computer printer.

The quality of this reproduction is dependent upon the quality of the copy submitted. Broken or indistinct print, colored or poor quality illustrations and photographs, print bleedthrough, substandard margins, and improper alignment can adversely affect reproduction.

In the unlikely event that the author did not send UMI a complete manuscript and there are missing pages, these will be noted. Also, if unauthorized copyright material had to be removed, a note will indicate the deletion.

Oversize materials (e.g., maps, drawings, charts) are reproduced by sectioning the original, beginning at the upper left-hand corner and continuing from left to right in equal sections with small overlaps. Each original is also photographed in one exposure and is included in reduced form at the back of the book.

Photographs included in the original manuscript have been reproduced xerographically in this copy. Higher quality 6" x 9" black and white photographic prints are available for any photographs or illustrations appearing in this copy for an additional charge. Contact UMI directly to order.

UMI

A Bell & Howell Information Company
300 North Zeeb Road, Ann Arbor MI 48106-1346 USA
313/761-4700 800/521-0600

Downloaded from SHAREOK. Persistent Handle URL: https://hdl.handle.net/11244/5641

UNIVERSITY OF OKLAHOMA

GRADUATE COLLEGE

A COUPLED MODEL FOR THE PREDICTION OF INTERFORMATION FLOW THROUGH AN ABANDONED WELL

A Dissertation

SUBMITTED TO THE GRADUATE FACULTY

in partial fulfillment of the requirements for the

degree of

Doctor of Philosophy

By

Elise Ann Striz

Norman, Oklahoma
1998

UMI Number: 9828794

Copyright 1998 by
Striz, Elise Ann

All rights reserved.

UMI Microform 9828794
Copyright 1998, by UMI Company. All rights reserved.

This microform edition is protected against unauthorized
copying under Title 17, United States Code.

UMI
300 North Zeeb Road
Ann Arbor, MI 48103

c Copyright by Elise Ann Striz 1998
All Rights Reserved.

A COUPLED MODEL FOR THE PREDICTION OF INTERFORMATION FLOW THROUGH AN ABANDONED WELL

A Dissertation APPROVED FOR THE
SCHOOL OF PETROLEUM AND GEOLOGICAL ENGINEERING

BY

ACKNOWLEDGMENTS

I would like to express my sincere appreciation for each of the faculty members who has served on my committee and has shared their expertise to advance my own. For Dr. Michael Wiggins, chair of my doctoral committee, who supported my idea for research and whose insight aided in its completion. He has taught me to visualize complexity and see simplicity. For Dr. Roy Knapp, who has been my source of sage advice. For Dr. Donald Menzie, who exemplifies the polish of years of experience. For Dr. Djebbar Tiab, who encouraged me to enter petroleum engineering and who has been a motivating force. And for Dr. Larry Canter, who was one of the first to address the problem of abandoned wells and whose questions led me to seek answers.

I would also like to express my great appreciation to the Department of Petroleum and Geological Engineering for their financial support which made my graduate study possible. This included their efforts on my behalf which led to my receiving the DOE EPSCoR Engineering Scholarship and the Mary Phelps Knowles Scholarship.

I would like to thank my husband, Fred, whose love and unwavering optimism has always been a source of strength for me. I would also like to thank my children, Leonhard, Anneliese, and Andrea, whose quick minds and smiling faces are the joy and the laughter in my life. Finally, I thank my parents, Dr. and Mrs. Donald and Elise Carpenter, and my sister, Susan Carpenter, who helped when times were tough and whose unconditional support embodies the meaning of family.

TABLE OF CONTENTS

Page

Chapter 1. Introduction 1

1.1 Abandoned Well Historical Problem 2
1.2 Research Objectives 5

Chapter 2. Critical Review of Abandoned Well Models 7

2.1 Analytical Models 7
2.2 Numerical Models 21
2.3 Discussion 28

Chapter 3. Development of Abandoned Well Model

3.1 Dynamics and Modeling of Abandoned Well Flow 47
3.2 'Series of Steady States' Coupled Abandoned Well Model 53
3.3 Wellbore Losses in Coupled Abandoned Well Model 62
3.4 Summary 72

Chapter 4. Computer Program for Coupled Abandoned Well Model 81

4.1 General Program Description and Input Requirements 81
4.2 Computer Program Algorithm 84
4.3 Coupled Model Verification and Sensitivity Analysis 86

Chapter 5. Application of Coupled Abandoned Well Model Program 101

5.1 Single Injection Well in Lower Formation 102
5.2 Production and Injection Wells in Either or Both the Lower and Upper Formation 109

Chapter 6. Field Case Studies 124

6.1 General Considerations for Field Application of Coupled Model 125
6.2 Evaluation of Potential for Abandoned Well Flow from Lower Tuscaloosa Sand Trend in Mississippi 129
6.3 Evaluation of Suspected Abandoned Well Flow from Lucas Formation in Sarnia, Ontario 140

Page

Chapter 7. Conclusions.....164

7.1 Summary.....164
7.2 Future Recommendations.....168

Nomenclature.....170

References.....175

Appendix A- Flow Charts for Main Program and Subroutines.....178

Appendix B- Field Unit Equations Used in Program.....188

Appendix C- Sample Input Data Files 191

Appendix D- Selected Lower Tuscaloosa Trend Field Study Input and Ouput Files.....193

Appendix E - Selected Sarnia Waste Disposal Field Study Input and Ouput Files.....204

LIST OF TABLES

Table		Page
1	Summary of characteristics of analytical abandoned well models	45
2	Summary of characteristics of numerical abandoned well models	46
3	Comparison of Avci's[17] analytical model and coupled abandoned well model results for dimensionless flow	94
D.1	Output file for Case PWC #1 for first 25 days	196
D.2	Output file for Case PWC #2 for first 25 days	197
D.3	Output file for Case PWC #3 for first 25 days	198
D.4	Output file for Case PWC #1 with plug for first 25 days	199
D.5	Output file for Case PWC #2 with plug for first 25 days	200
D.6	Output file for Case PWC #3 with plug for first 25 days	201
D.7	Output file for Case PWC #4 for first 25 days	202
D.8	Output file for Case PWC #5 for first 25 days	203
E.1	Output file for Case SWC #1a for first 25 days	207
E.2	Output file for Case SWC #2a for first 25 days	208
E.3	Output file for Case SWC #3a for first 25 days	209

LIST OF FIGURES

Figure		Page
1	Physical model of Javandel et al.[13] for the analysis of abandoned well flow	31
2	Results of Javandel et al.[13] for dimensionless flow through an abandoned well of varying resistance	32
3	Physical model of Silliman and Higgins[14] for the analysis of abandoned well flow	33
4	Dimensionless abandoned well flow results (adapted from Silliman and Higgins[14])	34
5	Physical model of Avci[16] for the analysis of abandoned well flow	35
6	Dimensionless abandoned well flow results (adapted from Avci[17])	36
7	Physical model of Chia and Chu[18] for abandoned well flow simulation	37
8	Horizontal finite difference grid showing injection and abandoned well locations (adapted from Warner[11])	38
9	Numerical simulation pressure change results (adapted from Warner[11]	39
10	Uncased wellbore simulation layers (adapted from Warner and McConnell[12])	40
11	Cased wellbore simulation layers (adapted from Warner and McConnell[12])	41
12	Horizontal finite difference grid showing injection and abandoned well locations (adapted from Warner and McConnell[12])	42
13	Finite element model with wellbore overlay (adapted from Lacombe et al.[21])	43
14	Physical model of Lacombe et al.[21] for abandoned well flow simulation	44
15	Physical system for development of abandoned well model	74

Figure Page

16 Pressure profiles developed for model of Avci[17] 75

17 Potential distributions developed for model of Silliman and Higgins[14] 76

18 Cartesian well locations and radii for use in superpostion to find pressure change at Point A 77

19 Location of constant potential radius marked with eight points relative to abandoned well and active well locations 78

20 Schematic of sand pack experiment used to evaluate spherical flow through a perforation 79

21 Dye profiles for sand pack experiment 80

22 Task flow chart for 'series of steady states' coupled abandoned well flow computer program 93

23 Comparison of dimensinless flow rates from Avci[17] and 'series of steady states' coupled model for one day time steps and a steady state radius of 55% R 95

24 Dimensionless flow rates from Avci[17] and 'series of steady states' coupled model for varying locations of steady state radii (.10R - .60R) and time steps of 1 day 96

25 Dimensionless flow rates from Avci[17] and 'series of steady states' coupled model for varying locations of steady state radii (.70R - 1.2R) and time steps of 1 day 97

26 Dimensionless flow rates from Avci[17] and 'series of steady states' coupled model for a steady state radius of 10% R and time steps of 0.1 days 98

27 Dimensionless flow rates from Avci[17] and 'series of steady states' coupled model for a steady state radius of 10% R and time steps of 0.5 days 99

28 Dimensionless flow rates from Avci[17] and 'series of steady states' coupled model for a steady state radius of 10% R and time steps of 1 day 100

Figure Page

29 Case 1 comparison of abandoned well flow for varying distance R between the abandoned well and the injection well....114

30 Case 2 comparison of abandoned well flow for varying permeability ratio, ξ....115

31 Case 3 comparison of abandoned well flow for different injection rates....116

32 Case 4 abandoned well flow in response to multiple injection rates....117

33 Case 6 comparison of abandoned well flow for different plug length and plug permeability of 0.1 md....118

34 Case 7 comparison of abandoned well flow for different perforation sizes....119

35 Case 8 comparison of abandoned well flow through an open wellbore or an open annulus....120

36 Case 8 comparison of abandoned well flow through a wellbore or annulus filled with a plug 100 ft long with 1 md permeability and an annulus with a 0.01 inch fracture in the plug....121

37 Case 9 comparison of abandoned well flow for different abandoned well locations in response to one injector at (500,0) and one producer at (-500,0) both operating at 100 bbls/day....122

38 Case 10 comparison of abandoned well flow in response to an injector or producer in the upper formation with no active wells in the lower formation....123

39 Cross section of Lower Tuscaloosa Sand trend and overlying formations showing location and rock properties of permeable and impermeable zones....151

40 Comparison of abandoned well flow for cases PWC #1 and PWC #2 in the field study of the Lower Tuscaloosa Sand trend....152

41 Comparison of abandoned well flow for cases PWC #1 and PWC #3 in the field study of the Lower Tuscaloosa Sand trend....153

Figure Page

42 Comparison of abandoned well flow for Cases PWC #1 and PWC #2 including a 100 ft 1.0 md plug in the field study of the Lower Tuscaloosa Sand trend.....154

43 Abandoned well flow for Case PWC #4 in the field study of the Lower Tuscaloosa Sand trend.....155

44 Abandoned well flow for Case PWC #5 in the field study of the Lower Tuscaloosa Sand trend.....156

45 Local region of Sarnia, Ontario showing location of specific wells (adapted from Lesage et. al[3]).....157

46 Typical disposal well used in Sarnia, Ontario injection operation (adapted from Lesage et al.[3]).....158

47 Cross section of Sarnia regional geology showing location and rock properties of permeable and impermeable zones.....159

48 Comparison of abandoned well flow for cases SWC #1a and b for contamination transport from Lucas formation to Rockport Quarry.....160

49 Comparison of abandoned well flow for cases SWC #2a and b for contamination transport from Lucas formation to Hungry Hollow.....161

50 Comparison of abandoned well flow for cases SWC #3a and b for contamination transport from Lucas formation to Fresh Water aquifer.....162

51 Comparison of abandoned well flow for cases SWC #4, #5, and #6 for contamination transport from Lucas formation with 100 ft 0.1 md plug.....163

A.1 General flow chart for Main Program.....178

A.2 General flow chart for subroutine TRANSF.....182

A.3 General flow chart for subroutine SILL.....183

A.4 General flow chart for subroutine POINTS.....186

A.5 General flow chart for subroutine AVEP.....186

Figure Page

A.6 General flow chart for subroutine ROOTS....186

A.7 General flow chart for subroutine BUILDUP....187

C.1 Sample input file demonstrating variable names....191

C.2 Sample input file for Avci[17] base case data used to verify the coupled model....192

D.1 Input file for Case PWC #1 for the field study of the Tuscaloosa Sand Trend....193

D.2 Input file for Case PWC #2 for the field study of the Tuscaloosa Sand Trend....194

D.3 Input file for Case PWC #3 for the field study of the Tuscaloosa Sand Trend....195

E.1 Input file for Case SWC #1a for the field study of Lucas formation at Sarnia....204

E.2 Input file for Case SWC #2a for the field study of Lucas formation at Sarnia....205

E.3 Input file for Case SWC #3a for the field study of Lucas formation at Sarnia....206

ABSTRACT

Abandoned wells may pose an environmental concern in Class II injection projects as a consequence of their potential to act as conduits for flow from the target reservoir to overlying formations. This work uses a novel approach to predict flow between two formations coupled by an abandoned well. A steady state abandoned well model is derived analytically and applied using a 'series of steady states' to create the transient flow response. The model is verified by comparison to the results from the one available transient analytical interformation well model for a single injector given by Avci. The new model is the first to include true pressure losses in the abandoned wellbore calculated from established equations for turbulent or laminar pipe flow, cement plugs, and a casing perforation. The model can also predict flow behind pipe through an open annulus, a plugged annulus or a fracture in the annular plug. Finally, the model is the first to incorporate the effect of pressure variations due to production or injection in the overlying formation on the well flow.

Application of the model is demonstrated in a computer program which is used to evaluate hypothetical field cases of varying producer/injector combinations and user defined abandoned well location and conditions. The results clearly demonstrate the impact of the evolving pressure distributions in the reservoir and overlying formation on the abandoned well flow, including the case where flow moves downhole. Pressure losses in the wellbore or behind pipe are shown to generally preclude flow. The model program is also applied to two field cases to demonstrate its use as a prediction and evaluation tool

for abandoned well transport. As opposed to the limited analytical solutions or complex numerical simulation methods currently available, the new abandoned well model provides a simple means to determine flow for any combination of abandoned well and formation conditions.

CHAPTER 1

INTRODUCTION

Improperly plugged abandoned wells are believed to pose an environmental concern as a consequence of their potential to act as conduits for flow between otherwise hydrogeologically isolated formations including Underground Sources of Drinking Water (USDW). The transport of fluids through abandoned wells is of particular interest to the petroleum industry as the pressure buildup from Class II injection wells in target reservoirs can act as a driving force for interformation flow.

The potential of abandoned wells to act as a source of contamination to USDW is a compelling problem. The huge number of abandoned wells from the oil and gas industry alone has often led to ubiquitous assumptions that they have acted and will act as pathways for contamination transport. However, there is practically no field evidence to support this conclusion. More importantly, there is no realistic and simple method to predict the transport of fluids between formations through an abandoned well. Therefore, there is no simple approach which can be applied to implicate or exonerate abandoned wells as a source of transport between formations.

As the oil and gas industry continues to mature, the use of Class II injection wells in secondary recovery operations will continue to increase. This will lead to even more concern about abandoned well transport. It is therefore critical to review the nature of the abandoned well problem and develop an abandoned well model which can simply and realistically predict flow between formations.

1.1 Abandoned Well Historical Problem

Several estimates exist on the number of abandoned wells in the United States. Canter[1] reported the number to be around 2.0 million. Anzollin et al.[2] reported that about 900,000 abandoned wells were believed to be located near Class II injection wells. The American Petroleum Institute[5] (API) estimated that about 2.2 million abandoned wells exist of which 1.2 million are plugged. The API numbers leave 1 million abandoned wells whose location and condition may be unknown. Wells abandoned before 1930 were not subject to regulation and were abandoned using plugging standards which were poor to non-existent. Beginning in the late 1930's, regulatory controls evolved in most states which required cement plugs to be placed in abandoned wellbore to prevent upward migration of fluids.[5]

Very few cases of abandoned well transport from Class II injection wells have been reported or confirmed in the literature. One suspected case of USDW contamination by abandoned well transport in the presence of injection wells was investigated recently by Lesage et al.[3] and Raven et al.[4], but was not verified. Canter[1] has noted the dearth of verifiable Class II injection well contamination to USDW but considered it to be due to the insidious nature of abandoned well transport. Based on the huge number of abandoned wells estimated to be near Class II injection projects and the persistent belief that abandoned well contamination to USDW is occurring, the Environmental Protection Agency (EPA) developed Underground Injection Control (UIC) regulations to protect USDW near Class II injection wells.

Class II injection wells are defined by the EPA as wells which are strictly associated with the production of oil and gas including produced salt water disposal wells and enhanced recovery wells (i.e. waterflood)[6]. Under the current Safe Drinking Water Act (SDWA) they are subject to 'Area of Review' (AOR) regulation which requires all abandoned wells within a 'radius of endangering influence' to be located and evaluated for plugging with corrective action to be taken if adequate plugging can not be demonstrated[6]. The 'zone of endangering influence' is determined by the calculation of pressure in the proposed injection zone using a simple Theis equation as given in 40 CFR 146.6[6]. This equation assumes an ideal reservoir with cylindrical geometry and homogeneous isotropic media. If the pressure provides a head higher than the location of the USDW, all abandoned wells within this region must be investigated and remediated if necessary. If information is not available the regulations arbitrarily assume a radius of one-quarter mile around the injection well. The current regulations exempt all injection wells 'authorized by rule' (i.e. those wells existing prior to implementation of the UIC program in 1980) from the AOR requirement[6].

In a recent study by EPA, an Advisory Committee recommended the promulgation of new regulations which would require AOR's to be conducted for all new and existing injection wells with corrective actions to be taken for all suspect abandoned wells[7]. The regulations were not passed but led to much concern in the petroleum industry as they were anticipated to have a highly unfavorable impact on oil and gas production[8]. Specifically, the Department of Energy (DOE) reported that the AOR investigations of abandoned wells and associated corrective actions would cause such unfavorable

economics that many secondary recovery projects would not be initiated and wells would be prematurely abandoned[8]. This ensued from the fact that the regulations arbitrarily assumed that any abandoned well in an AOR will act as a conduit for contamination in all injection operations. As such they would place a burden of proof on the operator to show that injection operations would not contaminate USDW through abandoned wells in the area of review. Operators would also be expected to provide corrective action to all abandoned wells suspected to be capable of contamination.

The Advisory Committee did attempt to mitigate the impact of these regulations by allowing that variances from the AOR may be obtained if the risk of migration into a USDW is minimal based upon[7]:

1. the absence of USDW,
2. pressure relationships between the injection well and overlying USDW,
3. presence of local geologic conditions that preclude fluid movement, and
4. other compelling scientific or engineering data supporting the issuance of a variance.

A methodology has been developed and applied to obtain variances for Class II injection projects that is based on the first three mitigating factors[9,10]. Two other studies have used single phase numerical simulation to show that transport would not occur for a proposed Class II injection well based on plugging in the abandoned wellbore and the geological setting of USDW relative to the injection zone[11,12]. This allowed a variance under 4 above, but the simulations were technically demanding and required large amounts of information.

Currently, there is no simple practical method to realistically quantify the fluid transport to USDW through an abandoned well in the area of a Class II injection operation to determine if a variance from the AOR regulations may be obtained. The literature contains analytical models which address simple physical systems or numerical simulations which are labor intensive and difficult to apply as a predictive tool. It is therefore essential that a method be developed to enable the transport through abandoned wells to be accurately and easily determined. This method would need to be versatile enough to address the numerous factors which can influence abandoned well flow and yet simple enough for use as a predictive tool. Such a model would enhance the understanding of factors which control abandoned well flow and identify the cases where abandoned wells are a potential threat to USDW and are in need of corrective action. The potential impact of a widely accepted predictive method could be to protect USDW and prevent the expense of millions of dollars in unnecessary abandoned well corrective actions which could force oil fields to be prematurely abandoned.

1.2 Research Objectives

Research was undertaken to provide a realistic and practical method to predict the transport of fluids between two formations coupled by an abandoned well. Such a model does not currently exist and would be of great value to determine the potential of abandoned wells to contaminate USDW. The model could also be used to evaluate the many factors which influence abandoned well transport to assess their impact on

enhancing or mitigating flow. Finally the model could be applied as a predictive tool to determine if proposed injection projects are a threat to USDW or used as an evaluation tool to determine if an abandoned well could be responsible for existing contamination to USDW. The objectives of this work are therefore:

1. To perform a critical review of the available models to predict abandoned well transport and assess their characteristics and applicability.
2. To identify the dynamics and essential factors controlling abandoned well transport between two formations including pressure distributions in the coupled formations from active wells, abandoned well location and abandoned well condition.
3. To develop a realistic and practical abandoned well model which captures these dynamics to predict the flow between the coupled formations for any set of active well operating conditions, abandoned well location and condition.
4. To develop a computer program to apply the model efficiently and easily.
5. To verify the abandoned well model using available analytical solutions.
6. To apply the model to determine the impact of varying abandoned well location, condition and active well operations in both formations on flow.
7. To apply the model to field cases to assess its applicability as a prediction and evaluation tool for abandoned well transport.

These objectives are addressed individually in this work and collectively produce an abandoned well model which is realistic and practical and can be applied to address the concerns of abandoned well transport between formations.

CHAPTER 2

CRITICAL REVIEW OF ABANDONED WELL MODELS

This chapter describes the currently available methods to predict interformation transport of fluids through an abandoned well. They include analytical models for steady state and transient abandoned well flow and numerical models. Where possible, the nomenclature has been changed from the original paper to provide a consistent nomenclature.

2.1 Analytical Models

The first analytical solution to determine the amount of flow through an abandoned well to an overlying formation in response to underground injection was published by Javandel, Tsang, and Witherspoon[13] in 1988. The authors used a physical model consisting of two homogeneous, isotropic formations separated by an aquitard as shown in Figure 1. The system included an injection well and an abandoned well. The injection well was completed across the entire section of target formation 1 and was operating at a constant rate. The abandoned well, which was assumed to be within the area of pressure influence of the injection well, was open to both the target formation 1 and the overlying formation 2. This allowed the abandoned wellbore to act as a conduit for flow between the two. Both formations were assumed to be saturated with a single phase fluid and the wellbore was filled with the same fluid.

Javandel et al.[13] proposed the abandoned well flow was a function of the pressure distribution in the lower formation, the natural potential gradient between the formations and the flow resistance of the wellbore. To determine the pressure change in formation 1 in response to a constant injection rate, the authors used the Theis equation which assumes the radial flow of a single phase Newtonian fluid in an infinite reservoir. At the location of the abandoned well, this pressure buildup, $\Delta P_I(R,t)$, was given by:

$$\Delta P_I(R,t) = \frac{-Q_I}{4\pi k_1 h_1} Ei\left(\frac{-\phi_1 \mu c R^2}{4k_1 t}\right) \tag{1}$$

Javandel et al. then assumed that flow into the abandoned well from formation 1, $Q_{AW}(t)$, would be radial and a function of time as it would vary with the pressure buildup created by the injection well. The existence of flow at the abandoned well itself created a pressure drawdown at the well location given by:

$$\Delta P(r_{AW},t) = \frac{1}{4\pi k_1 h_1} \int_0^t Q_{AW}(t') \left(\frac{\exp[-\phi_1 \mu c r_{AW}^2 / (4k_1(t-t'))]}{(t-t')}\right) dt' \tag{2}$$

Using the principle of superposition in an infinite reservoir, Javandel et al.[13] stated that the total change in pressure at the abandoned well, $\Delta P_T(r_{AW},t)$, was the difference between the injection pressure buildup and abandoned well drawdown:

$$\Delta P_T(r_{AW},t) = \Delta P_I(R,t) - \Delta P(r_{AW},t) \tag{3}$$

The original potentials in the formations, Φ_1 and Φ_2, were given by:

$$\Phi_1 = P_1 + \rho g z_1 \tag{4}$$

$$\Phi_2 = P_2 + \rho g z_2 \tag{5}$$

Combining these quantities, Javandel et al. presented the following equation for flow:

$$Q_{AW}(r_{AW},t)=\frac{\Phi_1+\Delta P_T(r_{AW},t)-\Phi_2}{\Omega} \tag{6}$$

where Ω was identified as the general resistance of the abandoned wellbore and was not otherwise defined.

To solve Eq. 6, Javandel et al.[13] assumed the initial potential in the overlying formation, Φ_2, was constant and equal to the initial potential Φ_1 in the target injection formation. This simplification meant the pressure change at the abandoned well due to injection buildup and drawdown given in Eq. 3 would be the only driving force for flow up the abandoned well. After substituting the expression for $\Delta P_T(r_{AW},t)$ into Eq. 6, Javandel et al.[13] obtained the following :

$$\Omega Q_{AW}(t)+\frac{1}{4\pi k_1 h_1}\int_0^t Q_{AW}(t')\frac{\exp[-\phi_1\mu c r_{AW}^2/(4k_1(t-t')]}{(t-t')}dt'=-\frac{Q_I}{4\pi k_1 h_1}Ei\left(\frac{-\phi_1\mu c R^2}{4k_1 t}\right) \tag{7}$$

which was transformed to Laplace space, solved and inverted back to real time to give the following solution for the abandoned well flow:

$$Q_{AW}(t)=Q_I-\frac{2Q_I}{\pi}\int_0^\pi \exp(-\frac{k_1 t}{\phi_1\mu c}u^2)\frac{J_0(uR)[4k_1h_1\Omega-Y_0(ur_{AW})]+J_0(ur_{AW})Y_0(uR)}{[4k_1h_1\Omega-Y_0(ur_{AW})]^2+J_0^2(ur_{AW})}\frac{du}{u} \tag{8}$$

The authors also presented the solution in dimensionless variables:

$$Q_{AWD}(t)=1-\frac{2}{\pi}\int_0^\infty e^{-v^2 t_D}\frac{J_0(v)[(2\Omega_D/\pi)-Y_0(vr_{AWD})]+J_0(vr_{AWD})Y_0(v)}{[(2\Omega_D/\pi)-Y_0(vr_{AWD})]^2+J_0{}^2(vr_{AWD})}\frac{dv}{v} \tag{9}$$

where:

$$Q_{AWD}(t)=\frac{Q_{AW}(t)}{Q_I} \tag{10}$$

$$t_D = \frac{k_1 t}{\phi_1 \mu c R^2} \tag{11}$$

$$r_{AWD} = \frac{r_{AW}}{R} \tag{12}$$

$$\Omega_D = 2\pi k_1 h_1 \Omega / \mu \tag{13}$$

The results for the dimensionless solution were reported by the authors for $r_{AWD} = 0.001$ and are shown in Figure 2. The figure shows that the abandoned well flow solution was very sensitive to the dimensionless general resistance factor, Ω_D. This term, however, was not physically defined by the authors and essentially functioned as a multiplication factor which by its magnitude acted to reduce or increase flow. The dimensionless flow values also increased with time as expected in response to the injection buildup. This response, however, was suprisingly large as exhibited by the result where nearly 50% of the injection fluids were transported through the well to the upper formation at large dimensionless times for the lowest resistance wellbore ($\Omega_D = 0.01$). Javandel et al.[13] recognized this problem and stated that it was a consequence of the constant potential assumption in the upper formation. This condition was not considered realistic as it did not account for the pressure buildup that occurs in the upper formation as it receives fluid. Ignoring this buildup led to the overestimation of flow volumes which was acknowledged by the authors.

The next analytical model for interformational flow through an open abandoned well was developed by Silliman and Higgins[14] in 1990 for steady state flow. Like Javandel et al.[13], the authors used a physical model in which an open wellbore acted as a conduit between two aquifers separated by an aquitard as shown in Figure 3. In their work,

however, there was no injection well present. Instead, a constant potential difference between the aquifers was the driving force for flow. The formations were assumed to be saturated with a single phase liquid. The authors also assumed that the unplugged well was filled with the same fluid.

Using the steady state solution for radial flow to the well, Silliman and Higgins[14] stated the flow rate from either aquifer to the well was:

$$Q_i = \frac{2\pi k_i h_i (\Phi_i - \Phi_{iAW})}{\mu \ln(r_i / r_{iAW})} \qquad i = 1,2 \tag{14}$$

where Φ_i represented the constant potential at a chosen steady state radius, r_i, and Φ_{iAW} represented the potential at the sandface of the abandoned well in either the upper or lower aquifer. In particular, the equations for flow to the abandoned well in formations 1 and 2 can be written respectively as:

$$Q_1 = 2\pi(\Phi_1 - \Phi_{1AW})\alpha \tag{15}$$

$$Q_2 = 2\pi(\Phi_{2AW} - \Phi_2)\beta \tag{16}$$

where:

$$\begin{aligned} \alpha &= k_1 h_1 / \mu \ln(r_1 / r_{1AW}) \\ \beta &= k_2 h_2 / \mu \ln(r_2 / r_{2AW}) \end{aligned} \tag{17}$$

represented the steady state productivity indices for the aquifers. Using conservation of mass, Silliman and Higgins stated the flows leaving formation 1, moving up the abandoned wellbore and entering formation 2 were the same to give:

$$Q_{AW} = Q_1 = -Q_2 \tag{18}$$

To solve for the abandoned well flow, Q_{AW}, the authors introduced a term for the pressure loss in the wellbore, ΔP_L, which was defined as the difference between the sandface potentials:

$$\Delta P_L = \Phi_{1AW} - \Phi_{2AW} \tag{19}$$

They solved Eq. 19 for Φ_{2AW} which was substituted into Eq. 16 to obtain an expression for Φ_{1AW}. The expression for Φ_{1AW} was substituted into Eq. 15 and led to the following solution for Q_{AW}:

$$Q_{AW} = \frac{2\pi(\Phi_1 - \Phi_2 - \Delta P_L)\alpha\beta}{(\alpha+\beta)} \tag{20}$$

which states that the steady state flow rate is a function of the constant potentials Φ_1 and Φ_2, a wellbore loss, ΔP_L, and the formation productivity indices α and β. Silliman and Higgins[14] assumed that the pressure loss term, ΔP_L, in the wellbore was proportional to the square of the flow rate and could be written as:

$$\Delta P_L = C_L Q_{AW}^{\ 2} \tag{21}$$

where C_L was identified as a well loss constant. Substituting this expression for ΔP_L into Eq. 20 and rearranging produced a quadratic equation in terms of Q_{AW}:

$$\frac{2\pi\alpha\beta C_L}{(\alpha+\beta)} Q_{AW}^2 + Q_{AW} - \frac{2\pi\alpha\beta\Delta\Phi}{(\alpha+\beta)} = 0 \tag{22}$$

where $\Delta\Phi = \Phi_1 - \Phi_2$. The solution to Eq. 22 gave this expression for Q_{AW}:

$$Q_{AW} = \frac{-1 + \sqrt{1 + 16\pi^2(\alpha^2\beta^2 C_L\Delta\Phi)/(\alpha+\beta)^2}}{4\pi\alpha\beta C_L/(\alpha+\beta)} \tag{23}$$

If no well losses were assumed in the wellbore, the equation for flow between the two formations reduced to:

$$Q_{AW} = \frac{2\pi\alpha\beta\Delta\Phi}{(\alpha + \beta)} \tag{24}$$

Silliman and Higgins[14] presented the abandoned well flow solution in terms of dimensionless variables:

$$Q = \frac{-(1+\tau) + \sqrt{(1+\tau)^2 + 16\pi^2\gamma\tau}}{4\pi\gamma\tau} \tag{25}$$

where:

$$Q = \frac{Q_{AW}}{(\alpha\Delta\Phi)} \tag{26}$$

$$\tau = \frac{\alpha}{\beta} \tag{27}$$

$$\gamma = \alpha\beta C_L \Delta\Phi \tag{28}$$

The results for the dimensionless flow as a function of γ and τ are shown in Figure 4. This figure demonstrates that a decrease in τ, the ratio of the lower aquifer to upper aquifer productivity indices, causes an increase in the dimensionless flow. The curves also show that an increase in γ leads to an asymptotic decrease in flow, presumably as the well loss term C_L becomes dominant. Unlike Javandel et al.[13] who ignored the pressure buildup from flow into the upper aquifer, the steady state results of Silliman and Higgins[14] showed that the flow rate is dependent on the relationship between the productivity indices of both formations.

To calculate abandoned well flow from field data using Eq. 20, it was necessary to determine the location of the constant potential radii, r_1 and r_2, in both formations.

Silliman and Higgins[14] stated that an empirical formula from Siechardt[15] could be used to determine the steady state radius in either formation:

$$r_{Si} = 3000 s_{Wi} K^{1/2} \tag{29}$$

where:

r_{Si} = steady state radius (m)

s_{Wi} = drawdown at the well location (m)

K= hydraulic conductivity (m/s)

Silliman and Higgins[14] did not describe how they chose the drawdown term, s_{Wi} , for the equation. The lack of a well defined method to find the radius of influence for the steady state was of concern because it influences the productivity indices and therefore the flows that can be obtained. Silliman and Higgins[14] recognized that errors in the location of the radius would produce differences in the estimates of flow. They argued that as the steady state radius only appears in the logarithm term in the productivity indices (Eq. 17), the errors would not be substantial.

The next model was developed by Avci[16] in 1992 and addressed the steady state flow of fluids through a vertical unplugged wellbore between two aquifers separated by an impermeable layer. The physical model used in the analysis is shown Figure 5. Unlike the previous models, Avci used two dimensions to account for vertical variation in flow in the vicinity of the wellbore. Avci's model also did not rely on a fully penetrating wellbore boundary condition but only on a wellbore opening at the interface between the aquifers and the impermeable boundary.

Using the paper's original groundwater nomenclature, Avci's[16] derivation began with the governing equation for drawdown, s_i, in either formation written in two dimensions as:

$$\frac{\partial^2 s_i}{\partial r_i^2} + \frac{1}{r_i}\frac{\partial s_i}{\partial r_i} + \frac{\partial^2 s_i}{\partial z_i^2} = 0 \tag{30}$$

It was subject to the following boundary conditions:

$$\frac{\partial s_i}{\partial z_i} = 0 \text{ at } z_i = L_i \tag{31}$$

$$\frac{\partial s_i}{\partial z_i} = \frac{q_{AW}}{K_i} \text{ for } 0 < r_i < a \text{ and } z_i = 0 \tag{32}$$

$$\frac{\partial s_i}{\partial z_i} = 0 \text{ for } r_i > a \text{ and } z_i = 0 \tag{33}$$

$$s_i = 0 \text{ at } r_i = R_i \tag{34}$$

where:

q_{AW} = uniform flux at borehole surface in either formation (m/s)

a = the radius of the wellbore (m)

K_i = hydraulic conductivity (m/s)

R_i = radius where constant potential is located (m)

Avci[16] solved the differential equation using separation of variables:

$$s_1(r_1, z_1) = R(r_1)Z(z_1) \tag{35}$$

which led to a general solution of:

$$s_1(r_1, z_1) = [A_1 \exp(\lambda_1 z_1) + B_1 \exp(-\lambda_1 r_1)]J_0(\lambda_1 r_1) \tag{36}$$

Applying the first boundary condition of no drawdown at the steady state radii, R_1, in formation 1, led to the expression:

$$J_0(\lambda_1 R_1) = 0 \tag{37}$$

The solution to Eq. 37 requires that the argument must equal the positive zeroes of the Bessel function. Since the zeroes are an infinite set of numbers, the solution was written as a infinite series:

$$s_1(r_1, z_1) = \sum_{n=1}^{\infty} [A_{1n} \exp(\lambda_{1n} z_1) + B_{1n} \exp(-\lambda_{1n} z_1)] J_0(\lambda_{1n} r_1) \tag{38}$$

Applying the last two boundary conditions allowed the expressions for the coefficients A_1 and B_1 to be obtained to give the complete solution for the drawdown in the lower aquifer:

$$s_1(r_1, z_1) = \frac{-2q_{AW}a}{K_1 R_1^2} \sum_{n=1}^{\infty} \{\exp(\lambda_{1n} z_1) + \exp[-\lambda_{1n}(z_1 - 2L_1)]\} \frac{J_1(\lambda_{1n} a) J_0(\lambda_{1n} r_1)}{\lambda_{1n}^2 [1 - \exp(2\lambda_{1n} L_1)][J_1(\lambda_{1n} R_1)]^2} \tag{39}$$

The same solution method was applied to give the expression for drawdown in the upper aquifer:

$$s_2(r_2, z_2) = \frac{2q_{AW}a}{K_2 R_2^2} \sum_{n=1}^{\infty} \{\exp(\lambda_{2n} z_2) + \exp[-\lambda_{2n}(z_2 - 2L_2)]\} \frac{J_2(\lambda_{2n} a) J_0(\lambda_{2n} r_2)}{\lambda_{2n}^2 [1 - \exp(2\lambda_{2n} L_2)][J_2(\lambda_{2n} R_2)]^2} \tag{40}$$

Avci[16] stated that flow through the abandoned wellbore could be described by:

$$Q_{AW} = \pi a^2 q_{AW} = \frac{\bar{h}_1 - \bar{h}_2}{\Omega} \tag{41}$$

where $\bar{h}_1$ and $\bar{h}_2$ represented the average head over the borehole openings in each aquifer respectively. As in the case of Javandel et al.[13], a general resistance term, Ω, was used to represent the head losses in the wellbore and was not further defined. Using the solutions for drawdown given by Eqs. 39 and 40, the average head, $\bar{h}_i$, across the borehole in either formation was determined from:

$$\bar{h}_i = H_i - \frac{2}{a^2}\int_0^a r_i s_i(r_i,0)dr_i \tag{42}$$

which gave:

$$\bar{h}_1 = H_1 + \frac{4q_{AW}}{K_1 R_1^2}\sum_{n=1}^{\infty}\frac{[1+\exp(2\lambda_{1n}L_1)][J_1(\lambda_{1n}a)]^2}{\lambda_{1n}^3[1-\exp(2\lambda_{1n}L_1)][J_1(\lambda_{1n}R_1)]^2} \tag{43}$$

$$\bar{h}_2 = H_2 + \frac{4q_{AW}}{K_2 R_2^2}\sum_{n=1}^{\infty}\frac{[1+\exp(2\lambda_{2n}L_2)][J_1(\lambda_{2n}a)]^2}{\lambda_{2n}^3[1-\exp(2\lambda_{2n}L_2)][J_1(\lambda_{2n}R_2)]^2} \tag{44}$$

The flow rate through the wellbore was then found by substitution of these expressions into Eq. 41 to give:

$$q_{AW} = \frac{\Delta H}{\left[\pi a^2\Omega - a\sum_{n=1}^{\infty}\left\{\left[\frac{J_1(\lambda_{1n}a)}{J_1(\lambda_{1n}R_1)}\right]^2\left[\frac{1+e^{(2\lambda_{1n}L_1)}}{1-e^{(2\lambda_{1n}L_1)}}\right]\beta_{1n} + \left[\frac{J_1(\lambda_{2n}a)}{J_1(\lambda_{2n}R_2)}\right]^2\left[\frac{1+e^{(2\lambda_{2n}L_2)}}{1-e^{(2\lambda_{2n}L_2)}}\right]\beta_{2n}\right\}\right]} \tag{45}$$

where:

$$\beta_{in} = \frac{1}{K_i R_i^2 \lambda_{in}^3} \tag{46}$$

The expression for the flux given in Eq. 45 could then be substituted into Eq. 41 to find the flow rate.

Although Avci[16] did not report any flow results from his solution, he did apply his equation to two field examples to perform a sensitivity analysis of the effect of the choice of the location of the steady state radii, R_1 and R_2, and wellbore resistance factor, Ω, on flow rate. In these case studies, Avci used the same expression as Silliman and Higgins[14] in Eq. 29 to calculate the steady state radius location for the constant potential in the formations. By varying the value chosen for drawdown in Eq. 29, Avci obtained different values for the steady state radii. Using these values in his flow expression, his results indicated the flow rates varied with the logarithm of the radius and an order of magnitude difference in the choice for radius caused less than a 10% difference in the flow rate prediction. The sensitivity analysis showed that the choice of magnitude for the resistance term, Ω, however, had a critical impact on the abandoned well flow rate as was reported by Javandel et al.[13]

The most current analytical model for fully transient flow through an abandoned well was given by Avci[17] in 1994. It was developed using an approach similar to Javandel et al.[13] and uses the same physical model as shown in Figure 1 which includes an injection and abandoned well. The injection well fully penetrates the target formation 1. The abandoned well fully penetrates both formations 1 and 2 to allow interformational flow. Once again, homogeneous, isotropic formations of infinite areal extent are assumed. Avci also assumed the formations were saturated with a single phase fluid and that the wellbore was filled with the same fluid. Flow in the well could be driven by the injection well or natural potential differences between the two formations.

Avci[17] defined the flow through the abandoned well using an equation similar to Eq. 6 from Javandel et al.[13] but included a term to account for the pressure buildup in the upper formation which had been neglected in their development. Therefore the equation describing flow was given as:

$$Q_{AW}(t) = \frac{\Delta P_I(t) + \Delta\Phi - [\Delta P_1(r_{AW},t) + \Delta P_2(r_{AW},t)]}{\Omega} \tag{47}$$

where:

$$\Delta\Phi = \Phi_1 - \Phi_2 \tag{48}$$

represented the difference in natural potential between the formations. The drawdown and buildup in formation 1 and 2 from flow through the abandoned well was given by:

$$\Delta P_i(r_{AW},t) = \frac{1}{4\pi k_i h_i}\int_0^t \frac{Q_{AW}(\tau)}{(t-\tau)} \exp\left[\frac{-r_{AW}^2 \phi_i \mu c}{4k_i(t-\tau)}\right] d\tau \qquad i = 1,2 \tag{49}$$

and the pressure buildup from injection was given by the Theis equation:

$$\Delta P_I(R,t) = -\frac{Q_I}{4\pi k_1 h_1} Ei\left(-\frac{R^2 \phi_1 uc}{4k_1 t}\right) \tag{50}$$

Avci[17] substituted these expressions into Eq. 47 and converted the expression to Laplace space using a Laplace parameter $\bar{z}$ to give:

$$\overline{Q}_{AW} = \frac{\frac{Q_I}{2\pi k_1 h_1} K_0\left[R\left(\frac{\bar{z}\phi_1 \mu c}{k_1}\right)^{1/2}\right] + \Delta\Phi}{\bar{z}\left\{\Omega + \frac{1}{2\pi k_1 h_1} K_0\left[r_{AW}\left(\frac{\bar{z}\phi_1 \mu c}{k_1}\right)^{1/2}\right] + \frac{1}{2\pi k_2 h_2} K_0\left[r_{AW}\left(\frac{\bar{z}\phi_2 \mu c}{k_2}\right)^{1/2}\right]\right\}} \tag{51}$$

Avci[17] then converted the equation to dimensionless form:

$$\overline{Q}_{AWD} = \frac{K_0\left[\left(z_D\right)^{1/2}\right] + \Delta\Phi_D}{z_D\left\{\Omega_D + \frac{k_1 h_1}{k_2 h_2} K_0\left[r_{AWD}\left(\frac{z_D \phi_2 k_1}{k_2 \phi_1}\right)^{1/2}\right] + K_0\left[\left(r_{AWD} z_D\right)^{1/2}\right]\right\}} \tag{52}$$

with dimensionless variables:

$$\overline{Q}_{AWD} = \frac{Q_{AW}}{Q_I} \tag{10}$$

$$t_D = t\frac{k_1}{\phi\mu c R^2} \tag{11}$$

$$r_{AWD} = \frac{r_{AW}}{R} \tag{12}$$

$$\Omega_D = 2\pi k_1 h_1 \Omega / \mu \tag{13}$$

$$z_D = z\frac{\phi_1 \mu c R^2}{k_1} \tag{53}$$

Avci used the Stehfest algorithm to numerically invert the solution from Laplace space.

The dimensionless flow results from Avci's solution for $r_{AWD} = 0.001$ are shown in Figure 6 for a case where the initial potential differences between the formations were assumed to be negligible and the thicknesses of the aquifers were assumed to be equal. The curves are a function of ξ, which is the ratio of the permeability of the upper aquifer to the lower aquifer. The curves are also a function of the dimensionless resistance factor Ω_D. Figure 6 shows the strong influence of the magnitude of the resistance factor, Ω_D, on the flow rate through the abandoned well. Like Javandel et al.[13], this resistance factor was undefined and acted as a multiplication factor which influenced flow accordingly. The ratio, ξ, also demonstrated that the permeability of the upper aquifer had a large impact

on the flow rate. For the case of no resistance in the wellbore ($\Omega_D = 0$), an ξ equal to 1.0 produced a late time flow rate equal to about 23% of the injection rate. A decrease in permeability of the upper aquifer by an order of magnitude to give ξ equal to 0.1 led to a decrease in this flow to 5% of the injection rate. An increase in the upper permeability by an order of magnitude to ξ equal to 10.0 led to an increase in this flow to 42.6% of the injection rate. In other results for a field case study, Avci also showed the abandoned well flow rate to be a strong function of the distance between the abandoned well and injection well, R. As expected, the flow rate decreased as this distance was increased.

Avci's[17] work demonstrated that an analytical solution for abandoned well flow which accounted for all pressure changes in the system could be obtained. Although it was only for the simple case of one injector driving flow it required a numerical solution, which made it the most complicated of the analytical models discussed. Avci's results, however, clearly showed the factors which strongly influenced flow including the permeability ratio between the two formations, the resistance of the abandoned wellbore, and the distance between the abandoned well and injection well.

2.2 Numerical Models

One of the first numerical simulations to predict abandoned well flow was that of Chia and Chu[18] in 1989. Chia and Chu investigated the transport of injected fluids up the microannuli and channels in the cement sheath and disturbed drilling zone surrounding an abandoned well as shown in Figure 7. They used the three dimensional finite difference

simulator SWIFT II[19] which is a single phase simulation package for contaminant transport. The abandoned well annular region was modeled as vertical grid blocks with user defined permeabilities. Their results showed that if the lowest formation was undergoing pressure buildup as a consequence of injection, transport of fluids up the disturbed region around the wellbore would occur. Chia and Chu also found that permeable formations next to this zone allowed the fluid to be transported horizontally away from the wellbore so that the majority of fluids did not continue upward migration. Chia and Chu's results did not include the actual flow rates expected but instead showed the magnitude of solute invasion into permeable zones overlying the lower formation.

Warner[11] also employed numerical simulation to infer the transport of fluids through an abandoned well to overlying formations in response to injection in a lower formation in 1988. Warner used a newer version of the three dimensional simulator SWIFT III[20] to model the response of an abandoned well of known location to a proposed injection well in the West Mallalieu Field in Mississippi. The study was initiated to determine if pressure buildup in the target Lower Tuscaloosa formation could move injected fluid through an abandoned well located within a quarter mile of the injection well into the Sparta formation which acted as an underground source of drinking water (USDW).

The simulation of abandoned well flow used a variable finite difference grid in which the well itself was represented as grid blocks. The injection well was treated using a source representation model. The simulation employed the horizontal finite difference grid in Figure 8 which shows the relative locations of the injection and abandoned well. The

vertical finite difference grid was composed of seven different layers to represent the geological formations. Because the condition of the abandoned well was unknown, the authors assumed it to be uncased. Three different cases of wellbore conditions were simulated by assigning different permeabilities to the wellbore blocks. The first case was for an open wellbore with grid blocks of 4000 darcys permeability. In the second case, the wellbore was open but included a 10 ft plug with 10^{-3} md permeability. The final case was also for an open wellbore with a 100 ft plug with 10^{-3} md permeability. All the cases were evaluated for different injection rates.

In his results, Warner[11] only presented the pressure profiles in the seven layers representing the formations to indicate flow. No actual cumulative flow volumes were reported. The results for the 'worst case' scenario of a high permeability open wellbore and a maximum injection rate of 200 bbls/day for 10 years are shown in Figure 9. As expected with an open wellbore, most of the flow which moved up the abandoned well grid blocks was transported into the overlying permeable formations as shown by their pressure buildup. There were no pressure changes in the Sparta USDW to indicate transport. For the cases of the 10 ft and 100 ft plugs in the wellbore, the results exhibited substantially lower pressure buildups in overlying formations which confirmed a decrease in fluid transport in the presence of increased wellbore resistance. Lower injection rates also produced lower pressure buildup.

The original work done by Warner [11] was extended by Warner and McConnell[12] in 1990 to evaluate the potential of abandoned wells in the entire Lower Tuscaloosa Sand trend in Mississippi to transport fluid to the overlying Sparta USDW. Warner and

McConnell collected and evaluated large amounts of data on the region which allowed a detailed simulation model to be prepared. The analysis included correlations of the stratigraphic units based on numerous logs from wells in the trend. Thorough descriptions of the geologic characteristics of each unit were also prepared. Furthermore, the authors also attempted to assess the condition of abandoned wells in the trend to aid in their description in the simulation. Based on their analysis, they described abandoned wellbore conditions which included estimates of expected thickness, porosity, and permeability of settled drilling muds and sloughed shale in the wellbore, as well as predictions of where corrosion in the casing might exist.

Warner and McConnell[12] once again used the three dimensional finite difference simulator SWIFT III[20] to determine the pressure profiles in the model. The simulations were all based on one injection well and one abandoned well. As in their previous work, the abandoned well was treated as grid blocks and the injection well was incorporated using a source representation well model. The authors investigated two scenarios which differed only in the definition of the characteristics of well blocks representing the abandoned wellbore. They considered these two cases of wellbore conditions to be representative of the abandoned wells in the trend. The first was for an uncased abandoned well which contained a sloughed shale column 154.5 feet thick overlain by a 4,620 foot column of settled mud solids. The wellbore and surrounding formations were modeled using 10 separate vertical layers as shown in Figure 10.

The second case was for a cased well with an annular region containing a sloughed shale column 200 feet thick and a settled mud column 3,740 feet thick on top of the

sloughed shale. It included a perforation in the casing roughly located in the center of the settled mud column which was modeled as a 1 ft open layer. The 12 vertical layers for the wellbore and formations used in the simulation for this case are shown in Figure 11. Wellbore blocks containing settled drilling mud were assigned a permeability of 1 md and the sloughed shale was assigned a permeability of 0.1 md. The well blocks which were filled with fluid were given a permeability of $3.7x10^8$ darcys. The horizontal grid for the location of the abandoned and injection well in the first case is shown in Figure 12. A slightly different grid was used for the second case but the distance between the injection and abandoned wells was identical.

Warner and McConnell[12] ran the simulation for both abandoned well cases over a time period of ten years. They reported the results in terms of flow into the abandoned well, but did not indicate the method used to calculate the flow from the pressures provided by the simulation. Their results showed a total absence of flow into the abandoned well in both cases in response to injection rates of up to 600 bbls/day. This result can be attributed to the resistance of the sloughed shale and mud layers in the wellbore and the annulus which acted as barriers to flow.

Based on their simulations, which only investigated the impact of one injector for highly resistive abandoned wellbore conditions, McConnell and Warner[12] concluded there were no conditions under which flow could be expected to move from the Lower Tuscaloosa through an abandoned well into the Sparta USDW. They did not consider the case of an abandoned well with no resistance. McConnell and Warner noted that the

numerical simulation method employed to determine abandoned well flow potential in the trend required large amounts of data and modeling which was not trivial.

The most recent numerical simulation of abandoned well flow was performed by Lacombe et al.[21] in 1995 who demonstrated the nature of cross formational contaminant transport through an abandoned well. Their physical model consisted of an upper aquifer, a middle aquitard, and a lower confined aquifer which were connected by an abandoned wellbore. The physical system was modeled using three dimensional finite element blocks where the wellbore was represented as one dimensional line elements which were superimposed on the finite element mesh as shown in Figure 13. The flow in the wellbore was described using the Darcy equation for one dimensional flow. Two wellbore conditions were considered. In one case, the wellbore was sediment filled and assigned a suitable permeability. In the other case, the wellbore was open and the wellbore conductivity was assigned by deriving a value using the Hagen and Poisueille equation for pipe flow:

$$K_w = r_s^2 \rho g / 8\mu \tag{54}$$

where:

K_w = wellbore conductivity (m/s)

r_s = the radius of the well screen (m)

The authors investigated three scenarios believed to create cross formational flow. The first case sought to determine how the location and condition of the borehole would impact the movement of a contaminant source on the surface of the upper formation to the lower formation within a natural groundwater flow regime. The second case involved

pumping the lower formation to determine how pumpage influenced contaminant movement. In the third case, the contaminant source was eliminated and the authors examined the effect of injection of wastes into the lower formation on the movement of fluids into the upper formation through the wellbore. The authors used a model of two 5 m thick aquifers separated by a 5 m aquitard to study all three cases. A single borehole fully penetrated the aquitard.

In the first case, the results showed that the borehole could rapidly transmit contaminants to the lower aquifer given a favorable natural groundwater flow gradient. If hydraulic gradients were sufficiently high, the entire plume was shown to be diverted to the lower aquifer. The flow rate was shown to dramatically increase with larger borehole size but this was limited by the natural groundwater flow gradients occurring in the upper aquifer. For the second case where the lower aquifer was pumped, the location of the abandoned wellbore was found to be critical in determining the arrival time and maximum concentration reaching the pumping well. The closer the location to the pumping well, the greater the concentrations of contaminant reaching the well at earlier times. In both cases, the sediment filled wellbore slowed the transport as compared to the open wellbore.

The third case is of the greatest interest in this work as it evaluated the impact of waste injection in the lower aquifer on flow through the abandoned wellbore to the upper aquifer. The physical model for this case is shown in Figure 14. The rock and fluid properties of both aquifer were set to the same values. The borehole existed only in the aquitard and was located at a distance of 500 m from the injection well. The injection well was operating at a rate of 200 l/min (1813 bbl/day). As shown in Figure 14, the natural

potential in the upper aquifer was greater than the lower aquifer which led to an initial gradient which created downward flow. Once injection was started, the resulting pressure buildup in the lower aquifer was shown to reverse flow up the wellbore and move wastes into the upper aquifer. The flow rate in the abandoned wellbore was reported be about 21 l/min (965m/d) after 2 years. This rate is equivalent to 190 bbls/day. The high flow rate through the borehole caused a significant diversion of the contaminant plume to the upper aquifer, but Lacombe et al.[21] noted that the plume was not completely redirected from the lower aquifer to the upper aquifer but continued to spread in the lower aquifer.

2.3 Discussion

The critical review of the methods to predict abandoned well flow shows that both analytical and numerical solutions can be used to describe interformational flow. A summary of the characteristics of the analytical models is given in Table 1 while Table 2 summarizes the characteristics of the numerical solutions.

The analytical models have provided solutions for steady and unsteady flow through abandoned wells. They have been limited to simple physical systems for which a solution is possible. In general, the driving force for flow is given by either natural potential differences between formations or the presence of an injection well in the lower formation. These models have demonstrated that the abandoned well flow is a function of the rock and fluid properties of the formations and the resistance of the wellbore. In cases where an injection well is present, the flow is also a function of the distance from the

injection well to the abandoned well. The critical problem with the analytical models is that although they identify the wellbore resistance term as a major factor in determining interformational flow, no attempt was made to define this term. The majority of the models, with the exception of Silliman and Higgins[14], supplied only a general resistance term which acted as a multiplier and could represent any number of values. None of the models considered the impact that a producing well in the lower formation may have on flow. They also did not consider the impact that wells in the upper formation may exert on the flow.

The numerical solutions for abandoned well flow have the capability of addressing more complex situations. They have been used to predict behind pipe flow and flow in the wellbore. The simulators were all limited to single phase fluids. In finite difference simulations, the SWIFT II[19] and III[20] three dimensional simulation packages were employed which required the wellbore to be represented as grid blocks. The resistance of the wellbore was incorporated by assigning the wellbore blocks user defined permeabilities to represent open holes, sloughed shales, or drilling muds. This technique of representing the well, however, leads to a lack of flexibility in choosing the abandoned well location as the grid must be re-established for each new location. The SWIFT simulations were able to incorporate the complex geology of a system as vertical layers and show that flow up the abandoned wellbore can be transported into a number of overlying permeable formations. Their application was demonstrated with simple single injector cases although they should be flexible enough to allow for other injector/producer schemes. The SWIFT[19,20] simulations were also not employed to evaluate the impact of injectors and

producers in the overlying formations on the abandoned well flow. The numerical simulation of Lacombe et al.[21] employed a finite element model. The simulation cases were performed using wellbore conditions which were homogeneous (completely open or completely sediment filled), but the finite element model appeared to have the capability to address other wellbore conditions. It was applied for the case of one injector in the lower aquifer but the description indicated it could incorporate more complex injection/production schemes including the presence of injection and production wells in the overlying formation.

In summary, the current analytical models are limited to simplistic physical systems involving flow between only two formations. They do not address wellbore condition and can not account for the impact of wells in overlying formation on well flow. Often, they require complex mathematical solutions and the most recent model given by Avci[17] requires a complex numerical inversion scheme to calculate flow rates. They are however very useful for identifying the parameters which affect the abandoned well flow. The current numerical solutions can be applied to more complex physical systems which may include numerous formations and many injectors/producers. The grid representation of the well can also represent realistic wellbore conditions, but leads to inflexibility in the choice of the abandoned well location. Because they require large amounts of data and analysis to define the grid block system and its characteristics, their application is complicated and labor intensive.

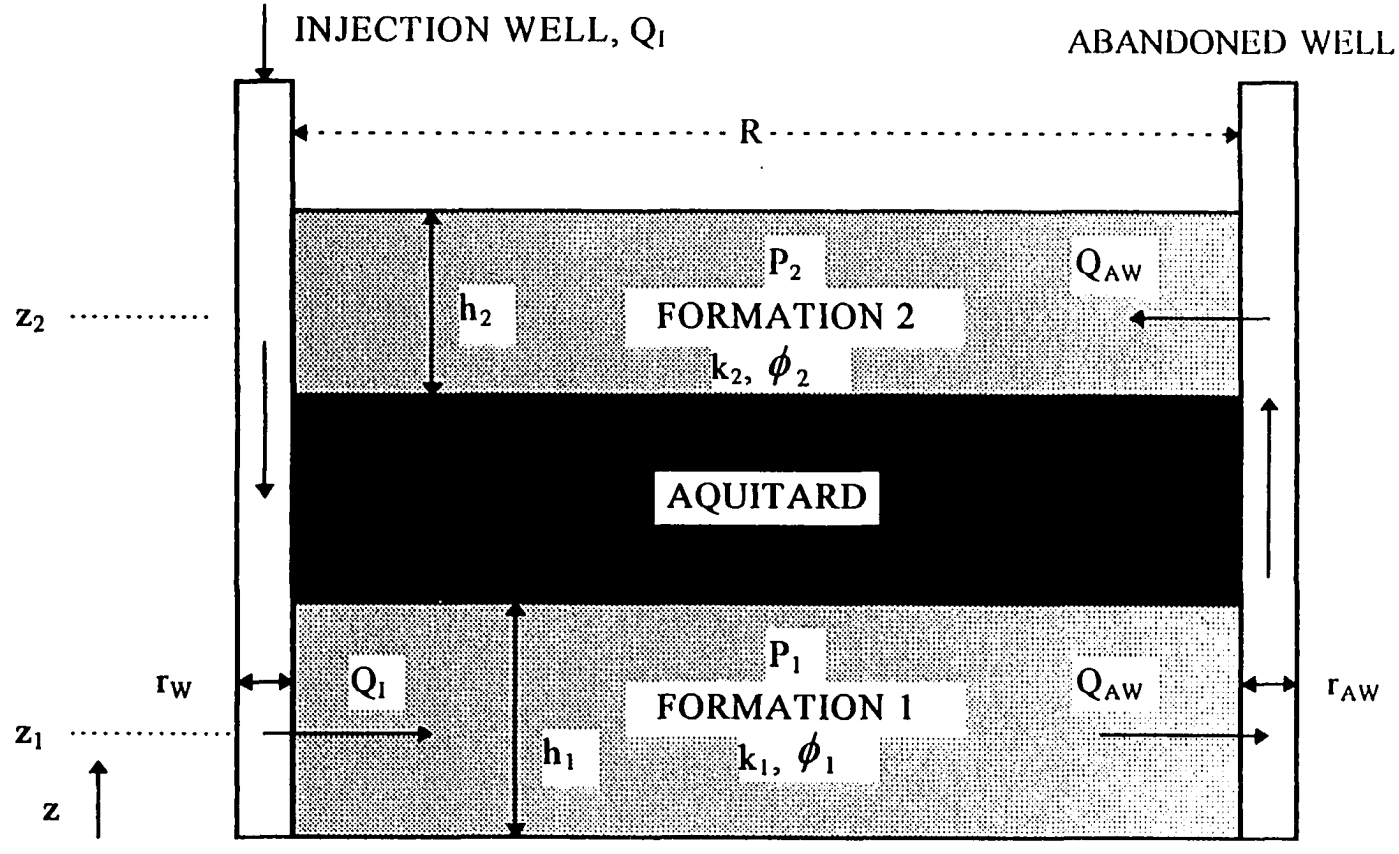


Figure 1. Physical model of Javandel et al.[13] for the analysis of abandoned well flow.

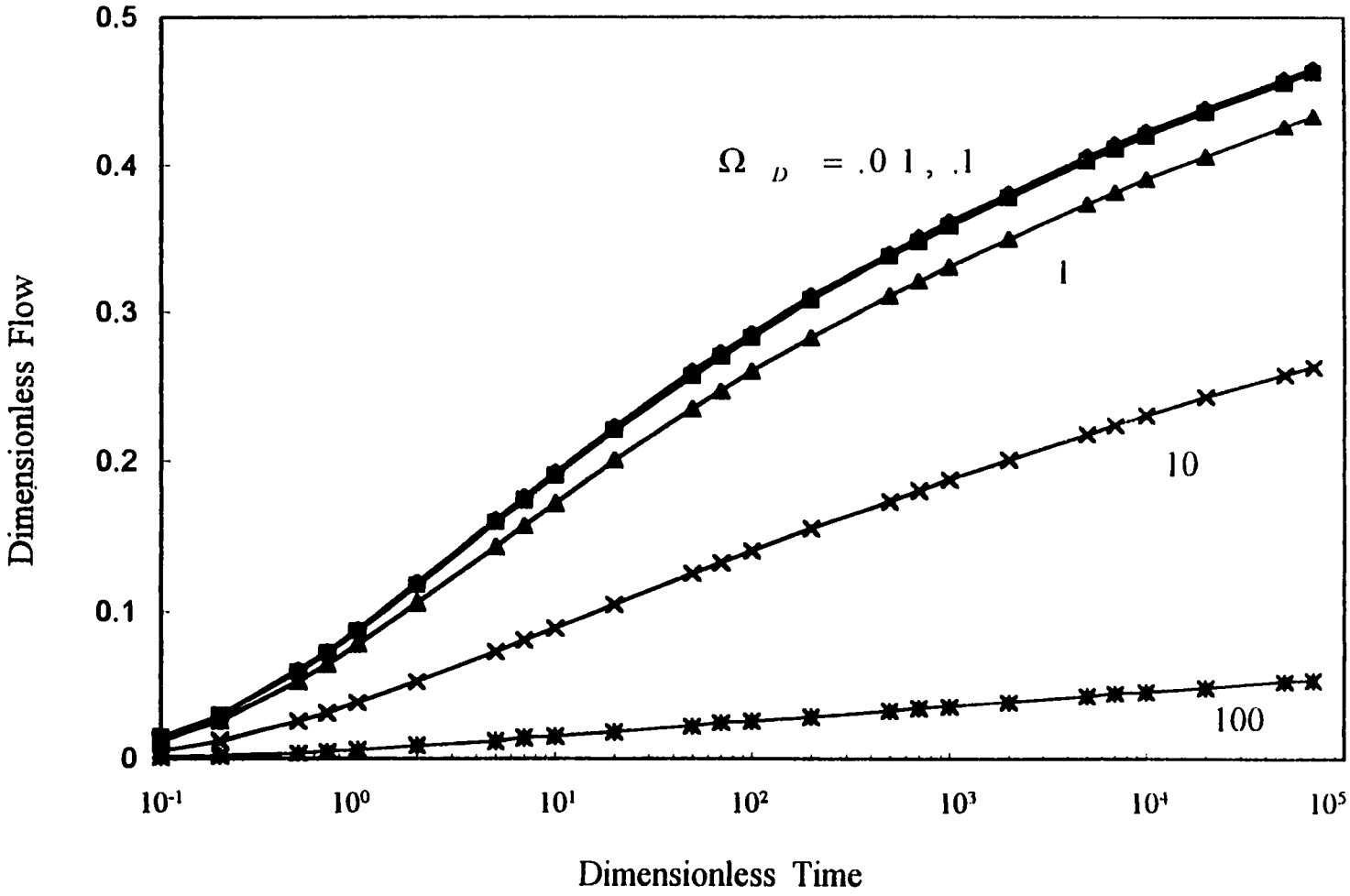


Figure 2. Results of Javandel et al.[13] for dimensionless flow through an abandoned well of varying resistance.

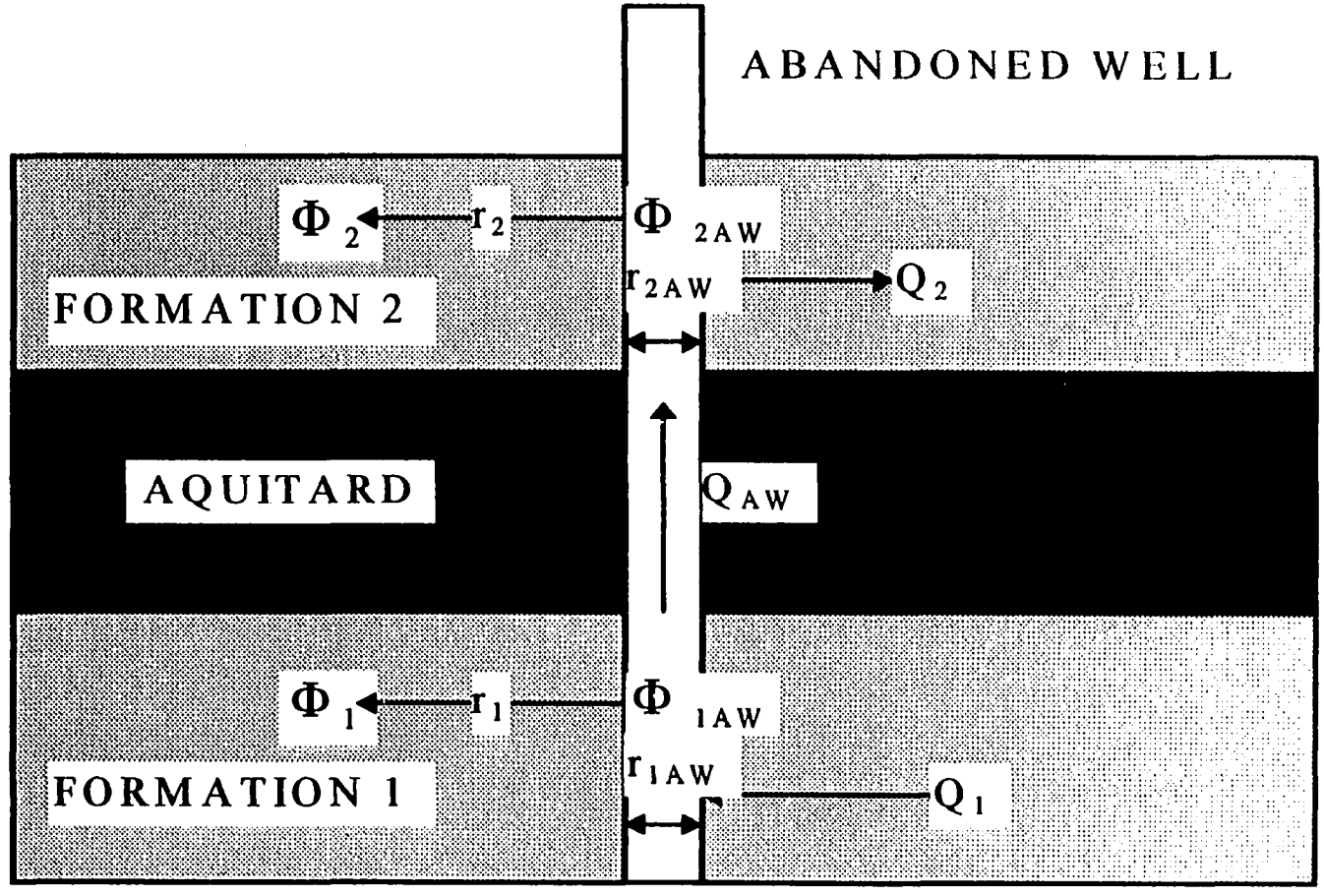


Figure 3. Physical model of Silliman and Higgins[14] for the analysis of abandoned well flow.

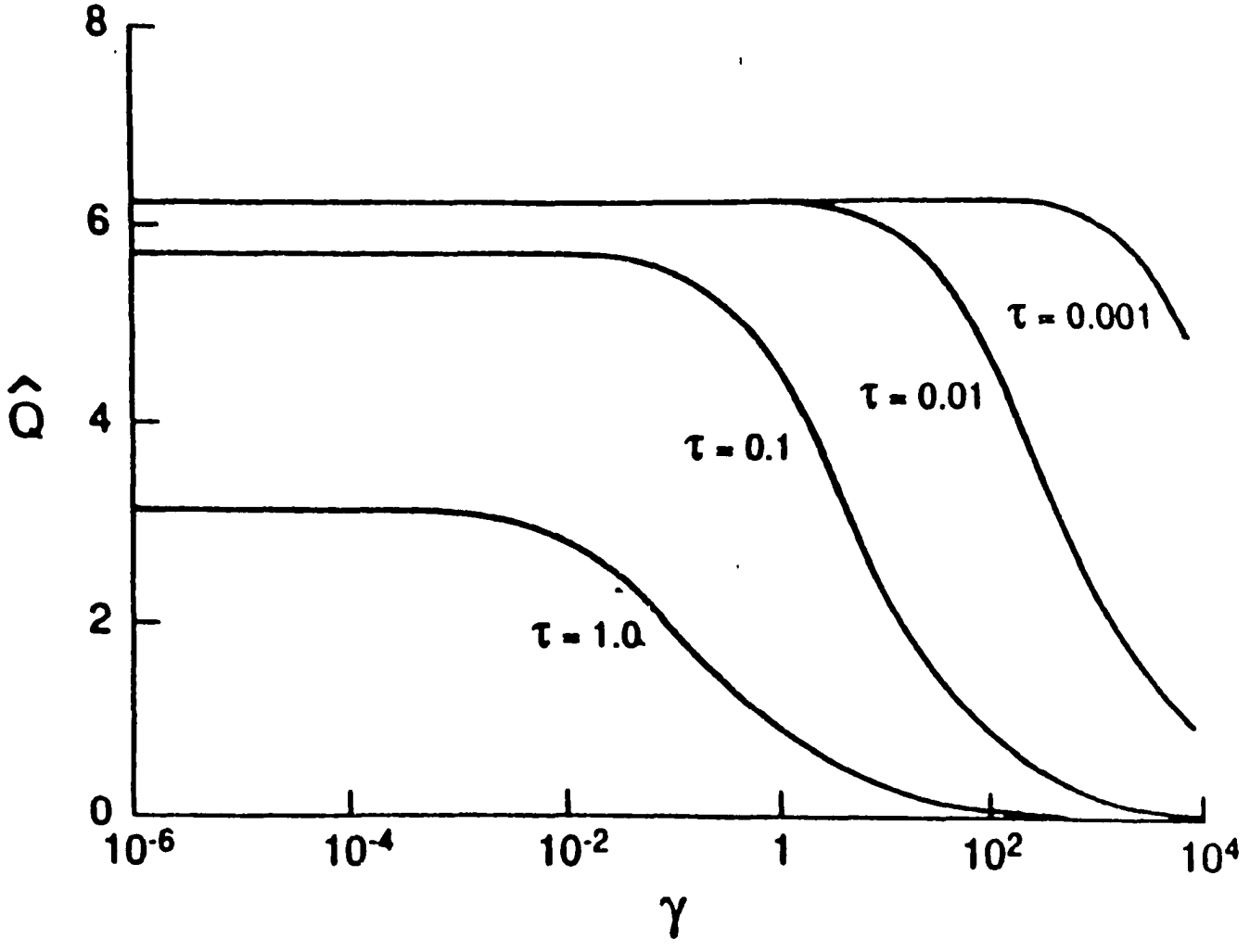


Figure 4. Dimensionless abandoned well flow results (adapted from Silliman and Higgins[14]).

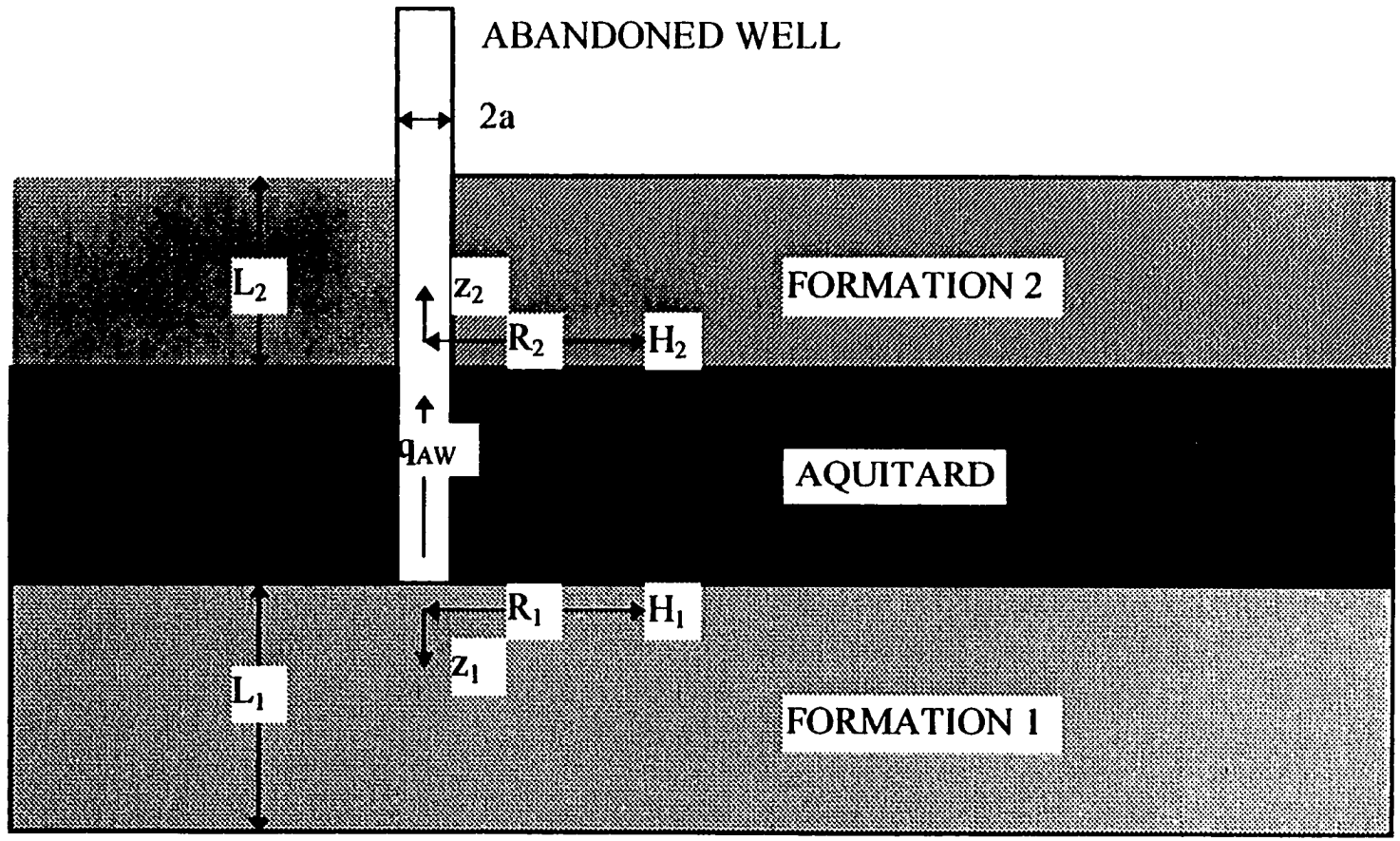


Figure 5. Physical model of Avci[16] for the analysis of abandoned well flow.

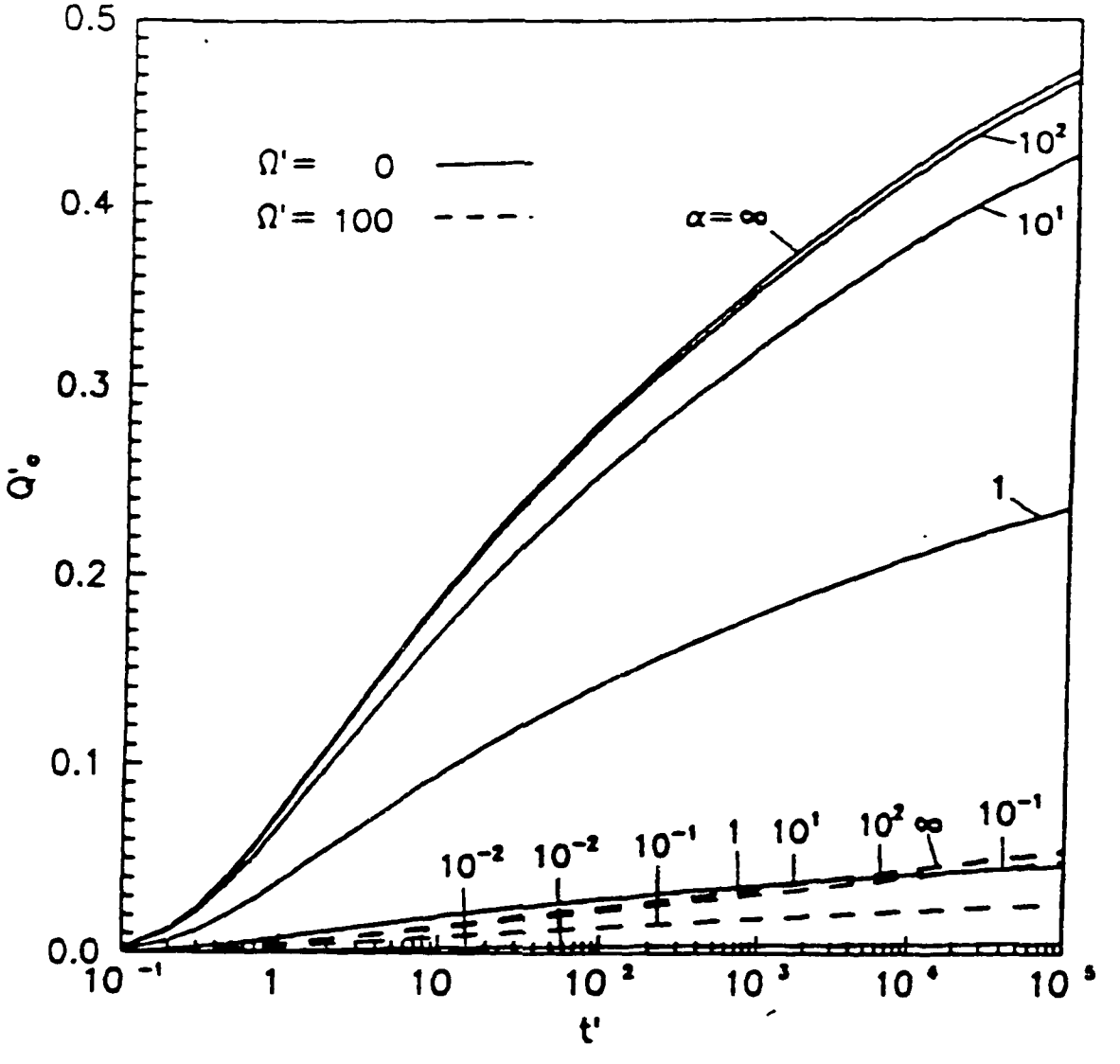


Figure 6. Dimensionless abandoned well flow results (adapted from Avci[17]).

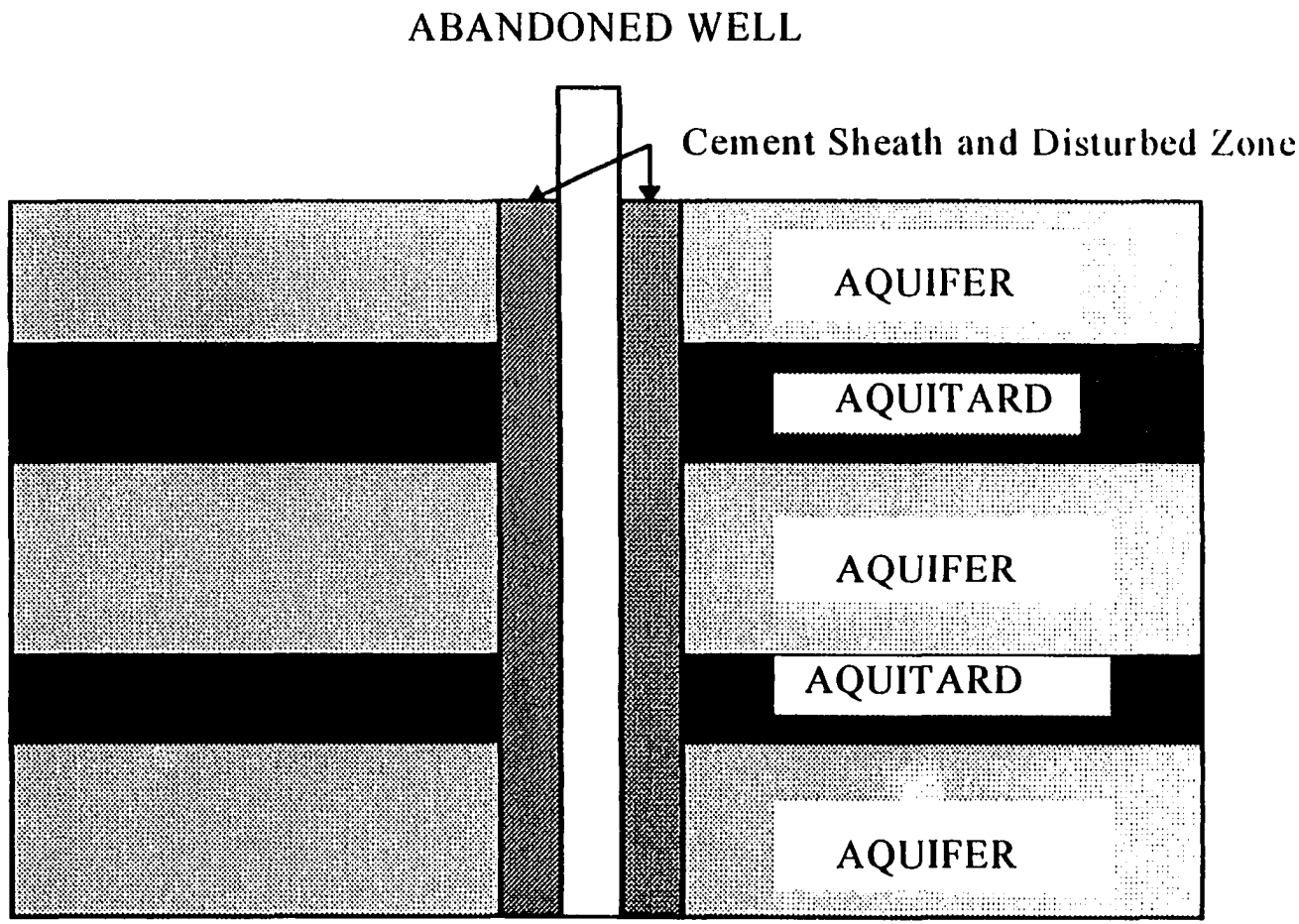


Figure 7. Physical model of Chia and Chu[18] for abandoned well flow simulation.

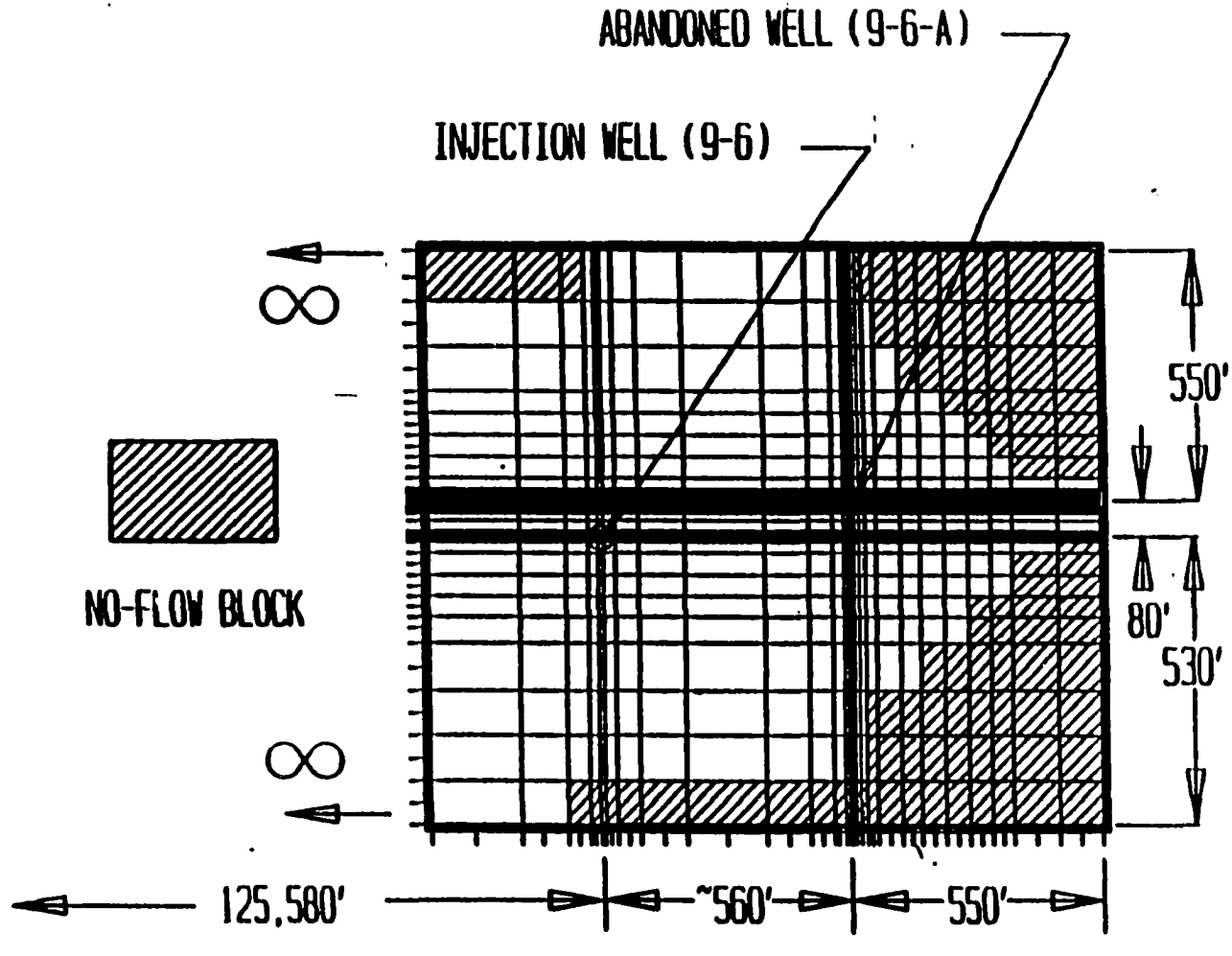


Figure 8. Horizontal finite difference grid showing injection and abandoned well locations (adapted from Warner[11]).

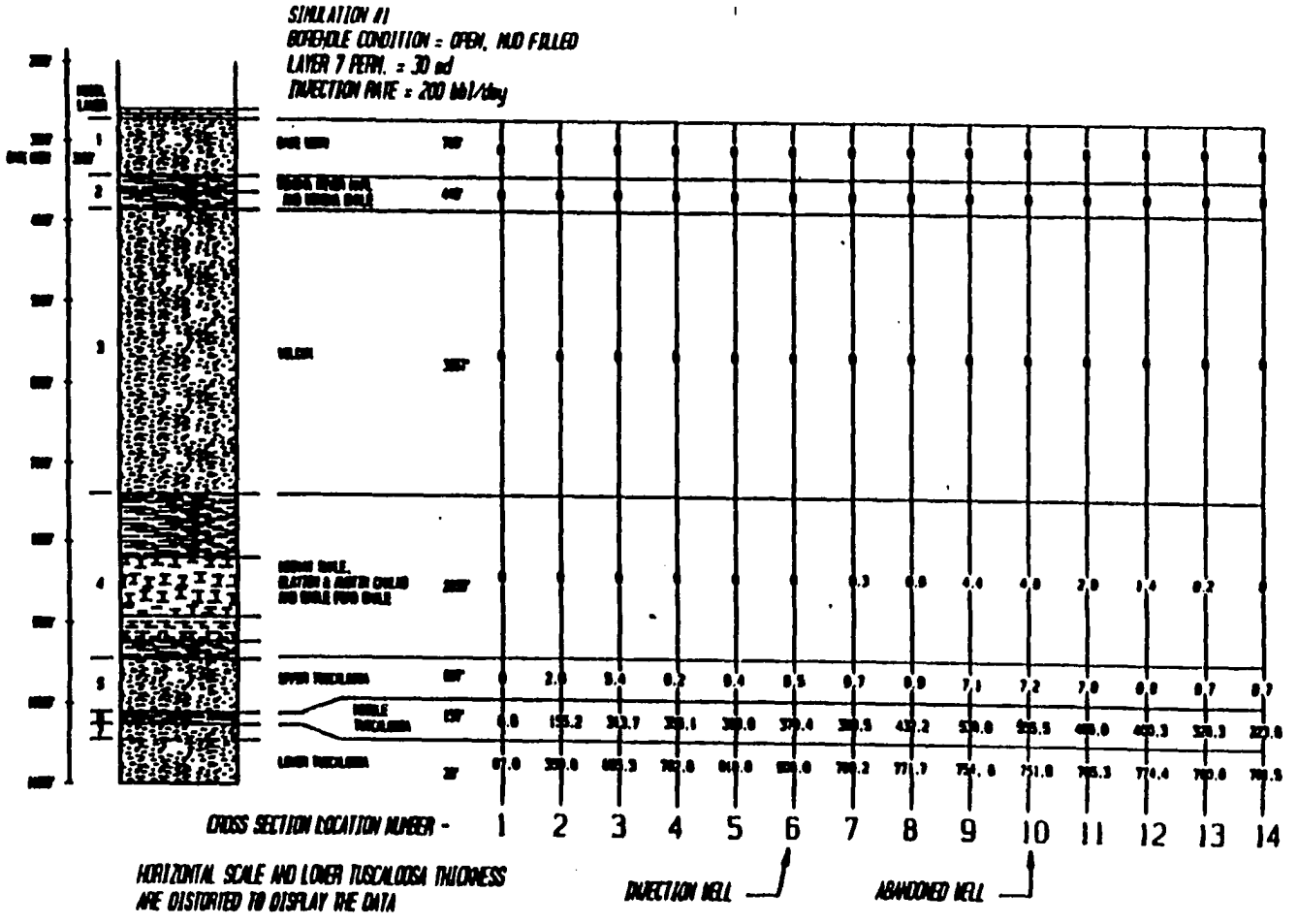


Figure 9. Numerical simulation pressure change results (adapted from Warner[11]).

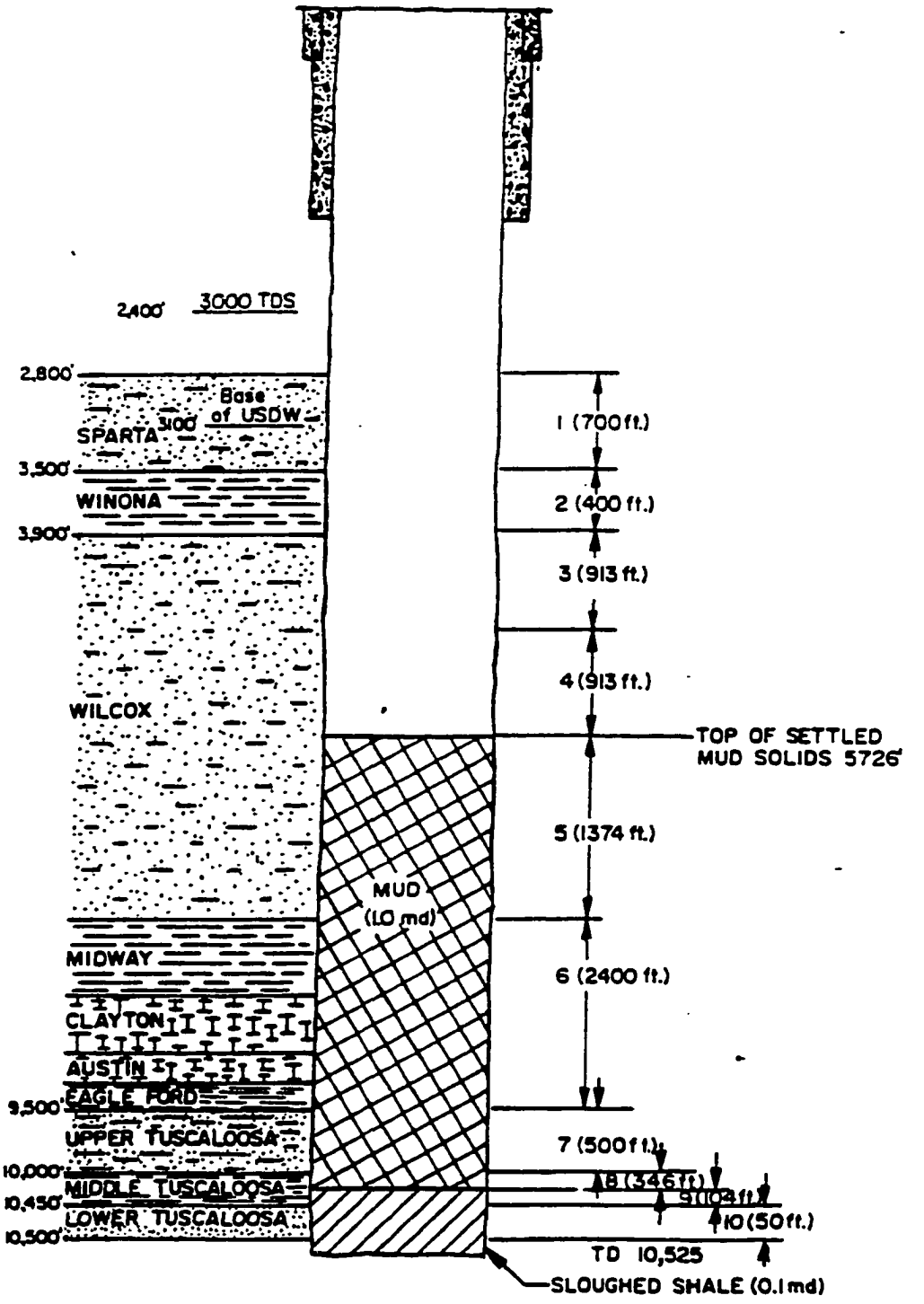


Figure 10. Uncased wellbore simulation layers (adapted from Warner and McConnell[12]).

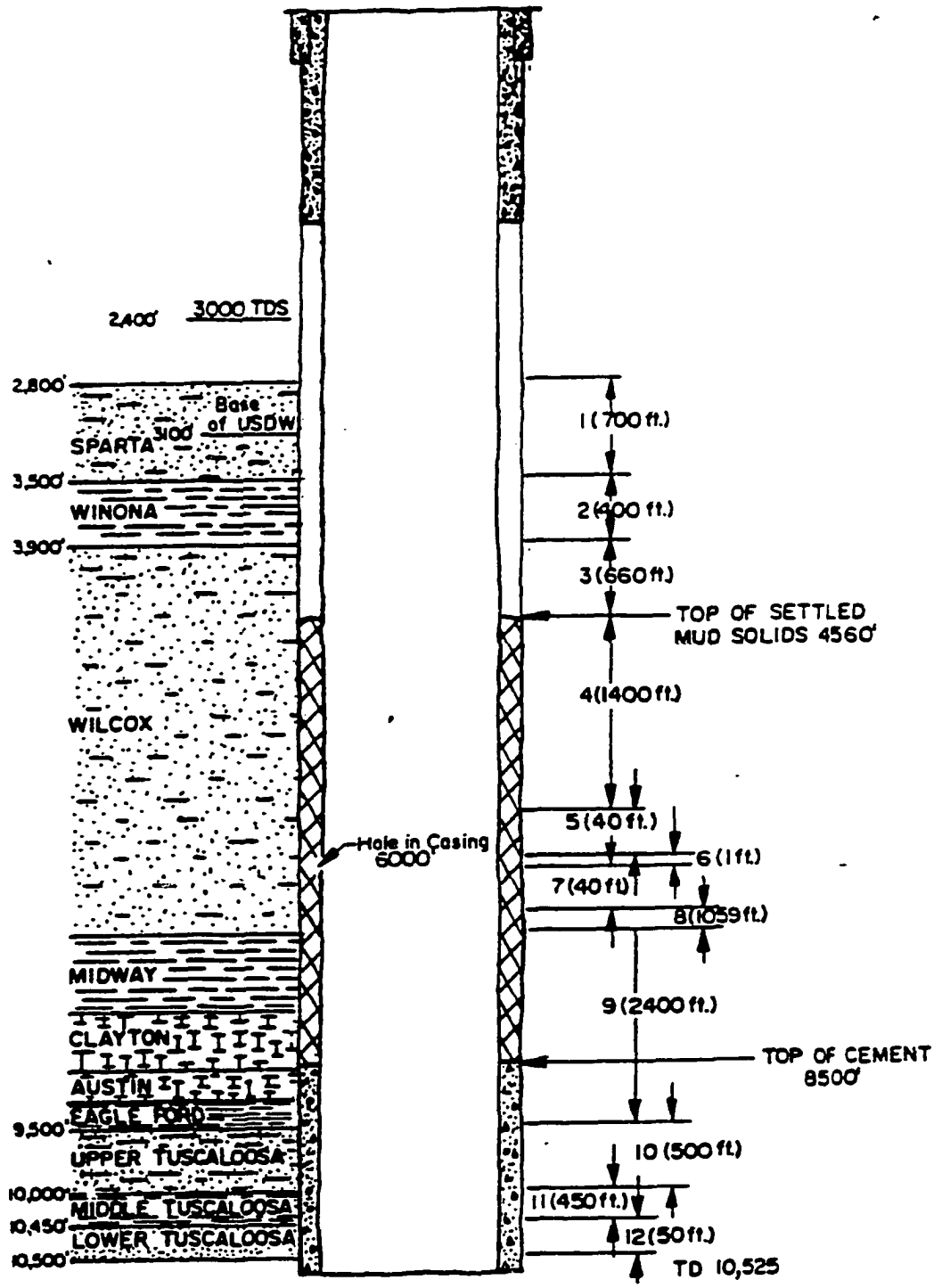


Figure 11. Cased wellbore simulation layers (adapted from Warner and McConnell[12]).

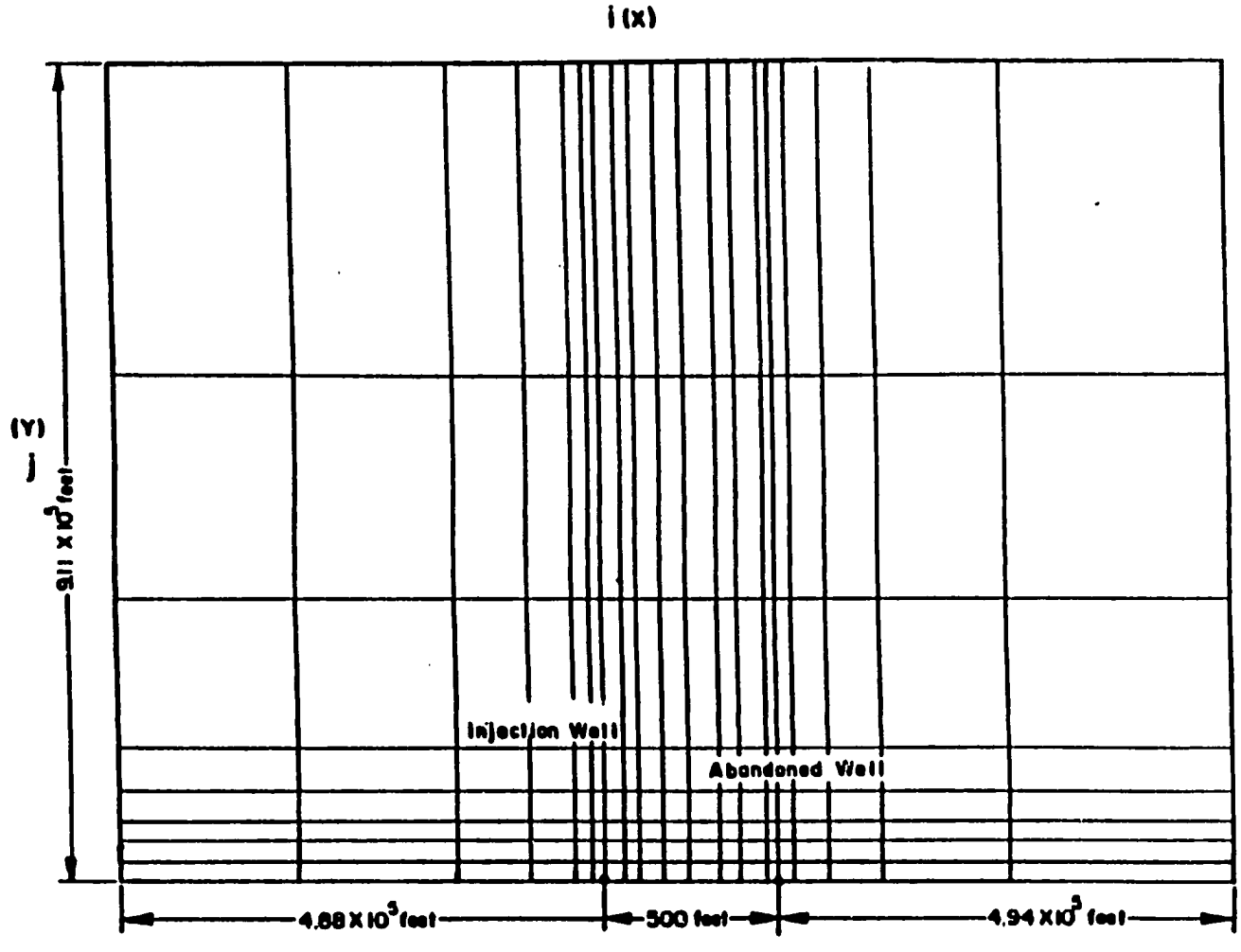


Figure 12. Horizontal finite difference grid showing injection and abandoned well locations (adapted from Warner and McConnell[12]).

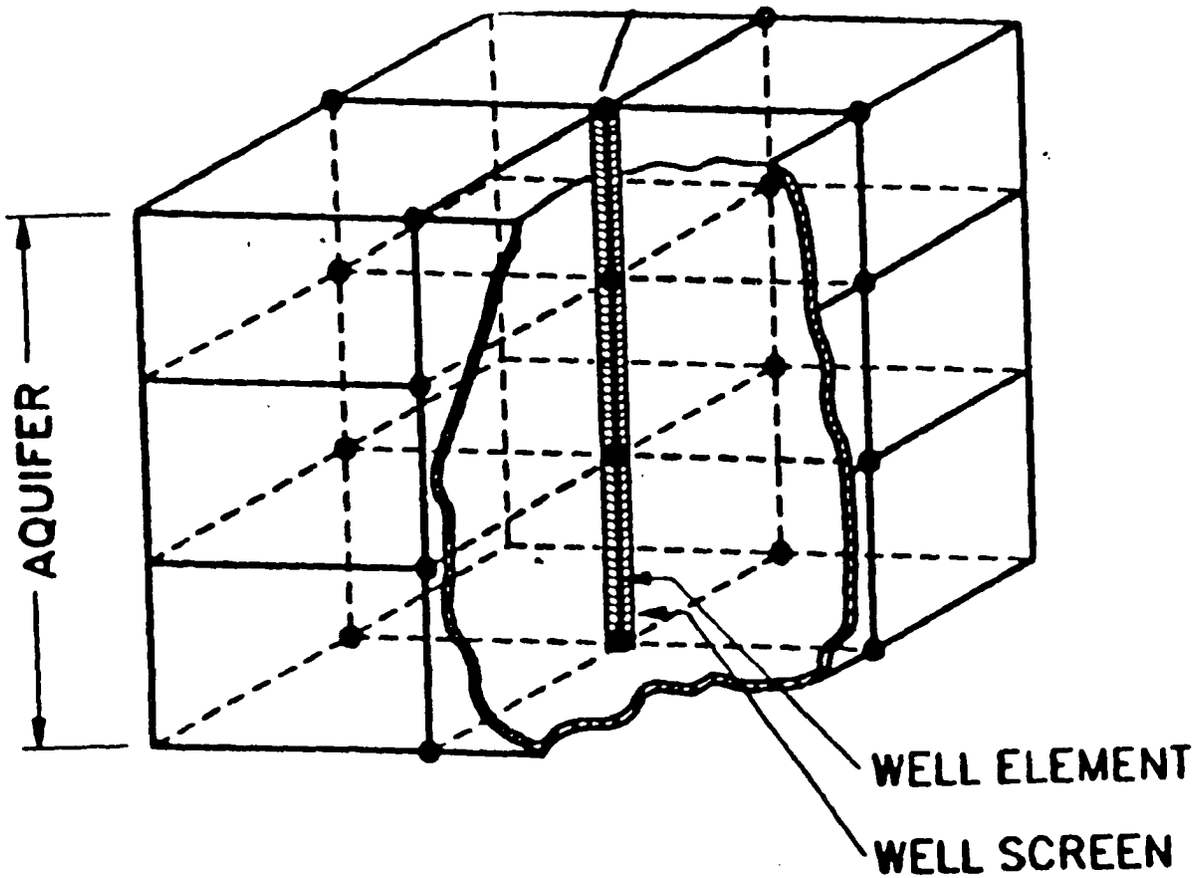


Figure 13. Finite element model with wellbore overlay (adapted from Lacombe et al.[21]).

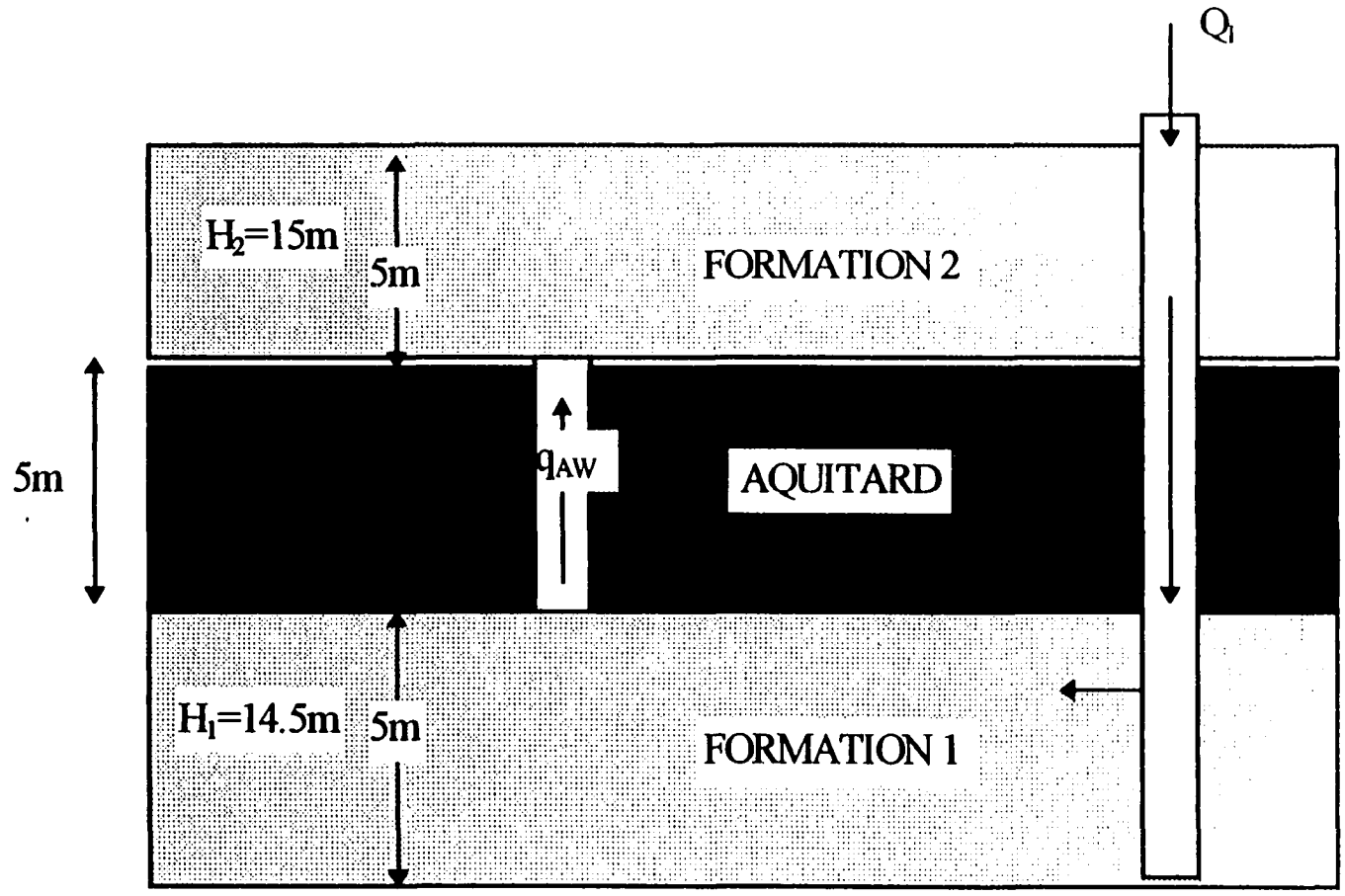


Figure 14. Physical model of Lacombe et al.[21] for abandoned well flow simulation.

Table 1. Summary of characteristics of analytical abandoned well models.

Category	Javandel 1988[13]	Silliman/Higgins 1990[14]	Avci 1992[16]	Avci 1994[17]
GENERAL	Unsteady State	Steady State	Steady State	Unsteady State
GEOLOGY	Homogeneous, isotropic, infinite	Homogeneous, isotropic, infinite	Homogeneous, isotropic, infinite	Homogeneous, isotropic, infinite
FLUIDS	single phase	single phase	single phase	single phase
DRIVING FORCE	single injector lower formation; no wells upper formation	natural potential between formations; no wells	natural potential between formations; no wells	single injector lower formation; natural potential; no wells in upper formation
WELLBORE CONDITION	General resistance term	General resistance term	General resistance term	General resistance term
COORDINATE SYSTEM	1D radial	1D radial	2D cylindrical	1D radial
SOLUTION	LaPlace Space with approximate inversion	Algebraic	Infinite Bessel Function Series	LaPlace Space with numerical inversion
PUBLISHED RESULTS	Flow rates	Flow rates	Flow rates	Flow rates

Table 2. Summary of characteristics of numerical abandoned well models.

Category	Chia and Chu 1989[18]	Warner 1988[11]	Warner and McConnell 1990[12]	Lacombe et al. 1995[12]
GENERAL	SWIFT II FD 3D simulator for fluid and contaminant transport	SWIFT III FD 3D simulator for fluid and contaminant transport	SWIFT III FD 3D simulator for fluid and contaminant transport	finite element simulation
GEOLOGY	user defined multilayer	user defined multilayer	user defined multilayer	user defined homogeneous, isotropic
FLUIDS	single phase	single phase	single phase	single phase
DRIVING FORCE	single injector lowest formation; no wells upper formations	single injector lowest formation; no wells in upper formations	single injector lowest formation; no wells in upper formations	natural potential between formations; single pumping well lower formation; single injector lower formation
WELLBORE DESCRIPTION	finely gridded multilayer vertical blocks for annulus with user defined permeabilities	finely gridded multilayer vertical blocks for wellbore with user defined permeabilities	finely gridded multilayer vertical blocks for wellbore with user defined permeabilites	1D vertical finite elements overlain on 3D finite element mesh with user defined permeabilites
PUBLISHED RESULTS	Solute invasion profiles in overlying formations	Pressure profiles in formations	Flow rates to USDW determined from pressure profiles	Plume concentration profiles in both formations, flow rate

CHAPTER 3

DEVELOPMENT OF ABANDONED WELL MODEL

3.1 The Dynamics and Modeling of Abandoned Well Flow

The intent of this research was to develop a model to predict flow through an abandoned well between formations that are hydraulically isolated from each other. For fluid transport to occur via the abandoned well in this system, a potential gradient must exist between the two formations. It may be a consequence of the natural potential difference, or active injection/production wells in either or both formations. As the abandoned well has no potential to initiate flow (it is neither receiving injection or being pumped), it will simply respond as a source or sink relative to the gradient, either moving fluid up or down the wellbore. The most cited case in the literature is for interformational abandoned well flow created in response to an injection well in the lower formation. Therefore the model development will focus on this case to allow comparisons to analytical and numerical solutions discussed in Chapter 2.

Figure 15 displays the physical system used in this work to demonstrate the dynamics involved in coupled abandoned well flow so a model can be developed to describe the flow. It is composed of two formations which are homogeneous, isotropic, of constant thickness and infinite in extent. They are separated by an impermeable formation which precludes vertical flow. The formations have rock properties given by permeabilities k_1 and k_2, porosities ϕ_1 and ϕ_2, and thicknesses h_1 and h_2. Both formations are

saturated with a single phase liquid of constant density. The wellbore between the two formations is filled with the same fluid, providing a hydraulic connection between them. The system contains two wells. One is an active well, which is capable of injection or production. It is completed across the entire interval in the lower formation and is not open to the upper formation. The second well is an abandoned well which penetrates both formations and is entirely open to both so it may act as a conduit for interformational flow. The initial pressures in the lower and upper formations are P_1 and P_2 respectively.

For the case of one injector and abandoned well as shown in Figure 15, the dynamic process of abandoned well flow may be visualized as follows. At some time after injection begins, the potential at the sandface of the abandoned well in formation 1 increases. This creates a potential gradient with the sandface of the overlying formation 2. The gradient produces radial flow into the abandoned well at formation 1, which becomes linear flow up the wellbore that is finally transformed to radial flow into formation 2. The movement of fluid out of the wellbore and into formation 2 lowers the sandface potential at formation 1. This process generates an abandoned well flow coupled to the evolving potential distributions in both formations.

At first it appears justifiable to assume that the potential at the abandoned well sandface in formation 1 is equivalent to its initial potential plus the pressure change created at the location by the injection well, but the problem is actually more subtle. Consider the analogous situation of the response of an observation well to an active injection well during an interference test. The observation well is synonymous to the case of an open abandoned well that is not hydraulically connected to an overlying formation.

In practice, the pressure change at the observation well has been matched to the exponential integral (Ei) transient pressure solution expected at the observation well location in response to the active injection well. This match, however, can only be true if the observation well is shut in at the sandface. In reality, the observation well is generally shut in at the surface and the potential created at the sandface by the active well generates radial flow into the wellbore. This discharge of fluid from the formation into the wellbore requires an additional pressure drop near the well which can not be accounted for by the traditional Ei solution used for interference tests.

Tongpenyai and Raghavan[22] and Ogbe and Brigham[23] recognized the existence of radial flow into the observation well when it is shut in at the surface during an interference test. They separately developed new dimensionless pressures for the response at the observation well during an interference test to include the effects of observation well flow. Their solutions were obtained by using superposition to account for the presence of radial flow at both the active well and the observation well. They also included a wellbore storage boundary condition. Their results clearly showed that flow at the observation well delayed and reduced the pressure response so that it did not match the Ei solution. This reduction can be attributed to the additional pressure drop necessary in the region of the abandoned well to move fluid radially from the porous media into the wellbore. Although this analogy does not entirely match the circumstances given in the model for interformational flow because it is not coupled to pressure changes in an overlying formation, it demonstrates that flow is moving into the abandoned well in response to

potential changes in the lower formation and that this flow requires an additional pressure drop in the region of the abandoned well.

The creation of radial flow to the abandoned wellbore in response to a potential gradient between formations formed the basis for the analytical solutions given in the literature and discussed in the Section 2.1. Of particular interest is the work done by Avci[17], who was the only author to provide an analytical solution for transient abandoned well flow which is coupled to the pressure changes in both formations. His work was once again based on flow initiated through an abandoned well in response to an injection well in the lower formation 1. The model he advanced for the coupled flow was:

$$Q_{AW}(t) = \frac{\Delta\Phi + \Delta P_I(R,t) - [\Delta P_1(r_{AW},t) + \Delta P_2(r_{AW},t)]}{\Omega} \tag{47}$$

In Eq. 47, the abandoned well flow was defined to be a function of the natural potential difference between the formations,

$$\Delta\Phi = \Phi_1 - \Phi_2 \tag{48}$$

where:

$$\Phi_1 = P_1 + \rho g z_1 \tag{4}$$

$$\Phi_2 = P_2 + \rho g z_2 \tag{5}$$

the pressure change at the abandoned well location created by the injection well,

$$\Delta P_I(R,t) = \frac{-Q_I}{4\pi k_1 h_1} Ei\left(\frac{-R^2\phi_1\mu c}{4k_1 t}\right) \tag{50}$$

the drawdown at the abandoned well location due to radial flow entering the abandoned well from formation 1,

$$\Delta P_1(r_{AW},t)=\frac{1}{4\pi k_1 h_1}\int_0^t \frac{Q_{AW}(\tau)}{(t-\tau)}\exp\left[\frac{-r_{AW}^2\phi_1\mu c}{4k_1(t-\tau)}\right]d\tau \tag{49}$$

and the buildup in formation 2 as consequence of radial flow entering this formation :

$$\Delta P_2(r_{AW},t)=\frac{1}{4\pi k_2 h_2}\int_0^t \frac{Q_{AW}(\tau)}{(t-\tau)}\exp\left[\frac{-r_{AW}^2\phi_2\mu c}{4k_2(t-\tau)}\right]d\tau \tag{55}$$

Avci's model also included the general resistance of the wellbore, Ω, to account for any losses in the well. But this term remained undefined as discussed in Section 2.1.

A graphical interpretation of the terms in Eq. 47 is shown in Figure 16 to demonstrate the general pressure profiles that are developed in the formations to support abandoned well flow. As can be seen in the figure, if the natural potentials are the same in both formations, the only driving force to move flow into the abandoned well from formation 1, up the wellbore and into formation 2 is provided by injection. The injection pressure buildup is a function of the rock and fluid properties of formation 1 and the distance between the injection well and the abandoned well. The pressure losses from drawdown and buildup caused by the abandoned well flow itself are a function of the rock and fluid properties in the respective formations. Any resistance in the well, which is not included in Figure 16, will incur another pressure loss which will diminish the flow.

Although Avci's[17] model is simple physically, its solution is difficult. First, the expressions for the pressure terms are substituted into Eq. 47 and it is transformed to Laplace space and solved. The actual values for the transient abandoned well flow are then obtained by numerical inversion to real space using the Stehfest algorithm. This solution demonstrates the difficulty involved in obtaining an analytical solution even for the simple case of abandoned well response to a single injector.

On the other hand a numerical solution can offer an abandoned well flow solution with the desired complexity. As discussed in Section 2.2, Warner and McConnell[12] used the SWIFT III[20] three dimensional numerical simulation for an injector and abandoned well in the lower formation. Although their work involved one injector only, SWIFT III is fully capable of addressing other injection/production well schemes in the lower formation. In these simulations, the abandoned well was treated as a section of vertical grid blocks. The permeability of the wellbore grid blocks were assigned to account for the resistance of the wellbore to flow. Because the well was incorporated as part of the grid, the numerical simulation could predict pressure changes within the abandoned well and the adjacent overlying formations which were modeled as permeable layers next to the well grid blocks. The pressure changes in the blocks were then used to determine the flow rates.

Although the well representation as grid blocks in the numerical simulation allows its resistance to be modeled, it adds complexity to the simulation because of the variable grid necessary to accommodate the well. If the resistances of the wellbore blocks are changed (i.e. the length of sloughed shales), the vertical grid must be modified. If a new abandoned well location is chosen, the horizontal grid must be modified. For Warner and McConnell's[12] work, the modeling of special wellbore conditions like a perforation or behind pipe flow required very small grid blocks on the order of 1 ft. The use of variable grids with such small block sizes to account for a well greatly increases computation time. Warner and McConnell stated that the simple one injector/ one abandoned well simulation for their case studies using SWIFT III[20] took around 4 hours of CPU time to run. Lacombe et al.'s[21] numerical simulation will suffer from the same inflexibility because the

well was treated as an overlay of one dimensional elements on a three dimensional finite element model.

3.2 'Series of Steady States' Coupled Abandoned Well Model

The objective of this work was to develop a realistic, flexible coupled abandoned well flow model which would be simple to apply as a predictive tool. For this goal to be met, the model would need to be capable of predicting flow for a potential gradient created from any injection/production scheme in either or both formations. The model would also need to address the actual wellbore conditions to account for the mitigating effect of these pressure losses on flow. Finally the model would need to be flexible enough to allow changes in the number and type of active wells in either formation and changes in abandoned wellbore conditions and location to be handled with ease. It was also desired that the model provide actual flow rates as results.

In considering an analytical approach, the work of Avci[17] demonstrated a solution for only one injector in the lower formation, did not realistically account for wellbore conditions and required a complex numerical solution. These limitations made it clear that the desired complexity in the new model would preclude a purely analytical solution. Warner and McConnell's[12] numerical simulation was also not an acceptable approach because it treated the well as a section of finite difference blocks. This required variable finite difference grids which were inflexible to explore the impact of abandoned wellbore conditions, locations and injection/production schemes on flow rate. These limitations

were also inherent to the numerical simulation of Lacombe et al.[21] who employed a finite element model for their work. Based on this analysis, it was apparent that another approach to the representation of an abandoned well would need to be considered.

In many numerical simulators, active wells are treated as sources in the finite difference equation for a particular well block. This allows the use of large constant grid block sizes for the simulation while retaining the capability to account for the effect of a well in a particular block. The well is often represented as a sink/source using the steady state analytical well model proposed by Peaceman[24]:

$$q = \frac{2\pi kh}{\mu} \frac{P_0 - P_{wf}}{\ln(r_o / r_w)} \tag{56}$$

where:

P_0 = the simulation well block pressure

r_0 = location of the steady state flowing well pressure equivalent to well block pressure

Peaceman found the equivalent radius to be equal to $0.2\Delta x$ for a square grid. In a simulation, the analytical well model is substituted for the source term in the finite difference equation for a block. This source representation of the well greatly reduces the number of equations which must be solved as compared to the case where the wellbore is incorporated as part of a variable grid. It also improves the flexibility of the simulation as the well location can be moved without resorting to changing the grid.

It is not possible to develop a true source representation model for an abandoned well and substitute it into the finite difference equations. This is due to the fact the abandoned well does not have an assigned rate or pressure as required in the source

representation but only develops a rate in response to active wells in the formations. In fact, the abandoned well rate varies with time as a consequence of the transient pressure distribution in the formations which the abandoned well couples. Like a source representation, however, the abandoned well can be defined using an analytical steady state model which instead of having an assigned rate or pressure will be driven by the evolving potential distributions generated by the active wells. This coupled steady state model can then be applied in a 'series of steady states' to provide a transient abandoned well response.

To use this approach, an analytical steady state abandoned well model must be available. As discussed in the Section 2.1, Silliman and Higgins[14] developed an analytical steady state equation for abandoned well flow in response to the difference in natural potentials between the two formations. The potentials were assumed to be constant to maintain steady flow. Their derivation led to following expression for flow:

$$Q_{AW} = \frac{2\pi(\Phi_1 - \Phi_2 - \Delta P_L)\alpha\beta}{(\alpha + \beta)} \tag{20}$$

where:

$$\begin{aligned} \alpha &= k_1 h_1 / \mu \ln(r_1 / r_{1AW}) \\ \beta &= k_1 h_1 / \mu \ln(r_2 / r_{2AW}) \end{aligned} \tag{17}$$

This equation states that the abandoned well flow is a function of the natural potentials, Φ_1 and Φ_2, which are constant at some steady state radii, r_1 and r_2. It is also a function of the terms α and β which represent the productivity indices of the formations. Finally, the equation includes a term, ΔP_L, which may be defined to account for potential losses in the wellbore. The inclusion of this term is an improvement over the general undefined

resistance term provided by Avci[17]. The potential distributions which are developed to support flow in this model are shown in Figure 17. These distributions are similar to those given in Figure 16 for Avci's model except they represent a constant well flow rate as opposed to Avci's transient rate produced in response to an injection well.

Silliman and Higgins'[14] model captures the essential dynamics of the problem and, because of its simplicity, is a good choice for a steady state analytical model of the abandoned well. In its current form, it is not capable of producing transient abandoned well flow coupled to the potential distributions created by active wells in the formations. One method to create transience from a steady state model is to use a 'series of steady states'. This approach relies on the assumption that a steady state equation may be applied over a series of time steps to produce an unsteady state response. The 'series of steady states' approach has been used by Muskat[25] for the determination of the productivity index in multiphase flow systems. It has also been routinely applied for water influx calculations in water drive reservoirs. Based on its success as a tool to produce transience from steady states in these applications, it was considered to be a possible approach to the problem of abandoned well flow.

The steady state model of Silliman and Higgins[14] relies on constant potentials described at the steady state radii, r_1 and r_2, in both the upper and lower formations to maintain a gradient which produces constant abandoned wellbore flow between them. For a system with active wells in either formation, one can recognize the potentials at these radii are not constant but are changing in time in response to active wells. The potentials

are therefore a function of time and the steady state model of Silliman and Higgins can be modified to account for the time dependence as follows:

$$Q_{1W}(t_i) = \frac{2\pi(\Phi_1(r_1,t_i) - \Phi_2(r_2,t_i) - \Delta P_L(t_i))\alpha\beta}{(\alpha+\beta)} \tag{57}$$

which is the first modification necessary to convert their equation to a form suitable for the 'series of steady states' approach. Instead of substituting expressions for the potentials as a function of time and solving for flow as done in the analytical solutions, the potentials can be approximated over a series of time steps and used directly in Eq. 57 to determine the transient flow rate.

In practice, the pressure and therefore potential at any time and location in a formation in response to production and injection may be determined by numerical simulation or superposition. Numerical simulation is limited to the calculation of average pressure for a well block and can not approximate location pressures unless one resorts to very fine grids. For the homogeneous, isotropic, infinite formations used in this model development, superposition of the Ei solution can be used to determine the pressure changes created in space and time by the injection/production wells so that the pressure may be found at any location. Consider the well system shown in Figure 18. The change in pressure at A created in response to an active well B located at a distance r_B away from A which has n rates is given by Matthews and Russell[26]:

$$\begin{aligned}\Delta P_{AB}(t) = &-\frac{Q_1\mu}{4\pi kh}Ei\left(\frac{-\phi\mu c r_B^2}{4kt}\right) - \frac{(Q_2-Q_1)\mu}{4\pi kh}Ei\left(\frac{-\phi\mu c r_B^2}{4k(t-t_1)}\right) \\ &- \frac{(Q_3-Q_2)\mu}{4\pi kh}Ei\left(\frac{-\phi\mu c r_B^2}{4k(t-t_2)}\right) - \cdots\cdots - \frac{(Q_n-Q_{n-1})\mu}{4\pi kh}Ei\left(\frac{-\phi\mu c r_B^2}{4k(t-t_{n-1})}\right)\end{aligned} \tag{58}$$

If there are other wells operating in the system, the pressure change they cause may also be calculated at A. For example, if wells C and D shown in Figure 18 are also operating, the pressure changes they produce at point A will be given in time as:

$$\Delta P_{AC}(t) = -\frac{Q_1\mu}{4\pi kh}Ei\left(\frac{-\phi\mu c r_C^2}{4kt}\right) - \frac{(Q_2-Q_1)\mu}{4\pi kh}Ei\left(\frac{-\phi\mu c r_C^2}{4k(t-t_1)}\right) - \frac{(Q_3-Q_2)\mu}{4\pi kh}Ei\left(\frac{-\phi\mu c r_C^2}{4k(t-t_2)}\right) - \ldots\ldots - \frac{(Q_n-Q_{n-1})\mu}{4\pi kh}Ei\left(\frac{-\phi\mu c r_C^2}{4k(t-t_{n-1})}\right) \quad (59)$$

$$\Delta P_{AD}(t) = -\frac{Q_1\mu}{4\pi kh}Ei\left(\frac{-\phi\mu c r_D^2}{4kt}\right) - \frac{(Q_2-Q_1)\mu}{4\pi kh}Ei\left(\frac{-\phi\mu c r_D^2}{4k(t-t_1)}\right) - \frac{(Q_3-Q_2)\mu}{4\pi kh}Ei\left(\frac{-\phi\mu c r_D^2}{4k(t-t_2)}\right) - \ldots\ldots - \frac{(Q_n-Q_{n-1})\mu}{4\pi kh}Ei\left(\frac{-\phi\mu c r_D^2}{4k(t-t_{n-1})}\right) \quad (60)$$

The pressure differentials generated by the individual wells may be added to give the total pressure change at A:

$$\Delta P_A(t) = \Delta P_{AB}(t) + \Delta P_{AC}(t) + \Delta P_{AD}(t) \quad (61)$$

and this value may then be subtracted from the initial formation pressure to give the new pressure at A for the desired time. Care must be taken to insure that the time total time, t, is the same for all wells but the calculation is otherwise unremarkable and may be used reliably to predict pressure changes at any point in a formation with any injection/ production operating schedule. To convert the pressure to potential only requires the effect of elevation be added such that:

$$\Phi_A(t) = P_A(t) + \rho g z_A \quad (62)$$

where z_A is the elevation defined relative to some datum.

The modified model of Silliman and Higgins[14] given in Eq. 57 requires that the potentials for both formations must be known at steady state radii surrounding the

abandoned wellbore at a given time. As explained above, the pressures on a chosen radius around the abandoned well can be calculated using the principle of superposition in space and time for all active wells in either formation. If one considers the simple case of one injector, it is apparent that in the lower formation, different pressures will be calculated on this radius and will not provide the constant potential boundary necessary for the modified model. This effect is also true when many active wells are present. So a question exists as to how one determines the constant potential at this radius.

The problem can be visualized as shown in Figure 19 for one formation. The abandoned well is assumed to be surrounded by a circle at some steady state radius where one must know the average potential. The circle is studded with eight points which represent the variable pressures that would be determined at these locations from superposition. This problem was evaluated by Muskat[27] who found that if an arbitrary pressure distribution exists over the radius, r_e, the total steady state flow into the well at r_w is the same as if the average of these pressures were applied over the boundary. This result means that if regional pressures vary on the outer radius one may average them and calculate the steady state flow as if it was in response to a constant pressure on the radius. Therefore, one can solve this problem of radial flow into the abandoned well by using superposition to calculate the pressure at points on this circle and then use the mean value theorem to predict the average pressure on the steady state radius:

$$\overline{P}(r_i) = \frac{\int_0^{2\pi} P(\theta)d\theta}{\int_0^{2\pi} d\theta} \tag{63}$$

which may be solved using numerical integration. The average pressure on the steady state radius will be a function of time and can be converted to potential for either formation using :

$$\Phi(r_i,t_i) = \overline{P}(r_i,t_i) + \rho g z_i \tag{64}$$

which will give the average potential in either formation as required in Eq. 57.

Another problem lies in the choice of radius, r_i, where the average pressure should be calculated. Silliman and Higgins[14] and Avci[16] recognized the difficulty in deciding where to place the steady state radii for a steady state model as discussed in Section 2.1. In their sensitivity analyses, however, they found very little variation in the flow value for a change in the choice of this radii. This result was considered to be a consequence of the fact that the radius appears in the logarithm term embedded in the productivity indices, α and β, in the steady state model. For the model developed in this work, the flow rates showed the same insensitivity to the choice of radius. This led to an empirical choice for radius based on a comparison of the model results to the published analytical results of Avci[17], which will be discussed in the Section 4.3. Intuitively, the radii should be located near the abandoned well to insure the pressure is determined in its region of influence.

To produce transient flow, the modified model must be applied using a 'series of steady states' approach. This requires the potentials at the steady state radii in each formation be determined over time steps and then used in Eq. 57 to determine the flow rate at a given time. As discussed these potentials are found by superposition in space and time of the active wells in each formation. After the first time step, however, the abandoned well may become active and the calculation of the potential on the constant

radius at the next time step must take into account the impact of this flow. Unlike active wells which supply their own potential for flow, the abandoned well transports fluids only in response to a potential gradient between the formations. If the abandoned well flows, the pressure consumed in the discharge of fluid from the lower formation into the wellbore and from the wellbore into the upper formation is lost from the system and must be subtracted from the new time step potential. Based on this analysis, Eq. 57 requires a second modification to include the effect of the abandoned well flow on the constant potential to give:

$$Q_{AW}(t_{i+1}) = \frac{2\pi((\Phi_1(r_1,t_{i+1}) - \Delta P_{AW}(r_1,t_i)) - \Delta P_L(t_{i+1}) - (\Phi_2(r_2,t_{i+1}) - \Delta P_{AW}(r_2,t_i))\alpha\beta}{(\alpha+\beta)} \tag{65}$$

where $\Delta P_{AW}(r_1,t_i)$ and $\Delta P_{AW}(r_2,t_i)$ represent the pressure consumed by the abandoned well in previous time steps on the constant radius to produce its flow. As time progresses, $\Delta P_{AW}(r_1,t_i)$ and $\Delta P_{AW}(r_2,t_i)$ must be calculated using the superposition of the abandoned well flow in time. The final 'series of steady states' coupled model shown in Eq. 65 can be applied over time to give the transient flow which accounts for all pressure changes in the system.

The process of using the 'series of steady states' coupled model to predict transient flow through an abandoned well between two formations can be summarized as follows. Using superposition and the mean value theorem, an average potential is calculated at the chosen steady state radii in each formation for the first time step and these potentials are used in Eq. 65 to calculate the abandoned well flow. For the next time step, new potentials at the radii are once again determined using superposition of the active wells in the system.

But the abandoned well in the next time step is now active and has a rate defined from the first time step. Therefore the pressure change from this rate must be subtracted from the superposition potential on the same radii to produce the new potential for flow in the new time step. Then the flow is calculated again using Eq. 65. This process is repeated for the desired total time period and the result is the transient flow rate through the abandoned well which is developed in response to the evolving pressure distributions in both formations.

3.3 Wellbore Losses in Coupled Abandoned Well Model

Aside from creating a physically realistic and simple model which provides transient flow in response to active wells in either or both of the formations, another objective of this work was to develop a model which was capable of directly and realistically addressing wellbore pressure losses and their impact on abandoned well flow. The 'series of steady states' coupled well model given in Eq. 65 contains a term $\Delta P_L(t_{i+1})$ to account for pressure losses in the wellbore. It is apparent from this equation and from a physical standpoint that any resistance in the wellbore will act to reduce flow by reducing the potential gradient.

The impact of resistance in the wellbore was discussed by Avci[17] who employed an undefined general resistance term in Eq. 47 to capture its presence. As shown by Avci in Figure 6, changes in the magnitude of this resistance term had a tremendous impact on dimensionless flow through the wellbore. The effect of wellbore resistance was also

investigated in the numerical simulations of Warner and McConnell[12] who used low permeability well blocks to represent sloughed shales and drilling mud layers in the wellbore and thus effectively eliminated flow. Unlike the methods used to include wellbore losses in the analytical models or numerical simulations, the existence of a separate term for wellbore losses in the coupled model provides the first direct method to assess their effect on well flow.

Since the wellbore losses are represented as a pressure term in the new model, it is possible to define this term using standard equations for pressure losses due to wellbore conditions. There are several sources of pressure losses that can exist in the wellbore. The first are those produced by pipe friction. These losses are dependent on whether flow is turbulent or laminar. For both cases, the head loss due to pipe friction, H_{Pf}, is given by:

$$H_{Pf} = f\frac{L}{D}\frac{V_{AW}^2}{2g} \tag{66}$$

where f represents the friction factor, L is the length of the pipe, D is the diameter of the pipe and V_{AW} is the velocity in the wellbore. For laminar flow, the friction factor is defined by:

$$f = \frac{64}{N_{Re}} \tag{67}$$

For turbulent flow, N_{Re}>2000, the friction factor is a function of the Reynolds number, N_{Re}, and relative pipe roughness, $\frac{\varepsilon}{D}$:

$$f = f(N_{Re}, \frac{\varepsilon}{D}) \tag{68}$$

and its value may be found by using the Moody diagram or the implicit Colebrook-White[28] formula on which it is based:

$$\frac{1}{\sqrt{f}} = -0.869 \ln\left[\frac{\varepsilon / D}{3.7} + \frac{2.523}{N_{Re}\sqrt{f}}\right] \tag{69}$$

An explicit equation for the turbulent friction factor is also given by[29]:

$$f = 0.001375\left[1 + \left(20{,}000\frac{\varepsilon}{D} + \frac{10^6}{N_{Re}}\right)^{\frac{1}{3}}\right] \tag{70}$$

which is within 5% of the Colebrook-White formula for Reynolds numbers between 4000 and 10,000,000 and $\frac{\varepsilon}{D}$ values up to 0.01.

If the head loss from pipe friction is substituted into the coupled model, the expression becomes:

$$Q_{AW}(t_{i+1}) = \frac{2\pi\alpha\beta}{\alpha+\beta}\left(\Phi(r_1, t_{i+1}) - \Delta P_{AW}(r_1, t_i) - \Phi(r_2, t_{i+1}) - \Delta P_{AW}(r_2, t_i) - \rho g f \frac{L}{D}\frac{(V_{AW})^2}{2g}\right) \tag{71}$$

where the velocity in Eq. 71 is the flow rate in the abandoned wellbore divided by the cross sectional area of the wellbore:

$$V_{AW} = \frac{Q_{AW}(t_{i+1})}{A_c} \tag{72}$$

If one substitutes this expression for velocity into Eq. 71, it gives an expression which is implicit in terms of the flow rate:

$$Q_{AW}(t_{i+1}) = \frac{2\pi\alpha\beta}{\alpha+\beta}[(\Phi(r_1,t_{i+1}) - \Delta P_{AW}(r_1,t_i)) - (\Phi(r_2,t_{i+1}) - \Delta P_{AW}(r_2,t_i)) - \rho g f \frac{L}{D}\frac{(Q_{AW}(t_{i+1})/A_c)^2}{2g}] \quad (73)$$

To find the flow rate, one can rewrite Eq. 73 as:

$$AQ_{AW}^2(t) + BQ_{AW}(t) + C = 0 \quad (74)$$

where:

$$A = \rho g f \frac{L}{D}\frac{(1/A_c)^2}{2g} \quad (75)$$

$$B = -\frac{\alpha+\beta}{2\pi\alpha\beta} \quad (76)$$

$$C = -\left[(\Phi(r_1,t_{i+1}) - \Delta P_{AW}(r_1,t_i)) - (\Phi(r_2,t_{i+1}) - \Delta P_{AW}(r_2,t_i))\right] \quad (77)$$

Once the values for the coefficients are determined, Eq. 74 may be solved for the flow rate using the quadratic equation.

Because the friction factor itself is dependent on the flow rate it is necessary to have an initial flow to solve for its value. In the application of the coupled model, an initial estimate of the flow may be calculated simply by setting ΔP_L to zero initially for each abandoned well flow calculation. This flow can be used to determine the velocity in the wellbore and the Reynolds number. Then the friction factor can be calculated and substituted into Eq. 75. The flow is then recalculated to include the friction losses in the pipe.

Another source of wellbore resistance which is important in the analysis of abandoned well flow is that of drilling muds, sloughed shales, and cement plugs. In their

numerical simulations, Warner and McConnell[12] demonstrated that these materials may be modeled as porous media in the wellbore to account for their impact on well flow. If one looks at the example of a cement plug in an abandoned well, the pressure loss is given by Darcy's law for linear flow as:

$$\Delta P_{PM} = \frac{Q_{AW}\mu}{k_{PM}A_c} L_{PM} \tag{78}$$

where ΔP_{PM} represents the pressure loss through the plug, L_{PM} is the length of the plug, k_{PM} is the permeability of the plug, and A_c is the cross sectional area of the plug. This expression may be substituted for the loss term to give:

$$Q_{AW}(t_{i+1}) = \frac{2\pi\alpha\beta}{\alpha+\beta}\left((\Phi(r_1,t_{i+1}) - \Delta P_{AW}(r_1,t_i)) - (\Phi(r_2,t_{i+1}) - \Delta P_{AW}(r_2,t_i)) - \frac{Q_{AW}(t_{i+1})\mu L_{PM}}{k_{PM}A_c}\right) \tag{79}$$

The resulting equation may be made explicit in Q_{AW} and solved directly. Therefore the coupled model can incorporate the impact of obstructions in the wellbore such as natural sloughed shales or drilling muds and artificial well cement plugs when they are represented as porous media losses in the wellbore. The model is very flexible with respect to these losses and can incorporate any number of different plugs or materials in the wellbore within a pressure loss term composed of the sum of separate porous media losses for cement plugs, shales, etc.

Another wellbore loss of importance is that created by a perforation. For an abandoned wellbore that is cased, a casing leak may develop next to the upper formation allowing fluid from the wellbore to be transported into the formation. Once again the

pressure loss term in the coupled model equation may be used to account for the frictional losses through the perforation. Physically, the casing leak may be represented as a single perforation and the following equation used to calculate its frictional losses[30]:

$$\Delta P_{perf} = \frac{0.2369 Q_{AW}^2 \rho}{N_p^2 D^4 C_D^2} \tag{80}$$

where :

Q_{AW} = abandoned well flow rate (bbl/min)

ρ = density (lb_m/gal)

C_d = discharge coefficient

N_P = number of perforations

D = diameter of perforation (in)

As in the previous cases, this equation may be substituted for ΔP_L in the coupled model and will lead to an equation which is implicit with respect to the flow. The resulting expression may once again be arranged into a quadratic equation as shown in Eq. 74 but coefficient A will be redefined to account for Eq. 80. The resulting quadratic equation may then be solved for its roots to give the flow.

The interesting complication arising from the perforation wellbore condition is that it contradicts the original assumption that the upper formation is completely open to the abandoned well. The boundary condition of a completely penetrating well forms the basis for the assumption of radial flow which was employed by Silliman and Higgins[14] in their original steady state model and is therefore imbedded in the coupled model. When one considers flow through a perforation, however, the radial flow assumption in the upper

formation is no longer valid. Therefore it is necessary to reassess the type of flow that is occurring.

Physically, the perforation acts like a point source in the formation. As such it can be visualized as a spherical source in the formation which produces spherical flow. To support this theory, a laboratory experiment was performed using a sand pack model to represent flow through a perforation to a formation. A schematic of the sand pack is shown in Figure 20. The sand pack was one foot square with a thickness of one inch and was filled with 40 mesh frac sand. One side of the sand pack had a 1/4 inch diameter hole drilled into it to represent a single perforation which acted as the entry point for fluid. The other side had 5 holes drilled into it to approximate an open side to discharge fluid. This discharge side was open to the atmosphere. The flow in the sand pack was created by a potential difference across the pack which was provided by a reservoir maintained at constant head by an overflow line. The head measured 9.5 inches which provided a differential of 0.343 psi. The discharge from the pack was collected in graduated cylinders. Initially, the sand pack was saturated with clear water and kept under hydrostatic conditions so that no flow existed. Then at time equal zero, the flow line was opened and a blue dye solution was allowed to enter the pack through the single opening under a constant head. The dye front was observed to see if it would produce a spherical flow pattern.

The propagation of the dye pattern is shown in Figure 21 at varying times. These profiles exhibit the evolution of spherical flow at the opening which expanded in time. Because of the large size of the opening relative to the sand pack width and the gradient,

the dye profiles begin to form a bullet shape and reached the center of the open end before intercepting the upper and lower boundaries of the sand pack. After breakthrough at the open end, the dye profile continued to expand until it covered the entire width of the pack. Based on these observations, it was apparent that spherical flow was created in response to flow through a single perforation into the pack. The presence of spherical flow is even more likely in the field where perforation diameters are around 0.25 inches which is 2-3 orders of magnitude smaller than typical formation thicknesses.

The existence of spherical flow is an important distinction for the model because it entails a much greater pressure loss in the formation which will act to reduce the abandoned well flow rate. The equation for steady state flow rate in a spherical system is given by Muskat[27] as:

$$Q = \frac{4\pi k(\Phi_e - \Phi_w)}{\mu\left(\frac{1}{r_w} - \frac{1}{r_e}\right)} \tag{81}$$

where the flow is a function of the potential at the outer radius and the wellbore but not of the thickness of the formation as in the case of radial flow. The coupled well model was based on Silliman and Higgins[14] original steady state model which assumed radial flow in the formations. If one returns to their derivation shown in the Section 2.1 and substitutes the spherical flow equation for the upper formation, the model obtained will have the same form as Eq. 20:

$$Q_{AW} = \frac{2\pi(\Phi_1(r_1) - \Phi_2(r_2) - \Delta P_L)\alpha\beta_{sph}}{(\alpha + \beta_{sph})} \tag{82}$$

in which α is defined based on radial flow into the lower formation:

$$\alpha = k_1 h_1 / \mu \ln(r_1 / r_{1,AW}) \tag{17}$$

but the β must be redefined for spherical flow into the upper formation:

$$\beta_{sph} = \frac{k_2}{\mu(1/r_{2,AW} - 1/r_2)} \tag{83}$$

Therefore for the case of flow through a perforation in the casing adjacent to the upper formation, the coupled model must be modified to account for spherical flow. This modification only requires the new definition for β.

The next problem lies in how to account for the pressure change on the constant radius for the spherical flow in the upper formation in the coupled model. As shown in the dye profiles of Figure 21, the spherical flow spreads across the entire formation by the time it reaches the outflow boundary. Therefore it is possible to assume that the radial superposition of the abandoned well flow rate could still be applied for both formations. This assumption will introduce some error but it will act conservatively on the flow calculation as the pressure loss would be greater if the spherical flow loss could be superimposed.

The last case which requires consideration in the prediction of abandoned well flow between formations is that of annular flow. For this case, the coupled model given in Eq. 65 is applicable because flow to the annulus in the lower formation and flow away from the annulus in the upper formation will be radial. The wellbore pressure loss term in the coupled model, however, must be changed to account for annular flow.

In the case of pipe wall friction in the annulus, the loss may be determined as in the case for the wellbore pipe friction but an equivalent hydraulic radius for the annulus must be used in the calculation. The hydraulic radius equation is:

$$R_h = \frac{A_c}{P_{wet}} \tag{84}$$

where A_c is the cross sectional area and P_{wet} is the wetted perimeter. For an annulus, the cross sectional area is:

$$A_c = \pi(r_o^2 - r_i^2) \tag{85}$$

where r_o is the outer radius and r_i is the inner radius. The wetted perimeter is:

$$P_{wet} = 2\pi(r_o + r_i) \tag{86}$$

Substitution of these definitions into Eq. 84 gives an annular hydraulic radius of:

$$R_h = (r_o - r_i) \tag{87}$$

The velocity in the wellbore is a function of the cross sectional area of the annulus and the Reynolds number must be calculated using a hydraulic diameter:

$$N_{Re} = \frac{\rho V_{AV} D_h}{\mu} \tag{88}$$

where:

$$D_h = 4R_h \tag{89}$$

The friction factors are then estimated using the same Eqs. 67-70 for either laminar or turbulent flow.

For the case of porous media losses in the annulus due to cement behind pipe or sloughed shales, the wellbore loss term will be treated as previously discussed for the

wellbore case. But the cross sectional area will now be determined for the annulus. It is possible for the cement in the annulus to have a fracture which allows flow. The pressure loss from fracture flow is given by[32]:

$$\Delta P_{PMF} = \frac{1.149*10^{-10} Q_{AW} \mu L}{W_F^{\,2} A_F} \tag{90}$$

where W represents the width of the fracture in feet and A_c is the cross-sectional area of the fracture in ft^2. This equation can be used to predict annular flow through a fracture by direct substitution for the porous media loss term ΔP_{PM}. Finally there is no need to consider a perforation case because flow is behind pipe and against the formation.

In conclusion, the wellbore losses may be defined in the model for pipe friction, plugs, or a single perforation. Annular losses may be defined for annular friction, plugs and a fracture behind pipe. The equation for an individual loss may be substituted into the model Eq. 65 and solved for the flow rate. Individual losses may also be combined in the pressure loss term as:

$$\Delta P_L = \Delta P_{Pf} + \Delta P_{PM} + \Delta P_{perf} \tag{91}$$

and substituted into the model. In both cases, the resulting equation will be implicit or explicit depending on which terms are included and may be solved directly or by root finding to ascertain the flow rate. As such the wellbore system can be viewed as an analog of an electrical circuit. For such an analog the potentials are set a both ends of the circuit and the current is determined simply by considering the resistances in between. Similarly the resistance within the abandoned wellbore determines the amount of flow that can develop.

3.4 Summary

The 'series of steady states' coupled model for abandoned well flow meets all of the research objectives. First, it is conceptually easy to understand and captures the dynamics of abandoned well flow. Second, it will predict flow which is driven by the pressure distributions produced in the formations for any number of production/injection wells. The ability to respond to these distributions means the well flow can show changes in flow rate as rates change in the active wells including cases where the flow moves downhole. This model also allows the position of the abandoned wellbore to be changed easily to evaluate the effect of its position relative to other wells on the flow rate. Finally, the model can evaluate the effects on flow of different wellbore conditions including annular flow, pipe friction, plugging materials, fractures behind pipe and a single perforation to represent a casing leak in the upper formation. The coupled model is dependent on the choice of the time step size and will require many iterations with time to provide the transient flow. However, the calculations may be efficiently handled by a computer algorithm as will be shown in Chapter 4.

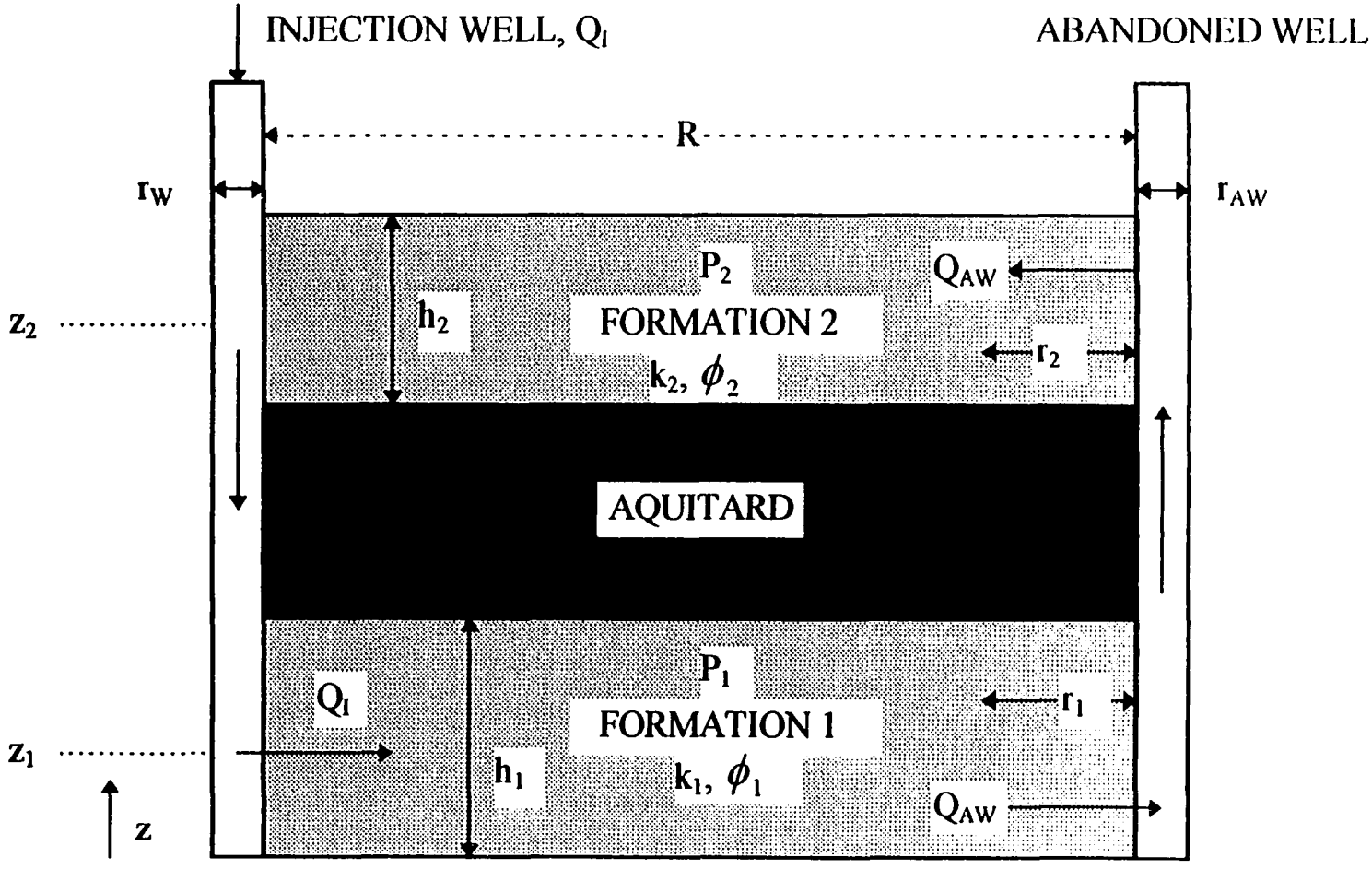


Figure 15. Physical system for development of abandoned well model.

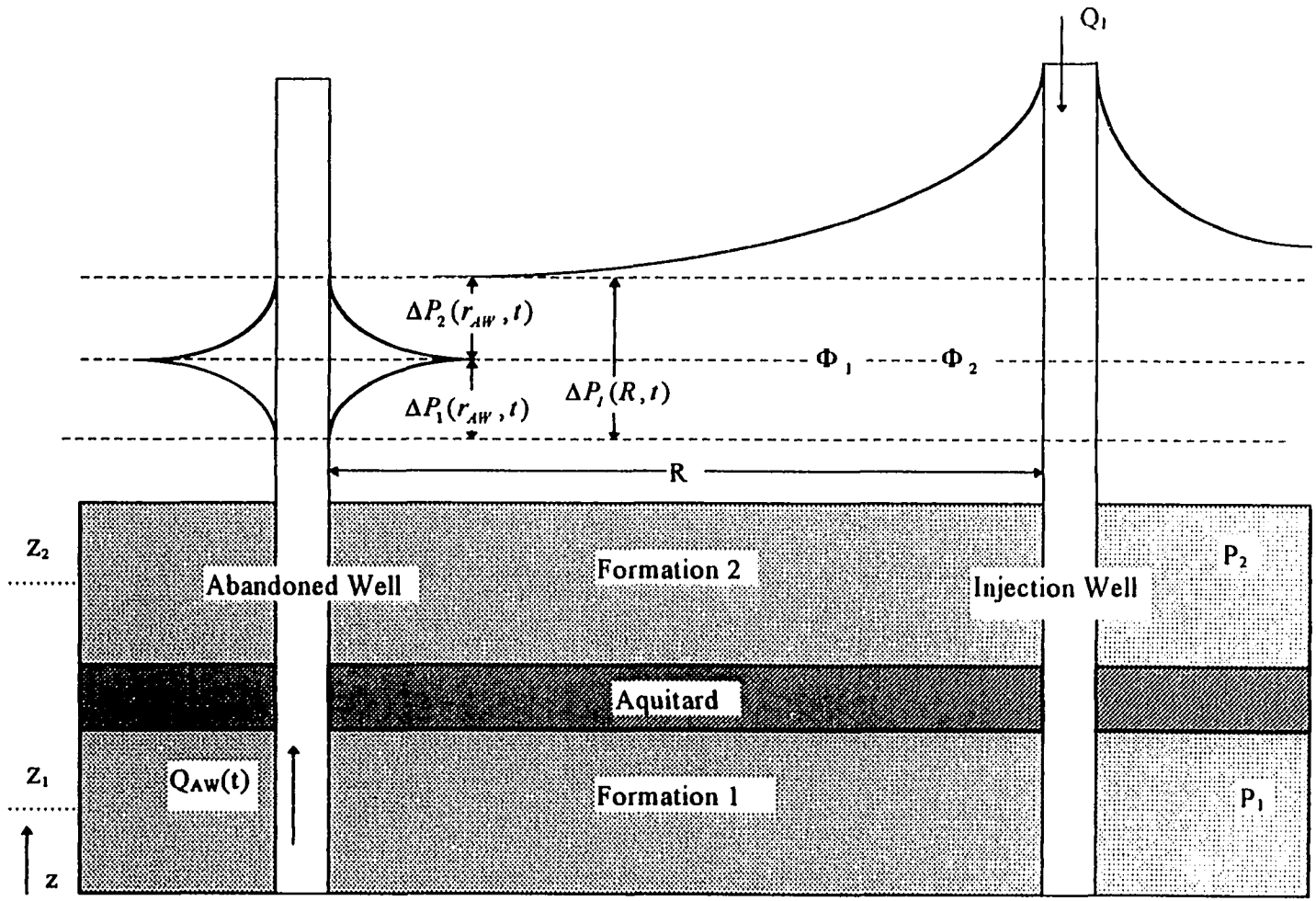


Figure 16. Pressure profiles developed for model of Avci[17].

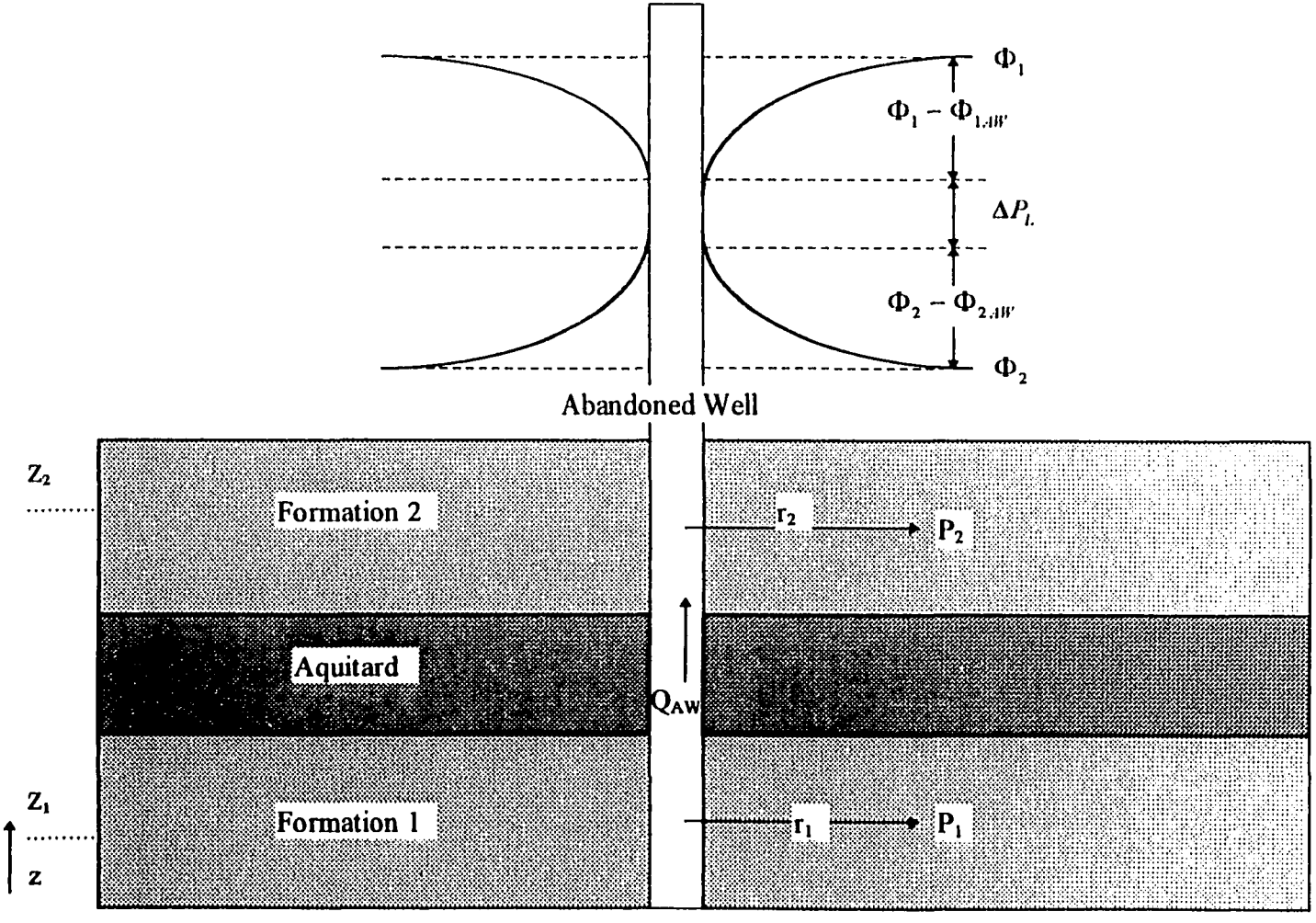


Figure 17. Potential distributions developed for model of Silliman and Higgins[14].

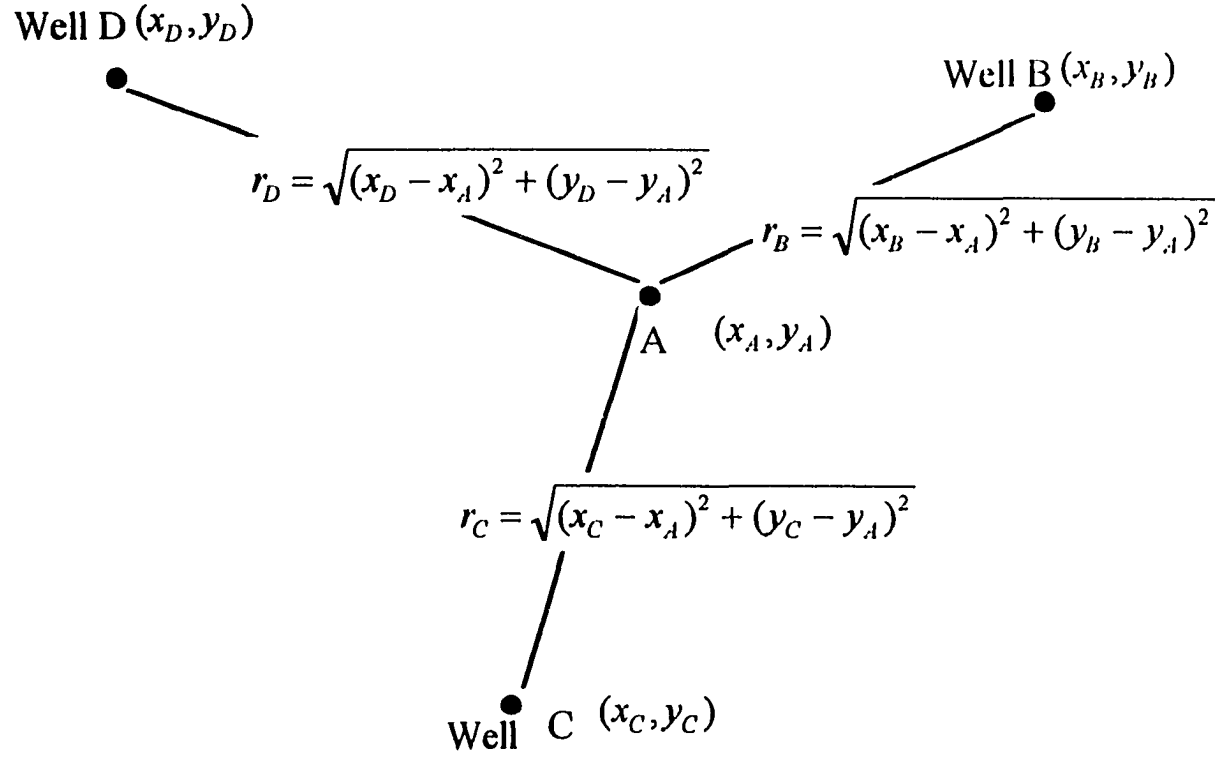


Figure 18. Cartesian well locations and radii for use in superposition to find pressure change at point A.

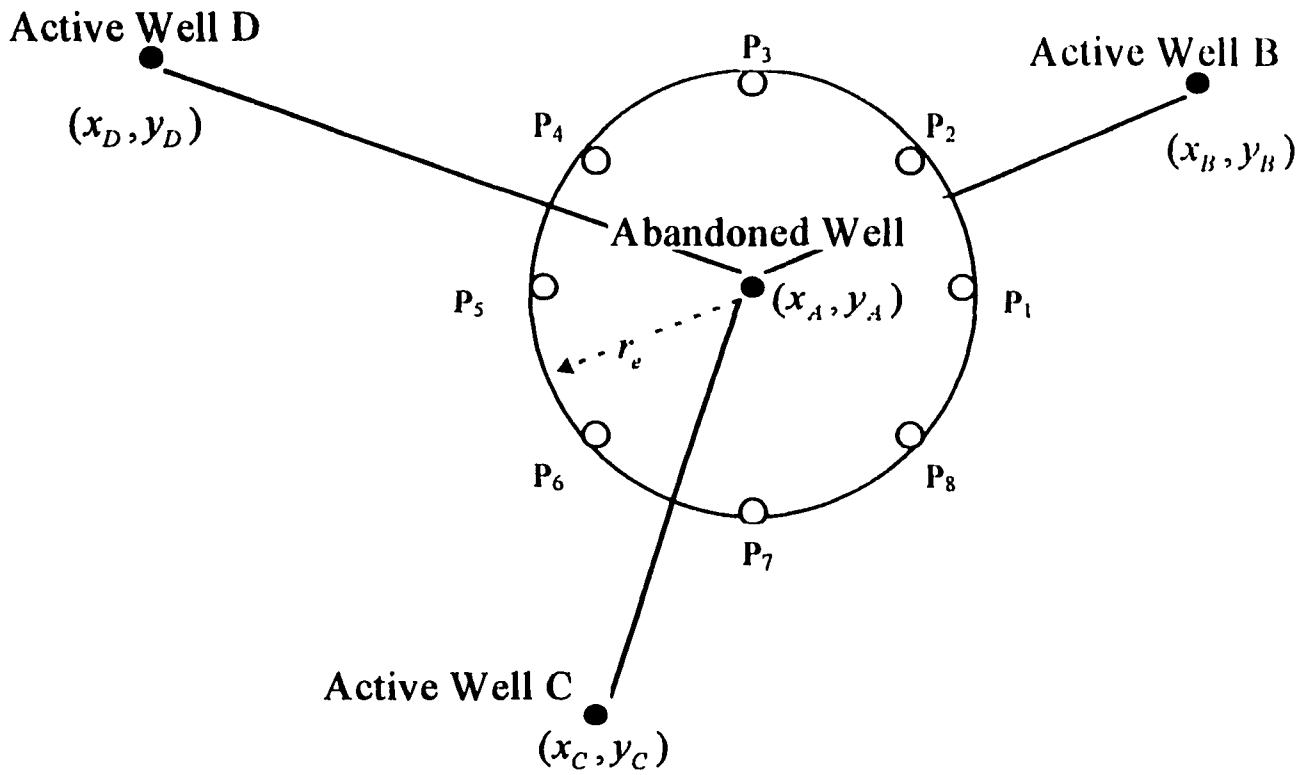


Figure 19. Location of constant potential radius marked with eight points relative to abandoned well and active well locations.

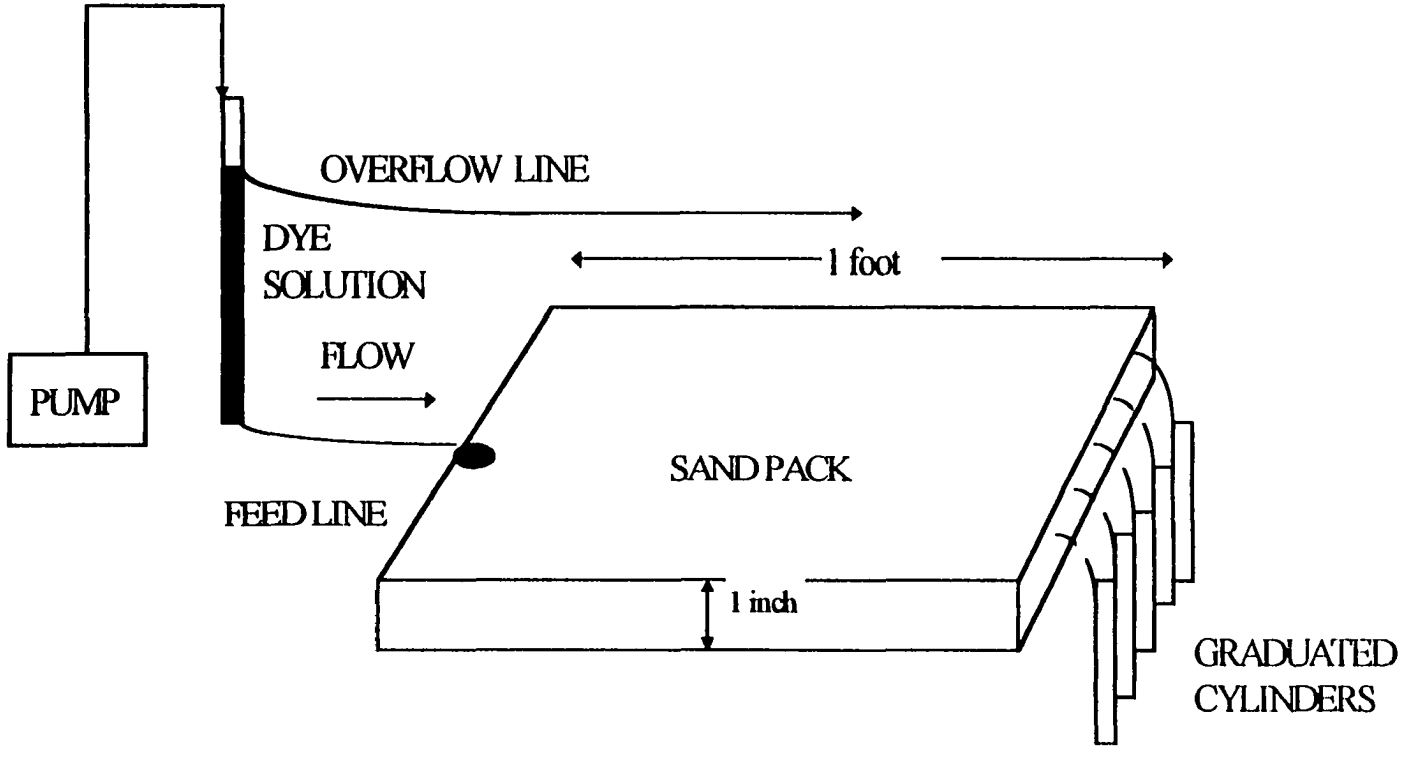


Figure 20. Schematic of sand pack experiment used to evaluate spherical flow through a perforation.

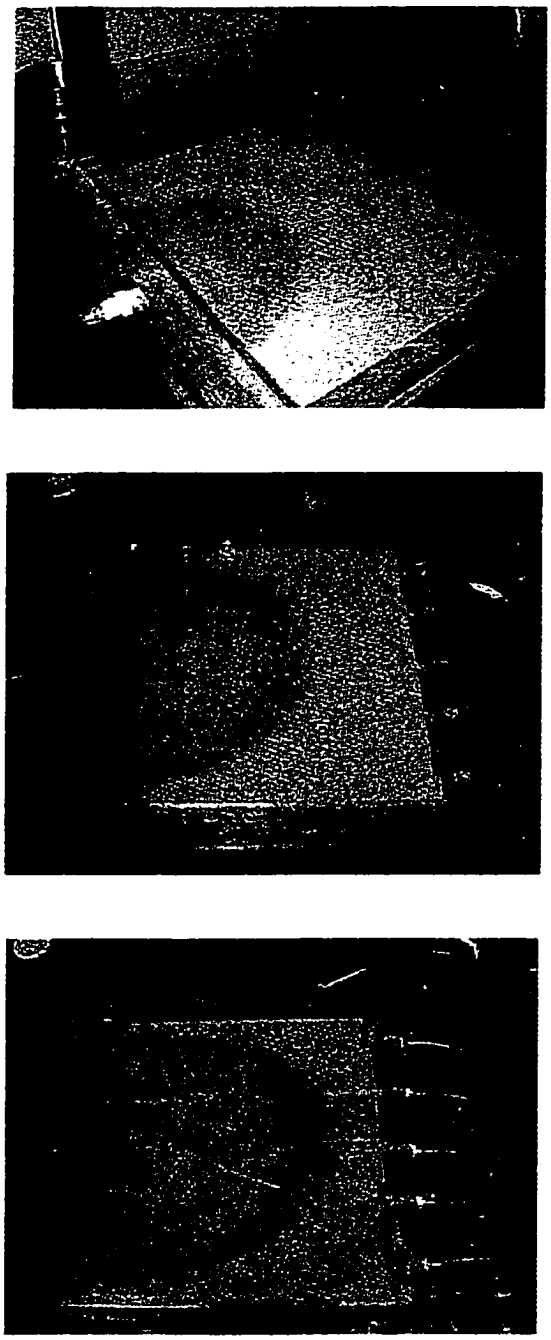


Figure 21. Dye profiles from sand pack experiment.

CHAPTER 4

COMPUTER PROGRAM FOR COUPLED ABANDONED WELL MODEL

As discussed in the previous chapter on development of the coupled abandoned well model, a 'series of steady states' approach is used in this work to create transient flow through an abandoned well between two formations. This approach is based on the modification of the steady state analytical abandoned well model originally proposed by Silliman and Higgins[14]. The coupled model not only expresses the flow as a function of the potential changes in both formations with time in response to active wells but also as a function of wellbore potential losses produced by pipe friction, plugs or a single perforation. It is a simple yet realistic and flexible model which when applied continuously over a series of time steps will produce transient flow through the abandoned well. The coupled model is particularly amenable to application using a computer algorithm to perform the steps required to calculate flow at each time.

4.1 General Program Description and Input Requirements

The coupled model was incorporated into a computer program to predict flow through an abandoned well. Based on the assumptions inherent to the model, the program was specifically designed for a physical system in which an abandoned well acts as a conduit for flow between two permeable formations separated by an impermeable

formation. An example is shown in Figure 15 with an active injection well in the lower formation. The formations are assumed to be homogeneous and infinite in extent.

The user supplies the rock properties and physical dimensions for each formation separately. The depth to the midpoint of each of the formations as well as their initial pressures must also be given. The potential for each formation is calculated using an elevation datum set to zero at the middle of the lower formation. The program is for single phase flow, so the user supplied fluid characteristics are the same for both formations.

Well locations in either formation are identified using a Cartesian coordinate system. The wells can be placed at (x,y) locations of the user's choice. Only one abandoned well location may be defined but both formations may have up to 10 separate active wells. The active wells may operate at up to 10 different rates at 10 different times. The number of wells and rates may be changed by redefining array sizes in the source code. The total time for all well operations must be the same for a computer run.

The time step for the calculations is supplied by the user in terms of days. The program accepts a maximum of 10,000 time steps for current source code array definitions. This allows computations which range from 27 years for a 1 day time step or 2.7 years for a 0.1 day time step. The time step is at the choice of the user. The value of steady state radii location around the abandoned well is also supplied by the user. The choice of time step and steady state radii influences the results at early time and will be discussed in the sensitivity analysis in Section 4.3.

The program also requires the description of the abandoned wellbore condition. Because the wellbore condition determines the nature of the pressure loss term which

influences the model solution, the program evaluates the input data and flags the program so that the appropriate calculations will be made. First, the user must indicate whether the program will be run to predict pipe flow or annular flow. The wellbore size is defined by hole diameter, casing inner diameter, and casing outer diameter at the location of each formation. The wellbore condition is flagged by the input values for the pipe roughness and the length and permeability of cement plugs, sloughed shales and drilling muds which are treated as porous media in the wellbore. It is also possible to run the program for a cased well with one perforation in the upper casing. The perforation size is declared by the user. The input of perforation data is also flagged. The program interprets the flags and the program runs the appropriate code to account for the wellbore conditions in the model solution. The wellbore may have no losses or may have all conditions at one time including pipe friction, plugs and one perforation.

The program is written in FORTRAN and was run on a Pentium 90 desk top PC using Microsoft FORTRAN Power Station 1.0. The program writes the results to an Microsoft Excel file which displays the cumulative time, flow rate, cumulative flow and average potentials at each of the steady state radii in the formations. Another diagnostic output file is printed to allow the user to view the original input data and a summary of the results of the calculations being performed at each time step. For the cases evaluated in this research, the program CPU run time was around 5 seconds for 1000 time steps.

4.2 Computer Program Algorithm

A task flow chart for the program is shown in Figure 22. This chart highlights the specific tasks carried out in the algorithm for discussion. Flow charts showing the major operations for the main program and main subroutines are given in Appendix A. As the program handles field data, some of the equations used in the development of the model required conversion to oil field units for the program and are described in Appendix B. A template input data file showing variable names and a sample input data file used to verify the model are given in Appendix C.

The first step in the task chart is the calculation of the average potential in the lower formation $\Phi_1(r_1, t_{i+1})$. The program uses superposition of the Ei solution to predict the pressure on eight points on a steady state radii circle around the abandoned well in each formation. For each formation, the location of the steady state radii is supplied by the user. The value is passed to a subroutine called POINTS which returns the location of eight equally spaced points on this radius as shown in Figure 19. The radial distances between these points and each of the active wells in the formation are then calculated. The individual pressures at the eight points on the steady state radii in formation 1 are determined using superposition in time and space. The calculations are performed in a subroutine called TRANSF which is called at each time step and calculates and sums the pressure changes created at each point by the active wells. TRANSF is able to test at every time step to evaluate if a rate change has occurred at any of the active wells and uses superposition in time to account for the effect of the rate change on the pressure. The

program uses a function EXPINT which returns the value of the exponential integral using a series expansion or the natural log approximation as shown in Eq. B.5 and B.6. Once the pressures are calculated at the eight points on the steady state radii, they are averaged using the mean value theorem shown in Eq. 63 which is solved with Simpson's multiple one-third rule in a subroutine called AVEP. The pressure is converted to potential using a datum defined with z equal to zero at the midpoint of the lower formation. This process is repeated in step 2 to give the average potential for the upper formation, $\Phi_2(r_2, t_{i+1})$.

Once the average potentials are determined in both formations, their values are passed down to the subroutine SILL which calculates the flow rate through the well. Step 3 in the task chart is performed in SILL and involves the definition of the wellbore loss term $\Delta P_L(t_{i+1})$ for use in the calculation of flow. The wellbore losses are derived from pipe friction, plug losses, one perforation or any combination of these. The program reads these values from the input file and flags determine which wellbore losses are present for consideration.

In Step 4, the program is designed to recognize whether substitution of the specific wellbore losses in the coupled model will lead to an equation which is explicit or implicit with respect to flow rate. It calculates the coefficients for the final flow rate equation as shown in Eq. 74. If the equation is explicit, the flow rate may be solved for directly. If it is implicit, it is solved for the flow rate using the subroutine ROOT which calculates the roots of the quadratic equation. A positive or negative flow rate is possible, where negative flow indicates flow down the wellbore.

Once the flow rate has been determined, the program in Step 5 passes its value to the subroutine BUILDUP. BUILDUP calculates the pressure change, $\Delta P_{AW}(r_1, t_i)$, on the steady state radius for the lower formation as a consequence of the abandoned well flow rate using superposition in time. This process is repeated for the upper formation in Step 6 to give $\Delta P_{AW}(r_2, t_i)$. The values for the pressure changes due to flow through the abandoned well are used to calculate flow in the next time step. Steps 1-6 are then repeated at each time step for the total time specified by the user.

4.3 Coupled Model Verification and Sensitivity Analysis

The computer program was verified by comparison of its results to the analytical solution results reported by Avci[17] for fully transient flow through an abandoned well between two formations which is driven by an injection well in the lower formation. Avci's published results were based on the system shown in Figure 1 with the following physical restrictions:

$$r_{AWD} = \frac{r_{AW}}{R} = .001 \tag{92}$$

$$h_1 = h_2 \tag{93}$$

$$\phi_1 = \phi_2 \tag{94}$$

and were reported using the following definitions for dimensionless time and flow:

$$Q_{AWD} = \frac{Q_{AW}}{Q_I} \tag{10}$$

$$t_D = \frac{k_1 t}{\phi \mu c R^2} \tag{11}$$

Avci's results were calculated for three separate permeability ratios, $\xi = k_2 / k_1$, where ξ was set to 0.1, 1.0, and 10.0 respectively. The program results can only be compared to the analytical results for the case of an open wellbore, Ω_D equal to zero, because Avci did not use any physical basis to define the resistance factor used in the analytical model as explained in the Section 2.1.

The input for the program was developed in field units and was designed to meet the physical restrictions placed on Avci's[17] reported results shown in Eqs. 90-92. The verification test data were also chosen to meet realistic formation and fluid conditions for the physical model in Figure 1. The permeabilities were 50 md, the thicknesses were 50 ft and porosities were 0.15. The fluid properties were for water and included a compressibility of 3×10^{-6} /psi, density of 67 lb/ft^3 and viscosity of 1 cp. The distance between the injection and abandoned well was 500 ft and the abandoned well had a borehole radius of 0.5 ft to meet the restriction given in Eq. 90. The steady state radii were chosen to be equal at 275 ft for reasons discussed in Section 4.3. The injection rate was 100 bbls/day. The initial pressure for the upper formation and the lower formation were given as 418.5 psi and 450 psi respectively. The lower formation had a depth of 1000 ft and the upper formation of 900 ft. Using a elevation datum of z equal to zero at the lower formation, the pressures gave a hydrostatic condition where the initial potentials for both formations were 465 psi. The time step was chosen as 1 day, which is a realistic time for a field study. The wellbore was treated as if it were totally open to flow so that no

wellbore losses were included. The input file for this Avci base case is shown in Figure C.2.

A comparison of Avci's[17] analytical and the program results is shown in Table 3 for the required permeability ratios of 0.1, 1.0, and 10.0. As the results of Avci were reported for dimensionless times and the program was run in one day real time steps, the program output shown in Table 3 was matched to Avci by calculating dimensionless times for the one day time steps and interpolating the program results. The true program output values and Avci's results for the case of ξ equal to 1.0 are plotted in Figure 23. As shown in the table and figure, the coupled model is almost an exact match to the analytical transient results of Avci for dimensionless times greater than 20, which is equal to around 7 days in real time for the field data. To ensure that the program produces the same dimensionless results for other field data, the program was run for other permeabilities and thicknesses as well as other fluid characteristics. The program outputs from these runs showed that as long as the conditions of equal formation permeability and thickness given in Eqs. 91-92 were met and the ratio of injector distance to abandoned well radius in Eq. 90 remained at 0.001, the results in Table 3 were duplicated.

For the results given in Table 3, the steady state radius in the formations, r_1 and r_2, was chosen at 275 ft which is 55% of the distance between the injector and producer. The choice of this radius is given as input from the user. As discussed in the development of the model there is uncertainty involved in the choice of steady state radius where the potentials $\Phi_1(r_1,t_i)$ and $\Phi_2(r_2,t_i)$ are calculated. Avci[16] and Silliman and Higgins[14]

recognized this dilemma and showed that for an analytical steady state model, the choice of radius did not greatly influence the steady state flow.

To evaluate the sensitivity of the coupled model to the location of the steady state radii in the formations, the program was run with test data for cases where the radii were set at 0.10 R, 0.20 R, 0.30 R, 0.40 R, 0.50 R, and 0.60 R. Figure 24 shows the dimensionless flow values derived from the program results for these cases along with the Avci[17] results. As can be seen in the figure, the dimensionless rates vary only at early time with these different radii and match the Avci results for later time. The coupled model also appears to be self correcting and at dimensionless times greater than 20 (7.1 days for test data) produces the same results for all radii choices. The program was also run for radii set at 0.70 R, 0.80 R, 0.90 R, 1.00 R, 1.10 R, and 1.20 R and the dimensionless flow rates for these program runs and Avci[17] are shown in Figure 25. The figure shows that for values at 100% R or greater, the program results begin to deviate from Avci's[17] results indicating that these steady state radii location are not acceptable. For this reason the program is designed to determine the distance between the abandoned well and the nearest active well and then set this value to R. The steady state radius is then chosen by the user as a percentage value of R less than 100%. For Avci's results the tabular data indicate that the best match appears to be for radii at 10-60% R and the exact choice of radius does not appear to be critical except at early time.

The values for the steady state radii are actually incorporated into the model as part of the productivity indices α and β:

$$\alpha = k_1 h_1 / \mu_1 \ln(r_1 / r_{1AW})$$

$$\beta = k_2 h_2 / \mu_2 \ln(r_2 / r_{2AW}) \quad (17)$$

where they appear in the natural log terms. For the field case, the preferred range for r_1 and r_2 at 10-60% of the distance between the injector and the abandoned well was equal to 50-300 ft. For a wellbore radius of 0.5 ft, this range leads to values of $\ln(r_1 / r_{1AW})$ and $\ln(r_2 / r_{2AW})$ between 4.6 and 6.4. Based on engineering judgment, in cases where the nearest active well may be at smaller or larger distances than the Avci[17] requirement of 0.001, the use of $\ln(r_i / r_{iAW})$ to choose the location of the steady state radii will ensure that it is placed within a reasonable range to represent the radius of influence of the abandoned well. Therefore for an individual formation, the program is designed to correct r_i to meet this range. Using formation 1 as an example, the program determines R as the distance from the abandoned well to the nearest active well. Next, the program finds r_1 as a user supplied percentage of R. The program then checks the value of $\ln(r_1 / r_{1AW})$. If this value does not fall into the range 4.6 to 6.4, the program calculates a value for r_1 to meet either the lower or upper limit for this range. If the value of $\ln(r_1 / r_{1AW})$ was below 4.6, it is set to 4.6 and a new r_1 is calculated. If the value of $\ln(r_1 / r_{1AW})$ is greater than 5.4, it is set to 5.4 and a new r_1 is determined. If no active well is present in a formation, r_i is determined using $\ln(r_i / r_{iAW})$ equal to 5.4. If a correction is made, the program prints an output statement warning the user that the substitution was required.

The results given in Table 3 were found using a time step of 1 day, which is a realistic time period for field data. However, the coupled model should give better results as one reduces the time step. To investigate the sensitivity of the model to time step, the

program was run with the test case data for time steps of 0.1 day, 0.5 day and 1 day at a radius of 0.10 R. This radius was chosen because it showed the greatest variation of results for the case of 1 day time steps shown in Figure 24. Figures 26-28 show the dimensionless flow results for these cases and for Avci[17]. The figures indicate that as time step is reduced, the early time variability in the dimensionless flow is also reduced and practically eliminated. In particular for time steps of 0.1 day, the program produced an almost exact match to Avci. This leads to a dilemma in choice for time step which can only be resolved by considering the trade-off between accuracy and computational time. If early time results are of critical interest, the program can be run with small time steps. If flow values at late time or a cumulative flow value are required then the amount of error introduced by a larger time step should be negligible and not worth the extra computational time.

In conclusion, the coupled model abandoned well flow program provides an almost exact match to the reported analytical results of Avci[17] for the case of transient abandoned well flow in response to one injector and no wellbore resistance. The program shows the expected dependence of the results on the choice of steady state radius and time step in which the model may produce variable flows at early times. These effects are considered negligible for practical application of the program where one is generally concerned with the cumulative flows. Therefore, the choice for the radii and time step are a matter of engineering judgment.

Based on the excellent match between the program results and the analytical results given by Avci[17], it is apparent the coupled model can reproduce the analytical

results for the case of one injector and an abandoned well. It is therefore within reason to expect the model should be capable of extension to estimate the quantity of abandoned well flow expected in response to active wells in either formation. Although there is no analytical solution available to verify the effects of wellbore conditions, the physical basis for their inclusion in the model is sound as discussed in the model development of Chapter 3.

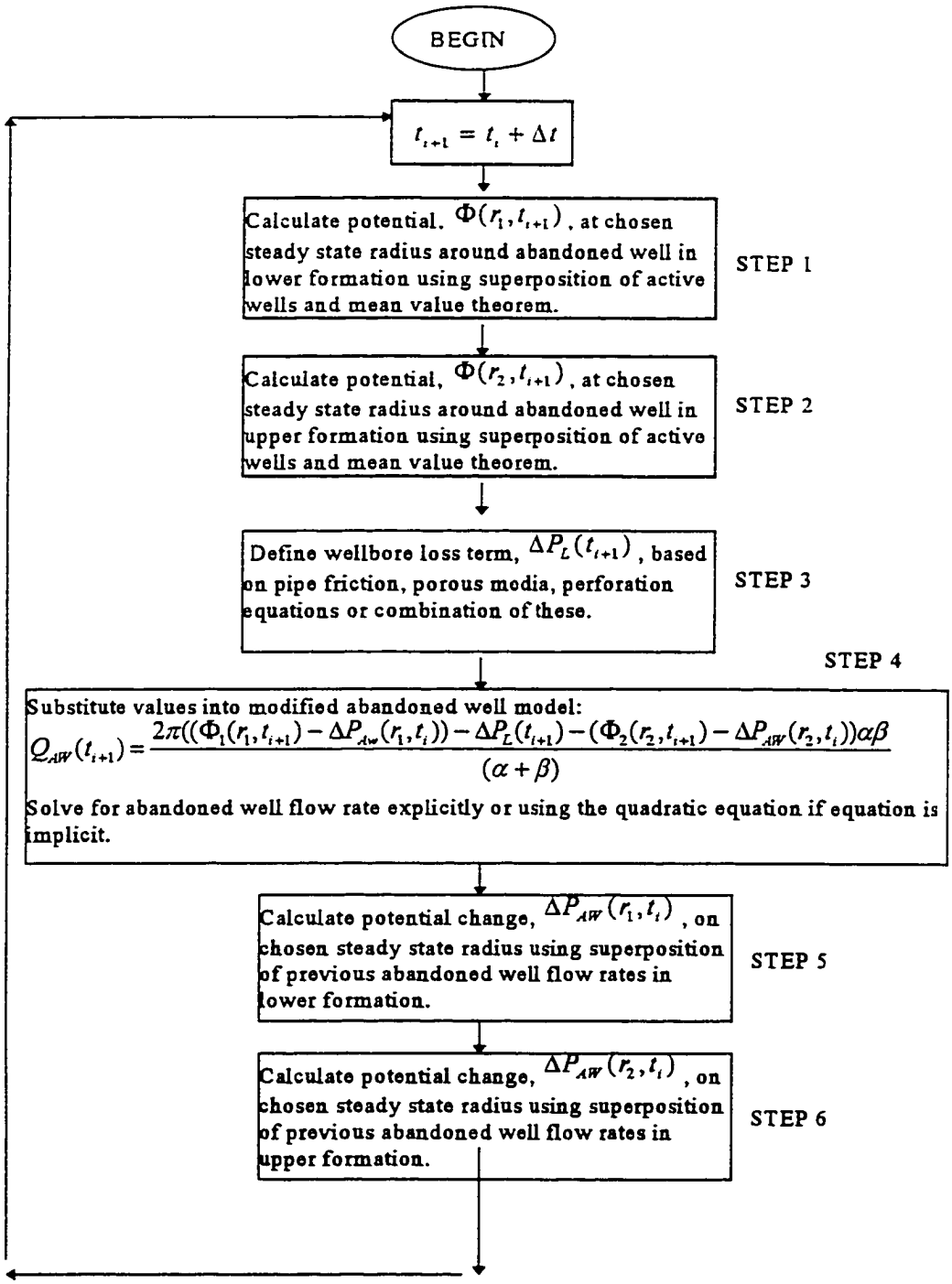


Figure 22. Task flow chart for 'series of steady states' coupled abandoned well flow computer program.

Table 3. Comparison of Avci's[17] analytical model and coupled abandoned well model program results for dimensionless flow.

	$\xi = 10.0$		$\xi = 1.0$		$\xi = .10$	
t_D	Avci Q_{AWD}	AW model Q_{AWD}	Avci Q_{AWD}	AW model Q_{AWD}	Avci Q_{AWD}	AW model Q_{AWD}
5	.1408	.1473	.0785	.0820	.0164	.0165
7	.1554	.1581	.0866	.0881	.0181	.0186
10	.1705	.1731	.0949	.0963	.0197	.0198
20	.1984	.1993	.1105	.1109	.0228	.0228
50	.2325	.2324	.1293	.1293	.0265	.0265
70	.2443	.2439	.1359	.1356	.0278	.0277
100	.2564	.2559	.1426	.1417	.0291	.0290
200	.2786	.2780	.1549	.1545	.0315	.0314
500	.3057	.3051	.1698	.1695	.0343	.0343
700	.3150	.3145	.1749	.1747	.0353	.0353
1000	.3248	.3242	.1804	.1801	.0363	.0363

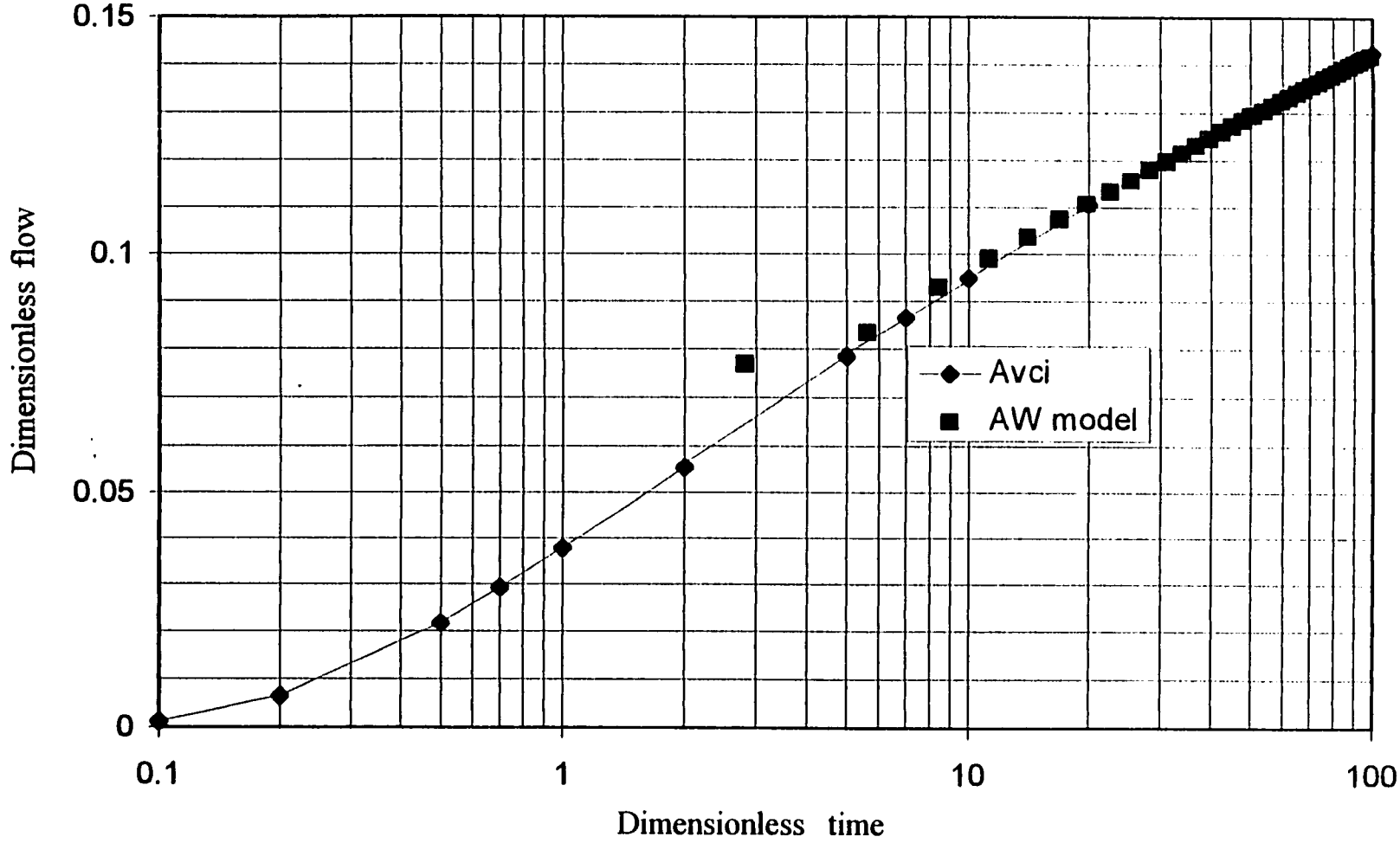


Figure 23. Comparison of dimensionless flow rates from Avci[17] and 'series of steady states' coupled model for one day time steps and a steady state radius at 55%R.

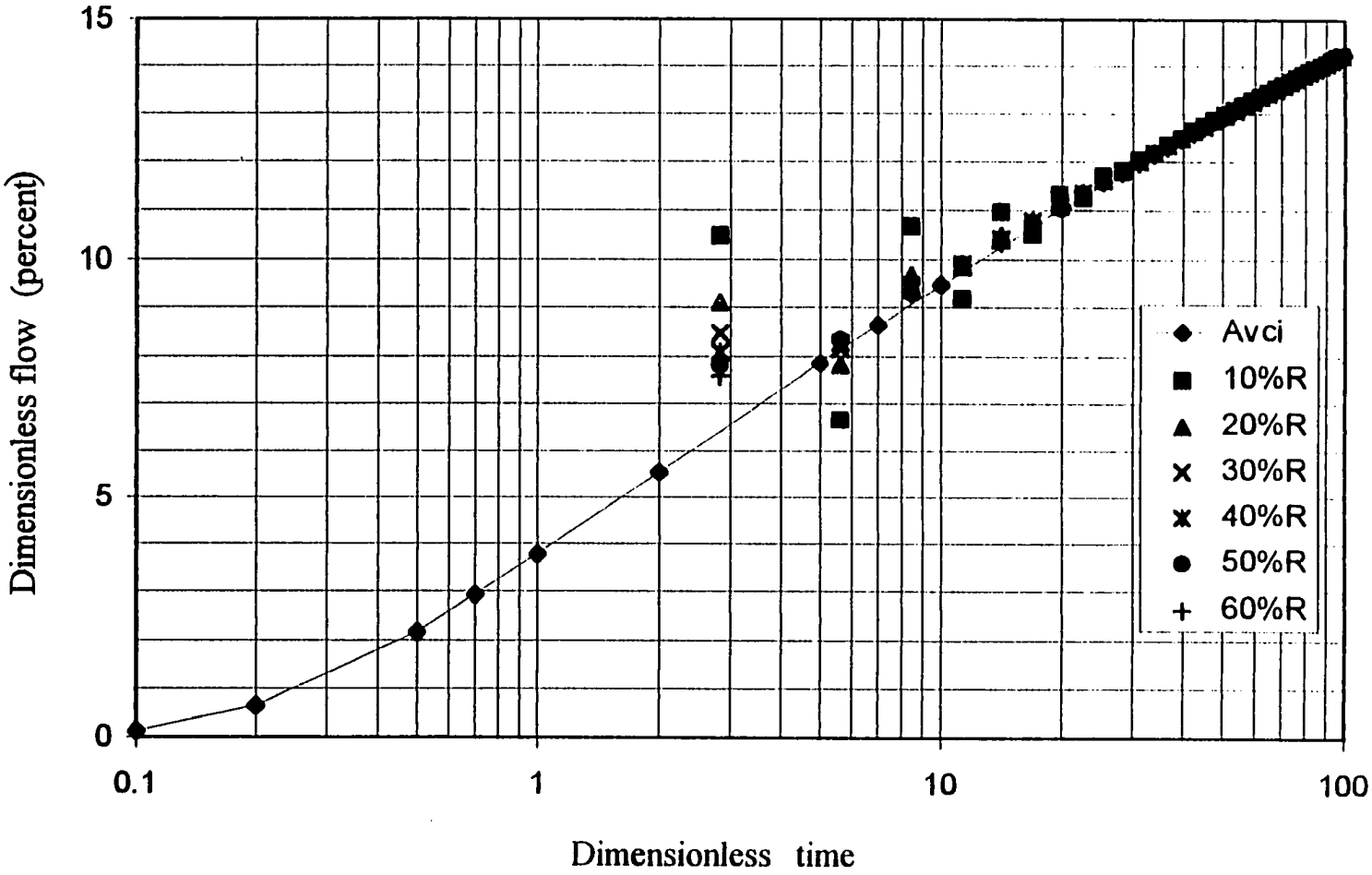


Figure 24. Dimensionless flow rates from Avci[17] and 'series of steady states' coupled model for varying locations of steady state radii (.10R-.60R) and time steps of 1 day.

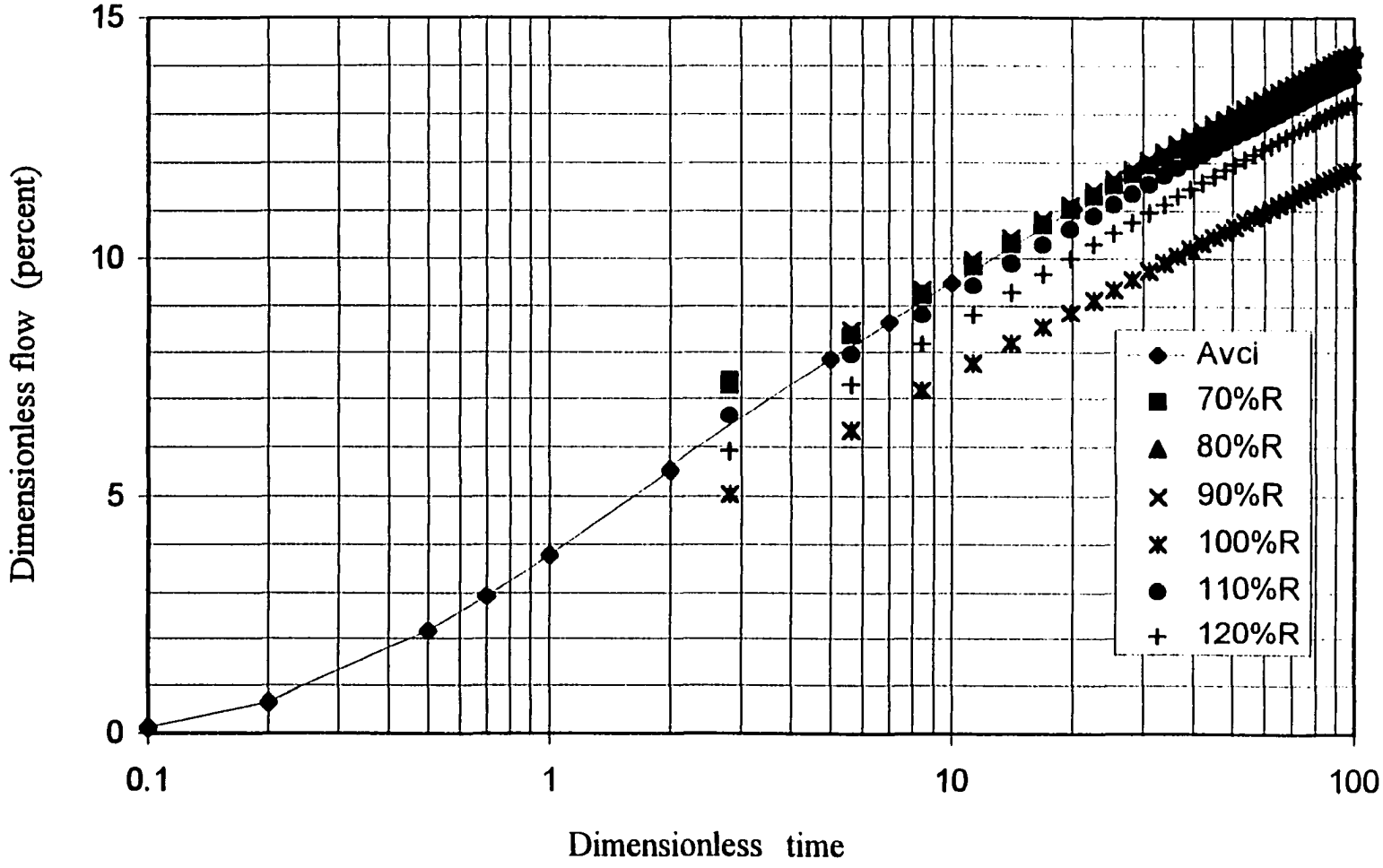


Figure 25. Dimensionless flow rates from Avci[17] and 'series of steady states' coupled model for varying locations of steady state radii (.70R-1.1R) and time steps of 1 day.

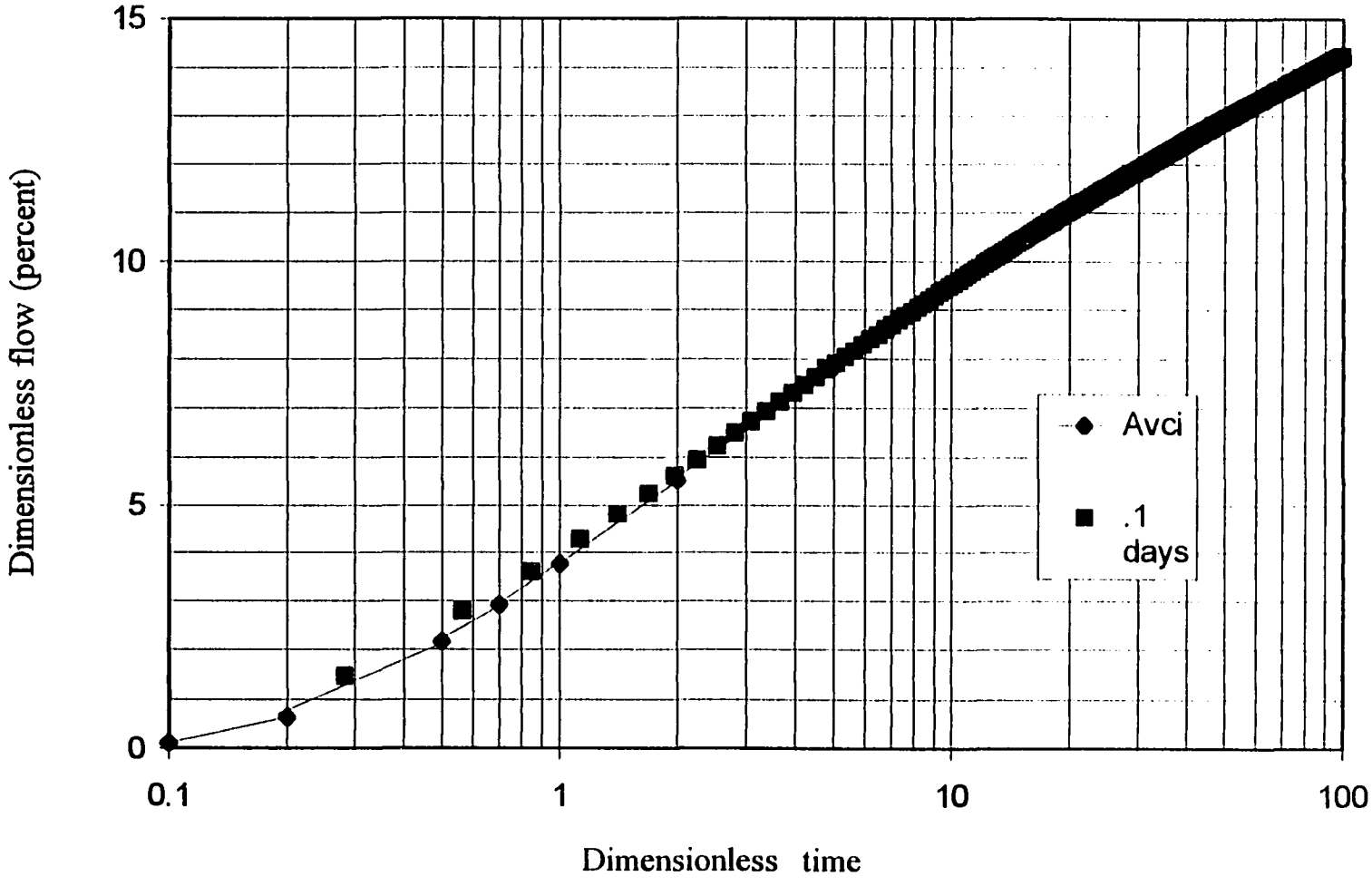


Figure 26. Dimensionless flow rates from Avci[17] and 'series of steady states' coupled model for a steady state radius of 10% R and time steps of 0.1 days.

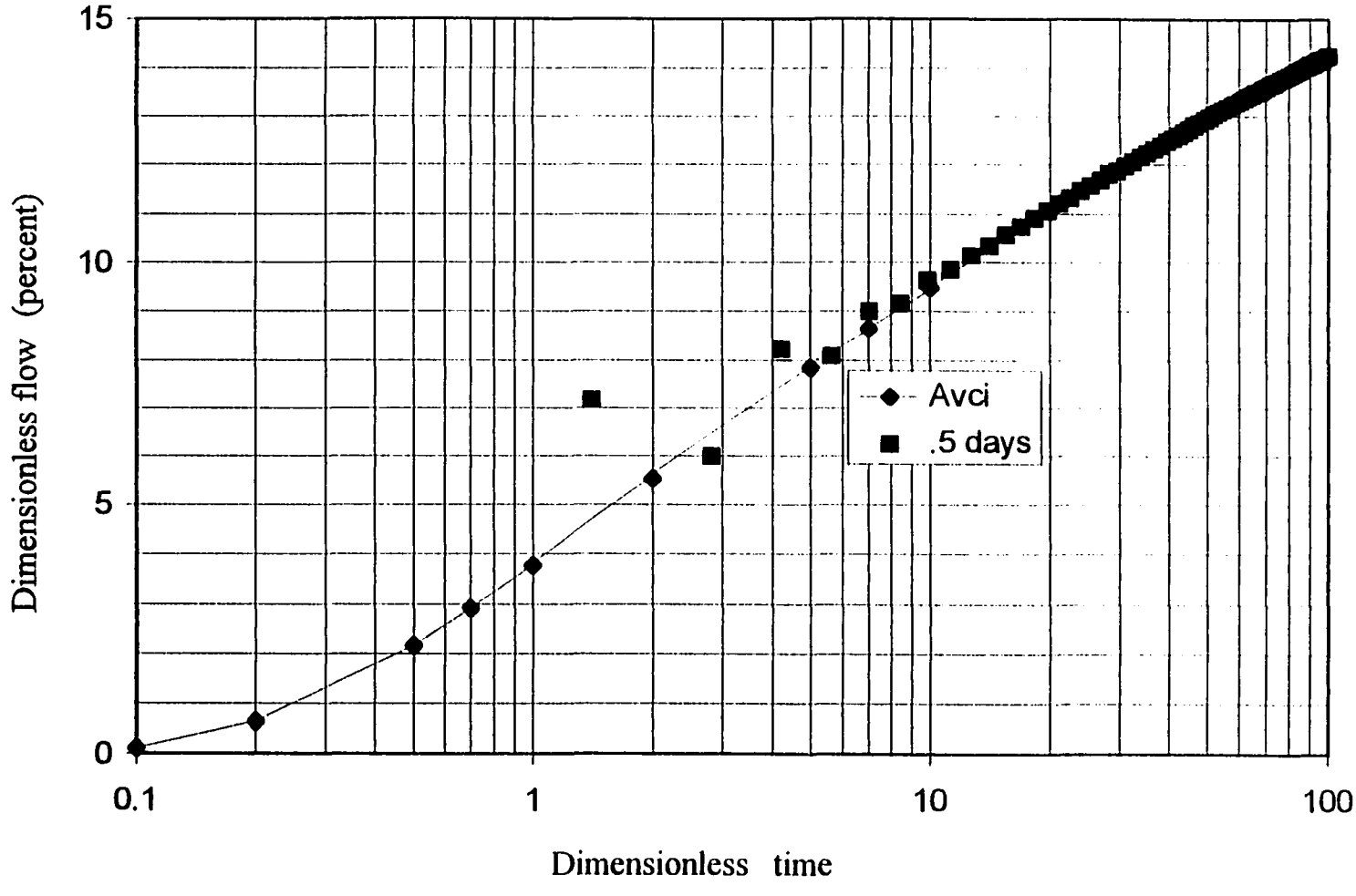


Figure 27. Dimensionless flow rates from Avci[17] and 'series of steady states' coupled model for a steady state radius of 10% R and time steps of 0.5 days.

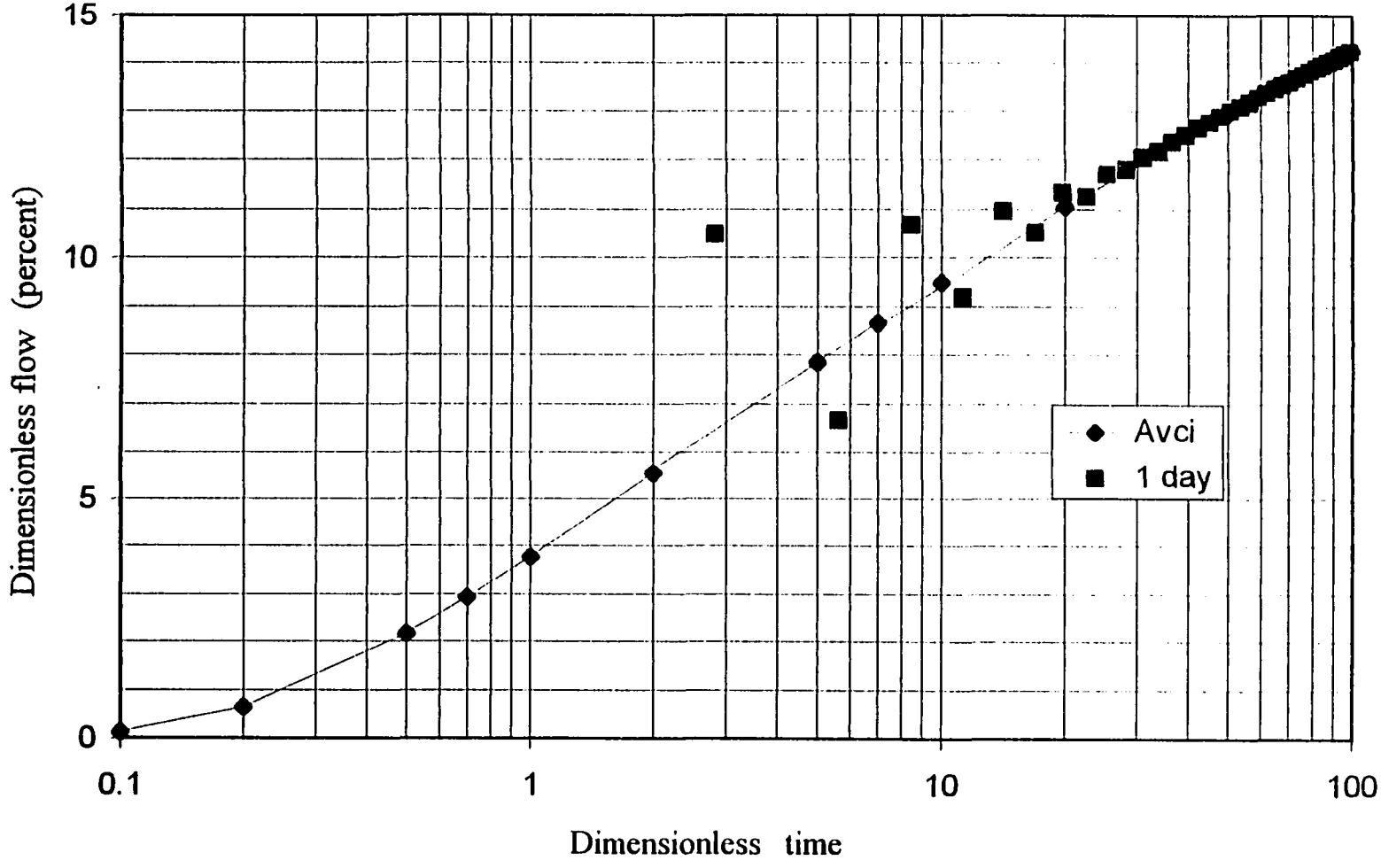


Figure 28. Dimensionless flow rates from Avci[17] and 'series of steady states' coupled model for a steady state radius of 10% R and time steps of 1 day.

CHAPTER 5

APPLICATION OF COUPLED ABANDONED WELL MODEL PROGRAM

The coupled abandoned well model developed in this research is unique in its simplicity and flexibility. The model can be employed to predict abandoned well flow in response to active wells in either formation. Flow through the wellbore may be up or down depending on the pressure distributions incurred by the active wells. The model may also include the wellbore conditions of pipe friction, plugging materials and a single perforation in the casing next to the upper formation. Finally it may be used to predict fluid transport between formations through the annulus. Its versatility allows it to be used as a tool to evaluate many of the parameters that determine if abandoned well flow will occur in a system and to what degree. There are numerous cases of interest which can be used to illustrate the effect of various conditions on flow. This section examines a select group to demonstrate the model's capabilities and the abandoned well flow responses.

The cases were run using the test data that were applied to verify the model with the analytical results of Avci[17] as discussed in the Section 4.3. These data were modified for each individual application to examine the sensitivity of the flow results to a particular change in condition. The basic test case data included formation permeabilities of 50 md, thicknesses of 50 ft and porosities of 0.15. The fluid properties were for water and included a compressibility of $3x10^{-6}$/psi, density of 67 lb/ft^3 and viscosity of 1 cp. The distance between the injection and abandoned well was 500 ft. The borehole diameter was 12 inches at both the upper and lower formation which gave an abandoned well radius of

0.5 ft. The casing outer diameter was 10.5 inches and the casing inner diameter was 10 inches. The steady state radii in the model were chosen to be at 50% R. A single injector was present in the lower formation with a rate of 100 bbls/day. The initial pressures for the upper formation and lower formation were 418.5 psi and 450 psi respectively. The lower formation was located at a depth of 1000 ft and the upper formation at 900 ft, which created an initial hydrostatic condition where the potentials for both formations were 465 psi. The time step was 1 day, which is a realistic time for a field study. The total time for all cases was 500 days. In the base case, the wellbore is initially treated as if it were totally open to flow so that no wellbore losses were included.

5.1 Single Injection Well In Lower Formation

In the study of abandoned well flow, the scenario which has received the greatest interest has been that of a single injection well near an abandoned well as shown in Figure 15. An example would be a salt water disposal well operating near an abandoned well. As discussed in the model development, the factors which have been shown to affect abandoned well flow for this case are the distance of the injection well from the abandoned well, the formation rock properties, the fluid properties, and the flow rate at the injection well. Within the wellbore, the flow rate may be affected by the presence of pipe friction, plugging materials or a single perforation. If the wellbore is plugged, it is necessary to consider the possibility of flow in the annulus. Therefore the coupled model program was used to evaluate the flow rates arising from individual variations in these conditions.

In Case 1, the program was applied to investigate the effect of the distance between the injection well and abandoned well on flow. The test data were modified to place the injection well at radial distances of 250, 500, 1000 and 2000 ft away from the abandoned well. Figure 29 shows the results of the program for these four distances. For a distance of 500 ft, the program results are almost an exact match to the analytical results of Avci[17] as discussed in Section 4.3. For all values of R, the results indicate a direct correlation between flow rate and the distance between the abandoned well and the injection well. As the distance between the wells is increased, the flow rate is decreased.

This result is anticipated. If one looks at the coupled model given in Eq. 65:

$$Q_{AW}(t_{i+1}) = \frac{2\pi((\Phi_1(r_1,t_{i+1}) - \Delta P_{AW}(r_1,t_i)) - \Delta P_L(t_{i+1}) - (\Phi_2(r_2,t_{i+1}) - \Delta P_{AW}(r_2,t_i))\alpha\beta}{(\alpha+\beta)} \tag{65}$$

the distance between wells is embedded in the $\Phi_1(r_1,t_{I+1})$ term which represents the potential on the chosen steady state radius in the lower formation 1. As explained in the model development, $\Phi_1(r_1,t_{I+1})$ is found by averaging the potentials from eight points on that radius. Each individual point potential is derived from the original potential plus the pressure change created by the injection well at that point and time which is given by:

$$\Delta P_I(R,t) = \frac{-Q_I}{4\pi k_1 h_1} Ei\left(\frac{-R_i^2 \phi_1 \mu c}{4k_1 t}\right) \tag{50}$$

where R_i represents the distance of the ith point from the injection well. If R_i is halved in Eq. 50 we obtain:

$$\Delta P_I(R,t) = \frac{-Q_I}{4\pi k_1 h_1} Ei\left(\frac{-0.25 R_i^2 \phi_1 \mu c}{4k_1 t}\right) \tag{95}$$

In Eq. 95, as the distance between wells is decreased, the Ei function value increases. This produces the larger pressure change which drives the higher flow rates.

As shown in Figure 29, as time progresses, the increase in flow rate becomes constant for each halving of the distance between the injector and the abandoned well. This is an interesting result that requires an explanation. Within the program, the Ei ($-\chi$) function is estimated by the natural log approximation :

$$Ei(-\chi) = \ln(\chi) + 0.577 \tag{96}$$

for values of $\chi < 0.01$ which occur after the first day for the test case data at a radius of 250 ft. The presence of the natural log function in the approximation is the reason why the difference between the flow rates becomes constant. If one begins with a χ value and quarters it as indicated by Eq. 95, one gets the following progression:

$$Ei(-\chi) = \ln(0.25\chi) + 0.577 = \ln(0.25) + \ln(\chi) + 0.577$$

$$Ei(-\chi) = \ln(0.25)(0.25)(\chi) + 0.577 = \ln(0.25) + \ln(0.25) + \ln(\chi) + 0.577$$

So for each successive halving of the radius, the log approximation provides a constant change of ln (0.25) in the Ei solution. As the Ei log approximation is used to find the potential in Eq. 65, the constant change in the natural log value manifests itself as the constant difference between flow rates.

Case 2 examined the effect of the ratio of the formation permeabilities on flow rate. The program was therefore run with the test case data but for four cases where the permeability of the upper formation was modified to 0.5 md, 5.0 md, 50.0 md, and 500.0 md to give permeability ratios of upper to lower permeability of 0.01, 0.1, 1.0, 10. The results for these cases are shown in Figure 30 and the flow rates for the ratios 0.1, 1.0 and

10.0 match the published analytical results given by Avci[17] as shown in Table 3. As can be seen in the figure, the flow rate is very sensitive to the permeability ratio. The highest flow rates are experienced when the permeability of the upper formation is greater than the lower.

The effect of the permeability ratio on flow rate is expected. Looking at Eq. 65:

$$Q_{AW}(t_{i+1}) = \frac{2\pi((\Phi_1(r_1,t_{i+1}) - \Delta P_{AW}(r_1,t_i)) - \Delta P_L(t_{i+1}) - (\Phi_2(r_2,t_{i+1}) - \Delta P_{AW}(r_2,t_i))\alpha\beta}{(\alpha+\beta)} \qquad (65)$$

the permeability values are embedded in every pressure term except the wellbore pressure losses. They are also present in the α and β terms which represent the productivity indices of the two formations. Although it is difficult to assess the impact of permeability ratio on each of these terms, its effect can be visualized physically. Simply stated, if the pressure losses across the upper formation are less because of its relatively lower permeability, more of the pressure buildup derived potential is available to move fluid up through the well.

In Case 3, the program was used to evaluate the impact of different injection rates on the flow rate through the abandoned well. The test data were changed to investigate injection rates of 25, 50, 100, and 200 bbls/day. The results for the flow rates in the abandoned well are shown in Figure 31 and demonstrate the flow rate through the abandoned well essentially doubles for every doubling of the injection rate. Once again this is a consequence of the transient pressure buildup in the lower formation which is directly dependent on the flow rate as given in:

$$\Delta P_I(R,t) = \frac{-Q_I}{4\pi k_1 h_1} Ei\left(\frac{-R_i^2 \phi_1 \mu c}{4k_1 t}\right) \qquad (50)$$

In Eq. 50, as the flow rate is doubled the pressure buildup is doubled. As this pressure buildup from the injection well is the driving force for flow in a single injection well system, doubling its value leads to a doubling of the flow rate in Eq. 65.

Case 4 investigated the abandoned well flow rate response to changes in the injection well rate over time. The injection well was programmed for six rates: 50 bbls/day for 100 days, 100 bbls/day for 100 days, 200 bbls/day for 100 days, 100 bbls/day for 100 days, 0 bbls/day for 50 days and 50 bbls/day for 50 days. Figure 32 demonstrates the coupled model program is fully capable of predicting the variable abandoned well flow rates expected to occur in response to changing rates at the injection well. The doubling of the rates from 50 to 100 to 200 bbls/day caused increases in flow rate which leveled off as expected in response to the slowing pressure buildup. Lowering the rates from 200 to 100 to 0 bbls/day showed the abandoned well rate will decrease quickly when the driving forces are reduced.

Up to this point, all the cases examined with the coupled model program have been based on flow through an abandoned wellbore with no resistance. The model, however, can also be applied to determine the impact of wellbore resistance from pipe friction, plugging materials and a single perforation on flow rates. In Case 5, the program was used to assess the effect of pipe friction in the open wellbore on the flow rates. The test case data were modified to include pipe roughness which was set to 2 different values of 0.01 ft (cement) and 0.00085 ft (cast iron). Injection rates were set at 25, 50, 100, and 200 bbls/day. But for all runs, it was found that for the test case where the pipe length between the formations is only 100 ft, the frictional losses in the wellbore were so small that they

were insignificant. The program therefore produced exactly the same results as shown in Figure 31. Although their effect was deemed negligible for the test data, the option to evaluate pipe friction is still included in the program. The program therefore retains the capability to address situations where pipe friction losses may become significant, i.e., when the distance between formations may be on the order of thousands of feet.

As discussed in the Section 2.3, the type of wellbore resistance which has the greatest effect on flow is the presence of plugging materials, such as a cement plug, shales or drilling mud, in the wellbore. In the numerical simulation of abandoned well flow done by Warner and McConnell[12], these impediments to flow were treated as porous media in the wellbore and were shown to totally eliminate flow. In the coupled model program they were also incorporated as porous media. In Case 6, the test data were modified to include the presence of one plug in the wellbore. Three separate runs were made for one plug with lengths of 100 ft, 10 ft and 1 ft and a permeability of 0.1 md. This permeability was identified by Warner and McConnell[12] as representative of the upper range for the permeability of sloughed shales within the wellbore. The flow rate results for Case 6 are shown in Figure 33 and demonstrate the strong influence of plugging materials which effectively eliminate flow through the wellbore even for the short length of only one foot. These results are expected because the frictional losses through porous media are high for relatively impermeable materials such as shales or drilling muds and therefore eliminate most of the potential developed from the pressure buildup.

Another type of wellbore condition that can reduce flow is that of a single perforation which represents a casing leak. Warner and McConnell[12] attempted to model a

perforation by treating it as a permeable wellbore block. The coupled model incorporates the perforation as an orifice with pressure losses given by Eq. 80. It also recognizes that a perforation acts as a spherical source and incorporates the spherical flow effect in the model. In Case 7, the program was applied to demonstrate the influence of a single perforation next to the upper formation on flow. The test case data were modified to include a perforation with three different sizes of 0.25, 0.50, and 1 inch. Figure 34 shows the results from these cases. As expected, the flow rates in the presence of a perforation are greatly reduced as compared to those of an open wellbore. The smallest perforation of 0.25 inches has the lowest flow rates as a consequence of the frictional loss and also its size as a spherical source. As the size of the perforation is increased the frictional losses are decreased and the source size is increased and both of these effects lead to an increase in the flow rate.

The final situation of interest for abandoned well flow in response to a single injector is that of the transport of fluid between formations through the annulus. If the wellbore contains plugging materials such as cement or sloughed shales, it has been shown to preclude flow. However, it is possible that flow can still move through the annulus. The coupled model program was employed in Case 8 to determine the rates that can arise from annular flow. The annular flow rate was investigated for an open annulus, an annulus filled with 100 ft of 1 md disturbed zone materials, and a cement filled annulus with a 0.01 in fracture extending the vertical distance between the formations The results for the open annulus flow are shown in Figure 35 beside the flow rates for an open wellbore. Figure 35 shows that the results for the open annulus and open wellbore are exactly the same

because the frictional effects over 100 ft are negligible. The results for a plugged annulus are shown in Figure 36 along with the results for a wellbore filled with 100 ft of 1 md plugging materials and the annulus with a fracture for comparison. Figure 36 shows a 100 ft plug greatly reduces the flow in both the wellbore and annulus, but the annular flow is much less because of the smaller annular cross sectional area. The presence of the fracture increases the flow rate but it is still substantially less than the open annular case.

5.2 Production and Injection Wells in Either or Both the Lower and Upper Formations

The results from Cases 1-8 discussed above for the simple example of a single injector in the lower formation near an abandoned well provide significant insight into the types of conditions which influence flow rates through an abandoned wellbore. The coupled model program was developed, however, to handle much more complex systems which involve the presence of many active wells in either the upper or lower formation and their influence on the flowrate. This is an important aspect of the program because if other active wells are present they can mitigate or enhance the probability of abandoned well flow. This situation has been neglected in almost all of the published work on abandoned well flow models which have been limited to the case of a single injection well in the lower formation[11-14,16-18]. Only one study[21] examined the impact of a producer in the lower formation on the flow rate.

The program was therefore used to evaluate the abandoned well flow rates in cases involving one or more active wells in either formation. The first investigation in Case 9 centered on the relatively simple yet realistic situation of an abandoned well located on a straight line between one injector and one producer in the lower formation. The injector and producer were both operating at 100 bbls/day. The formation and fluid properties and other input data were the same as for the single injector test case described earlier. The abandoned well was assumed to have no resistance. The injector was located at (500,0) and the producer was located at (-500,0). The program was run for three abandoned well locations. The first was exactly halfway between the wells at (0,0). The second was near the injection well at (250,0). The third was near the producing well at (-250,0).

The flow rate results for the three abandoned well locations are shown in Figure 37 and clearly display the influence of the active wells. If the abandoned well is located at (0,0), which is exactly between the injection and production wells, the pressure change at this location is zero and represents a no flow boundary. The abandoned well rate from the program results reflects this no flow boundary with a rate of zero for all time. If the abandoned well is located at (250,0), it is closer to the injection well and demonstrates a positive flow rate (up the wellbore) in response to the injection pressure buildup. But unlike the case for the single injector this rate does not continue to increase, but decreases with time because of the reduction in pressure derived from the producing well drawdown. In the same manner, when the abandoned well is located at (-250,0) which is close to the production well, the abandoned well shows that the flow rate is negative (down the

wellbore) in response to the production drawdown. Once again the rate does not increase with time but is decreased by the injection rate pressure buildup.

Another case of interest is when the active wells are located in the upper formation. Depending on the type, number and locations of the active wells, the pressure distribution they induce within in the upper formation may also move flow up or down the wellbore. To examine this possibility, Case 10 was run first for an injection well operating in the upper formation and then for a producing well operating in the upper formation. The lower formation had no active wells. The formation and fluid properties and other input data were the same as for the single injector test case data. The abandoned wellbore was assumed to be open. The two cases were run with the injector or producer located at 500 ft from the abandoned well.

The results for Case 10 are shown in Figure 38 and demonstrate the symmetry expected from the coupled model. For the case of a producer in the upper formation operating at 100 bbls/day, the results are the same as if an injector operating under the same conditions was present in the lower formation. Now instead of raising concerns about the transport of fluids up the wellbore from injection in the lower formation, this case raises concerns that fluid transport occurs through abandoned wells in response to production in the upper formation. For the case of the injection well in the upper formation, the flow is the same magnitude but reversed as anticipated.

The results from these cases demonstrate an important point about abandoned well flow which has been neglected in the literature. Abandoned well flow is coupled to the pressure distribution induced by active wells in either or both formations. Because of this

dependence, the flow may move up or down the wellbore in response and may reverse under appropriate conditions. The possibility of two way flow has been almost completely ignored in the modeling of abandoned well flow, but it can have numerous implications.

If the abandoned well is near a producing well in the lower formation or an injection well in the upper formation, the pressure distribution near the well may move the fluids down hole. For example, if an oil producing well is near an abandoned well which is hydraulically connected to an overlying brine aquifer, it is possible that part of the produced water may be derived from abandoned well flow down the wellbore. Such produced water can lead to premature abandonment of the well.

If the abandoned well is near a injection well in the lower formation or a producing well in the upper formation, fluid should move up hole. This means that injection fluids may be transported to overlying formations including underground sources of drinking water. For salt water disposal wells, the salt water may escape up the wellbore. For injection wells used in secondary recovery projects such as waterfloods, fluids may be transported through the abandoned well to overlying formations and lower the displacement efficiency of the flood.

Finally the presence of balanced production and injection active wells may eliminate the potential for flow to occur in the abandoned well. This is likely in the spot patterns of producers and injectors normally used in secondary and tertiary recovery projects whose flow rates should mitigate the abandoned well flow because the pressure buildup created by injection wells is balanced by the pressure drawdown at the producing wells.

In conclusion, there are a myriad of conditions which influence the flow rates between formations through an abandoned well. The rates are dependent on formation rock properties and fluid properties. They also depend on the wellbore condition. More importantly, however, they depend on the number and type of active wells operating in either or both formations. Because of the simplicity and flexibility of the coupled model program, the problem of abandoned well flow can be solved for numerous conditions and scenarios to allow the prediction of the nature and amount of flow for a particular situation.

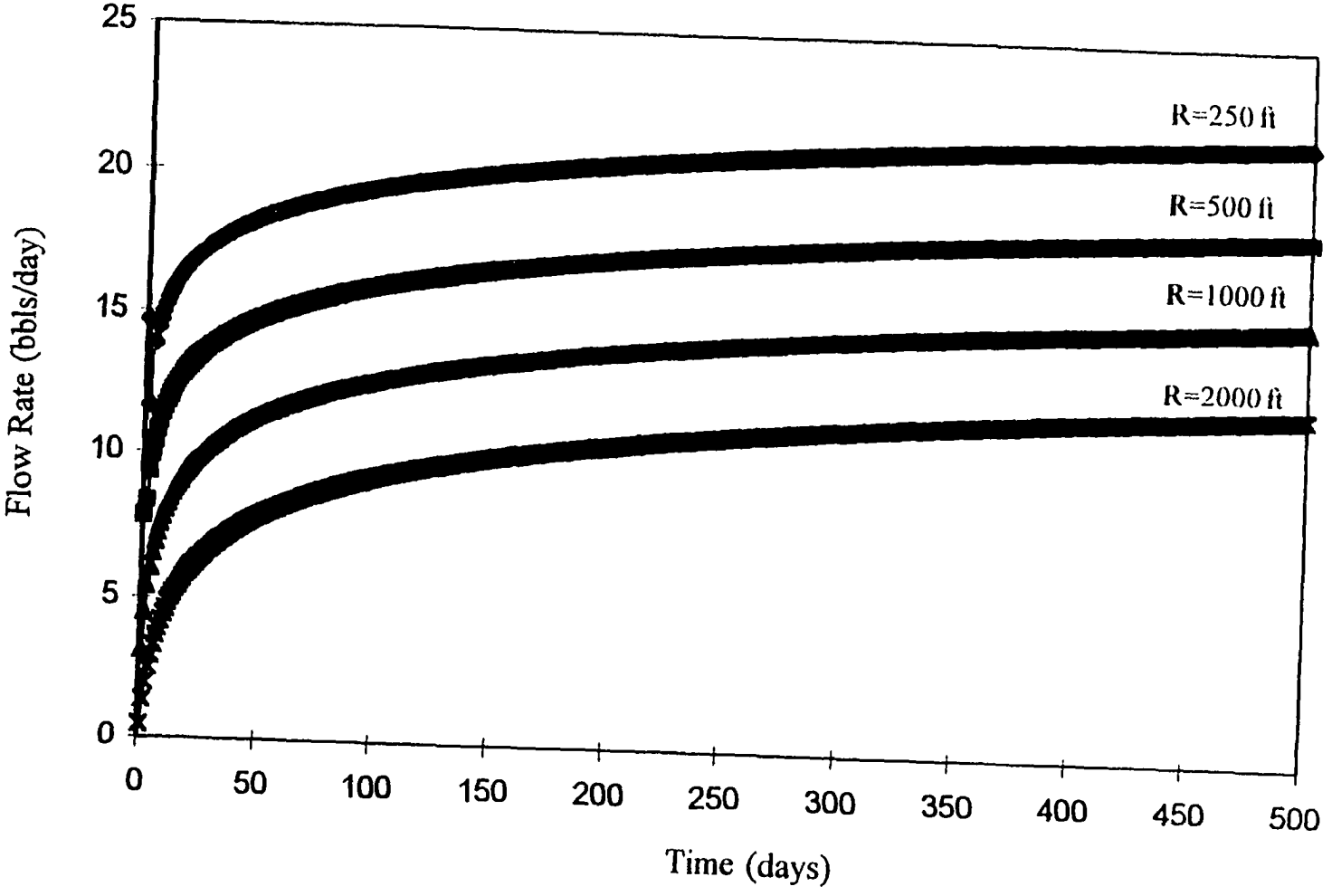


Figure 29. Case 1 comparison of abandoned well flow for varying distance R between the abandoned well and injection well.

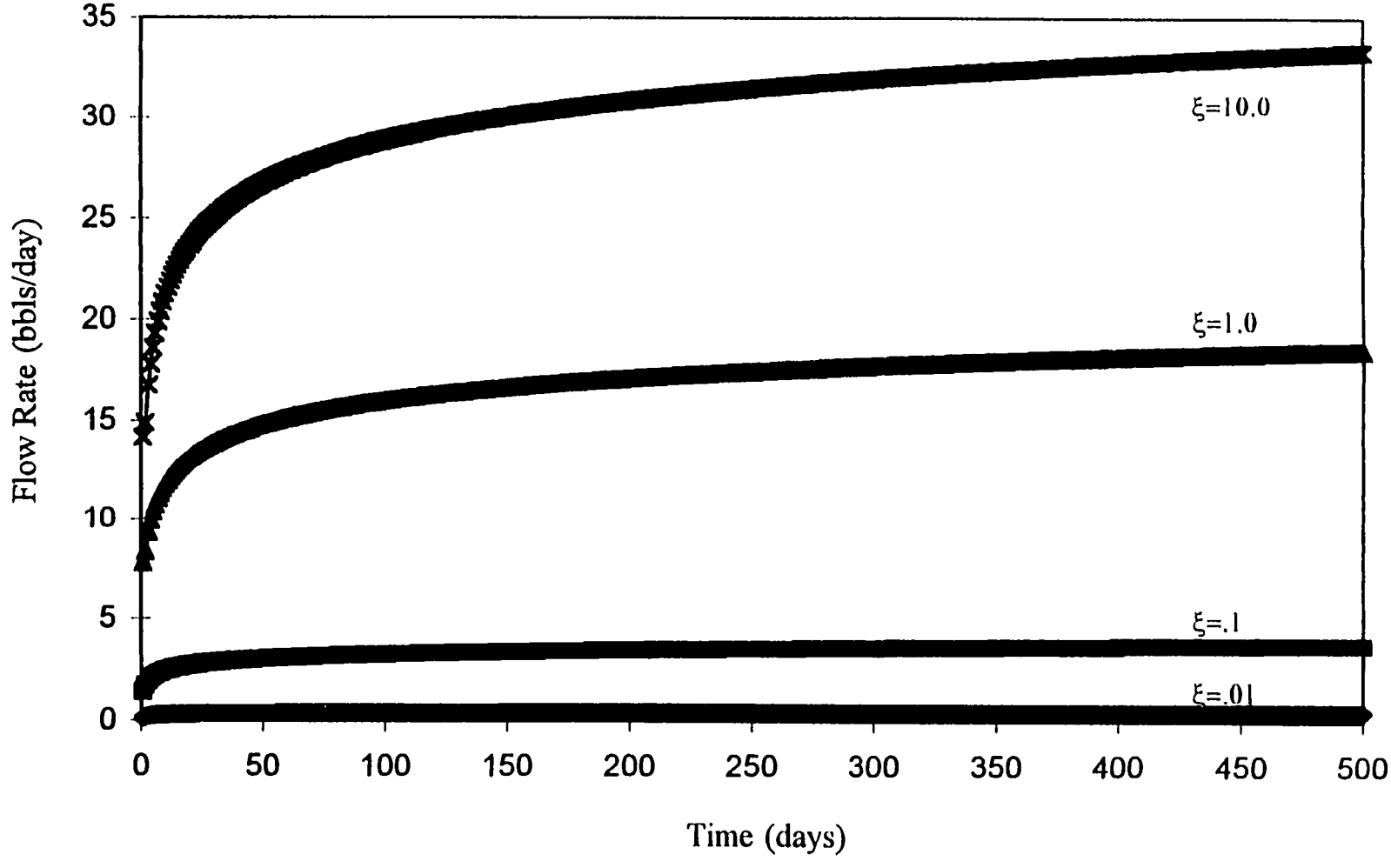


Figure 30. Case 2 comparison of abandoned well flow for varying permeability ratio, ξ .

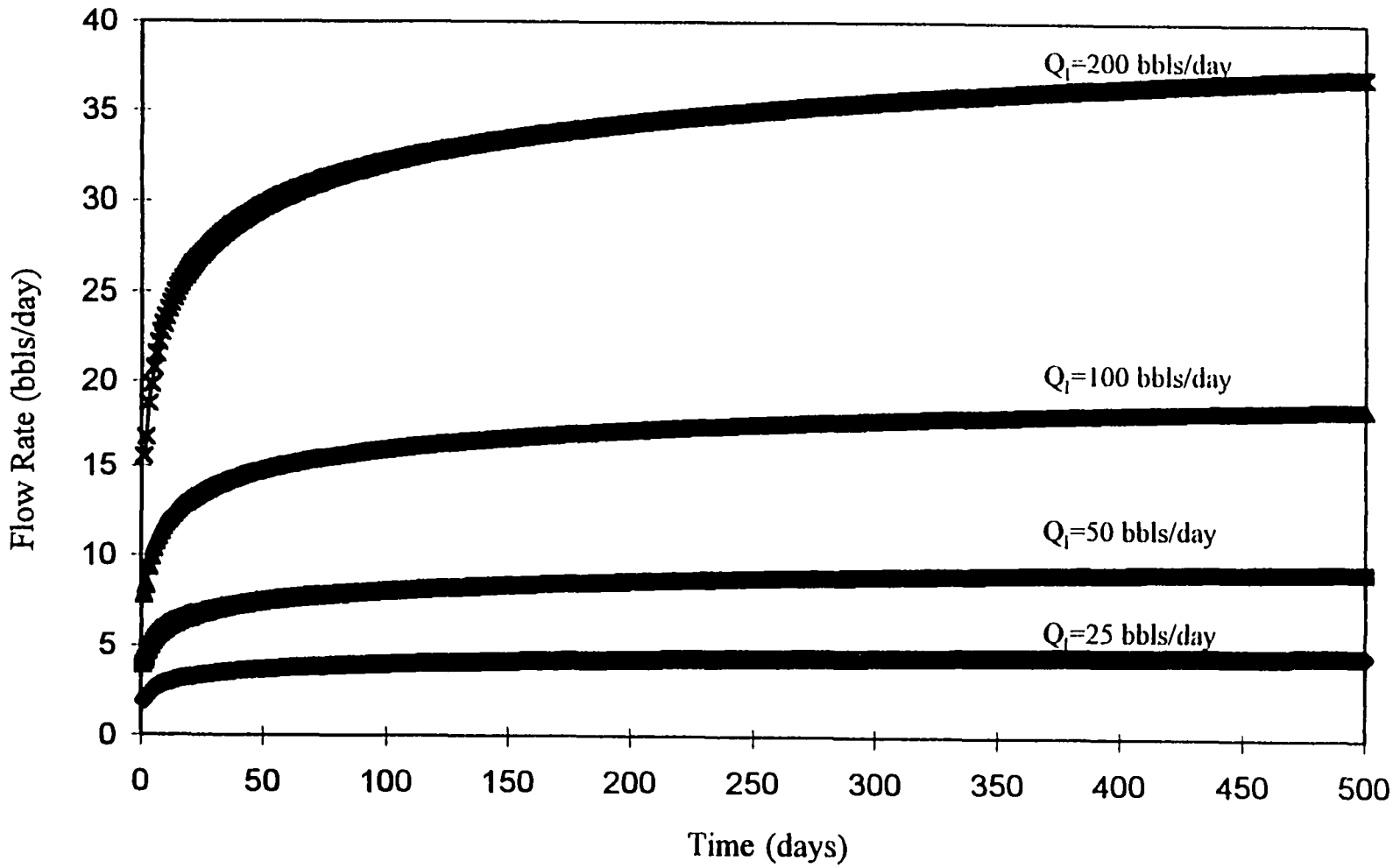


Figure 31. Case 3 comparison of abandoned well flow for different injection rates.

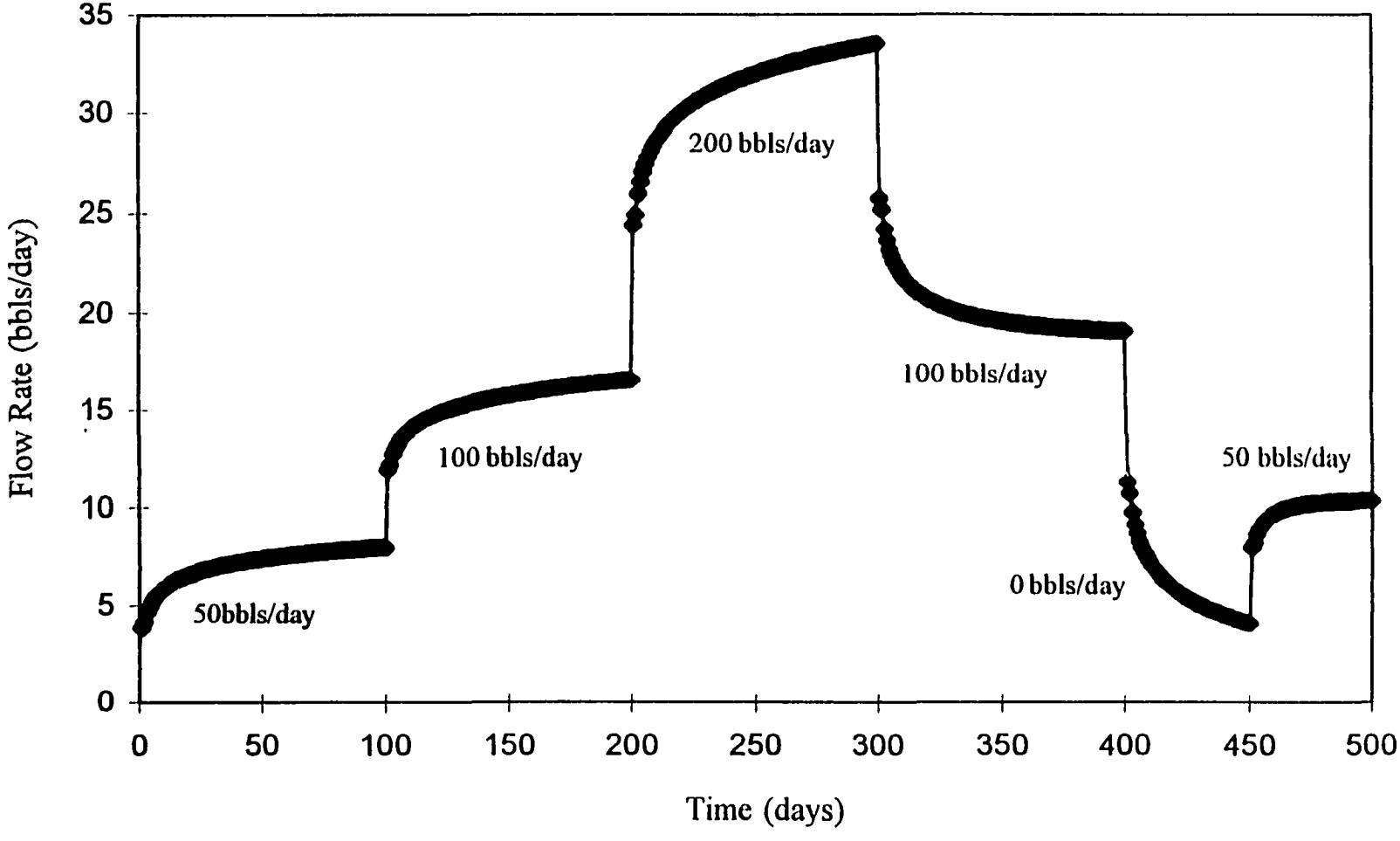


Figure 32. Case 4 abandoned well flow in response to multiple injection rates.

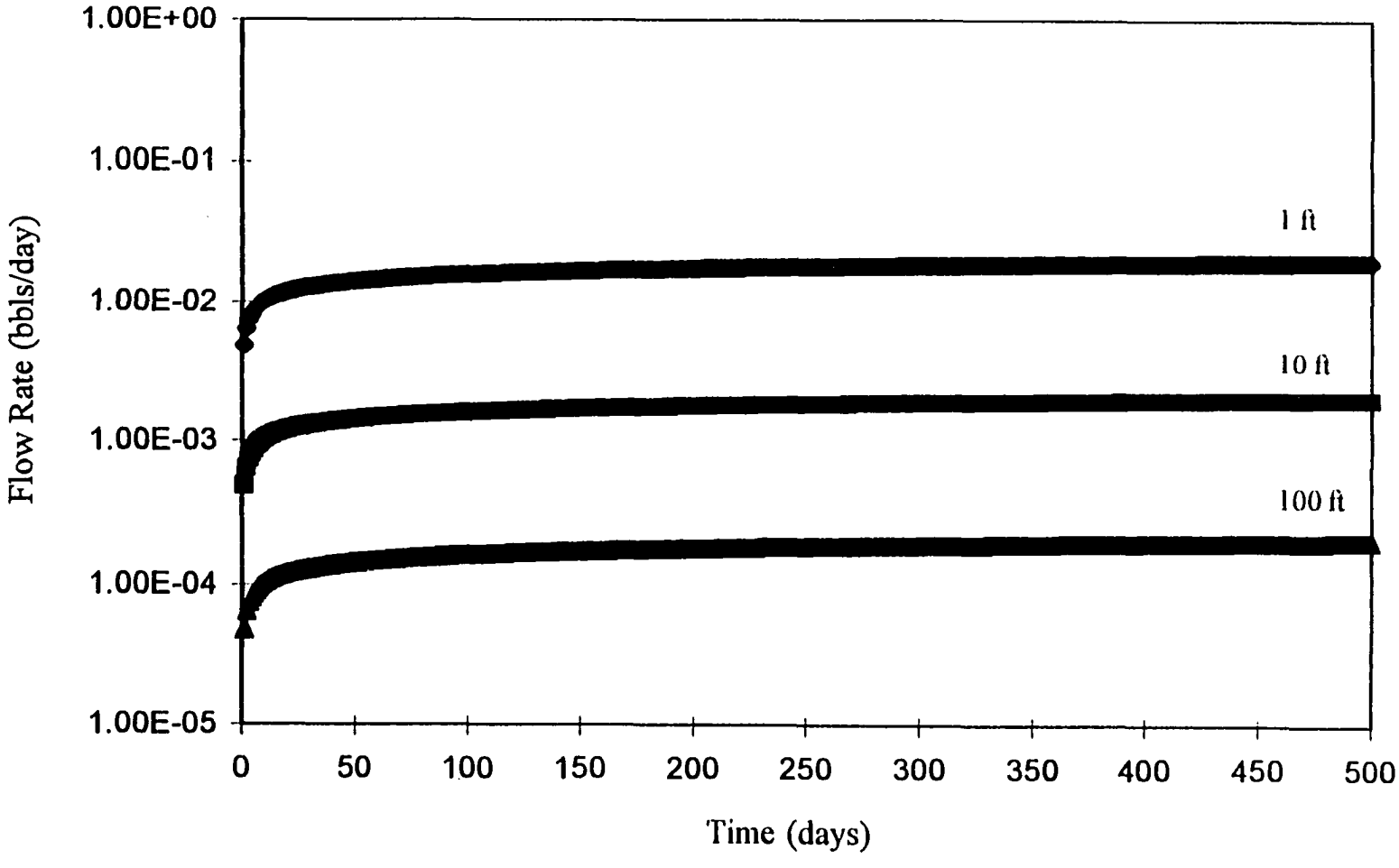


Figure 33. Case 6 comparison of abandoned well flow for different plug lengths and plug permeability of 0.1 md.

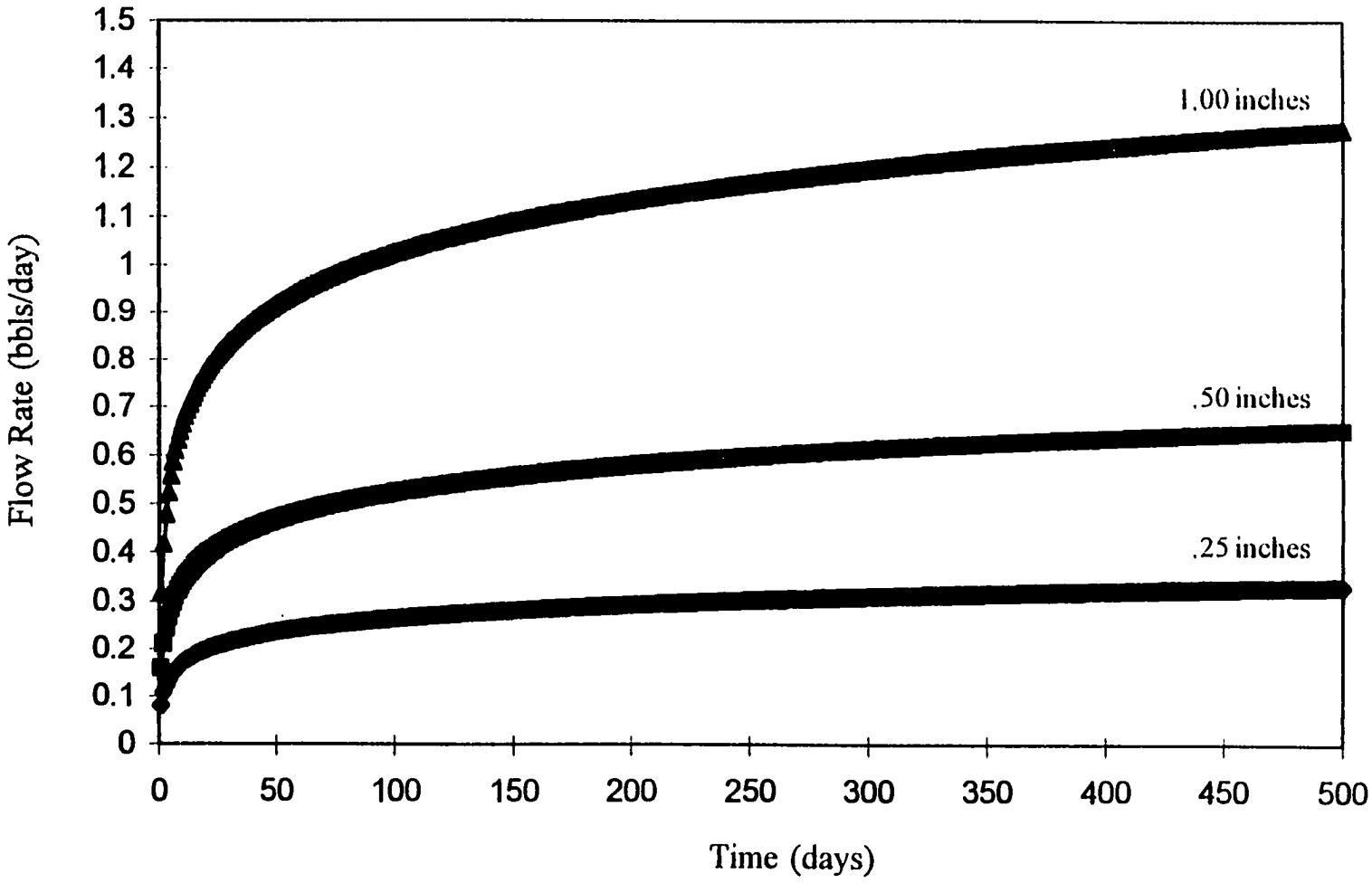


Figure 34. Case 7 comparison of abandoned well flow for different perforation sizes.

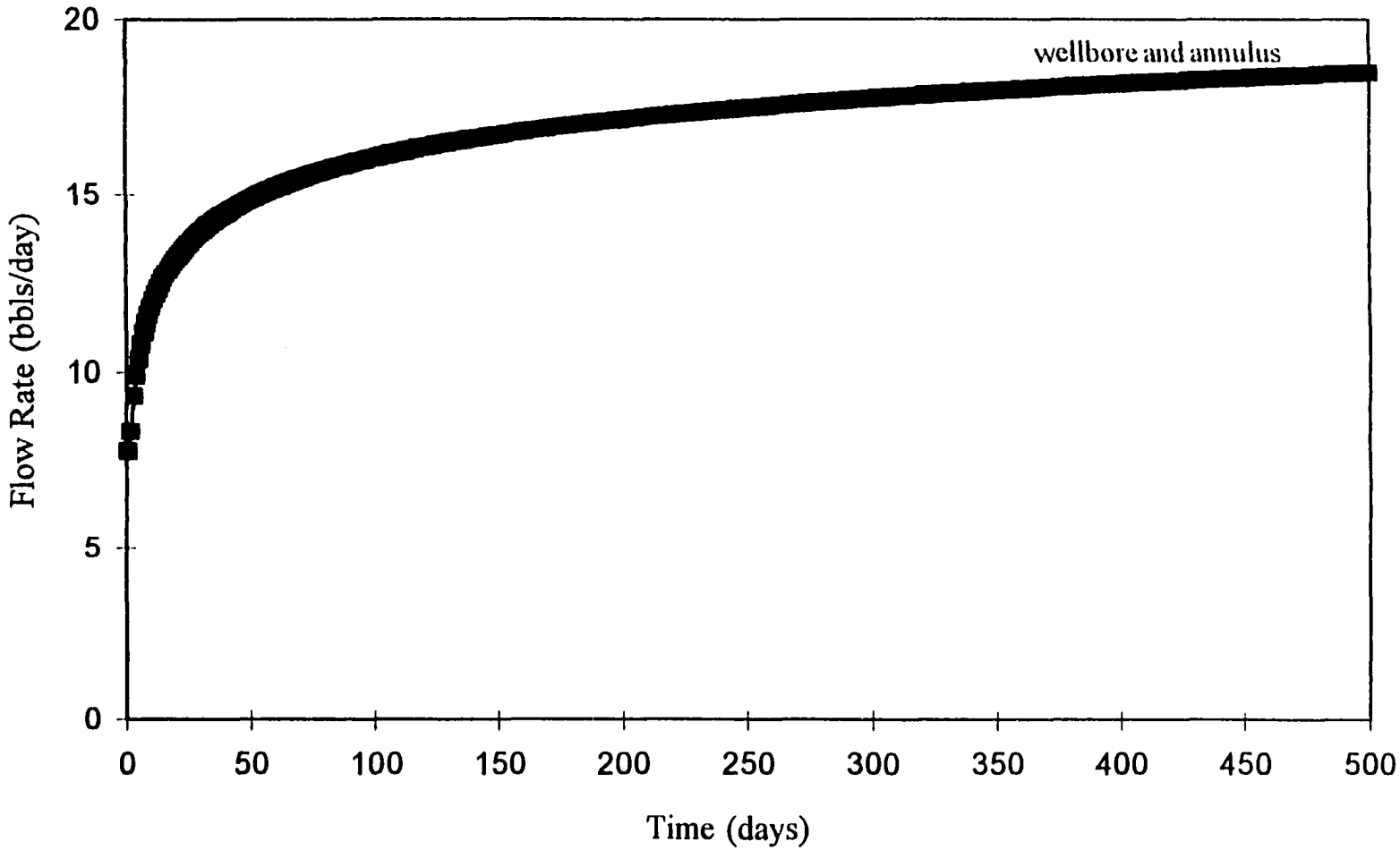


Figure 35. Case 8 comparison of abandoned well flow through an open wellbore or an open annulus.

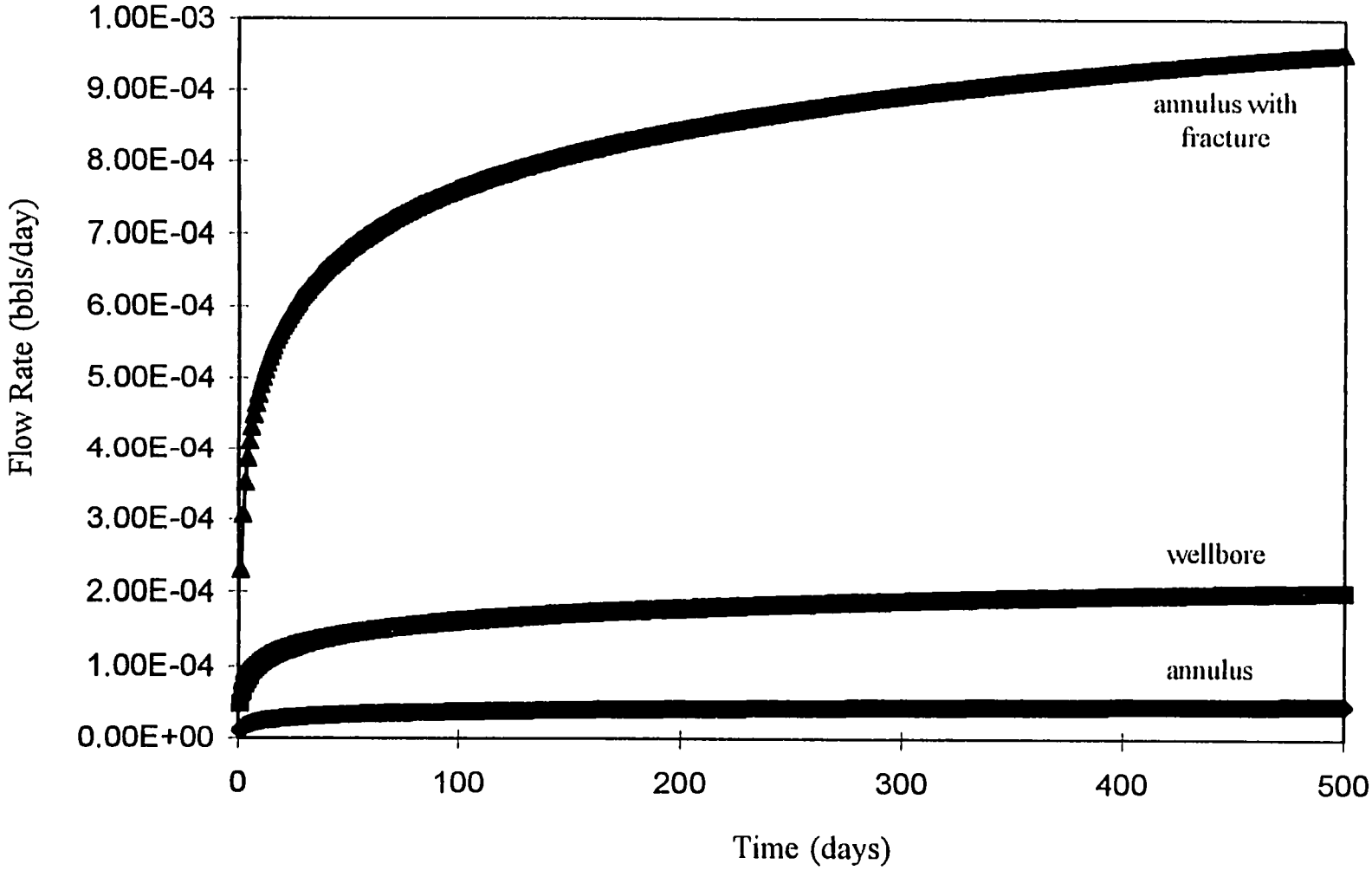


Figure 36. Case 8 comparison of abandoned well flow through a wellbore or annulus filled with a plug 100 ft long with 1 md permeability and an annulus with a 0.01 inch width fracture in the plug.

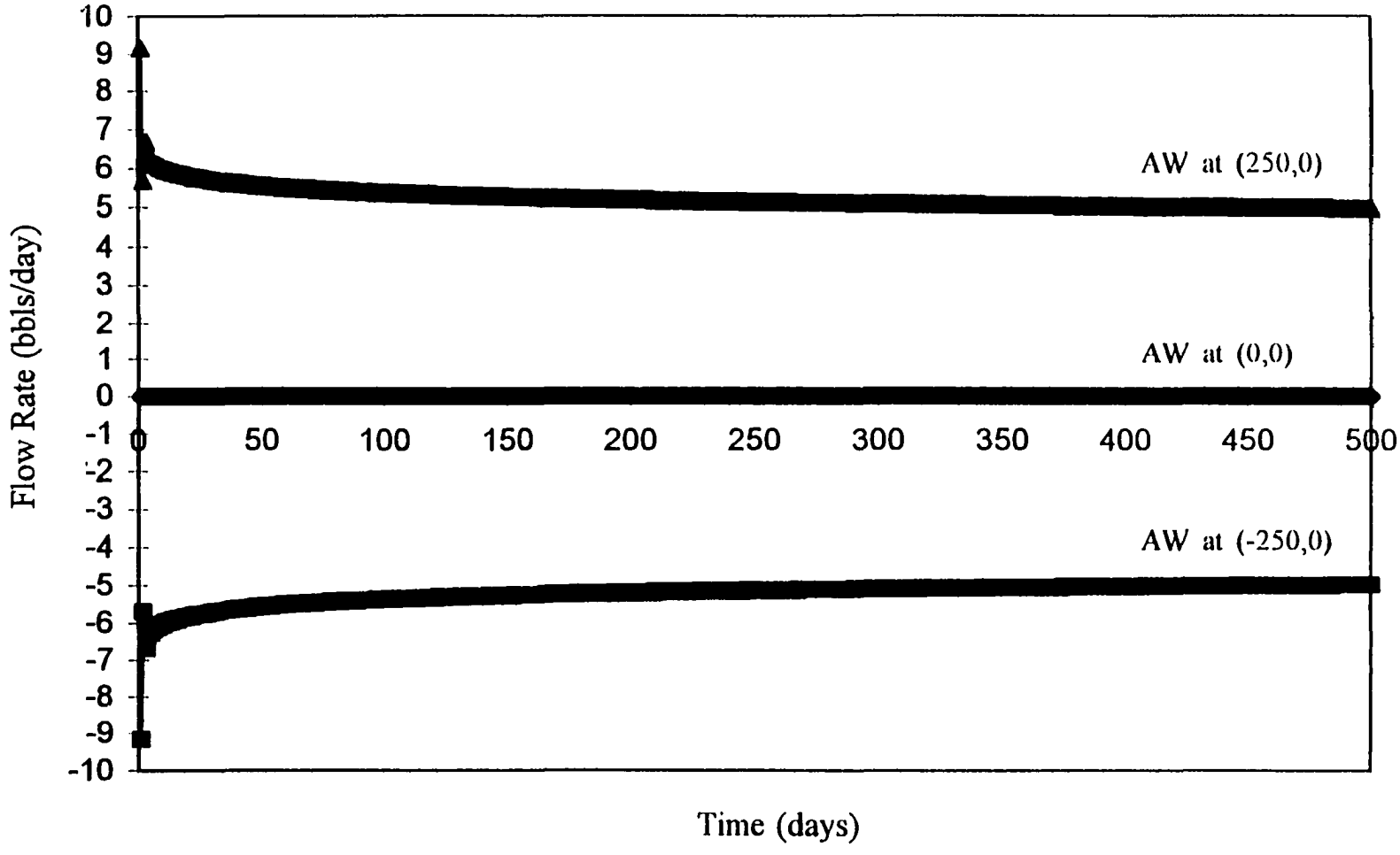


Figure 37. Case 9 comparison of abandoned well flow for different abandoned well locations in response to one injector at (500,0) and one producer at (-500,0) both operating at 100 bbls/day.

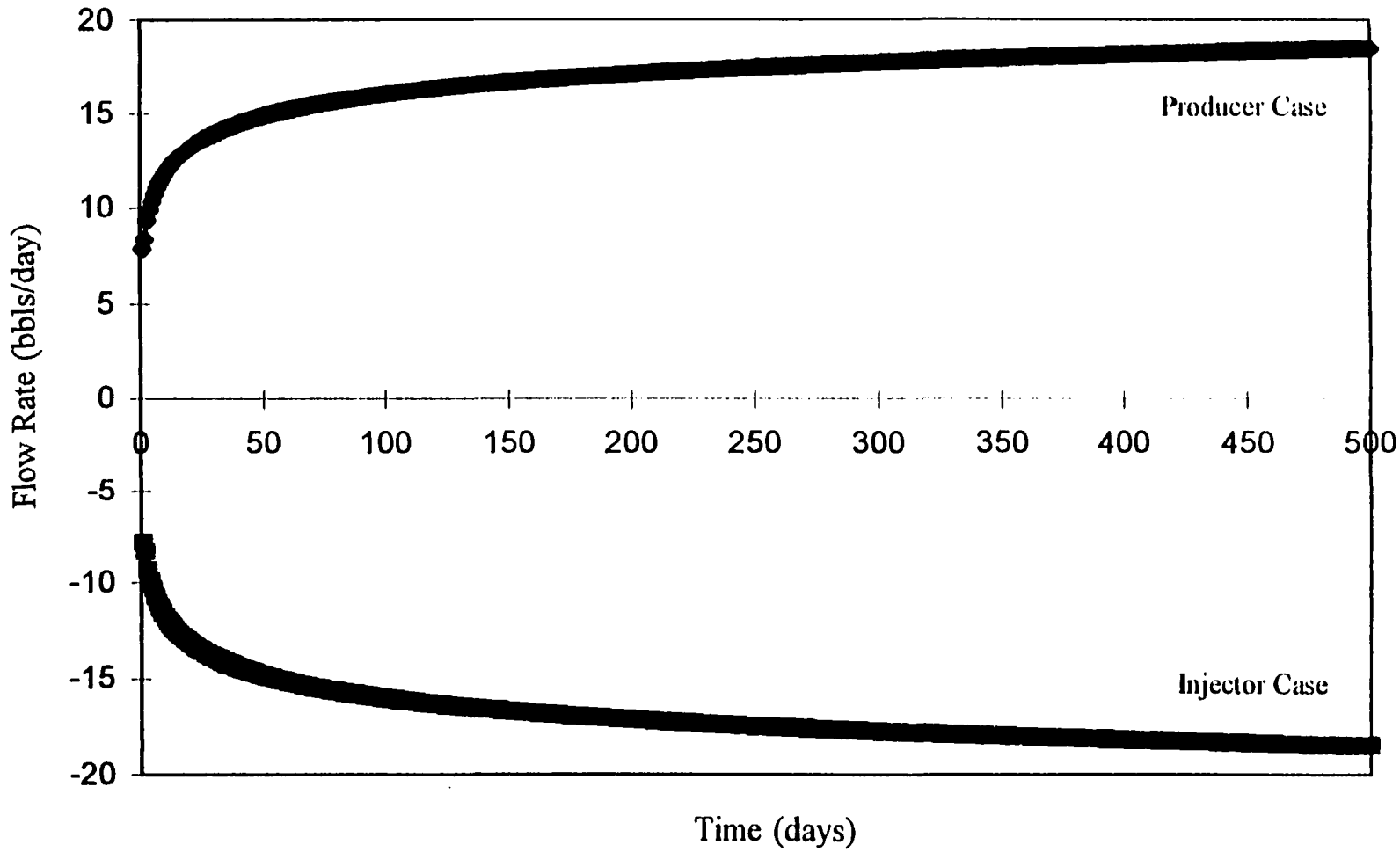


Figure 38. Case 10 comparison of abandoned well flow in response to an injector or producer in the upper formation with no active wells in the lower formation.

CHAPTER 6

FIELD CASE STUDIES

The 'series of steady states' coupled abandoned well model was shown in Chapter 5 to be a simple and flexible tool to predict abandoned well flow between formations. It can be applied for different formation properties and abandoned wellbore conditions. It is also unique in its ability to incorporate the impact of active wells in either formation on the flow. As a consequence of its versatility, it is especially suited to application to field data to predict abandoned well flow in response to operating conditions in the formations. As explained earlier in Section 1.1, the ability to predict abandoned well flow is necessary to meet 'Area of Review' (AOR) regulations for Class II injection wells. Aside from its use as a prediction tool, the model can also be employed as an assessment tool for cases of contamination suspected to be a consequence of fluid transport through abandoned wells.

This chapter examines the application of the model program to two field cases. The first example involves the use of the model as a prediction tool. For this case, the model is applied to determine if abandoned well fluid transport to an underground source of drinking water (USDW) will occur in response to a planned secondary recovery injection well in an oil reservoir. This field example was previously evaluated by Warner and McConnell[12] using a numerical simulation as presented in Section 2.2.

The second case involves the application of the model as an assessment tool to ascertain if suspected contamination of a particular formation can be attributed to abandoned well transport occurring in response to waste disposal operations in an

underlying formation. The field example for this case was a large waste injection disposal operation in Sarnia, Ontario which was presented by Lesage et al.[3] and Raven et al.[4]. These authors suspected abandoned wells as a source of contamination to overlying formations based on chemical fingerprinting of formation fluids but did not identify any abandoned wells or perform any abandoned well modeling to support this claim.

6.1 General Considerations for Field Application of Coupled Model

In Chapter 3, it was shown that the prediction of abandoned well flow between formations was dependent on several key factors. These factors included:

1. The rock/fluid properties and potentials of the coupled formations.
2. The number and rates of injection/production wells in the coupled formations.
3. The location and wellbore condition of the abandoned well.

In Chapter 5, the importance of these factors was confirmed and their particular influence on abandoned well flow was demonstrated. To obtain estimates of abandoned well flow which can be used with some confidence, it is essential that each of these factors be addressed in as much detail as possible. For field application of the model, however, the data to describe these factors is often not available and their values must be estimated using engineering judgment.

The first information critical to the model is the rock/fluid properties and pressures of the formations coupled by the abandoned well. The abandoned well model can be used to predict transport between any two formations of the user's choice. Rock properties

required for each of these formations include permeability, porosity, and thickness. Fluid properties are assumed to be the same in both formations and include density, viscosity and compressibility. It is also important to have the pressures for the formations. If pressures are not available, it may be possible under certain conditions to assume the formations are normally pressured. If the pressure head of the formation undergoing injection is less than the distance between the coupled formations, their is no hydraulic connection and the model program reports that flow can not occur. The pressure head in the lower formation must be shown to support a condition of a wellbore full of fluid between the formations before the program will execute.

For Class II injection well regulations, the permeable formations which act as USDW are singled out for evaluation when considering abandoned well fluid transport from the injection zone. However, there may be many formations above the injection zone which are permeable enough to receive fluid and act to divert fluid from the USDW. Therefore to consider all possible formation combinations for fluid transport from the injection formation, it is essential to identify the rock properties of all the permeable and impermeable zones the abandoned well penetrates.

For a particular operation involving injection for secondary recovery or fluid disposal, the rock properties of the injection zone are usually well documented by logs, cores, and well testing. Average pressure can be obtained from shut-in tests. Overlying formations which act as USDW are usually as well described. The problem lies in obtaining the rock properties of the formations between the USDW and the injection zone. This region is important because intermediate permeable zones can act to divert fluid and

minimize transport to USDW. Pressures in these formations are generally documented in drilling logs or can be assumed to be normally pressured if no wells are operating. If active wells are present in such a zone, shut-in tests may be available. The geology, thickness, and porosity of the overlying formations can usually be identified by well logs in the region. Unfortunately, permeability values which are obtained from cores and well testing are not usually available. The assignment of permeability to these overlying formations then becomes a matter of engineering judgment based on the geology and porosity.

The second type of information which is critical to the model is the location, number, and operating data of active production and injection wells in the coupled formations. Once again for the injection zone, this information is generally available for both secondary recovery operations and waste disposal operations and includes injection and production rates and times of operation. Overlying USDW production/injection information is also generally available. The problem lies in determining the operation of any injection or production wells in permeable formations between the injection zone and the USDW. For example, brine aquifers overlying the injection zone may be tapped as an injection water source or disposal operations may be occurring in an overlying formation. The existence of such operations in intermediate formations will greatly influence the abandoned well transport. In all cases, efforts must be made to determine the location and operations of active wells in the overlying formations.

The third type of information necessary to the modeling is the determination of the abandoned well location and its wellbore condition. The location of the abandoned well is one of the most critical factors in the modeling and also one of the most elusive. The

number of wells abandoned between 1859 and 1974 has been estimated at greater than 1.6 million and a large number have either unknown or inaccessible locations[1,2]. Wells abandoned before 1930 are of special concern because abandonment practices were not established prior to this date. Determining the location of undocumented abandoned wells is difficult and magnitude of the problem has not lead to any easy or certain solution[31].

The AOR regulations for Class II injection wells require that all abandoned wells which penetrate the injection formation within a quarter mile of a proposed injection well must be identified and evaluated for their potential to allow transport to USDW. For field cases, the records for any documented abandoned well locations within this radius can be evaluated to determine depth of penetration and completion information on casing and borehole size. The plugging practices used for the abandonment may also be available. Wells abandoned before 1930 are of particular concern as previously mentioned.

Once the known abandoned wells are identified, the model can be used to determine any transport through them to USDW. If the abandonment plugging procedures are documented, the length and permeability of the plugs can be entered into the model to estimate transport. If plugging practices are unknown for a well, the well can be assigned a hypothetical condition. The model allows the user to assign any number of wellbore conditions as discussed in Section 3.3. For example, realistic conditions include a cased well with a perforation near a permeable zone or an open well with sloughed shales in the wellbore. In 'worst case' scenarios, it may be assumed to be totally open or totally plugged with an annulus open to flow.

The model can also be applied to evaluate the transport through any undocumented wells. Abandoned well locations can be assumed at any location within the quarter mile radius of the injection well. For example, well locations could be set at 500 ft, 1000 ft, 2000 ft from the injection well. Wellbore conditions for undocumented wells can be assigned as desired by the user. Then the model can be run separately for each location and condition to predict the flow that would occur through this well. If the model indicates transport is probable for these hypothetical well locations, a search for undocumented abandoned wells can be undertaken.

6.2 Evaluation of Potential for Abandoned Well Flow from Lower Tuscaloosa Sand Trend in Mississippi

The first field case demonstrates the use of the coupled model as a prediction tool. The study is based on the work published by Warner and McConnell[12] who investigated the potential for abandoned well transport to USDW in response to a planned secondary recovery injection well in the Lower Tuscaloosa Sand trend in Mississippi. Warner and McConnell[12] used numerical simulation for their predictions and a summary of their work and results was presented and discussed in Section 2.2. The case was re-evaluated using the data collected in their study and the coupled model.

The numerical simulation of Warner and McConnell[12] included one injection well and one abandoned well 500 ft apart. The abandoned well was given two possible wellbore conditions. The first was for a open wellbore with sloughed shales and drilling

muds in the well. The second was for a cased well with a perforation next to a permeable zone. The numerical simulation was separately run for each of these cases using two different injection rates and injection zone permeabilities. Given the highly obstructed wellbore conditions, the simulations showed no flow to overlying formations for any of the examples.

The work of Warner and McConnell[12] was presumably limited to these cases because of the complexity involved in preparing the simulation grids and also the amount of time required for each simulation run. The coupled model's versatility, however, allows the prediction to be quickly performed for numerous cases. Changes in the abandoned well location are easily made. The coupled model may also be run for numerous and variable injection rates. The model can also include other active wells in the injection zone and in the overlying permeable formations. Finally the model is capable of addressing many wellbore conditions. This versatility allows the model to be used to quickly examine numerous factors which can affect the abandoned well flow rate in a particular setting.

The first information necessary to the application of the coupled model was the rock/fluid properties and pressure of the formations in the trend. Warner and McConnell[12] had prepared an extensive description of the geology of the formations above the Lower Tuscaloosa Sand trend using well logs. The geological cross section they used in their work is shown in Figures 10 and 11 along with their assumed abandoned wellbore conditions. Warner and McConnell[12] also described the fluid properties of the injection zone as density of 67.3 lb/ft^3, viscosity of 1 cp, and compressibility of $3x10^{-6}$/psi. Unfortunately, they did not state the pressures of any formations.

For the coupled model, it is first necessary to identify the permeable and impermeable zones in the region. Using the data of Warner and McConnell[12], the geological cross section was reduced to impermeable and permeable zones as shown in Figure 39. The rock properties and depths for these formations were documented by Warner and McConnell[12] and are shown in Figure 39. Based on this figure, it can be seen there are three permeable formations overlying the injection zone. They are the Upper Tuscaloosa Sand, the Wilcox Sand and the Sparta Sand. The Sparta Sand was identified as a USDW. The model may be used to evaluate transport from the Lower Tuscaloosa to any of these permeable formations individually.

The second information necessary to the model is the number, location and operating data on the active wells in either of the coupled formations. Warner and McConnell[12] limited their study to just one injection well 500 ft from the abandoned well operating at 200 or 600 bbls/day. In a secondary recovery project, however, there are also production wells present in the injection zone and their impact on the abandoned well flow was shown to be of great significance in Section 3.2. It is also important to consider the presence of a production well in overlying formations, such as an USDW, which may act as a municipal water source.

The final type of information critical to the case study is the condition of the abandoned wellbore. The abandoned well was completed using 5 1/2 inch, 17 lb/ft N-80 casing. The casing inner diameter was therefore 4.892 inches. The roughness of the wellbore was assumed to be .00015 for steel. The borehole size was not given and was assumed to be 7 inches. Warner and McConnell[12] evaluated flow for two wellbore

conditions as described previously in which the wellbore and annulus were effectively plugged by large amounts of sloughed shales and settled drilling muds. Warner and McConnell[12] however did not consider the case for an open well or a cased well with a perforation across from the permeable zone.

Any of the permeable formations may be coupled to the Lower Tuscaloosa Sand injection zone in the model to evaluate transport through an abandoned well with different wellbore conditions. For this field example, the cases of greatest concern are those that result in transport to USDW. Therefore this study will be limited to the determination of the 'worst case' scenarios in which transport occurs from the Lower Tuscaloosa injection zone to the Sparta Sand.

To determine 'worst case' scenarios it is important to consider the nature of the operation. The project under consideration is a water injection well for secondary recovery. Before secondary recovery is initiated, the reservoir has usually already undergone pressure depletion so it may be possible that there is not enough pressure head in the Lower Tuscaloosa to provide a hydraulic connection to the USDW. If the pressure in the Lower Tuscaloosa is sufficient to reach the Sparta, it is only likely to happen in a cased well with a perforation next to these formations. This is because in an open well the fluid would have flowed into the Upper Tuscaloosa or Wilcox before reaching the USDW as shown by Warner[11].

The 'worst case' scenario is therefore for transport to the Sparta Sand USDW through a perforation in the casing. The study will therefore examine transport through a cased abandoned well for a one inch perforation placed at a depth of 3150 ft in the middle

of the Sparta Sand for varying operations in the formations. Because Warner and McConnell[12] did not provide any pressure data for the formations, they were treated as normally pressured and hydrostatic. Using a elevation datum of z equal to zero at the middle of the Lower Tuscaloosa, the potential in both the Lower Tuscaloosa and the Sparta will be hydrostatic at about 4896 psi. This assumption will produce the most transport because in reality the potential in the Lower Tuscaloosa after depletion should be less than the Sparta. Two cases will be run to demonstrate the transport expected through a newly opened one inch perforation when the Lower Tuscaloosa has a potential which is 500 and 200 psi less than the Sparta.

For the prediction of transport with an initial hydrostatic condition between the two formations, the first case evaluated will be for one injection well operating in the Lower Tuscaloosa. Then a second case will be run to include the impact of one producing well in the Lower Tuscaloosa. The third case will include one injection and production well in the Lower Tuscaloosa and a municipal water well operating in the Sparta Sand. All cases will be run first as an open cased wellbore and next with a 100 ft 1.0 md plug. For the fourth and fifth case where the initial condition is not hydrostatic, only one injection well will be operating in the Tuscaloosa and the wellbore will be cased and open with a perforation. All other data required for these cases were given by Warner and McConnell[12] including the rock/fluid properties for the two formations, the casing and borehole sizes, and the pipe roughness.

In summary, the 'Prediction Worst Case' (PWC) scenarios to be evaluated in the field study of the potential for abandoned well flow to USDW in the Lower Tuscaloosa Sand trend are:

1. PWC #1. Cased abandoned well at (0,0) with 1 inch perforation at 3150 ft next to Sparta Sand. Coupled formations are in hydrostatic equilibrium at a potential of 4896 psi. Lower Tuscaloosa Sand has one injection well operating at 600 bbls/day at (500,0). No active wells are in the Sparta Sand. Abandoned wellbore may be open or with one 100 ft 1.0 md plug.
2. PWC #2. Cased abandoned well at (0,0) with 1 inch perforation at 3150 ft next to Sparta Sand. Coupled formations are in hydrostatic equilibrium at a potential of 4896 psi. Lower Tuscaloosa Sand has one injection well operating at 600 bbls/day at (500,0) and one active production well operating at 300 bbls/day at (-500,0). No active wells are in the Sparta Sand. Abandoned wellbore may be open or with one 100 ft 1.0 md plug.
3. PWC #3. Cased abandoned well at (0,0) with 1 inch perforation at 3150 ft next to Sparta Sand. Coupled formations are in hydrostatic equilibrium at a potential of 4896 psi. Lower Tuscaloosa Sand has one injection well operating at 600 bbls/day at (500,0) and one active production well operating at 300 bbls/day at (-500,0). One active municipal water well is operating at 600 bbls/day in the Sparta Sand at (500,0). No active wells are in the Sparta Sand. Abandoned wellbore may be open or with one 100 ft 1.0 md plug.

4. PWC #4. Cased abandoned well at (0,0) with newly opened 1 inch perforation at 3150 ft next to Sparta Sand. Lower Tuscaloosa is at a potential of 4396 psi and the Sparta Sand is at a potential of 4896 psi. Lower Tuscaloosa Sand has one injection well operating at 600 bbls/day at (500,0). No active wells are present in the Sparta Sand.
5. PWC #5. Cased abandoned well at (0,0) with newly opened 1 inch perforation at 3150 ft next to Sparta Sand. Lower Tuscaloosa is at a potential of 4696 psi and the Sparta Sand is at a potential of 4896 psi. Lower Tuscaloosa Sand has one injection well operating at 600 bbls/day at (500,0). No active wells are present in the Sparta Sand.

The input data files for Case PWC #1, PWC #2, and PWC #3 for an open wellbore are given in Appendix D Figures D.1, D.2, and D.3. All cases were run for a total of 500 days using 1 day time steps. The choice for steady state radius location was placed at 50% for both formations. Portions of the output file for each case are shown in Tables D.1, D.2, and D.3 respectively for the first 25 days. The output files show not only flow rates but also the cumulative flow and the potential values as a function of time for both the reservoir and the USDW. The potential values allow the user to check the pressure trends in the coupled formations for consistency.

Figure 40 displays the flow rate results for PWC #1 and PWC #2 for an open wellbore. This figure shows that for an initial hydrostatic condition the addition of an injection well in Case PWC #1 to the Lower Tuscaloosa will produce very large flow

rates. When the producing well is added in Case PWC #2, these rates show a substantial decrease in response to the pressure relief incurred by the production well.

Figure 41 exhibits the results for PWC #1 and PWC #3 with an open wellbore. Once again the single injection well in PWC #1 produces large flows. The addition of the producing well in the Lower Tuscaloosa and a municipal water well in the Saprta for PWC #3 produce almost the same results as PWC #2. This result is not unexpected. At first one may think the addition of a producing well in the Sparta would greatly increase transport but the Sparta is highly transmissive with a thickness of 700 ft and a permeability of 1 Darcy. Therefore the pressure decrease around the abandoned well in the Sparta is only enough to increase the flow by about 0.25 bbls/day.

The cases of PWC #1, PWC #2 and PWC #3 were next run with the addition of a 100 ft 1.0 md plug. The input files for these case only required the addition of the plug data and are otherwise identical to the input files for the open well case. All cases were run for 500 days with time steps of 1 day. Portions of the output file for each case are shown in Tables D.4, D.5, and D.6, respectively, for the first 25 days.

Figure 42 displays the flow rate results for PWC #1 and PWC #2. As shown in the figure, the flow rate is dramatically reduced to negligible values for the two cases when a plug is added. PWC #1 shows a slightly larger flow rate for the one injector case as expected. The results for PWC #3 are indistinguishable from PWC #2 because of the small impact of the water well in the Sparta on the flow rate and were not plotted. All these examples corroborate the original work done by Warner and McConnell[12] who also showed the elimination of flow in the presence of plugs. These authors, however used

much larger plug lengths and lower permeabilities as presented in Section 2.2. These cases all demonstrate the physical reality that even a small porous media resistance in the wellbore in the form of plugs essentially eliminates all flow between formations.

The final cases evaluated in this field study were for one injector in the Lower Tuscaloosa in the presence of a non-hydrostatic initial potential condition. This condition was created by assuming the reservoir had undergone depletion before the injection and the perforation at the Sparta was opened at time equal to zero. The input file for PWC #4 and PWC #5 are exactly the same as PWC #1 in Figure D.1 except the original pressure in the reservoir was assumed to be 4396 psi and 4696 psi respectively. The case was also run for 500 days and with 1 day time steps. The choice for steady state radius location was placed at 50% for both formations. A portion of the output file for the cases are shown in Tables D.7 and D.8 for the first 25 days.

The flow rate results for PWC #4 are shown in Figure 43. The figure clearly shows that flow is moving downhole from the Sparta Sand to the Tuscaloosa Sand in response to the 500 psi potential gradient. The flow is decreasing in time because the injection well is creating a pressure buildup. At some late time this pressure buildup may lead to a zero flow rate which will finally reverse flow up the wellbore to the Sparta. If a production well is added, the reversal of flow may not occur and flow will continuously remain downhole, never posing a threat to USDW except to deplete the aquifer.

The flow rate results for PWC #5 are shown in Figure 44. The figure clearly shows that flow is initially moving downhole from the Sparta Sand to the Tuscaloosa Sand in response to the 200 psi potential gradient. The flow is decreasing in time because the

injection well is creating a pressure buildup. At 10 days this pressure buildup leads to a zero flow rate which then reverses flow up the wellbore to the Sparta. If a production well is added to the reservoir, the reversal of flow may not occur and flow will continuously remain downhole, never posing a threat to USDW except to deplete the aquifer.

Cases PWC #4 and PWC #5 demonstrate an important point about abandoned well flow. With coupled formations, the abandoned well will flow in either direction depending on the gradient between them. The very real possibility of downward flow has been neglected in the study of abandoned well flow as discussed in Section 5.2. However, it must be considered a probable scenario, especially when evaluating Class II injection wells in reservoirs undergoing secondary recovery. These reservoirs are often at a lower potential than overlying formations from primary production so the coupled gradient favors downward flow. The reservoirs also possess numerous injection and production wells so any pressure buildup is optimally consumed by the production. Therefore, in a secondary recovery project, an abandoned well should experience upward flow to only a limited degree if near an injector, or the abandoned well should experience downward flow if near a producer. It is therefore critical when evaluating abandoned well flow to consider the impact of all active wells in the reservoir. The coupled model is the first which allows these cases to be investigated to show how all these factors mitigate the possibility of flow to USDW.

In summary, the field study to predict abandoned well flow from the Lower Tuscaloosa Sand to the Sparta USDW in the Lower Tuscaloosa trend shows varying results depending on formation potentials, wellbore condition and active well operations.

The definition of these factors is dependent on the availability of information on the geological setting, abandoned wells and proposed operations. For the case of the Tuscaloosa Sand trend, the geological setting was well defined by Warner and McConnell[12] and the abandoned well condition was estimated for 'worst case' scenarios. Unfortunately, information on original pressures and secondary recovery operations was not available and was estimated.

Transport to the Sparta Sand USDW was demonstrated through an abandoned well perforation for cases PWC #1, PWC #2 and PWC #3, all of which had an open wellbore and an initial hydrostatic condition. Transport was most severe for a single injection well in the reservoir and the flow was greatly reduced by the addition of a producing well in the reservoir. For true secondary recovery operations the flow should be even less as the production and injection operations will be balanced. The addition of a producing water well in the highly transmissive Sparta Sand had little impact on the flow rate. When a plug was added to wellbore in these cases, the flow to the USDW was effectively eliminated. In Cases PWC #4 and PWC #5, the Sparta was initially at a higher potential than the depleted Lower Tuscaloosa Sand and one injection well was present in the reservoir. The results showed that flow will be downhole from the USDW to the reservoir and the injection buildup may reverse the flow up hole.

6.3 Evaluation of Suspected Abandoned Well Flow from the Lucas Formation in Sarnia, Ontario

The second field case demonstrates the use of the coupled model as an evaluation tool to determine if abandoned well transport of fluids has occurred for a particular operation. The example is based on the work of Lesage et al.[3] and Raven et al.[4] who investigated suspected abandoned well contamination from a large waste disposal injection operation. Over 17 years from 1958 to 1974, a total of approximately 1.7 billion gallons of industrial waste composed of spent caustic, phenols and sulfides was injected into the Lucas formation at Sarnia, Ontario through eight injection wells operating at rates ranging from 250 to 2500 bbls/day[3,4]. During the disposal operations, several occurrences of waste flow on the surface occurred within 3-4 km of the disposal wells although exact locations were not reported[3,4]. Because the region was an oil and gas producing area during the late 1800's and early 1900's, abandoned wells were suspected as the source of the surface flow. They were also suspected of causing contamination to formations overlying the Lucas including the Fresh Water aquifer which was a USDW[3,4]. Neither of the studies[3,4], however, identified the location or condition of any abandoned wells so the suspicions remain speculative. The coupled model was therefore applied to determine if an unknown abandoned well could have been the source of contamination.

The area of waste disposal and the locations of the eight disposal wells to the Lucas Formation in Sarnia, Ontario are shown in Figure 45[3]. A multi-level monitoring well reaching the Lucas and a network of shallow Fresh Water aquifer monitoring wells used to

identify contamination are also shown in Figure 45. The geological cross section of the region and typical disposal well used in the operation are shown in Figure 46[3].

The Lucas formation was identified by Raven et al.[4] as micro-crystalline dolomites with halite and anhydrite layers. The Lucas is overlain by the Dundee limestone which is oil and gas bearing and reported to contain numerous exploratory wells[3]. The Hamilton Group overlying the Dundee is composed of several layers of shale and limestone. It contains two permeable limestone layers, the Rockport Quarry and Hungry Hollow, which are gas bearing. The Kettle Point formation is composed of black bituminous shales and forms the bedrock surface for the region. The Fresh Water aquifer is a thin sand, gravel and fractured shale aquifer which serves as a USDW. The Fresh Water aquifer is overlain by approximately 100 ft of clay till.

The regional geology, operations, and contamination at the Sarnia disposal site were studied by Raven et al.[4] and Lesage et al.[3] Raven et al.[4] employed a 300 m deep multi-level monitoring well to the Lucas formation to assess the geochemical and hydrogeologic conditions in the subsurface formations. They found evidence of residual waste in the Lucas formation and some contamination in the Rockport Quarry and Hungry Hollow limestones of the Hamilton Group.[4] Lesage et al.[3] evaluated the nature and extent of any contamination to the Fresh Water aquifer using a network of 29 monitoring wells. They found no evidence of contamination to the Fresh Water aquifer. Based on the information provided in the studies performed by these authors, it was possible to apply the coupled model to evaluate if and how a hypothetical abandoned well could have acted

as a conduit for contamination transport from the Lucas to these overlying permeable formations.

The first step in the application of the coupled model as an evaluation tool to ascertain if abandoned well transport has occurred was to identify the permeable formations which could be coupled to the injection zone. Based on specific information on the geological cross section at the multi-level monitoring well and Disposal Well #1 given by Lesage et al.[3] and Raven et al.[4], a cross section of permeable and impermeable zones was created for the model and is shown in Figure 47. The permeable zones included the Lucas formation, the Rockport Quarry limestone, the Hungry Hollow limestone and the Fresh Water aquifer. The permeabilities of these formations from core analysis and pressure testing were reported by Raven et al.[4] and are shown in Figure 47. Only the porosity of the Lucas was reported[4]. The porosities of the other permeable zones were estimated in this work and are shown in Figure 47.

Next, the fluid properties in the formations were required. Unfortunately, very little information was reported on the nature of the waste fluid, excepting one evaluation of its chemical composition which showed it to be essentially an aqueous solution with concentrations of phenol, ammonia, and mercaptans. As the coupled model is single phase, it was assumed that the aqueous waste fluid would be diluted by the Lucas formation fluids to allow the model application to be based on the properties of the Lucas formation brine. The density of the brine in the Lucas was given by Raven et al.[4] as about 67 lb/ft^3. The compressibility and viscosity were not reported and were estimated to be $3x10^{-6}$/psi and 1 cp respectively.

The next data required in the model were the pressures in the injection zone and the permeable zones. Injection into the Lucas formation began in 1958 and continued through 1974. Raven et al.[4] reported that there was no information available on pre-disposal pressures. In May 1988, Raven et al.[4] measured pressures in the formations in 26 packer isolated zones in the multi-level monitoring well. The measurements were reported as freshwater heads and have been converted to pressures in this study. The Lucas formation had a pressure of 278 psi at 630 ft which was somewhat underpressured. This value however clearly indicated that the buildup from the waste disposal operations had dissipated. The Rockport Quarry limestone was found to contain gas and was highly overpressured at 315 psi at 395 ft. The Hungry Hollow limestone was also found to be gas bearing and overpressured at 176 psi at 233 ft. Raven et al.[4] noted that similar observations of high pressures have been made in the Hamilton Group shales and limestones of southern Ontario and stated that the cause was unknown. They did indicate the presence of 'squeezing' shales in the Hamilton Group, which are often identified with overpressured zones. Finally, the pressure in the Fresh Water aquifer was reported to be 44 psi at 100 ft which was close to normally pressured.

The next information required in the model was the number, location, and operating data on the active wells present in the coupled formations. Figure 45 displays the locations of all the active disposal wells in the operation. For the purposes of evaluating abandoned well flow transport in the current study, it was decided to limit the investigation to Disposal Well #1. This well was chosen because it was close to the multi-level deep monitoring well which showed contamination. It was also close to two fresh

water aquifer monitoring wells which showed no evidence of contamination. Disposal Well #1 well was completed into a 157 ft thick section of the Lucas formation and operated at an average rate of 1200 bbls/day from 1958-1967. No active wells were noted to be in the overlying permeable formations and water withdrawals from the Fresh Water aquifer were not reported.

The final information necessary to the model was the location and condition of the abandoned wells in the regions. Unfortunately, none of the studies identified the location or condition of any abandoned wells in the Sarnia region. It was reported, however, that the region had numerous oil and gas exploratory wells drilled in the late 1800s and early 1900's. It was therefore assumed that some of these wells reached the Lucas formation. Since the wells were drilled before 1930, no consistent abandonment procedures were practiced and it is possible that some of these wells were not plugged. The wells may be cased or uncased. If cased, they are likely to be severely compromised. Therefore for a 'worst case' scenario, it was assumed that the abandoned well would be unplugged and uncased. The average wellbore size was unknown and was estimated to be 7 inches. As formations in the region were identified as having shale, it was possible that the wellbore would contain sloughed shales.

Based on the information available, several cases were run to assess if abandoned well transport could occur to the overlying formations in response to injection in Disposal Well #1. No abandoned well locations were identified in the region, so one was chosen to be located 2000 ft away from Disposal Well #1. This distance represented the distance between Disposal Well #1 and the multi-level monitoring well where contamination was

found. Since contamination was located in both the Rockport Quarry and Hungry Hollow formation, abandoned well transport to these zones was investigated in 'Sarnia Worst Case' SWC #1 and SWC #2, respectively. Abandoned well transport to the Fresh Water aquifer USDW was also investigated in SWC #3. Because pre-disposal pressures were unknown, two initial pressure scenarios were run for each case. In the first, the formation pressure values reported by Raven et al.[4] were used. In the second, all the formations were assumed to be normally pressured. The potential datum was assumed to be zero at the middle of the Lucas formation at 630 ft. Finally, in SWC #4, SWC #5, and SWC #6, all three cases were re-run with a wellbore containing 100 ft of 0.1 md sloughed shale using the pressures reported by Raven et al.[4]

In summary, the cases to evaluate the abandoned well transport from the Lucas Formation to overlying permeable zones are described as follows:

1. SWC #1 a and b. Abandoned well at (0,0) open to the Rockport Quarry Limestone. One injection well operating in the Lucas formation at (2000,0) at a rate of 1200 bbls/day. For (a), the Lucas formation is at a pressure of 278 psi and the Rockport Quarry is at 315 psi. For (b), the Lucas formation and Rockport Quarry are at a hydrostatic potential of 300 psi.
2. SWC #2 a and b. Abandoned well at (0,0) open to the Hungry Hollow Limestone. One injection well operating in the Lucas formation at (2000,0) at a rate of 1200 bbls/day. For (a), the Lucas formation is at a pressure of 278 psi and the Hungry Hollow is at 176 psi. For (b), the Lucas formation and Hungry Hollow are at a hydrostatic potential of 300 psi.

3. SWC #3 a and b. Abandoned well at (0,0) open to the Fresh Water aquifer. One injection well operating in the Lucas formation at (2000,0) at a rate of 1200 bbls/day. For (a), the Lucas formation is at a pressure of 278 psi and the Fresh Water aquifer is at 44 psi. For (b), the Lucas formation and Fresh Water are at a hydrostatic potential of 300 psi.

4. SWC #4. Abandoned well at (0,0) open to the Rockport Quarry Limestone. One injection well operating in the Lucas formation at (2000,0) at a rate of 1200 bbls/day. The Lucas formation is at a pressure of 278 psi and the Rockport Quarry is at 315 psi. The wellbore contains 100 ft of sloughed shale with 0.1 md permeability.

5. SWC #5. Abandoned well at (0,0) open to the Hungry Hollow Limestone. One injection well operating in the Lucas formation at (2000,0) at a rate of 1200 bbls/day. The Lucas formation is at a pressure of 278 psi and the Hungry Hollow is at 176 psi. The wellbore contains 100 ft of sloughed shale with 0.1 md permeability.

6. SWC #6. Abandoned well at (0,0) open to the Fresh Water aquifer. One injection well operating in the Lucas formation at (2000,0) at a rate of 1200 bbls/day. The Lucas formation is at a pressure of 278 psi and the Fresh Water aquifer is at 44 psi. The wellbore contains 100 ft of sloughed shale with 0.1 md permeability.

The input data files for Case SWC #1a, SWC #2a, and SWC #3a are given in Appendix E in Figures E.1, E.2, and E.3. All cases were run for a total of 500 days using 1 day time steps. The choice for steady state radius location was placed at 50% for both

formations. Portions of the output file for each case are shown in Tables E.1, E.2, and E.3 respectively for the first 25 days. The output files show not only flow rates but also the cumulative flow and the potential values as a function of time for both the Lucas and the overlying formation. The potential values allow the user to check the pressure trends in the coupled formations for consistency.

Figure 48 displays the flow rate results for SWC #1 a and b. This figure shows that for initial condition (a), where the Rockport Quarry is overpressured, the flow will be downhole for about ninety days and will then reverse. This leads to an abandoned well flow rate of about 60 bbls/day by 500 days in response to the large injection rate. If the Lucas and Rockport Quarry are in hydrostatic equilibrium as shown in (b), the rates of transport are even greater. Based on these results, it is probable that if an open abandoned well was present, it could have acted as a conduit for contamination to the Rockport Quarry as suspected. In fact, since the injection operation was carried out for many years at high rates, even larger flow rates would be expected.

Figure 49 shows the flow results for abandoned well transport to the Hungry Hollow as described in Case SWC #2 a and b. The results show that in the normally pressured and overpressured cases, flow rates of 90 and 75 bbls/day, respectively, would be occurring from the Lucas to the Hungry Hollow by 500 days. Therefore, the source of contamination to the Hungry Hollow formation could also be attributed to abandoned well flow.

Figure 50 shows the flow results for Case SWC #3 a and b. As in the previous two cases, the program results show that if an abandoned well was present, almost 100

bbls/day of flow would occur to the Fresh Water aquifer from the Lucas formation in response to the injection rate at Disposal Well #1 by 500 days.

Based on the results of the first three cases, it can be seen that the operating conditions in the Lucas formation were sufficient to create abandoned well contamination to the Rockport Quarry, Hungry Hollow and Fresh Water aquifer in the Sarnia region. These results were based on a case for only 500 days and one disposal well. If the cases had been run for more time and the impacts of all the disposal wells had been included, the flow rates would be even greater. If abandoned wells had been located in the Lucas and were open to the overlying formations, the flow rates predicted by the model in these cases should have created a contamination event.

Raven et al.[4] reported the existence of some contamination to the Rockport Quarry and the Hungry Hollow formations which is supported by this modeling. However, in a study by Lesage et al.[3], the Fresh Water aquifer was found to have no evidence of contamination as verified by extensive testing of the 29 monitoring wells. Two of these monitoring wells were located near Disposal Well #1 and neither showed contamination.

The modeling in this study, however, indicates that if an open uncased abandoned well had been present fluid would have moved from the Lucas formation to the Fresh Water aquifer. The lack of contamination to this aquifer may be a consequence of several factors. The first explanation is that if the abandoned well was open to all the formations as assumed, the Rockport Quarry and Hungry Hollow layers would have taken on a substantial amount of the flow, therefore diverting it from the Fresh Water aquifer. Another explanation may be the presence of casing in the wellbore. Since the Fresh Water

aquifer lies around 100 ft below the surface, it is possible that surface casing was set and remains intact. If the lower hole was open, the flow would have been taken by the Hungry Hollow and Rockport Quarry formations and the Fresh Water aquifer would have been protected by this casing. It is also possible that very few wells were drilled into the Lucas formation, as the Dundee formation was the oil and gas bearing zone in the region. But this would not explain the contamination to the Rockport Quarry or Hungry Hollow. Until a search to determine the location and condition of abandoned wells in the region is undertaken, it is not possible to assess these cases.

The most likely reason for the lack of transport is the presence of plugging materials in the wellbore. Although no abandonment procedures were consistently practiced at the time most of the exploratory wells were drilled in the Sarnia region, it is possible that some plugs were set. It is also possible that the well could be plugged by sloughed or swelling shales. The regional geology of the Sarnia region shows that the Fresh Water aquifer is underlain by the Kettle Point Formation which is composed of black bituminous shales. Below this, the Hamilton group contains numerous shale layers including 15-18 m of Bell shale and 35 m of Arkona shale. Raven et al.[4] described the shales in the region as 'squeezing' shales which would prevent upward migration through fractures. In an open hole, the presence of large shale layers supports the existence of wellbore plugging by shales. The shales may either slough off into the wellbore or they may swell and plug portion of the well at different locations.

Figure 51 shows the flow results for Cases SWC #4, SWC #5 and SWC #6, which investigated the transport to each formation in the presence of a 100 ft 0.1 md shale plug.

This figure shows that in all cases, the flow is essentially eliminated. Since some contamination was located in the Rockport Quarry and Hungry Hollow formations, it is possible that the Kettle Point shale, which is located directly below the Fresh Water aquifer, swelled and effectively cutoff wellbore communication to the aquifer. As these shales are present under the aquifer in the entire Sarnia region, this could explain the lack of contamination to the entire Fresh Water aquifer in the presence of such large disposal operations.

In conclusion, the modeling in the Sarnia region shows the disposal operations in the Lucas formation would have produced large amounts of transport to overlying formations if one assumes open uncased abandoned wells had been present to act as conduits. The presence of major contamination, however, was not discovered in any of the formations in the region. The total lack of contamination to the Fresh Water aquifer could be a consequence of protection by casing, or interception of flow by the Rockport Quarry and Hungry Hollow formations. The most likely explanation, however, is the presence of shale plugging in the abandoned wellbore which would eliminate transport. It is also entirely possible that no abandoned wells are present in the Lucas. Until an attempt is made to assess the location and condition of the abandoned wells in the Sarnia region, it is not possible to determine exactly what role, if any, they played in contamination transport.

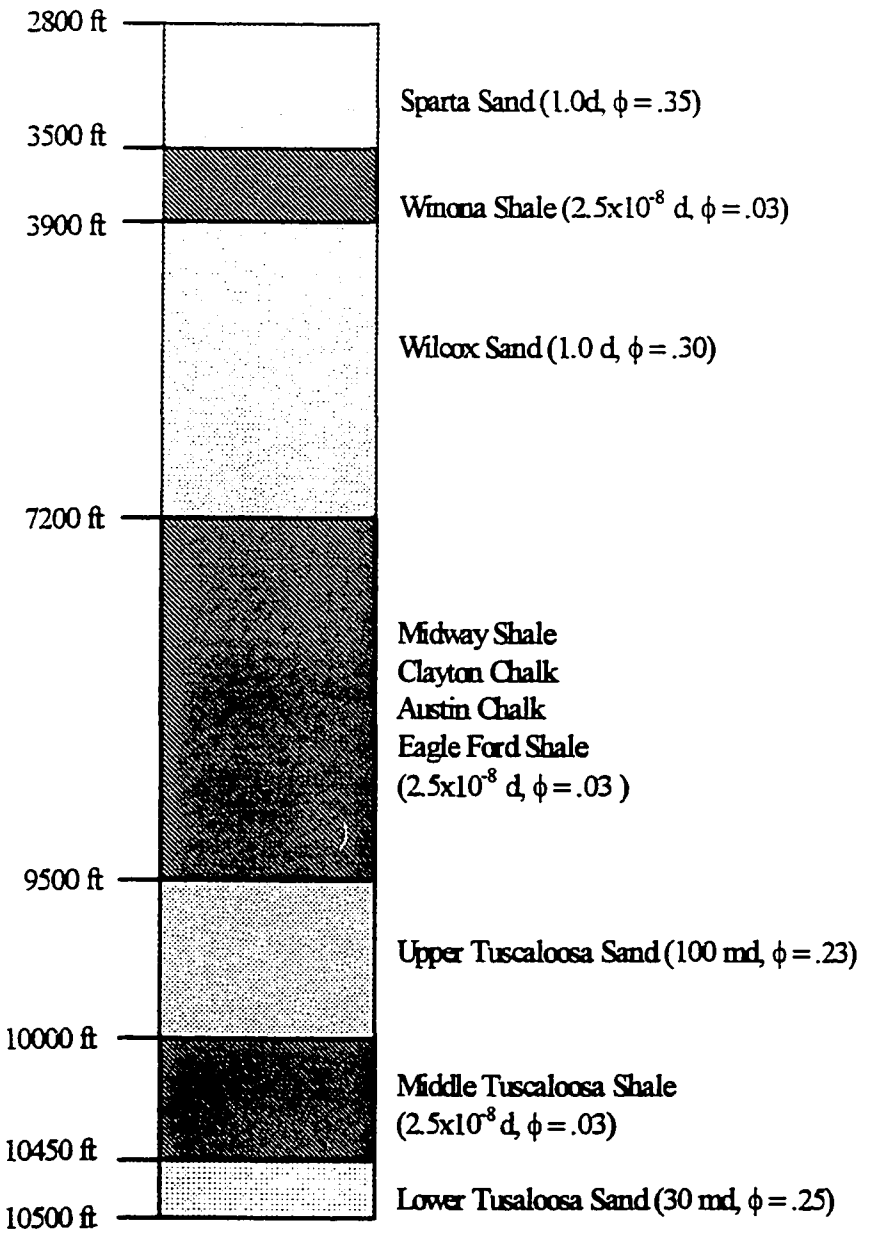


Figure 39. Cross section of Tuscaloosa Sand trend and overlying formations showing location and rock properties of permeable and impermeable zones.

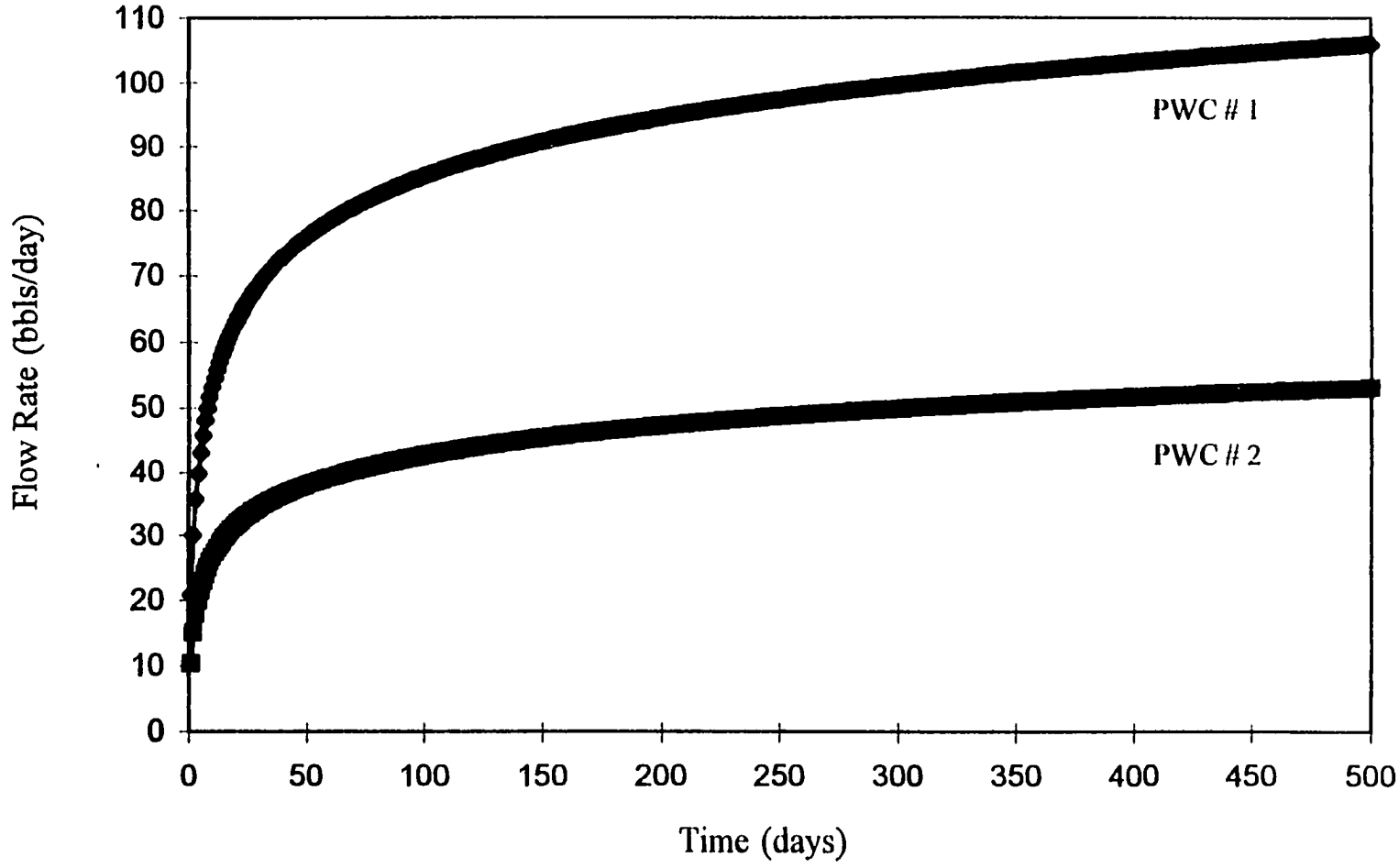


Figure 40. Comparison of abandoned well flow for cases PWC #1 and PWC #2 in the field study of the Tuscaloosa Sand trend.

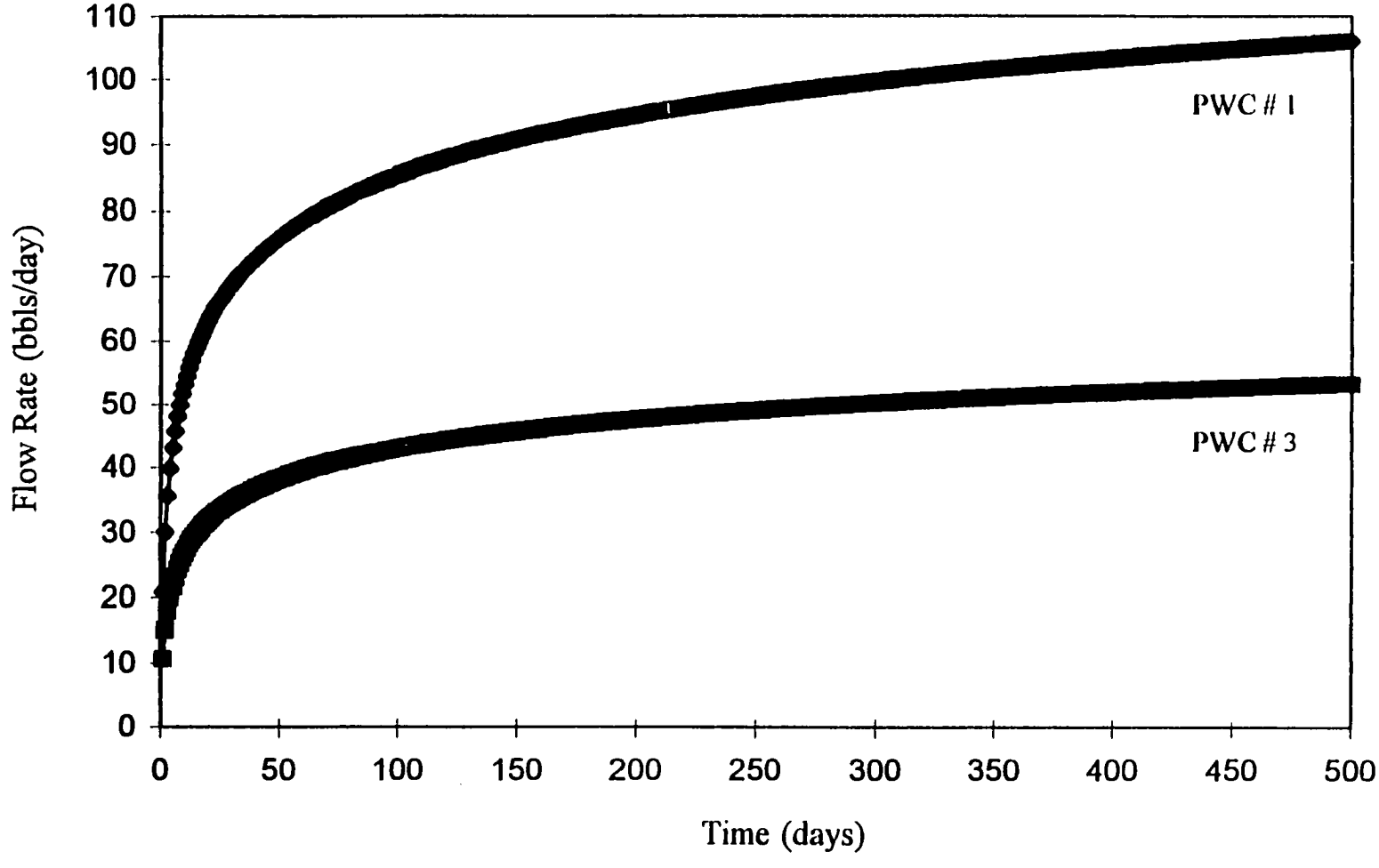


Figure 41. Comparison of abandoned well flow for cases PWC #1 and PWC #3 in the field study of the Tuscaloosa Sand trend.

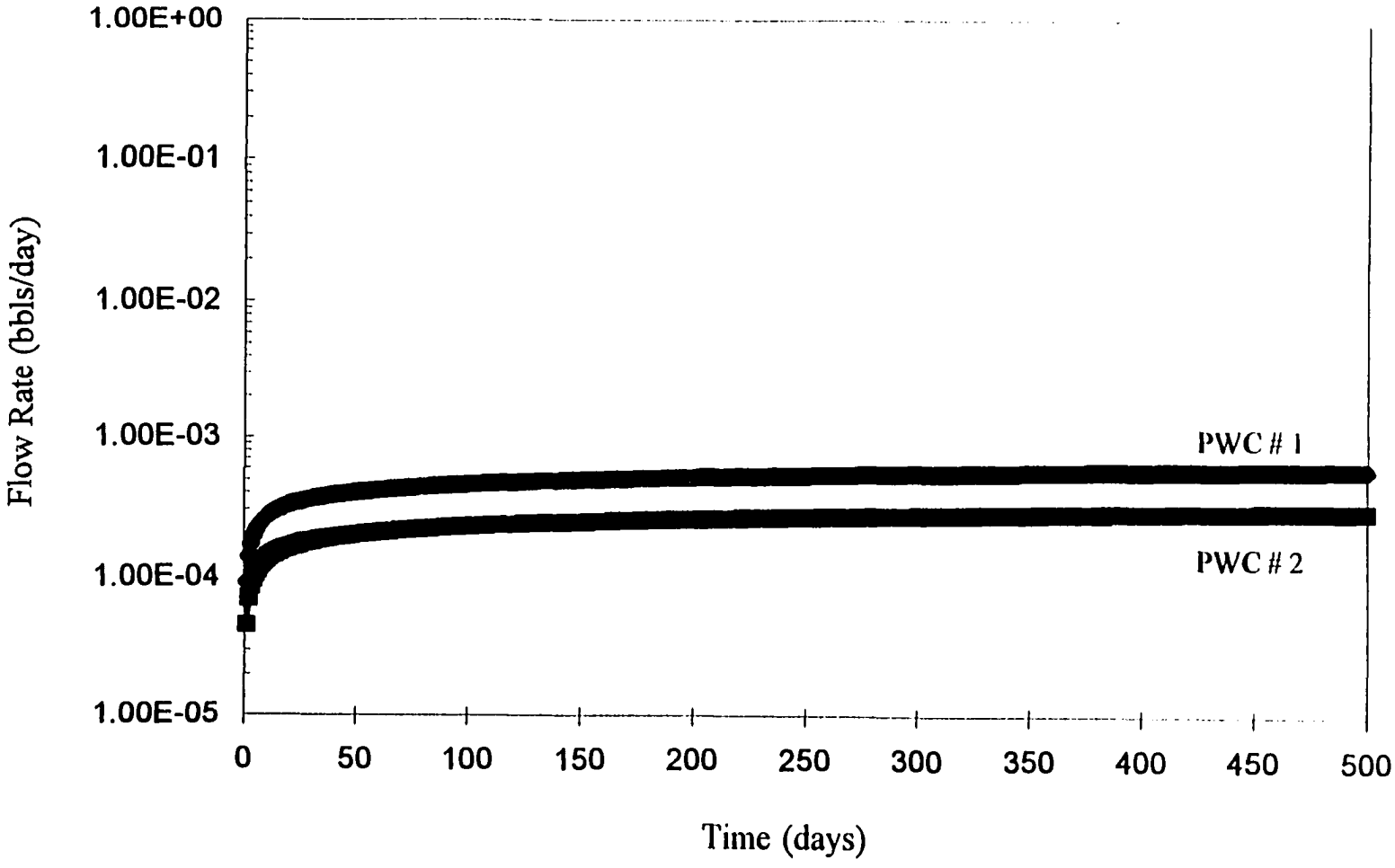


Figure 42. Comparison of abandoned well flow for cases PWC #1 and PWC #2 including a 100 ft 1.0 md plug in the field study of the Tuscaloosa Sand trend.

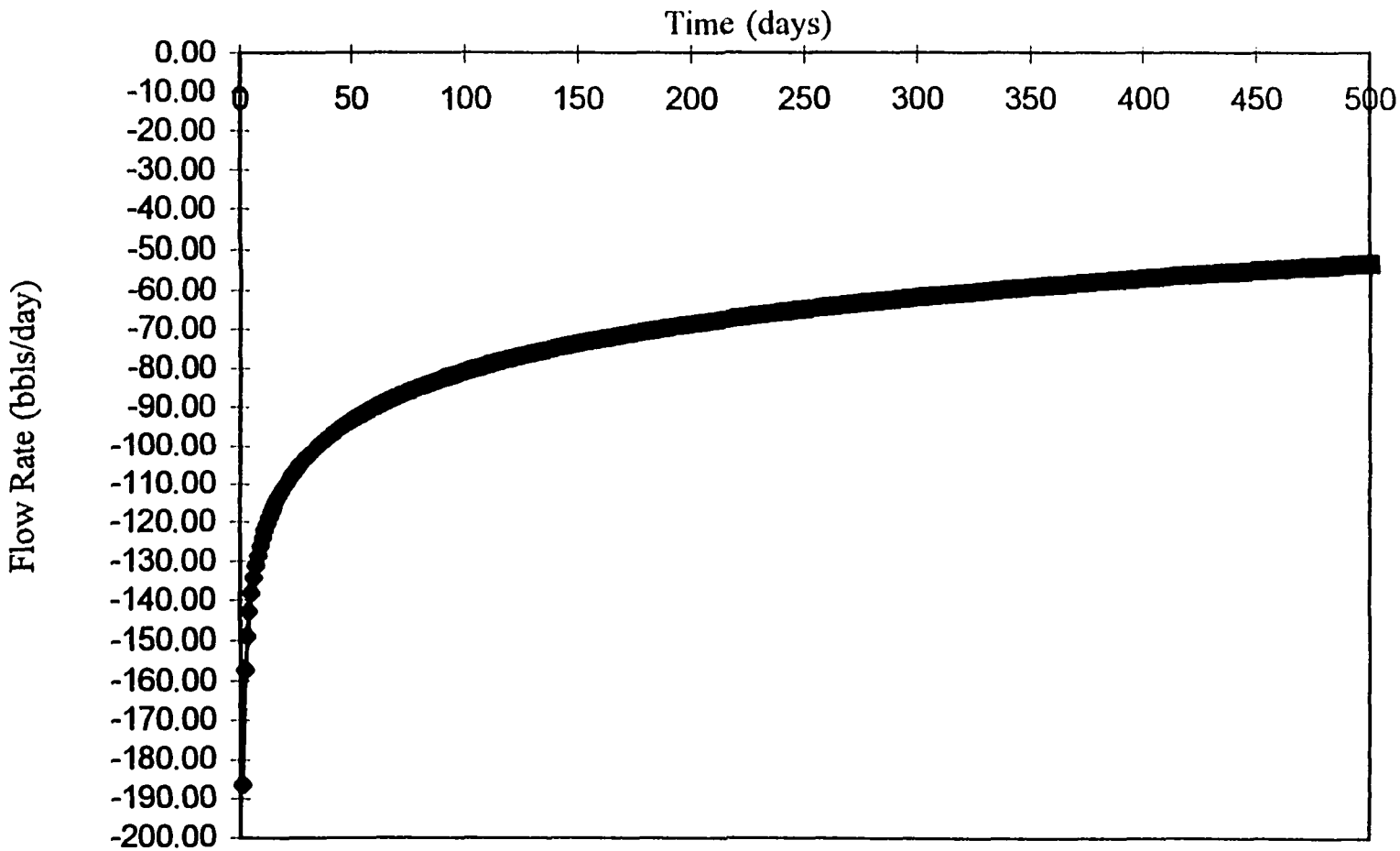


Figure 43. Abandoned well flow for case PWC #4 in the field study of the Tuscaloosa Sand trend.

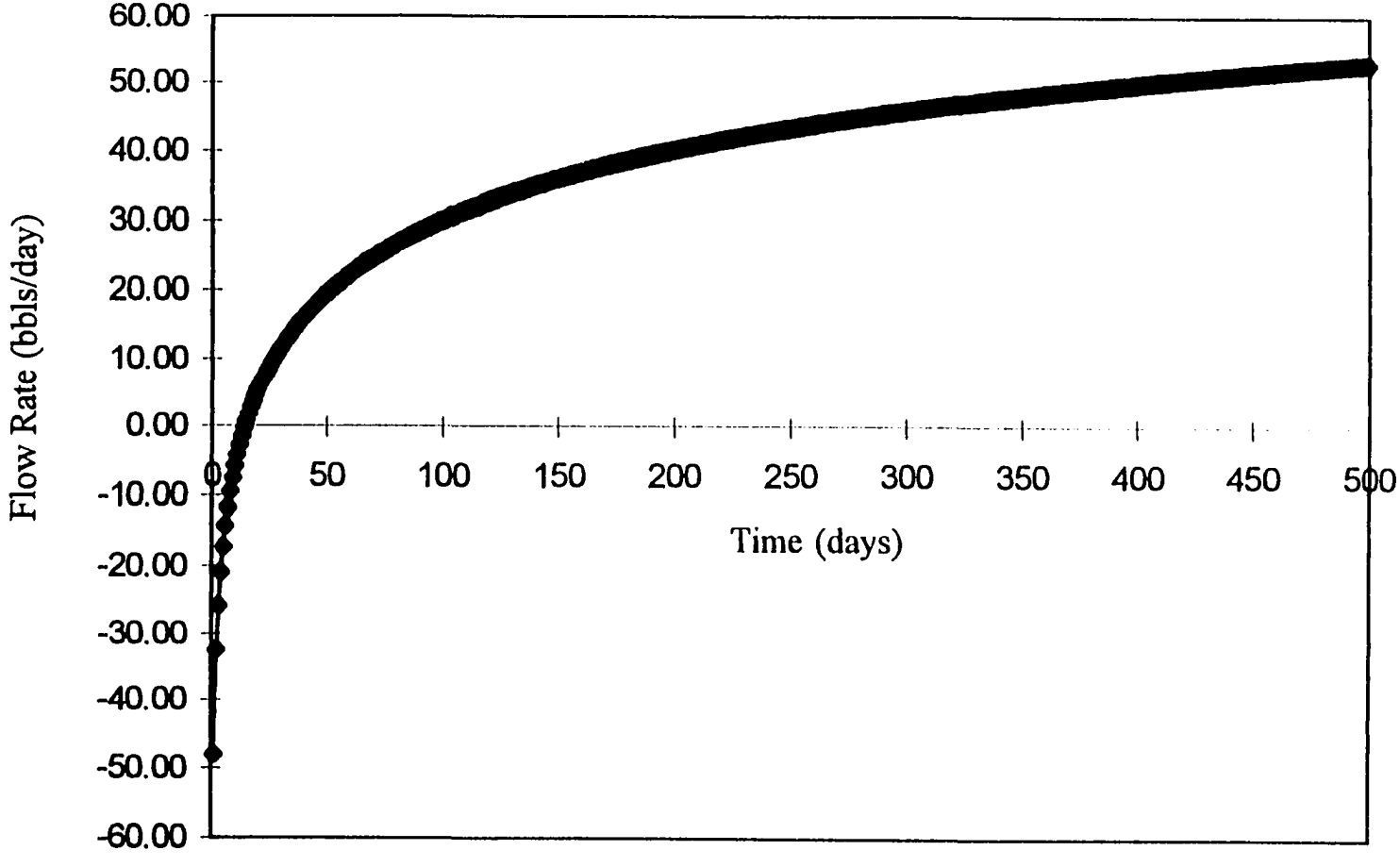


Figure 44. Abandoned well flow for case PWC #5 in the field study of the Tuscaloosa Sand trend.

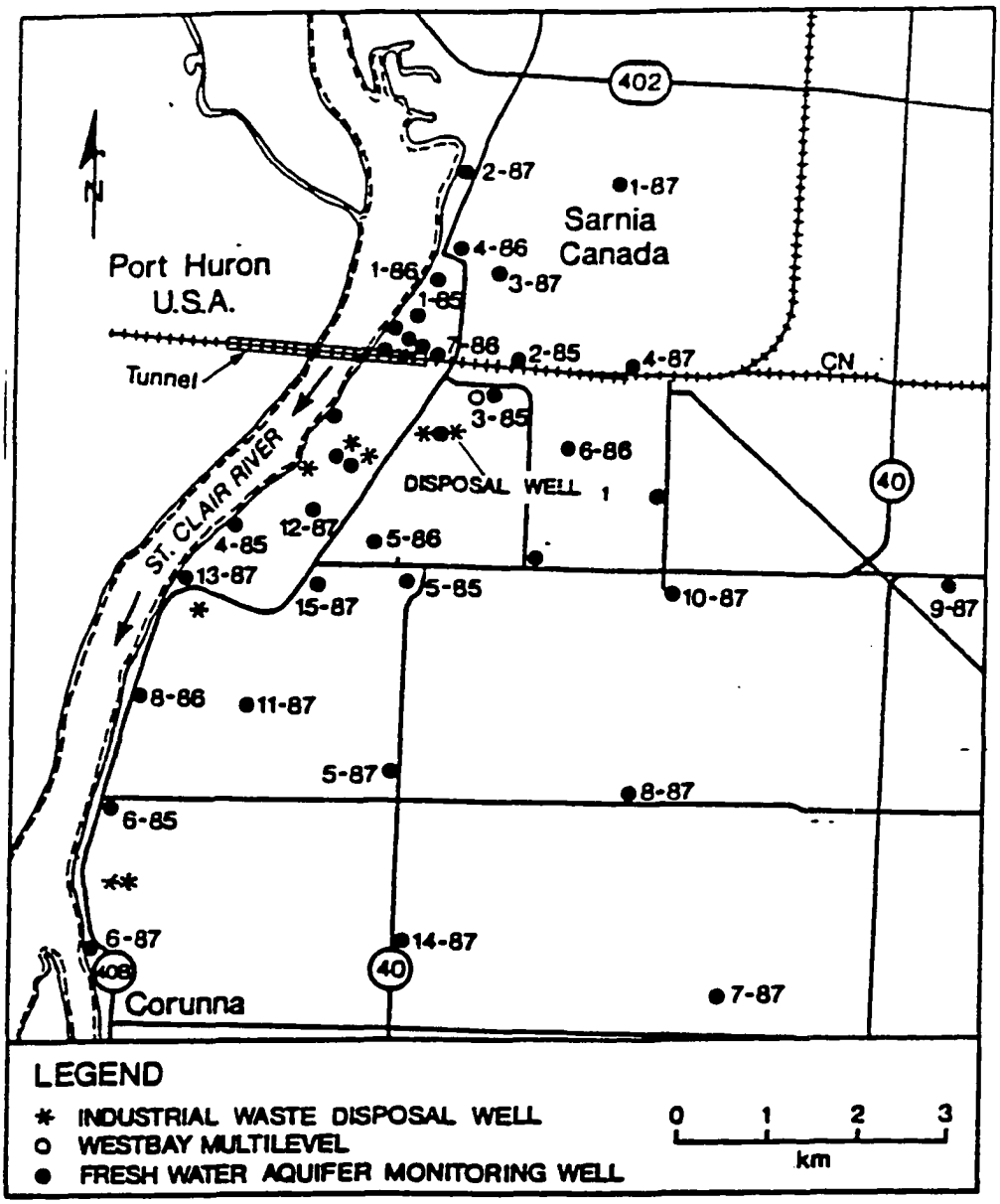


Figure 45. Local region of Sarnia, Ontario showing location of specific wells (adapted from Lesage et al.[3]).

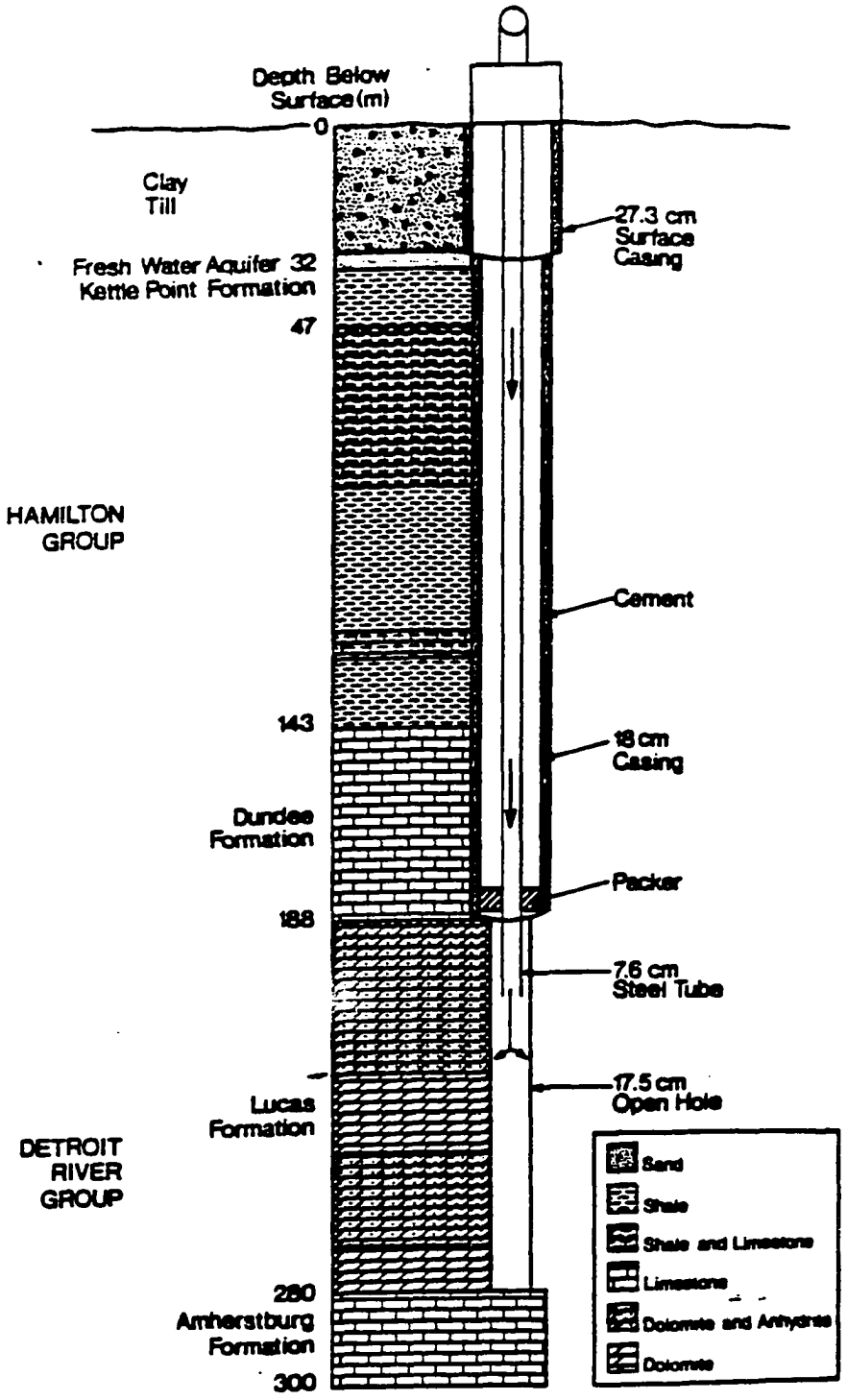


Figure 46. Typical disposal well used in Sarnia, Ontario injection operation (adapted from Lesage et al.[3]).

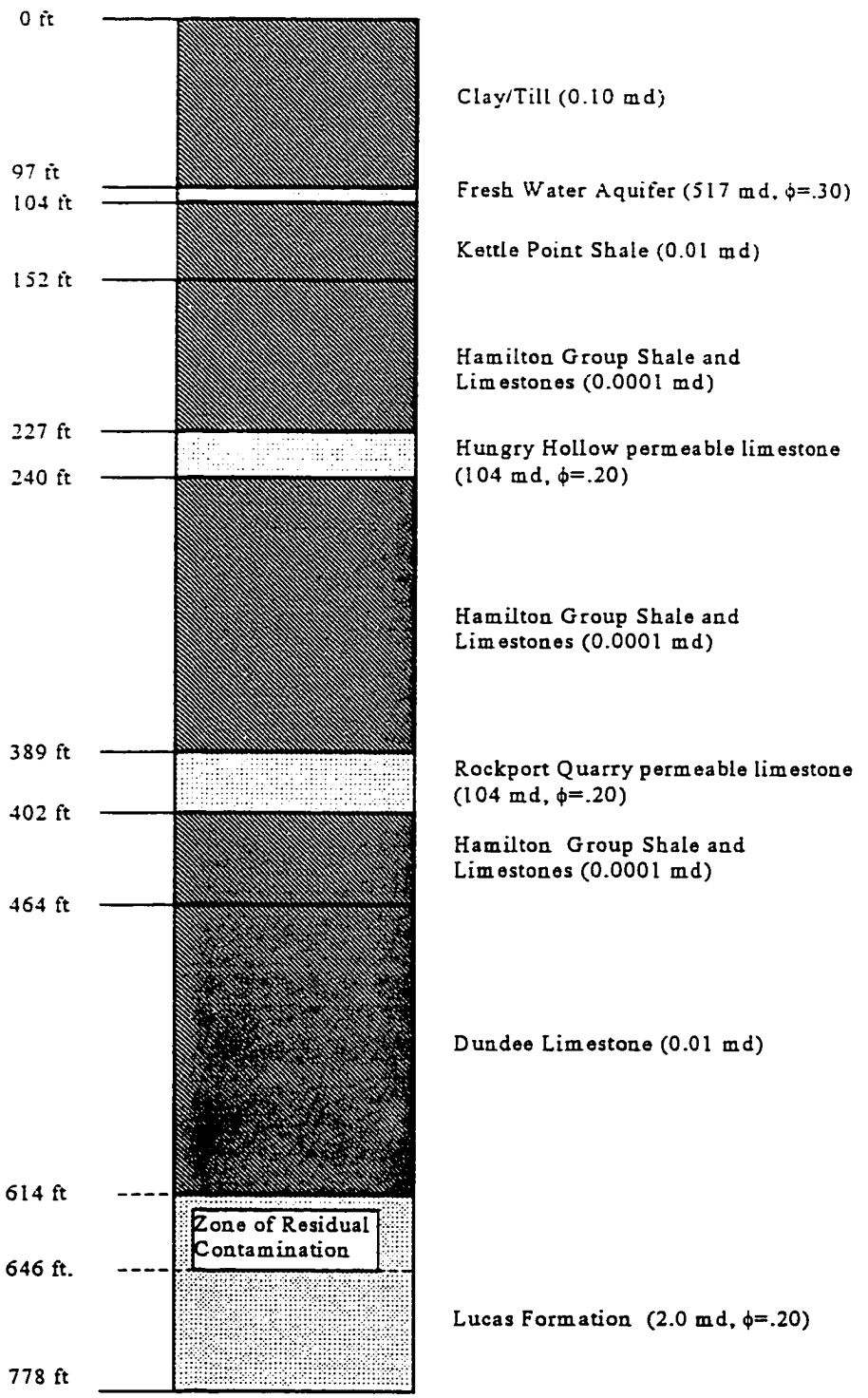


Figure 47. Cross section of Sarnia regional geology showing location and rock properties of permeable and imperemable zones.

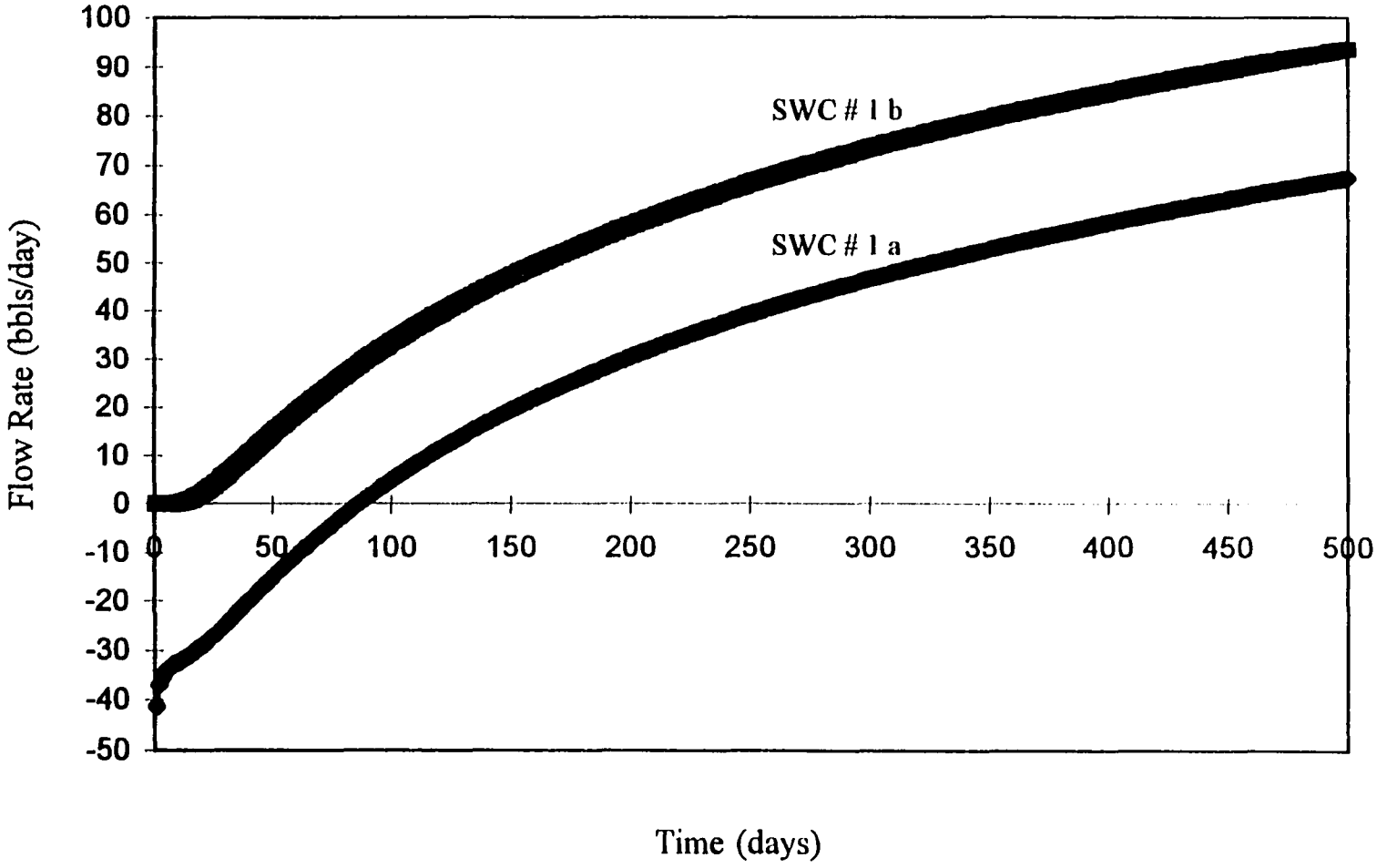


Figure 48. Comparison of abandoned well flow for cases SWC #1 a and b for contamination transport from Lucas formation to Rockport Quarry.

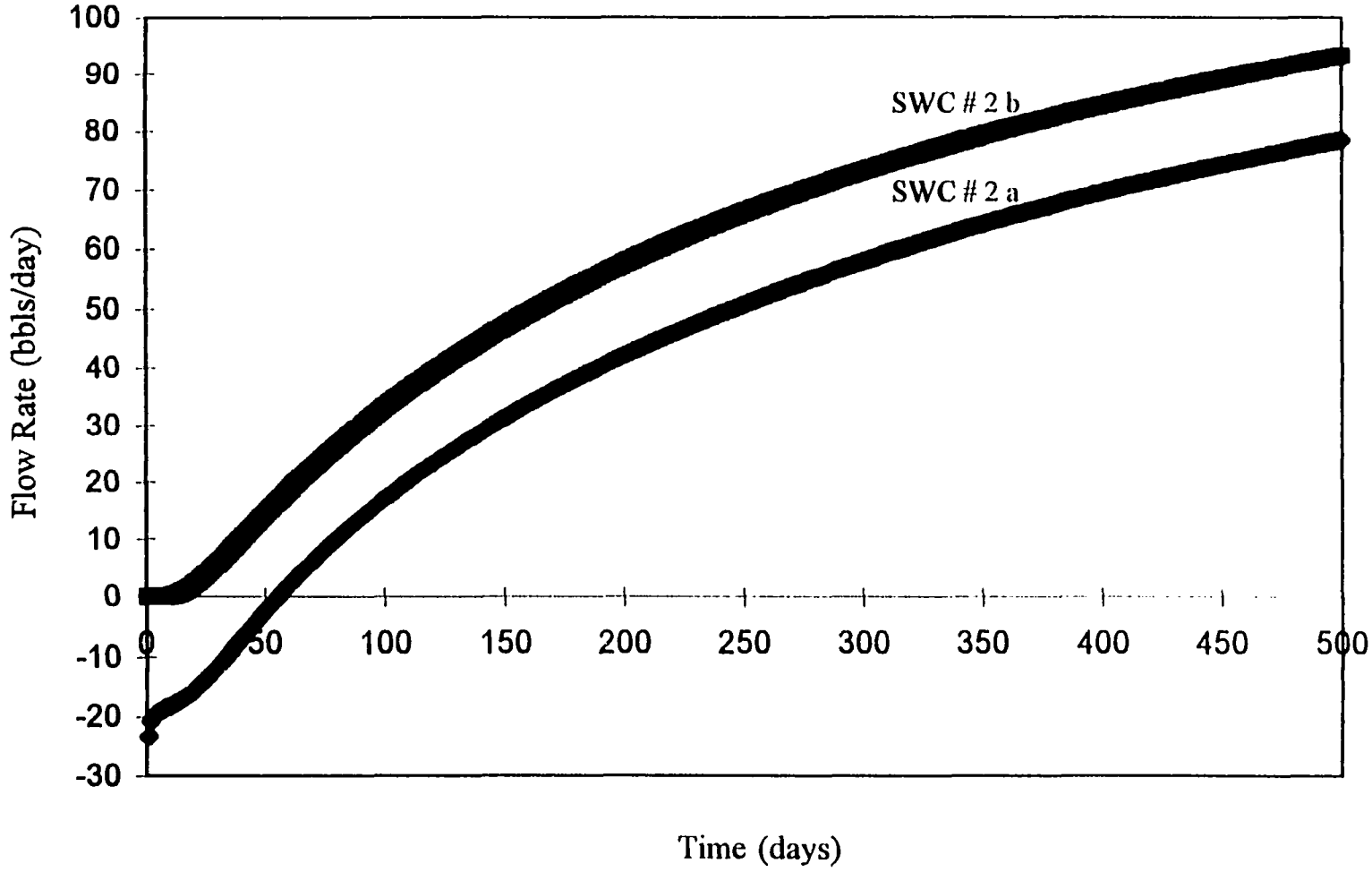


Figure 49. Comparison of abandoned well flow for cases SWC #2 a and b for contamination transport from Lucas formation to Hungry Hollow.

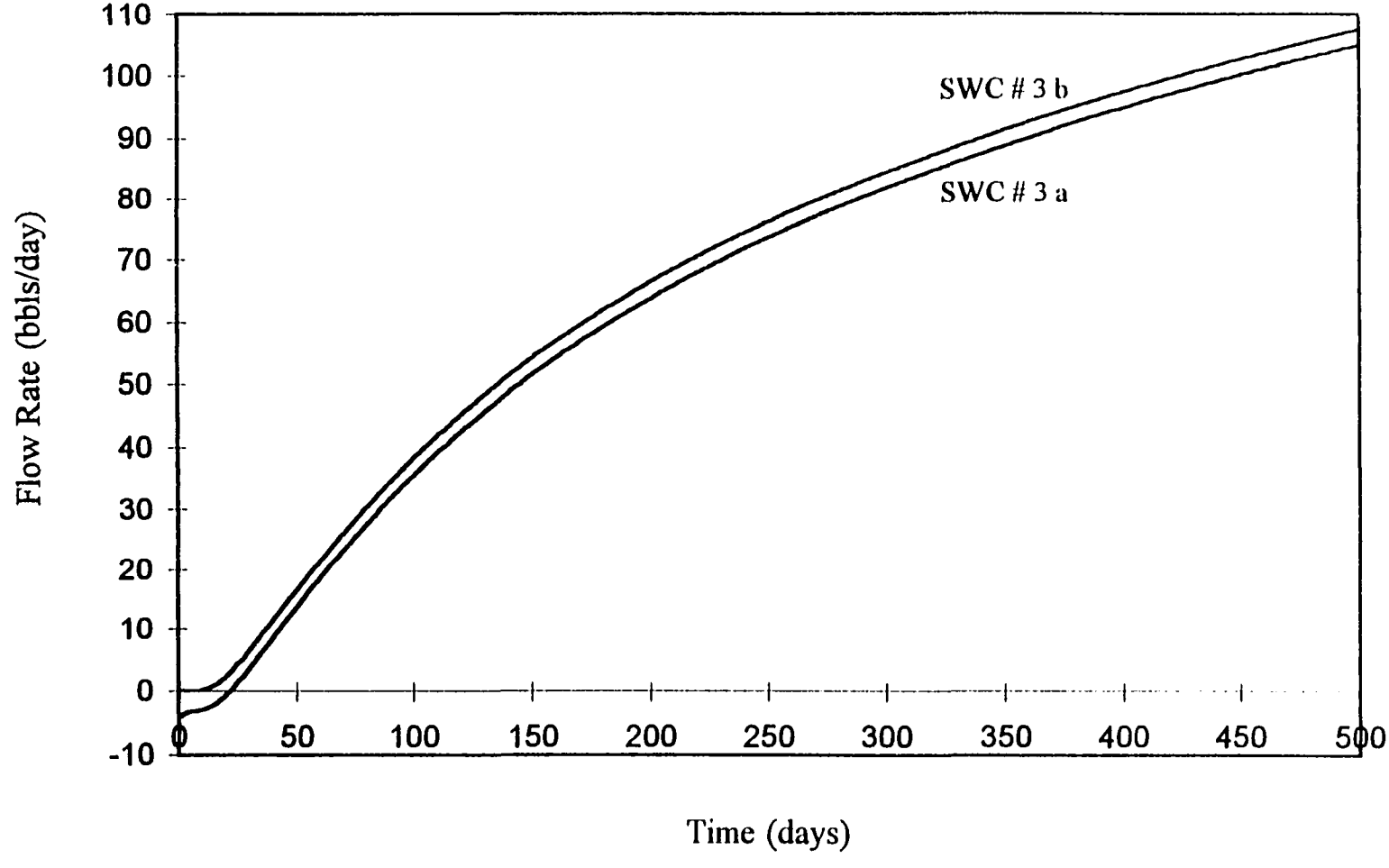


Figure 50. Comparison of abandoned well flow for cases SWC #3 a and b for contamination transport from Lucas formation to Fresh Water aquifer.

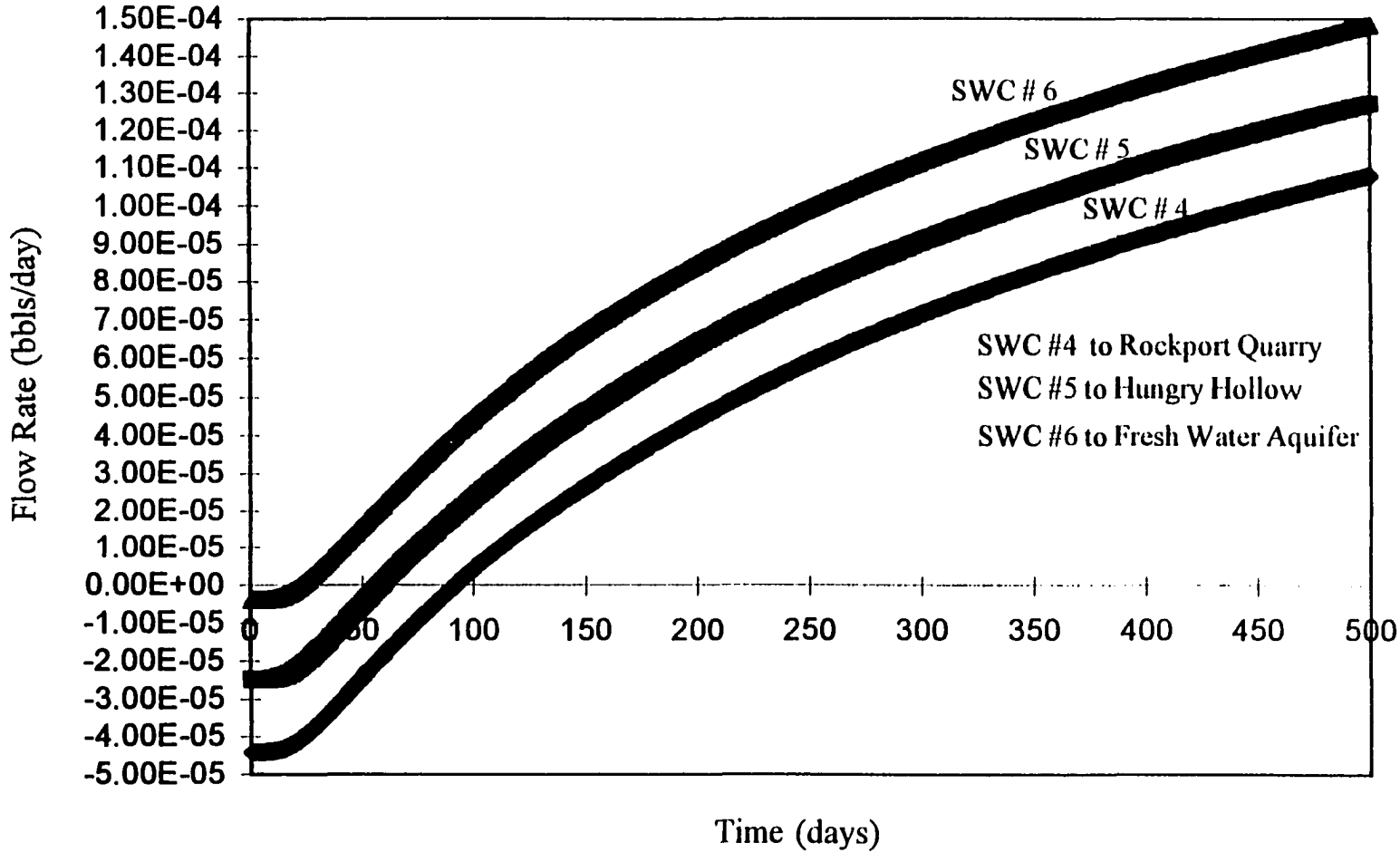


Figure 51. Comparison of abandoned well flow for cases SWC #4, #5 and #6 for contamination transport from Lucas formation with a 100 ft 0.1 md plug.

CHAPTER 7

CONCLUSIONS

7.1 Summary

This research was undertaken to address the problem of abandoned wells which may act as conduits for flow between formations. Of special concern is contamination transport to overlying USDW in the presence of Class II injection wells which has led to the regulation of these wells under EPA AOR regulations. These regulations require that whenever a new Class II injection well is brought into operation, all abandoned wells within a 'radius of endangering influence' must be evaluated for their potential to act as a contamination pathway to overlying USDW. If sufficient plugging can not be shown, the abandoned wells in this zone must be remediated. Under particular conditions, including the demonstration that flow is unlikely based on engineering analysis, injection wells can obtain a variance from AOR regulations.

A review of the literature for current methods to predict interformation abandoned well transport showed that the flow was dependent on the rock/fluid properties and pressure distributions in both formations. It was also dependent on the abandoned well condition and its location. The available methods incorporated most of these factors but were limited to either simple analytical models for one injector which required difficult solutions or to complicated numerical solutions in which the abandoned well was treated as vertical grid blocks. None of the methods was able to address flow coupled to the presence of active wells in either or both formations. They were also not able to easily

address variable abandoned wellbore conditions such as plugs and perforations. Because no model was currently available to predict abandoned well flow for these conditions, the primary objective of this research was to develop a simple and realistic model to predict the transport between two formations coupled by an abandoned well.

The model was developed using a novel approach. First, an analytical equation for steady state abandoned well flow developed by Silliman and Higgin's[14] was used as the base well model. It was then modified to be a function of time and applied in a 'series of steady states' to create transient flow. The model captures the essential dynamics of the problem. It contains terms which address the dependency of flow on the rock/fluid properties of the formations, the active wells in either formation and the location and condition of the abandoned well.

The model is the first to predict flow which is coupled to the evolving pressure distributions created by the active wells in the formations. This is accomplished by calculating the potential in both formations at steady state radii around the abandoned well using the superposition of the active wells in space and time. The impact of the abandoned well flow on the potential at the steady state radii is also included using superposition. These potentials are then used to calculate the gradient which drives flow between the formations over time.

The coupled model is the first transient model which contains a term for the wellbore pressure losses. The wellbore losses can be represented by pipe friction, porous media plugs, and a single perforation near the upper formation. The pressure loss can also be written as a combination of these terms. The model may also be used to predict annular

flow if the wellbore is plugged. It can account for friction through the annulus using pipe friction factors based on the annular hydraulic diameter. Plug losses in the annulus can also be evaluated based on the annular cross section. Flow may also be determined for the case where the annular plug contains a continuous fracture. All pressure losses are subtracted from the potential gradient and act to reduce flow.

The coupled model is applied using a 'series of steady states' which requires its calculation at numerous times steps. It was therefore incorporated into a computer program to allow its efficient execution. The results of the model program were verified using the analytical results of Avci[17] for a single injection well in the lower formation. The model was found to produce almost an exact match to these results at all but early time. The sensitivity of the model to time step was evaluated and reducing the time step was shown to produce an almost exact match even at early time. The sensitivity of the model to the choice of steady state radius where the potentials in the formations are calculated for the model was also evaluated. The impact of steady state radius choice was not significant until it approached the location of the nearest active well. It was therefore chosen to be between the abandoned well and nearest active well to keep it within the radius of influence of the abandoned well.

The program was applied to evaluate the effect of different variables on the abandoned well flow rate and demonstrate how these factors mitigate or enhance transport between formations. The presence of active wells in either formation was shown to move flow up or down the wellbore in response to the evolving pressure distributions. Any resistance in the wellbore was shown to greatly reduce or preclude flow.

The model program was also applied to field cases to demonstrate its use as a tool to predict or evaluate abandoned well flow. All of the application cases demonstrated the unique versatility of the model which was able to show the abandoned well flow expected between permeable formations in the presence of true field operating conditions. Flow was also predicted based on known or estimated 'worst case' wellbore conditions.

Based on the results of this research, the following conclusions are offered:

1. A novel coupled abandoned well model to predict interformation flow was developed using a 'series of steady states' approach to create transient flow and has been verified by comparison to the analytical results of Avci[17]. The coupled model can be incorporated into a computer program to allow efficient calculation of the flow.
2. Abandoned well flow between two formations is a function of the rock/fluid properties and the evolving pressure distributions in the coupled formations. The flow responds to rates in the active wells in either formation and it may be up or down the wellbore.
3. Abandoned well flow is a function of the location and condition of the abandoned well. Pressure losses in the wellbore from friction in the pipe or annulus have little to no effect on flow rate. Pressure losses from a perforation next to the upper formation reduce flow substantially and the reduction is dependent on the size of the perforation. Pressure losses from plugs in the wellbore or annulus effectively eliminate flow. A fracture in the annular plug allows slightly greater transport compared to a solid plug.
4. The coupled model can be applied to predict or evaluate abandoned well flow in field cases using available field data, engineering estimates and application of 'worst case' scenarios for unknown abandoned well locations and conditions as necessary.

These conclusions meet the objectives outlined for the research. They demonstrate that the coupled abandoned well model is a versatile and simple tool to evaluate transport between formations through an abandoned well. It has the potential to be applied in numerous field cases to predict or evaluate abandoned well flow. For Class II injection wells it can be used to predict if abandoned well flow is probable, to protect USDW or obtain variances from AOR regulations.

7.1 Future Recommendations

The coupled model has been verified using the analytical results from Avci[17] for a single injection well in the lower formation. It would, however, be useful to verify the model in a well documented field application. The field test would require a relatively homogenous injection zone with a fully penetrating injection well. An open well would be required near the injection well to act as the 'abandoned well'. The 'abandoned well' would need to be hydraulically connected to an overlying formation through an open casing or perforation. Plugs in the wellbore could also be added. The flow into the upper zone could be evaluated by pressure measurements in monitoring wells near the 'abandoned well'. Although such a test would be a substantial undertaking, it would allow a verification of the model to be made under field conditions.

The coupled model was developed to predict flow between two formations. It may be possible to modify the model to extend it to the prediction of flow between several overlying formations at a time. The model is essentially based on the analog of an

electrical circuit which predicts flow in the presence of two formation potentials and the resistance of the formations and wellbore. The circuit analog can be evolved to include loops into other formations with defined resistances and potentials. The new analog would require the solution of a system of linear algebraic equations at each time step to determine the flow to each formation. It would increase the complexity of the model, but would address the potential of other formations to divert flow from the wellbore.

Finally, it may be possible to incorporate the coupled abandoned well model into a numerical simulator. This could be accomplished by assigning the abandoned well to a particular well block. The average pressure of the well block could be used as the potential in the lower formation to predict flow to the overlying formation. The calculated abandoned well flow could be used for the block flow rate in the next time step to calculate a new average pressure for the block. If the model is incorporated into such a simulation, the effects of geologic complexity and muliphase flow pressure changes could be included in the determination of the abandoned well flow.

If the coupled model can be verified in the field and modified to encompass other situations it will enhance its applicability. This will further the formulation of a method to truly address the potential of numerous abandoned wells to act as a source of contamination to overlying formations. The coupled model developed in this research and future advancements will move the problem of abandoned well transport out of the realm of speculation and into the realm of engineering analysis.

NOMENCLATURE

a = radius of abandoned borehole (m)

B_w = formation volume factor (bbls/STB)

A_{1n} = general solution coefficient

B_{1n} = general solution coefficient

A, B, C = coefficients and constant of quadratic equation, $Ax^2+Bx+C=0$

A_c = cross sectional area (cm^2, ft^2)

A_F = cross sectional area of fracture (ft^2)

c = compressibility of formation fluid (atm^{-1}, psi^{-1})

D = diameter (cm, in, ft)

D_h = hydraulic diameter (cm, ft)

C_L = wellbore loss coefficient (atm s^2/cm^6)

C_D = coefficient of discharge (dimensionless)

f = friction factor (dimensionless)

g = gravity (cm/s^2, ft/s^2)

$\overline{h}_1$ = average pressure head across borehole opening of lower formation (m)

$\overline{h}_2$ = average pressure head across borehole opening of upper formation (m)

h_1 = thickness of lower formation (cm, ft)

h_2 = thickness of upper formation (cm, ft)

H = pressure head (m, ft)

H_1 = initial pressure head in lower formation (m, ft)

H_2 = initial pressure head in upper formation (m, ft)

K = hydraulic conductivity (cm/s, m/s)

K_1 = hydraulic conductivity in lower formation (m/s)

K_2 = hydraulic conductivity in upper formation (m/s)

K_w = hydraulic conductivity of wellbore (m/s)

k_{PM} = permeability of plug in abandoned wellbore (d, md)

k_1 = permeability of lower formation (d, md)

k_2 = permeability of upper formation (d, md)

L_i = thickness of formation (m)

L_1 = thickness of lower formation (m)

L_2 = thickness of upper formation (m)

L = length of pipe (cm, ft)

L_{PM} = length of plug in abandoned wellbore (cm, ft)

N_{Re} = Reynolds number (dimensionless)

N_p = number of perforations (dimensionless)

P_{wet} = wetted perimeter (cm, ft)

$\overline{P}$ = average pressure (atm, psi)

P = pressure (atm, psi)

P_1 = initial pressure in lower formation (atm, psi)

P_2 = initial pressure in upper formation (atm, psi)

ΔP_{AW} = change in pressure at steady state radius around abandoned well (atm, psi)

ΔP_1 = change in pressure at abandoned well in lower formation (atm, psi)

ΔP_2 = change in pressure at abandoned well in upper formation (atm, psi)

ΔP_I = change in pressure from injection well rate (atm, psi)

ΔP_T = total change in pressure (atm, psi)

ΔP_{PM} = pressure loss for flow through plug (atm, psi)

ΔP_{PMF} = pressure loss for flow through fracture in plug (psi)

ΔP_{Pf} = pressure loss from pipe friction (atm, psi)

ΔP_{Perf} = pressure loss for perforation (atm, psi)

ΔP_L = pressure loss through wellbore (atm, psi)

P_o = simulation well block pressure (atm, psi)

P_{wf} = well flowing pressure (atm, psi)

q_{AW} = uniform flux on wellbore (m/s)

Q = flow rate (cm^3/s, bbls/day)

Q_1 = flow rate in lower formation (cm^3/s, bbls/day)

Q_2 = flow rate in upper formation (cm^3/s, bbls/day)

Q_D = dimensionless flow rate

Q_I = injection well rate (cm^3/s, bbls/day)

$\overline{Q}_{AW}$ = abandoned well flow rate in Laplace space (cm^3/s)

$\overline{Q}_{AWD}$ = dimensionless abandoned well flow rate in Laplace space

Q_{AWD} = dimensionless abandoned well flow rate = Q_{AW}/Q_I

Q_{AW} = abandoned well flow rate (cm^3/s, bbls/day, bbls/min)

R = distance between injection well and abandoned well (cm, ft)

R_i = location of constant potential radius in Eq. 34(m), or distance between active wells and points on steady state radius (m, ft)

R_h = hydraulic radius (cm, ft)

r_{AW} = radius of abandoned well (cm, ft)

r_i = radial dimension in Eq. 30 (m)

r_1 = steady state radius in lower formation (cm, ft)

r_2 = steady state radius in upper formation (cm, ft)

r_o = location of flowing well pressure in well block in Eq. 56 (cm) or outer radius of casing (cm, ft)

r_i = inner radius of casing (cm, ft)

r_{1AW} = radius of abandoned well in lower formation (cm, ft)

r_{2AW} = radius of abandoned well in upper formation (cm, ft)

r_{AWD} = dimensionless radius of abandoned well, r_{AW}/R

r_e = outer radius of reservoir (cm, ft)

r_w = radius of well (cm, ft)

r_{si} = steady state radius of well (m)

r_s = radius of well screen (cm, ft)

s_i = drawdown (m)

s_1 = drawdown in lower formation (m)

s_2 = drawdown in upper formation (m)

s_{wi} = drawdown at well location (m)

t = time (s, hrs)

t_D = dimensionless time

V_{AW} = velocity in abandoned well bore (cm/s, ft/s)

W_F = width of fracture (ft)

x = well location Cartesian coordinate (cm, ft)

y = well location Cartesian coordinate (cm, ft)

z = elevation of formation (cm, ft)

$\bar{z}$ = Laplace variable

z_i = vertical dimension in Eq. 30(m)

z_i = elevation of formation (cm, ft)

z_l = elevation of lower formation (cm, ft)

z_2 = elevation of upper formation (cm, ft)

z_D = dimensionless Laplace variable

Greek Symbols

α = productivity index of lower formation (cm^3/s/atm, bbls/day/psi)

β = productivity index of upper formation (cm^3/s/atm, bbls/day/psi)

β_{in} = variable group in Eq. 46

β_{sph} = productivity index for spherical flow (cm3/s/atm, bbls/day/psi)

ε = pipe roughness (ft)

ξ = ratio of upper formation permeability to lower formation permeability (dimensionless)

τ = ratio of lower formation productivity index to upper formation productivity index, α/β

γ = variable group, $\alpha\beta C_L \Delta\Phi$, in Eq. 28.

λ_{in} = eigenvalue

ϕ = porosity (fraction)

ϕ_l = porosity of lower formation (fraction)

ϕ_2 = porosity of upper formation (fraction)

Φ = potential (atm, psi)

$\Delta\Phi$ = change in potential (atm, psi)

$\Delta\Phi_D$ = dimensionless change in potential (atm, psi)

Φ_{1AW} = abandoned well potential at sandface of lower formation (atm, psi)

Φ_{2AW} = abandoned well potential at sandface of upper formation (atm, psi)

Φ_1 = potential of lower formation (atm, psi)

Φ_2 = potential of upper formation (atm, psi)

Φ_e = potential at outer radius(atm, psi)

Φ_w = potential at wellbore (atm, psi)

ρ = fluid density (g/cm^3, lb/ft^3, lbs/gal)

μ = viscosity (cp)

Ω = resistance of abandoned wellbore (atm s/cm^3, s/m^2)

Ω_D = dimensionless resistance of abandoned wellbore

REFERENCES

1. Canter, L.W., "Problems of Abandoned Wells", Proceedings of the First National Conference on Abandoned Wells: Problems and Solutions, edited by D. M. Fairchild, pp. 164-185, Environmental Ground Water Institute, University of Oklahoma, Norman, 1984.

2. Anzollin, A.R. and Graham, L.L., "A Regulatory Perspective", Proceedings of the First National Conference on Abandoned Wells: Problems and Solutions, edited by D.M. Fairchild, pp. 17-36, Environmental Ground Water Institute, University of Oklahoma, Norman, 1984.

3. Lesage, S., Jackson, R.E., Priddle, M., Beck, P., and Raven, K.G., "Investigation of Possible Contamination of Shallow Ground Water by Deeply Injected Liquid Industrial Wastes", Ground Water Monitoring Review, Winter, 1991.

4. Raven, K.G., Lafleur, D.W., and Sweezy, R.A., "Monitoring Well into Abandoned Deep-Well Disposal Formations at Sarnia, Ontario", Journal of Canadian Geotechnology, pp. 105-188, Vol. 27, 1990.

5. American Petroleum Institute, "Environmental Guidance Document: Well Abandonment and Inactive Well Practices for U.S. Exploration and Production Operations", API Bulletin E3, 1st Edition, Jan 31, 1993.

6. "Underground Injection Control: Criteria and Standards Applicable to Class II Wells", Code of Federal Regulations, 40 CFR Chapter 1, Part 146, Subpart C, 7-1-93 Edition, 1993.

7. Smith, J.B. and Browning, L.A., "Proposed Changes to EPA Class II Well Construction Standards and Area of Review Procedures", paper SPE 25961 presented at the 1993 SPE/EPA Exploration and Production Environmental Conference, San Antonio, Mar. 7-10.

8. Department of Energy, "Potential Cumulative Impacts of Environmental Regulatory Initiatives on U.S. Crude Oil Exploration and Production, Volume 2: Final Report", DOE/FE/61679P-H1, Dec. 1990.

9. Dunn-Norman, S., Warner, D.L., Koederitz, L.F., Laudon, R.C.,"Application of an Area of Review Variance to the San Juan Basin, New Mexico", SPE 29762 ,SPE Advanced Technology Series, Vol. 4, No. 2, 1996.

10. Warner, D.L., Koederitz, L.F.,Laudon, R.C., and Dunn-Norman, S.,"An Area of Review Variance of the East Texas Field", paper SPE 36641 presented at the 1996 SPE Annual Technical Conference and Exhibition, Denver, Oct. 6-9.

11. Warner, D. L., "Response of Abandoned Well 9-6A to Injection through Well 9-6, West Mallelieu Field, Mississippi", 1988, Appendix 1, API Publication No. 4507, pp. 1-19, June 1990.

12. Warner, D. L., and McConnell, C. L., "Abandoned Oil and Gas Industry Wells- A Quantitative Assessment of Their Environmental Implications", API Publication No. 4507, pp. 1-45, June 1990.

13. Javandel, I., Tsang, C.F., Witherspoon, P. A., and Morganwalp, D., "Hydrogeologic Detection of Abandoned Wells Near Proposed Injection Wells for Hazardous Waste Disposal", Water Resources Research, Vol. 24, No. 2, pp. 261-170, Feb. 1988.

14. Silliman, S. and Higgins, D., "An Analytical Solution for Steady State Flow between Aquifers through an Open Well", Ground Water, Vol. 28, No. 2, pp. 184-190, 1990.

15. Bear, J., Hydraulics of Groundwater, McGraw-Hill, New York, p.306, 1979.

16. Avci, C. B., "Flow Occurrence between Confined Aquifers through Improperly Plugged Boreholes", Journal of Hydrology, Vol. 139, pp. 97-114, 1992.

17. Avci, C.B., "Evaluation of Flow Leakage through Abandoned Wells and Boreholes", Water Resources Research, Vol. 30, No. 9, pp. 2565-2578, Sept. 1994.

18. Chia, Y. and Chu, J., "Upward Migration of Underground Injected Wastes through Hydrologic Conduits Around the Wellbore.", DOE/DE89-005839,1989.

19. Reeves, M., Johns, N.D., and Cranwell, R.M., "Theory and Implementation for SWIFT II, The Sandia Waste Isolation Flow and Transport Model for Fractured Media Release 4.84", NUREG/CR-3328, SAND83-1159, Sandia National Laboratories, Albuquerque, NM.,1986

20. Ward, D.C., "Modifications to Reeves et al., 1986", Geotrans, Inc., Herndon, VA, 1987.

21. Lacombe, S., Sudicky, E.A., Frape, S.K., and Unger, A.J.A., "Influence of Leaky Boreholes on Cross-Formational Groundwater Flow and Contaminant Transport", Water Resources Research, Vol. 31, No. 8, pp. 1871-1882, Aug. 1995.

22. Tongpenyai, J. and Raghavan, R., "The Effect of Wellbore Storage and Skin on Interference Test Data", Journal of Petroleum Technology, pp. 151-160, Jan. 1981.

23. Ogbe, O. D. and Brigham, W.E., " A Model for Interference Testing with Wellbore Storage and Skin Effects at Both Wells", paper SPE 13253 presented at the 1984 SPE Annual Technical Conference and Exhibition, Houston, Sept. 16-19.

24. Peaceman, D. W., "Interpretation of Well-Block Pressures in Numerical Reservoir Simulation", SPEJ, Trans. AIME, pp. 183-194, June 1978.

25. Evinger, H.H. and Muskat, M., "Calculation of Theoretical Productivity Factor", Trans. AIME, Vol. 146, pp. 126-139, 1942.

26. Matthews, C.S. and Russell, D.G., Pressure Buildup and Flow Tests in Wells, Society of Petroleum Engineers, 1967.

27. Muskat, M., The Flow of Homogeneous Fluids through Porous Media, McGraw-Hill, pp. 164-169, 1937.

28. Streeter, V. L. And Wylie, E.B., Fluid Mechanics, Mc Graw-Hill, 1985.

29. Fox, J.A., Hydraulic Analysis of Unsteady Flow in Pipe Networks, John Wiley and Sons, 1977.

30. Crump, J.B. and Conway, M.W., "Effects of Perforation Entry Friction on Bottomhole Treating Analysis", paper SPE 15474 presented at the 1986 SPE Annual Technical Conference and Exhibition, New Orleans, Oct. 5-8.

31. Aller, L., "Survey of Available Technologies for Locating Abandoned Wells", Proceedings of the First National Conference on Abandoned Wells: Problems and Solutions, edited by D. M. Fairchild, pp. 125-143, Environmental Ground Water Institute, University of Oklahoma, Norman, 1984.

32. Craft, B. C. and Hawkins, M., Applied Petroleum Reservoir Engineering, 2nd Edition, Prentice-Hall, 1991.

APPENDIX A

FLOW CHARTS FOR MAIN PROGRAM AND SUBROUTINES

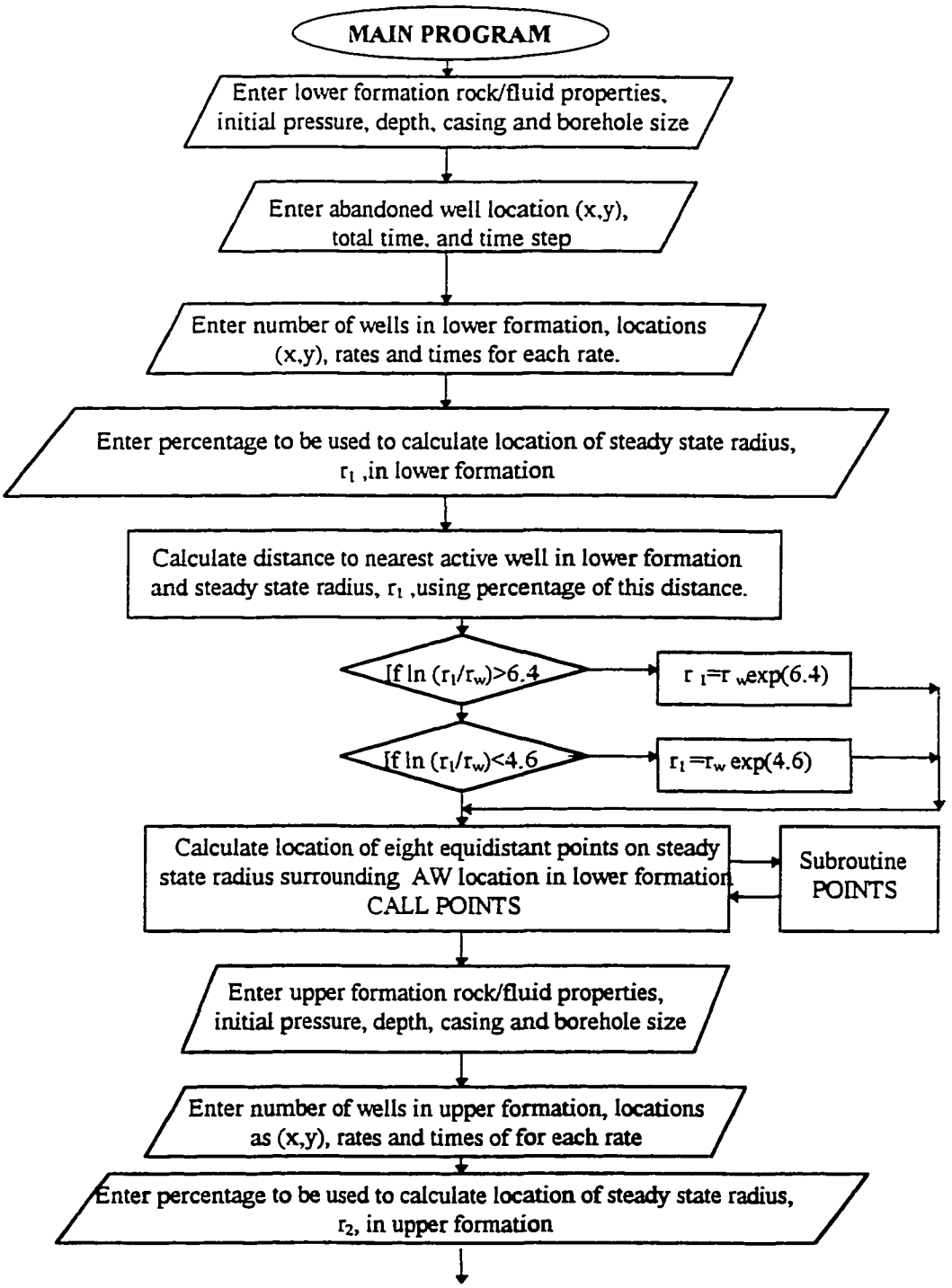


Figure A.1 General flow chart for Main program

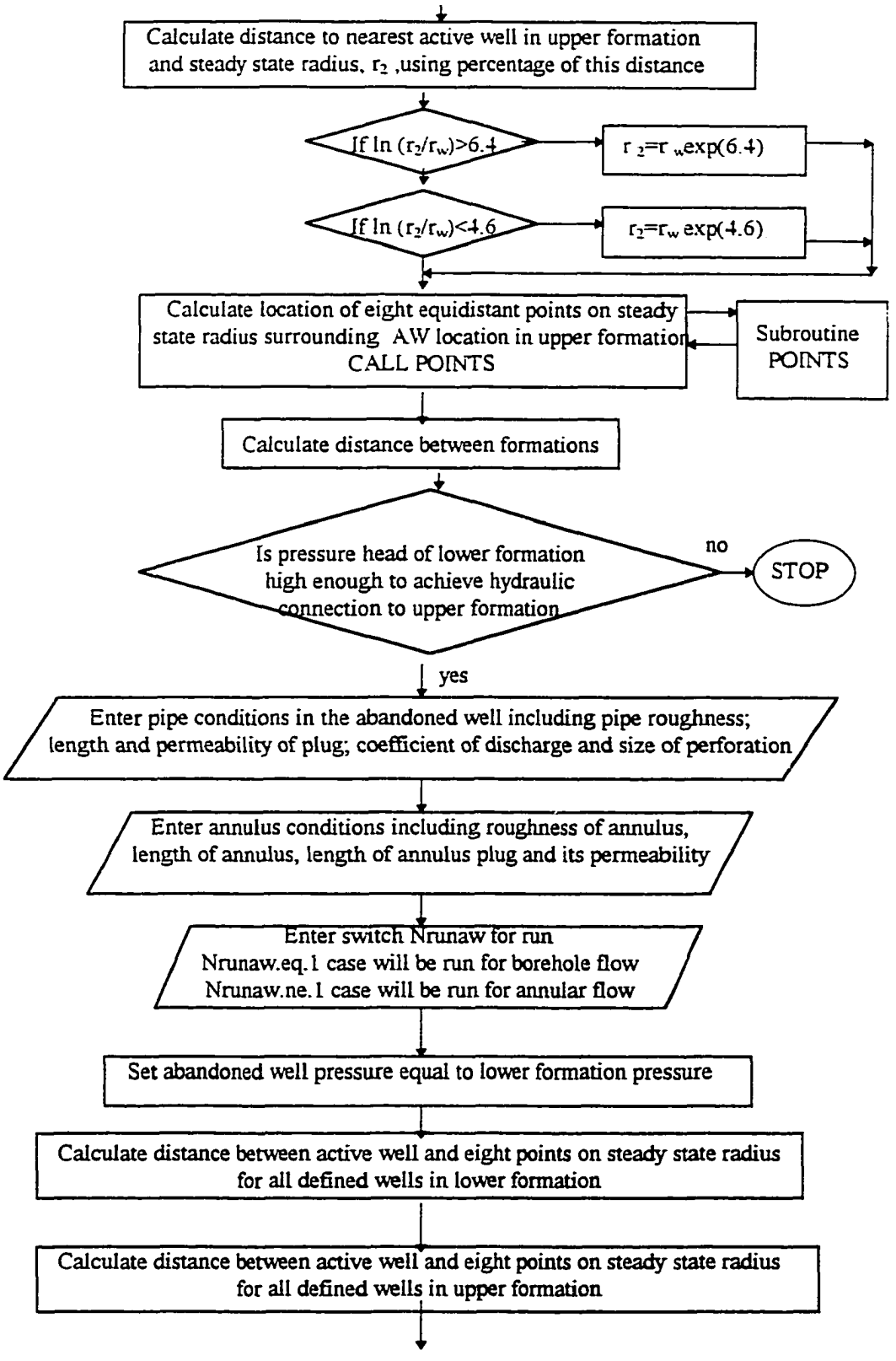


Figure A.1 continued.

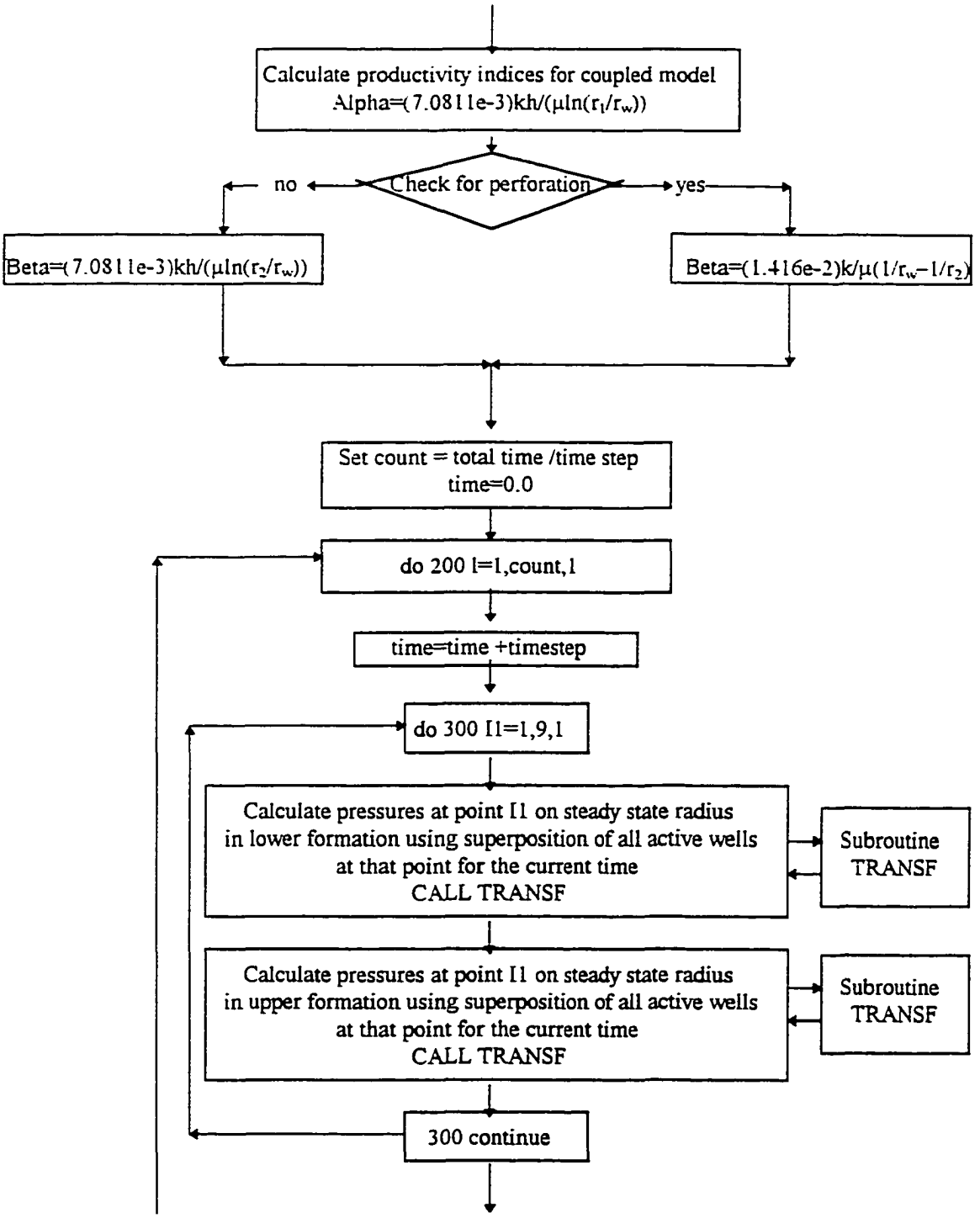


Figure A.1 continued

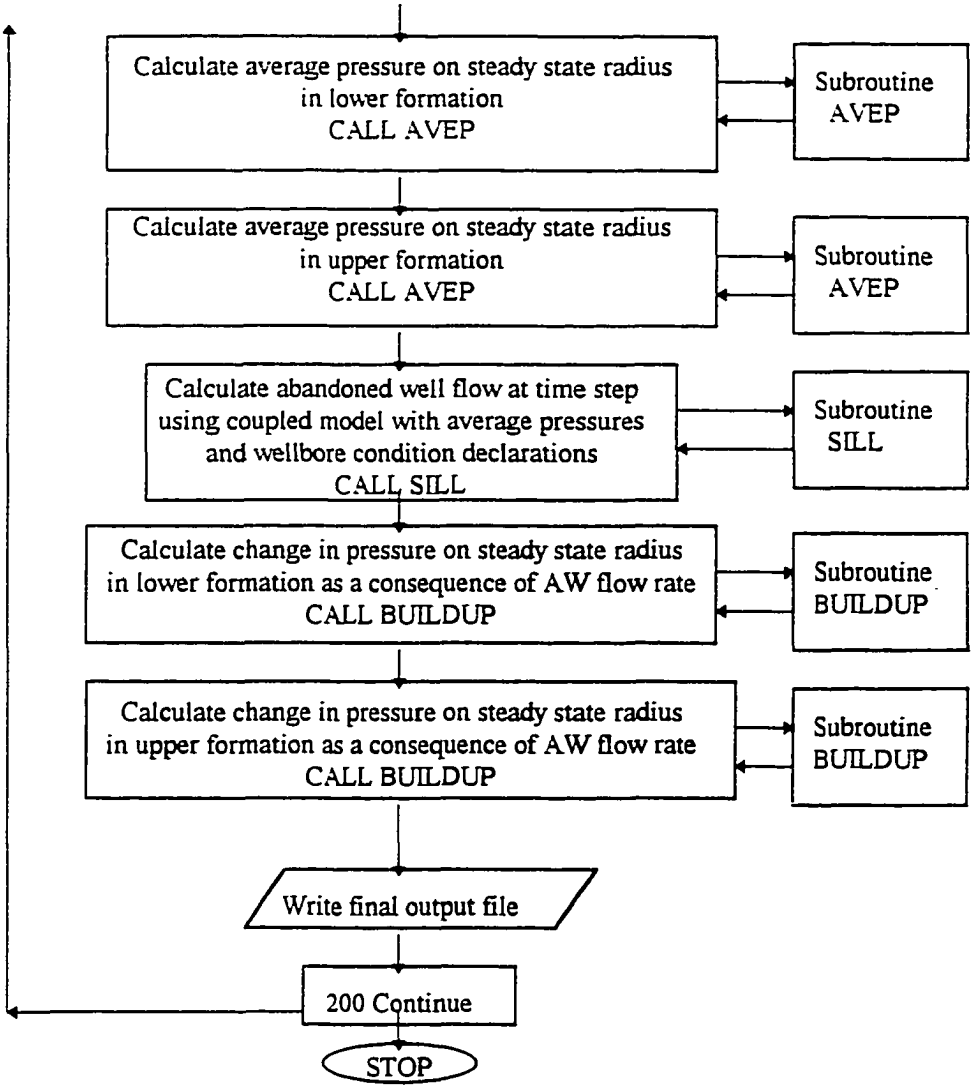


Figure A.1 continued

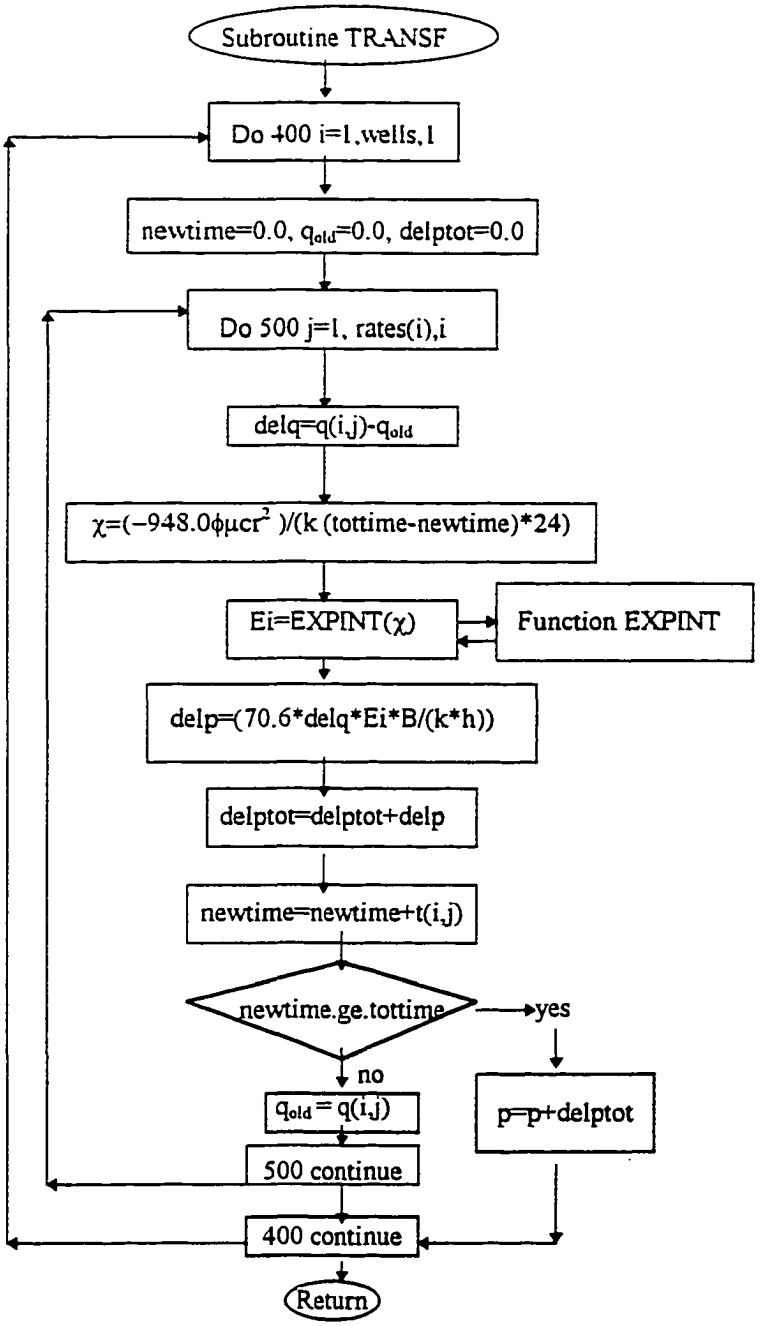


Figure A.2 General flow chart for subroutine TRANSF.

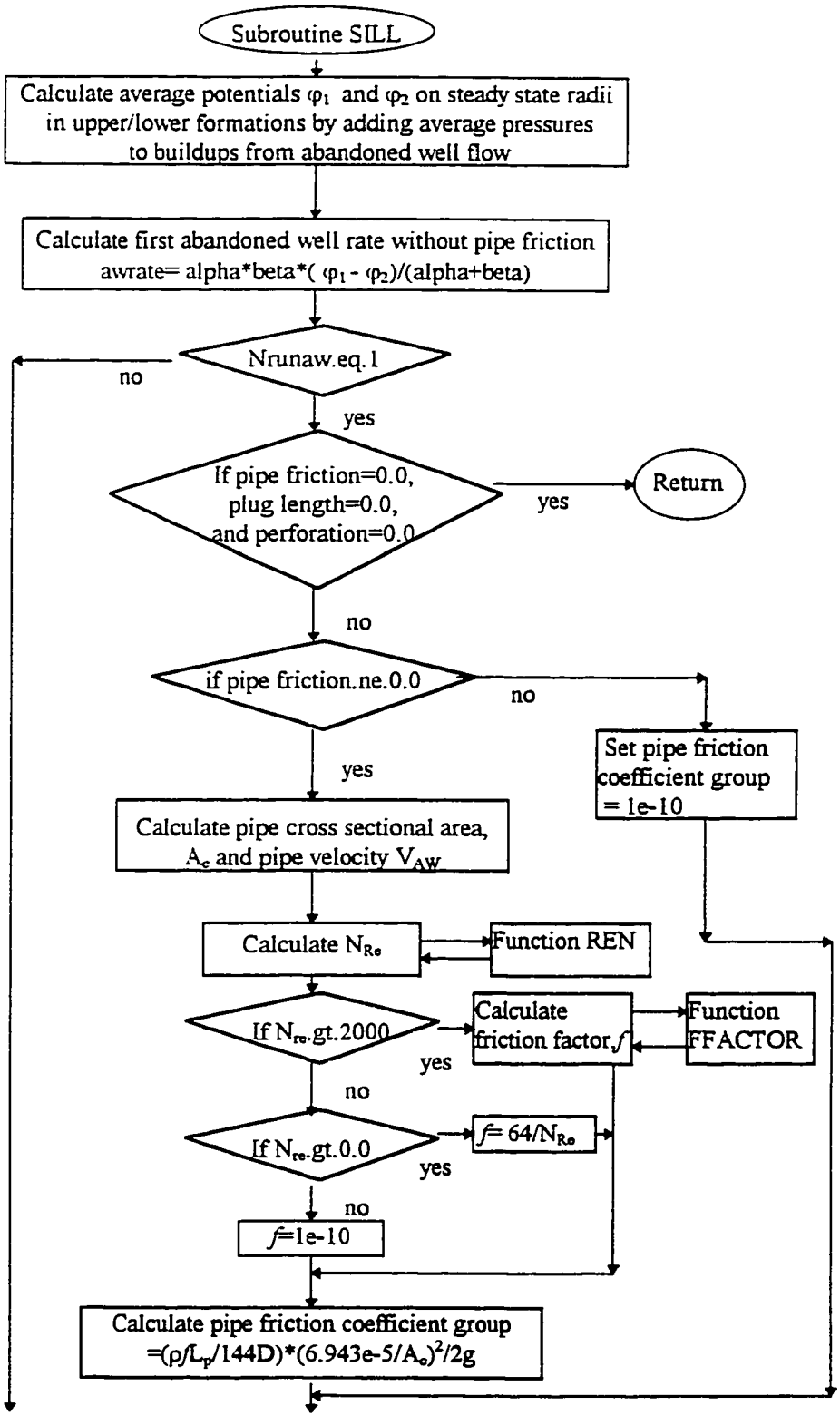


Figure A.3 General flow chart for subroutine SILL.

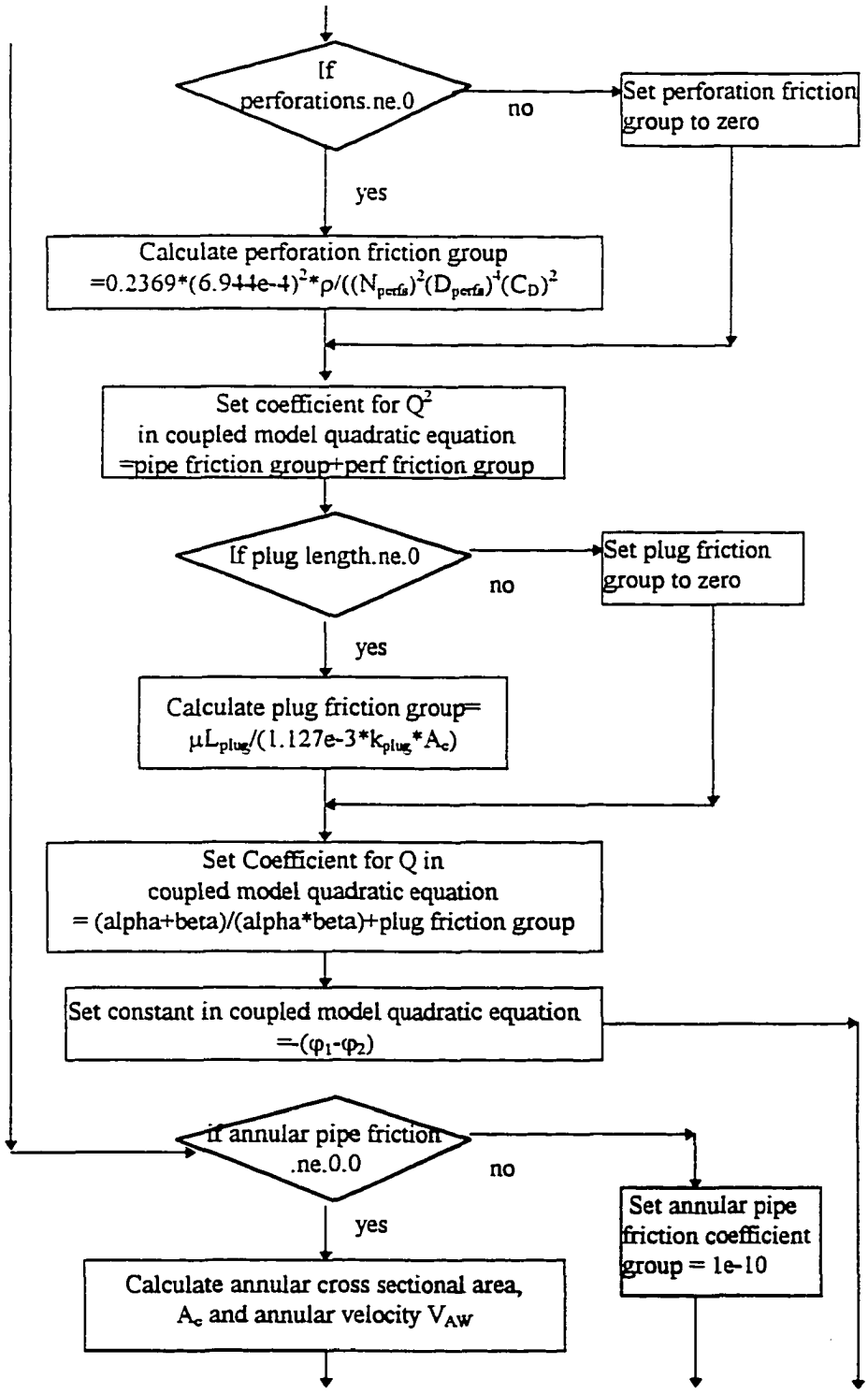


Figure A.3 continued

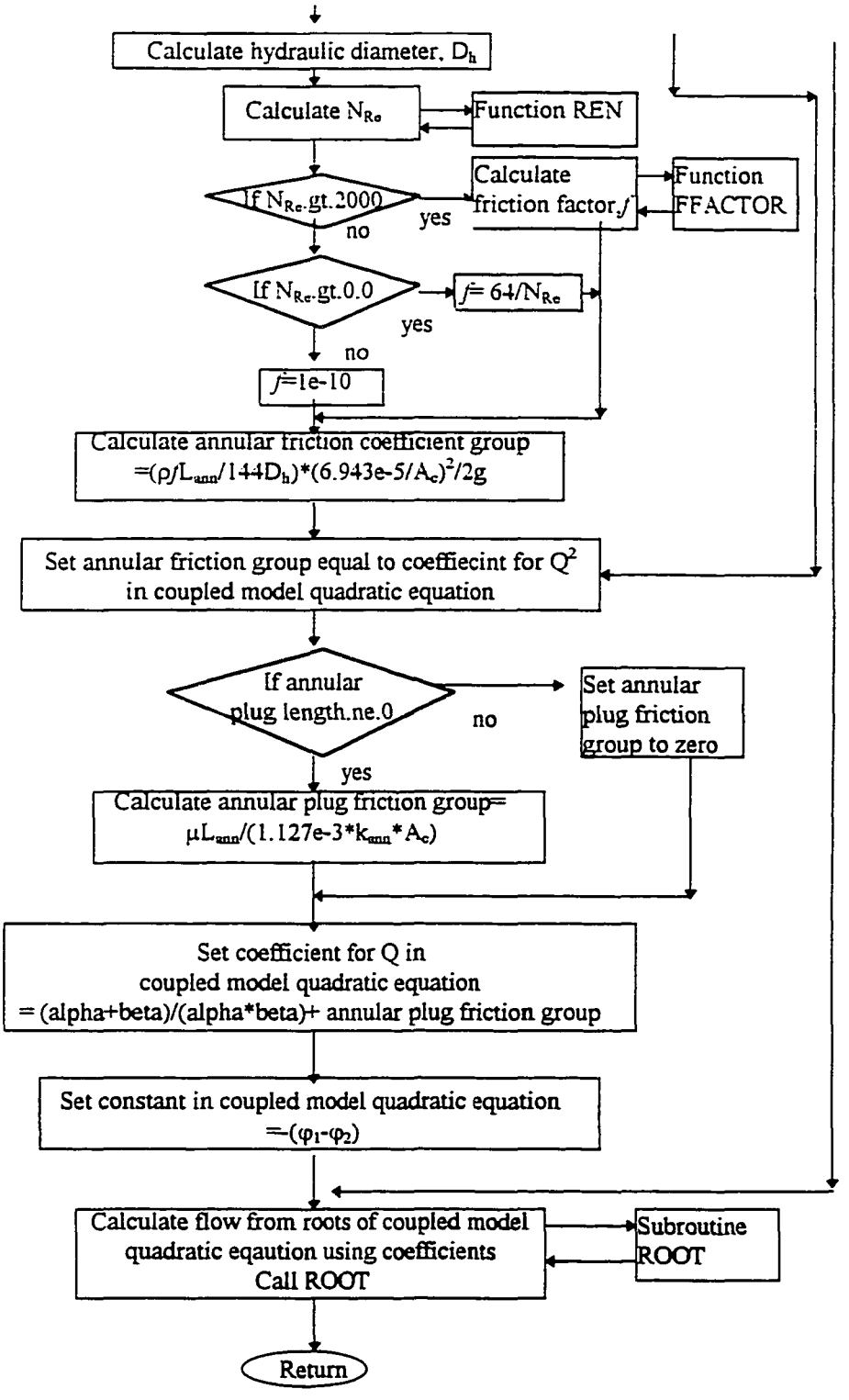


Figure A.3 continued

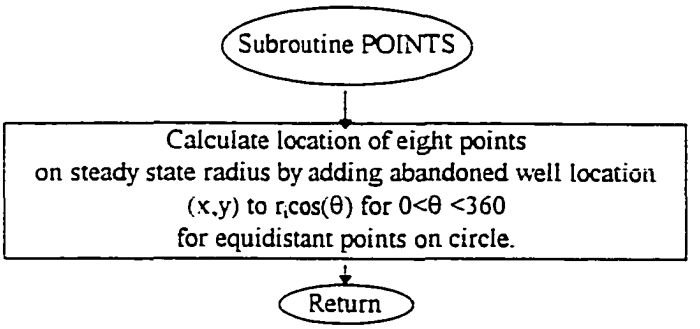


Figure A.4. General flow chart for subroutine POINTS.

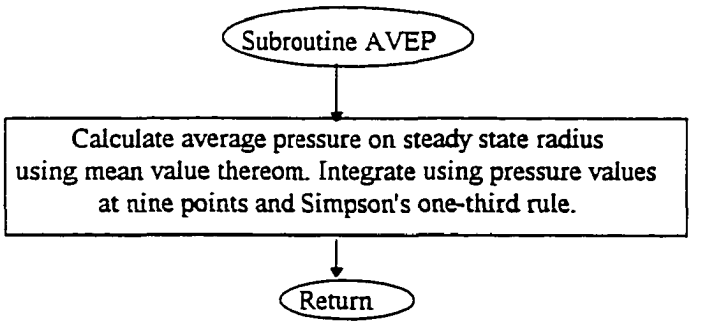


Figure A.5. General flow chart for subroutine AVEP.

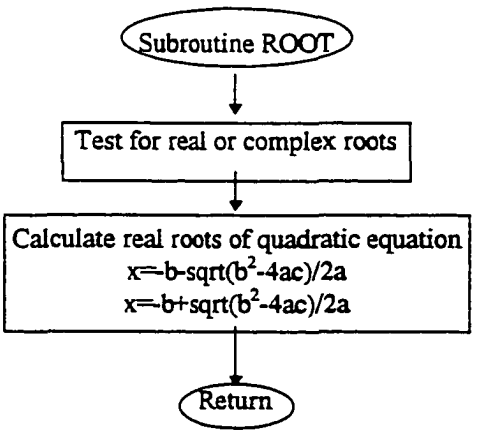


Figure A.6. General flow chart for subroutine ROOTS.

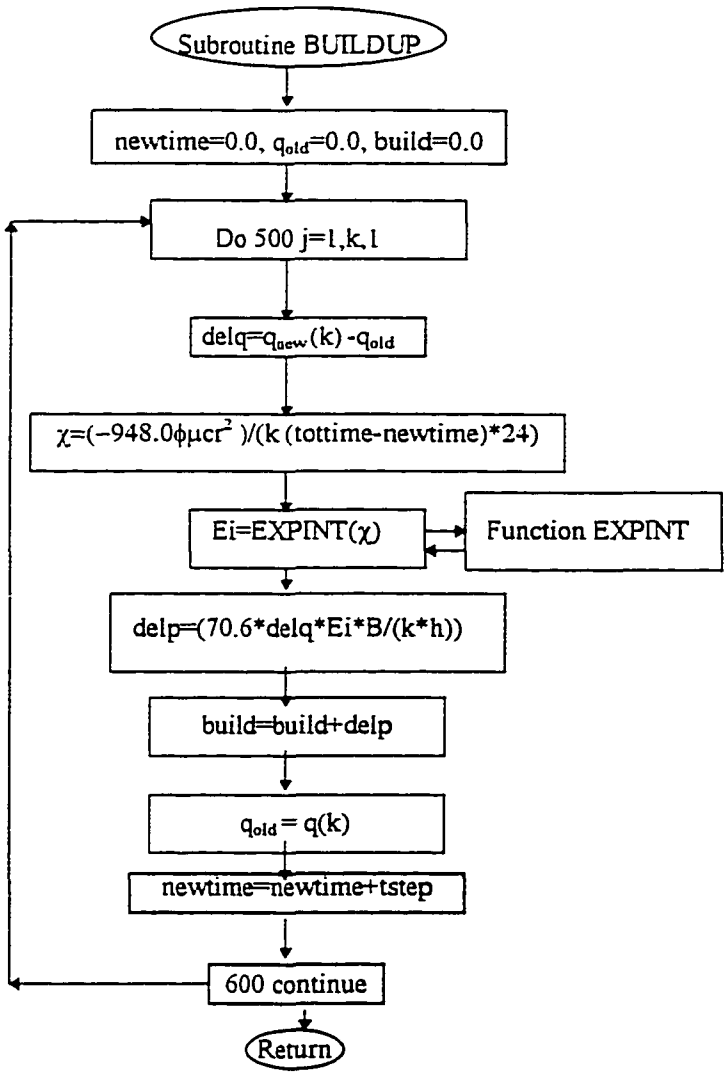


Figure A.7 General flow chart for subroutine BUILDUP.

APPENDIX B

FIELD UNIT EQUATIONS USED IN MODEL PROGRAM

The computer program for the coupled abandoned well model was written for calculations done in oil field units. The general oil field units are:

B_w = formation volume factor of water (bbls/STB)

c = compressibility (1/psi)

h = thickness (ft)

k = permeability (md)

L = length (ft)

P = pressure (psi)

Q = flow rate (bbls/day)

r = radius (ft)

t = time (hrs)

ϕ = porosity (fraction)

μ = viscosity (cp)

These units were used in the following equations which were incorporated into the coupled abandoned well program:

A. Darcy's Law

1. Linear

$$Q = 1.127*10^{-3}\frac{k}{\mu}\frac{\Delta P}{\Delta L} \tag{B.1}$$

2. Radial

$$Q = 7.0811*10^{-3}\frac{kh}{\mu}\frac{P_e - P_w}{\ln(r_e / r_w)} \tag{B.2}$$

3. Spherical

$$Q = 1.416*10^{-2}\frac{k}{\mu}\frac{P_e - P_w}{\frac{1}{r_w} - \frac{1}{r_e}} \tag{B.3}$$

B. Transient Flow Equation

$$\Delta P = -70.6\frac{quB_w}{kh}Ei\left(\frac{-948\phi\mu cr^2}{kt}\right) \tag{B.4}$$

C. Exponential Integral, $Ei(-\chi)$

1. $$\chi = \frac{948\phi\mu cr^2}{kt} \tag{B.5}$$

2. for $\chi < 0.01$

$$Ei(-\chi) = \ln(\chi) + 0.577 \tag{B.6}$$

3. for $0.01 \le \chi \le 10.0$

$$Ei(-\chi) = \left[\ln(x) - \frac{x}{1!} + \frac{x^2}{2(2!)} - \frac{x^3}{3(3!)} + \cdots\cdots + \frac{(-1)^n x^n}{n(n!)}\right] \tag{B.7}$$

4. for $\chi > 10.0$

$$Ei(-\chi) = 0 \tag{B.8}$$

The following equations were described in the main text and were also incorporated into the program with the designated field units:

D. Pipe Friction Factors

1. Laminar Flow

$$f = \frac{64}{N_{Re}} \tag{B.9}$$

2. Turbulent Flow

$$f = 0.001375 + \left[1 + \left(20{,}000\frac{\varepsilon}{D} + \frac{10^6}{N_{Re}}\right)^{1/3}\right] \tag{B.10}$$

ε = pipe roughness in ft
D = pipe diameter in ft

E. Perforation Friction Loss

$$\Delta P_{perf} = \frac{0.2369 Q^2 \rho}{N_p^2 D^4 C_D^2} \tag{B.11}$$

ΔP_{perf} = friction loss (psi)
Q = flow rate (bbls/min)
ρ = fluid density (lb/gal)
N_p = number of perforations
D = perforation diameter (inches)
C_D = coeffeicient of discharge

APPENDIX C

SAMPLE INPUT DATA FILES

```
'RTITLE'
RPERM RH RPOR RC RU  RB RPRESI RDENS
RDEPTH
RWCSID RWCSOD RBDIAM
XA YA
ALLTIME TIMESTEP
NWELLS
RX(I) RY(I) NRATES
Q(I,J) T(I,J)
REPER
'ATITLE'
AQPERM AQH AQPOR AQC AQU AQB AQPRESI AQDENS
AQDEPTH
AQCSID AQCSOD AQBDIAM
NAWELLS
ARX(I) ARY(I) NARATES
AQ(I,J) AT(I,J)
AQPER
'PTITLE'
ROUGH
LPLUG KPLUG
CDISCH  PERFD PERFN
'ANTITLE'
ANROUGH ANLENG
LANN PANN AFRACW AFRACH
NRUNAW
```

Figure C.1 Sample input file demonstrating variable names.

```
'Avci case for model verification,one injector in lower formation'
50. 50. .15 .000003  1.00  1. 465.  66.96
1000.
10.0 10.5 12.0
0. 0.
500. 1.
1
500. 0. 1
-100. 500.
.50
'No wells in upper formation'
50. 50. .15 .000003 1.00 1. 418.5  66.96
900.
10.0 10.5 12.0
0
.50
'AW flow with pipe friction'
.00085
0.0  0.0
0.0  0.0  0.0
'Nrunaw =1 flow thorugh wellbore'
.00085 100.0
100.0 1.0  0.0 0.0
1
```

Figure C.2 Sample input file for Avci base case data used to verify the coupled model.

APPENDIX D

SELECTED LOWER TUSCALOOSA TREND FIELD STUDY INPUT AND OUTPUT FILES

```
'PWC#1 Tuscaloosa Sand Trend- One injector in Lower Tuscaloosa'
30. 50. .25 .000003  1.00  1. 4895.6  67.3
10475.
4.892 5.5 7.0
0. 0.
500.0 1.0
1
500. 0. 1
-600. 500.
.50
'No wells in Sparta'
1000. 700. .35 .000003 1.00 1. 1472.2  67.3
3150.
4.892 5.5 7.0
0
.50
'AW flow with frictional losses and one perforation at Sparta'
.00015
0.0 0.0
.85  1.0  1.0
'Nrunaw=1 flow through wellbore'
0.0 0.0
0.0 0.0 0.0 0.0
1
```

Figure D.1. Input file for case PWC #1 for the field study of the Tuscaloosa Sand Trend.

```
'PWC#2 Tuscaloosa Sand Trend- injector and producer in Lower Tuscaloosa'
30. 50. .25 .000003  1.00  1. 4895.6  67.3
10475.
4.892 5.5 7.0
0. 0.
500.0 1.0
2
500. 0. 1
-600. 500.
-500. 0. 1
300. 500.
.50
'No wells in Sparta'
1000. 700. .35 .000003 1.00 1. 1472.2  67.3
3150.
4.892 5.5 7.0
0
.50
'AW flow with frictional losses and one perforation at Sparta'
.00015
0.0 0.0
.85  1.0  1.0
'Nrunaw=1 flow through wellbore'
0.0 0.0
0.0 0.0 0.0 0.0
1
```

Figure D.2. Input file for case PWC #2 for the field study of the Tuscaloosa Sand Trend.

```
'PWC#3 Tuscaloosa Sand Trend- injector and producer in Lower Tuscaloosa'
30. 50. .25 .000003  1.00  1. 4895.6  67.3
10475.
4.892 5.5 7.0
0. 0.
500.0 1.0
2
500. 0. 1
-600. 500.
-500. 0. 1
300. 500.
.50
'1 producing water well in Sparta'
1000. 700. .35 .000003 1.00 1. 1472.2  67.3
3150.
4.892 5.5 7.0
1
500. 0.  1
600. 500.0
.50
'AW flow with frictional losses and one perforation at Sparta'
.00015
0.0 0.0
.85  1.0  1.0
'Nrunaw=1 flow through wellbore'
0.0 0.0
0.0 0.0 0.0 0.0
1
```

Figure D.3. Input file for case PWC #3 for field sudy of the Tuscaloosa Sand Trend.

Table D.1. Output file for Case PWC#1 for first 25 days.

Time (days)	Flow Rate (bbls/day)	Cumulative Volume (bbls)	Reservoir Potential (psi)	USDW Potential (psi)
1	20.93	20.93	4925.965	4895.620
2	30.02	50.95	4939.167	4895.633
3	35.74	86.70	4947.469	4895.640
4	39.89	126.59	4953.493	4895.645
5	43.15	169.74	4958.214	4895.649
6	45.81	215.55	4962.081	4895.652
7	48.06	263.61	4965.351	4895.655
8	50.01	313.62	4968.182	4895.658
9	51.73	365.35	4970.676	4895.660
10	53.26	418.61	4972.904	4895.662
11	54.63	473.25	4974.894	4895.664
12	55.90	529.15	4976.730	4895.665
13	57.06	586.20	4978.415	4895.667
14	58.13	644.34	4979.972	4895.668
15	59.13	703.46	4981.417	4895.669
16	59.99	763.45	4982.677	4895.671
17	60.87	824.33	4983.956	4895.672
18	61.70	886.03	4985.153	4895.673
19	62.48	948.50	4986.281	4895.674
20	63.21	1011.71	4987.351	4895.675
21	63.91	1075.62	4988.365	4895.676
22	64.57	1140.20	4989.330	4895.677
23	65.21	1205.41	4990.251	4895.678
24	65.81	1271.22	4991.130	4895.679
25	66.39	1337.62	4991.973	4895.680

Table D.2. Output file for Case PWC #2 for first 25 days.

Time (days)	Flow Rate (bbls/day)	Cumulative Volume (bbls)	Reservoir Potential (psi)	USDW Potential (psi)
1	10.46	10.46	4910.783	4895.620
2	15.01	25.47	4917.384	4895.626
3	17.87	43.33	4921.535	4895.630
4	19.94	63.28	4924.548	4895.633
5	21.57	84.85	4926.908	4895.635
6	22.90	107.75	4928.841	4895.636
7	24.03	131.78	4930.477	4895.638
8	25.00	156.78	4931.892	4895.639
9	25.86	182.65	4933.139	4895.640
10	26.63	209.28	4934.252	4895.641
11	27.32	236.59	4935.247	4895.642
12	27.95	264.54	4936.166	4895.643
13	28.53	293.07	4937.008	4895.644
14	29.06	322.13	4937.786	4895.644
15	29.56	351.70	4938.509	4895.645
16	30.00	381.69	4939.139	4895.646
17	30.44	412.13	4939.779	4895.646
18	30.85	442.98	4940.376	4895.646
19	31.24	474.22	4940.941	4895.647
20	31.61	505.82	4941.475	4895.647
21	31.96	537.78	4941.982	4895.648
22	32.29	570.07	4942.465	4895.648
23	32.61	602.67	4942.925	4895.649
24	32.91	635.58	4943.365	4895.649
25	33.20	668.78	4943.786	4895.650

Table D.3. Output file for Case PWC #3 for first 25 days.

Time (days)	Flow Rate (bbls/day)	Cumulative Volume (bbls)	Reservoir Potential (psi)	USDW Potential (psi)
1	10.63	10.63	4910.783	4895.378
2	15.19	25.81	4917.361	4895.343
3	18.06	43.87	4921.505	4895.322
4	20.14	64.02	4924.512	4895.308
5	21.78	85.79	4926.868	4895.296
6	23.11	108.90	4928.798	4895.287
7	24.24	133.15	4930.431	4895.279
8	25.22	158.37	4931.844	4895.272
9	26.09	184.46	4933.089	4895.266
10	26.86	211.32	4934.200	4895.260
11	27.55	238.86	4935.193	4895.255
12	28.18	267.04	4936.110	4895.251
13	28.76	295.80	4936.951	4895.247
14	29.30	325.11	4937.728	4895.243
15	29.80	354.91	4938.449	4895.240
16	30.24	385.14	4939.078	4895.236
17	30.68	415.82	4939.716	4895.233
18	31.09	446.91	4940.313	4895.230
19	31.48	478.40	4940.876	4895.228
20	31.85	510.25	4941.410	4895.225
21	32.20	542.45	4941.916	4895.223
22	32.54	574.99	4942.397	4895.220
23	32.85	607.84	4942.857	4895.218
24	33.16	641.00	4943.296	4895.216
25	33.45	674.45	4943.716	4895.214

Table D.4. Output file for Case PWC #1 with plug for first 25 days.

Time (days)	Flow Rate (bbls/day)	Cumulative Volume (bbls)	Reservoir Potential (psi)	USDW Potential (psi)
1	9.14E-05	9.14E-05	4925.965	4895.620
2	1.40E-04	2.31E-04	4942.068	4895.620
3	1.71E-04	4.02E-04	4952.299	4895.620
4	1.93E-04	5.95E-04	4959.801	4895.620
5	2.11E-04	8.06E-04	4965.725	4895.620
6	2.26E-04	1.03E-03	4970.621	4895.620
7	2.38E-04	1.27E-03	4974.792	4895.620
8	2.49E-04	1.52E-03	4978.426	4895.620
9	2.59E-04	1.78E-03	4981.646	4895.620
10	2.68E-04	2.05E-03	4984.536	4895.620
11	2.76E-04	2.32E-03	4987.135	4895.620
12	2.83E-04	2.61E-03	4989.535	4895.620
13	2.90E-04	2.90E-03	4991.748	4895.620
14	2.96E-04	3.19E-03	4993.799	4895.620
15	3.01E-04	3.49E-03	4995.712	4895.620
16	3.07E-04	3.80E-03	4997.413	4895.620
17	3.12E-04	4.11E-03	4999.102	4895.620
18	3.16E-04	4.43E-03	5000.697	4895.620
19	3.21E-04	4.75E-03	5002.206	4895.620
20	3.25E-04	5.07E-03	5003.639	4895.620
21	3.29E-04	5.40E-03	5005.002	4895.620
22	3.33E-04	5.74E-03	5006.302	4895.620
23	3.37E-04	6.07E-03	5007.546	4895.620
24	3.41E-04	6.41E-03	5008.736	4895.620
25	3.44E-04	6.76E-03	5009.879	4895.620

Table D.5. Output file for Case PWC #2 with plug for first 25 days.

Time (days)	Flow Rate (bbls/day)	Cumulative Volume (bbls)	Reservoir Potential (psi)	USDW Potential (psi)
1	4.57E-05	4.57E-05	4910.783	4895.620
2	6.99E-05	1.16E-04	4918.834	4895.620
3	8.53E-05	2.01E-04	4923.949	4895.620
4	9.66E-05	2.98E-04	4927.701	4895.620
5	1.06E-04	4.03E-04	4930.662	4895.620
6	1.13E-04	5.16E-04	4933.110	4895.620
7	1.19E-04	6.35E-04	4935.196	4895.620
8	1.25E-04	7.60E-04	4937.013	4895.620
9	1.30E-04	8.89E-04	4938.623	4895.620
10	1.34E-04	1.02E-03	4940.067	4895.620
11	1.38E-04	1.16E-03	4941.367	4895.620
12	1.41E-04	1.30E-03	4942.568	4895.620
13	1.45E-04	1.45E-03	4943.674	4895.620
14	1.48E-04	1.59E-03	4944.700	4895.620
15	1.51E-04	1.75E-03	4945.656	4895.620
16	1.53E-04	1.90E-03	4946.506	4895.620
17	1.56E-04	2.05E-03	4947.352	4895.620
18	1.58E-04	2.21E-03	4948.148	4895.620
19	1.60E-04	2.37E-03	4948.903	4895.620
20	1.63E-04	2.54E-03	4949.619	4895.620
21	1.65E-04	2.70E-03	4950.301	4895.620
22	1.67E-04	2.87E-03	4950.951	4895.620
23	1.69E-04	3.04E-03	4951.573	4895.620
24	1.70E-04	3.21E-03	4952.168	4895.620
25	1.72E-04	3.38E-03	4952.739	4895.620

Table D.6. Output file for Case PWC #3 with plug for first 25 days.

Time (days)	Flow Rate (bbls/day)	Cumulative Volume (bbls)	Reservoir Potential (psi)	USDW Potential (psi)
1	4.64E-05	4.64E-05	4910.783	4895.378
2	7.08E-05	1.17E-04	4918.834	4895.337
3	8.63E-05	2.03E-04	4923.949	4895.313
4	9.76E-05	3.01E-04	4927.701	4895.295
5	1.07E-04	4.08E-04	4930.662	4895.282
6	1.14E-04	5.22E-04	4933.110	4895.271
7	1.20E-04	6.42E-04	4935.196	4895.261
8	1.26E-04	7.68E-04	4937.013	4895.253
9	1.31E-04	8.98E-04	4938.623	4895.246
10	1.35E-04	1.03E-03	4940.067	4895.240
11	1.39E-04	1.17E-03	4941.367	4895.234
12	1.43E-04	1.31E-03	4942.568	4895.229
13	1.46E-04	1.46E-03	4943.674	4895.224
14	1.49E-04	1.61E-03	4944.700	4895.219
15	1.52E-04	1.76E-03	4945.656	4895.215
16	1.54E-04	1.92E-03	4946.506	4895.211
17	1.57E-04	2.07E-03	4947.352	4895.208
18	1.59E-04	2.23E-03	4948.148	4895.204
19	1.62E-04	2.39E-03	4948.903	4895.201
20	1.64E-04	2.56E-03	4949.619	4895.198
21	1.66E-04	2.72E-03	4950.301	4895.195
22	1.68E-04	2.89E-03	4950.951	4895.192
23	1.70E-04	3.06E-03	4951.573	4895.189
24	1.72E-04	3.23E-03	4952.168	4895.187
25	1.73E-04	3.41E-03	4952.739	4895.184

Table D.7. Output file for Case PWC #4 for first 25 days.

Time (days)	Flow Rate (bbls/day)	Cumulative Volume (bbls)	Reservoir Potential (psi)	USDW Potential (psi)
1	-186.28	-186.28	4625.965	4895.620
2	-157.20	-343.48	4667.891	4895.506
3	-148.81	-492.29	4680.037	4895.511
4	-142.64	-634.93	4688.958	4895.510
5	-138.02	-772.94	4695.645	4895.510
6	-134.23	-907.18	4701.121	4895.511
7	-131.08	-1038.26	4705.688	4895.511
8	-128.37	-1166.62	4709.609	4895.512
9	-125.99	-1292.62	4713.043	4895.512
10	-123.88	-1416.50	4716.097	4895.512
11	-122.00	-1538.50	4718.821	4895.513
12	-120.27	-1658.78	4721.320	4895.513
13	-118.69	-1777.47	4723.607	4895.514
14	-117.24	-1894.71	4725.715	4895.514
15	-115.89	-2010.60	4727.670	4895.514
16	-114.69	-2125.29	4729.403	4895.515
17	-113.50	-2238.79	4731.123	4895.515
18	-112.39	-2351.18	4732.732	4895.515
19	-111.34	-2462.52	4734.250	4895.516
20	-110.35	-2572.87	4735.685	4895.516
21	-109.41	-2682.28	4737.046	4895.516
22	-108.52	-2790.79	4738.340	4895.517
23	-107.66	-2898.46	4739.575	4895.517
24	-106.85	-3005.31	4740.752	4895.517
25	-106.07	-3111.38	4741.880	4895.518

Table D.8. Output file for Case PWC #5 for first 25 days.

Time (days)	Flow Rate (bbls/day)	Cumulative Volume (bbls)	Reservoir Potential (psi)	USDW Potential (psi)
1	-48.05	-48.05	4825.965	4895.620
2	-32.33	-80.38	4848.729	4895.591
3	-25.72	-106.10	4858.314	4895.597
4	-20.90	-127.00	4865.304	4895.600
5	-17.19	-144.20	4870.681	4895.603
6	-14.16	-158.35	4875.083	4895.605
7	-11.60	-169.96	4878.785	4895.607
8	-9.40	-179.36	4881.980	4895.609
9	-7.47	-186.83	4884.788	4895.610
10	-5.74	-192.57	4887.291	4895.612
11	-4.20	-196.77	4889.525	4895.613
12	-2.78	-199.55	4891.582	4895.615
13	-1.48	-201.03	4893.467	4895.616
14	-0.28	-201.31	4895.208	4895.617
15	0.83	-200.48	4896.823	4895.618
16	1.81	-198.67	4898.240	4895.619
17	2.79	-195.88	4899.667	4895.620
18	3.71	-192.17	4901.000	4895.621
19	4.58	-187.59	4902.259	4895.621
20	5.40	-182.19	4903.450	4895.622
21	6.18	-176.01	4904.580	4895.623
22	6.92	-169.09	4905.655	4895.624
23	7.63	-161.47	4906.680	4895.625
24	8.30	-153.17	4907.659	4895.625
25	8.95	-144.22	4908.597	4895.625

APPENDIX E

SELECTED SARNIA WASTE DISPOSAL FIELD STUDY INPUT AND OUPUT FILES

```
SWC#1 Lucas Formation- One injector. Transport to Rockport'
2. 157. .20 .000003  1.00  1. 278. 66.96
630.
4.892 5.5 7.0
0. 0.
500.0 1.0
1
2000. 0. 1
-1200. 500.
.50
'No wells in Rockport overpressured'
104. 13. .30 .000003 1.00 1. 315.  66.96
395.5
4.892 5.5 7.0
0
.50
'AW flow with frictional losses'
.00015
0.0 0.0
0.0  0.0  0.0
'Nrunaw=1 flow through wellbore'
0.0 0.0
0.0 0.0 0.0 0.0
1
```

Figure E.1. Input file for case SWC #1 a for field study of Lucas formation at Sarnia.

```
'SWC#2 Lucas Formation- One injector. Transport to Hungry Hollow'
2. 157. .20 .000003  1.00  1. 278.  66.96
630.
4.892 5.5 7.0
0. 0.
500.0 1.0
1
2000. 0. 1
-1200. 500.
.50
'No wells in Hungry Hollow, overpressured'
104. 13. .20 .000003 1.00 1. 176.  66.96
233.
4.892 5.5 7.0
0
.50
'AW flow with frictional losses'
.00015
0.0 0.0
0.0  0.0  0.0
'Nrunaw=1 flow through wellbore'
0.0 0.0
0.0 0.0 0.0 0.0
1
```

Figure E.2. Input file for case SWC #2 a for field study of Lucas formation at Sarnia.

```
'SWC#3 Lucas Formation- One injector. Transport to FWA'
2. 157. .20 .000003  1.00  1. 278.  66.96
630.
4.892 5.5 7.0
0. 0.
500.0 1.0
1
2000. 0. 1
-1200. 500.
.50
'No wells in FWA, overpressured'
517. 7. .30 .000003 1.00 1. 44.0  66.96
100.5
4.892 5.5 7.0
0
.50
'AW flow with frictional losses'
.00015
0.0 0.0
0.0  0.0  0.0
'Nrunaw=1 flow through wellbore'
0.0 0.0
0.0 0.0 0.0 0.0
1
```

Figure E.3. Input file for case SWC #3 a for field study of Lucas formation at Sarnia.

Table E.1. Output file for Case SWC #1a for first 25 days.

Time (days)	Flow Rate (bbls/day)	Cumulative Volume (bbls)	Lucas Potential (psi)	Rockport Quarry Potential (psi)
1	-41.17	-41.17	278.000	424.043
2	-36.76	-77.94	285.078	415.471
3	-35.43	-113.37	289.258	414.922
4	-34.61	-147.98	291.731	414.485
5	-34.03	-182.00	293.484	414.178
6	-33.58	-215.58	294.839	413.943
7	-33.21	-248.79	295.968	413.754
8	-32.89	-281.68	296.957	413.598
9	-32.59	-314.27	297.877	413.467
10	-32.31	-346.57	298.772	413.358
11	-32.03	-378.60	299.676	413.267
12	-31.74	-410.34	300.611	413.193
13	-31.45	-441.79	301.592	413.135
14	-31.14	-472.93	302.631	413.092
15	-30.82	-503.75	303.731	413.062
16	-30.49	-534.25	304.895	413.046
17	-30.14	-564.39	306.124	413.043
18	-29.78	-594.17	307.415	413.051
19	-29.41	-623.58	308.765	413.070
20	-29.02	-652.60	310.173	413.100
21	-28.62	-681.22	311.634	413.140
22	-28.21	-709.42	313.146	413.189
23	-27.78	-737.21	314.701	413.246
24	-27.35	-764.56	316.298	413.312
25	-26.91	-791.47	317.931	413.385

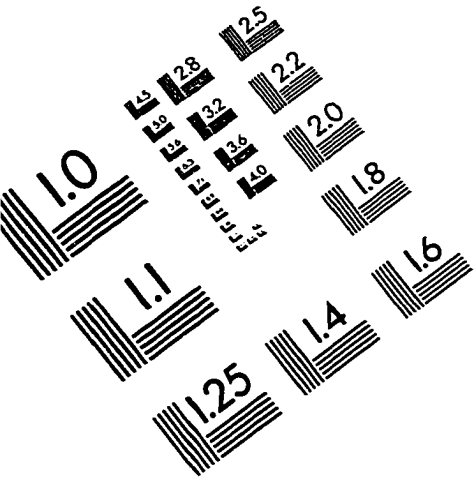
Table E.2. Output file for Case SWC #2a for first 25 days.

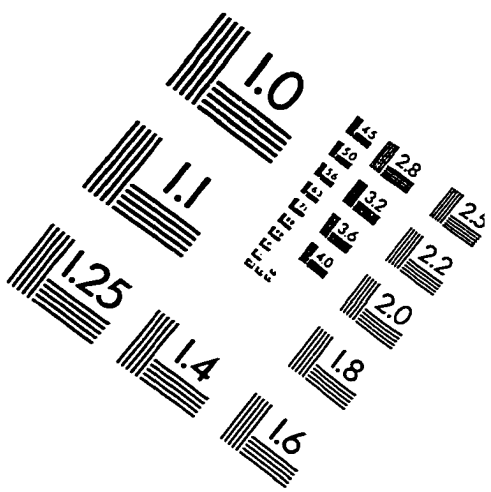
Time (days)	Flow Rate (bbls/day)	Cumulative Volume (bbls)	Lucas Potential (psi)	Hungry Hollow Potential (psi)
1	-23.29	-23.29	278.000	360.605
2	-20.66	-43.95	282.004	355.277
3	-19.93	-63.88	284.344	355.036
4	-19.47	-83.35	285.732	354.804
5	-19.15	-102.50	286.719	354.641
6	-18.90	-121.40	287.486	354.515
7	-18.69	-140.08	288.140	354.414
8	-18.50	-158.58	288.732	354.332
9	-18.31	-176.89	289.311	354.264
10	-18.13	-195.02	289.907	354.210
11	-17.94	-212.96	290.548	354.169
12	-17.73	-230.69	291.246	354.140
13	-17.51	-248.20	292.013	354.123
14	-17.27	-265.47	292.856	354.118
15	-17.01	-282.49	293.776	354.124
16	-16.74	-299.23	294.774	354.142
17	-16.44	-315.67	295.849	354.171
18	-16.13	-331.80	296.995	354.210
19	-15.80	-347.60	298.210	354.259
20	-15.46	-363.06	299.491	354.317
21	-15.10	-378.16	300.833	354.384
22	-14.73	-392.88	302.231	354.460
23	-14.34	-407.22	303.678	354.544
24	-13.94	-421.17	305.173	354.635
25	-13.54	-434.71	306.709	354.732

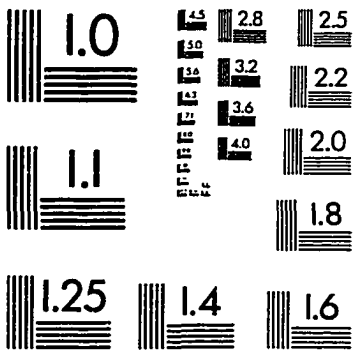
Table E.3. Output file for Case SWC #3a for first 25 days.

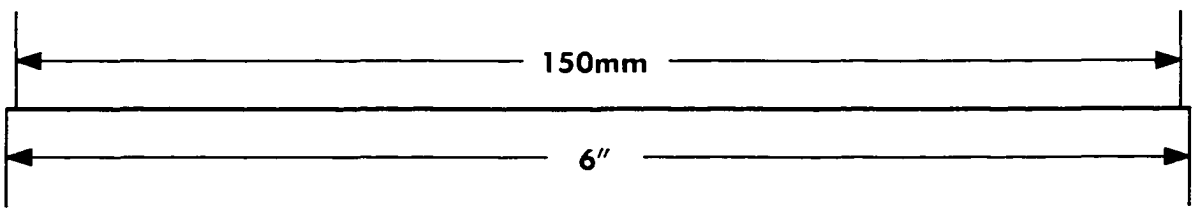
Time (days)	Flow Rate (bbls/day)	Cumulative Volume (bbls)	Lucas Potential (psi)	Fresh Water Potential (psi)
1	-3.91	-3.91	278.000	290.218
2	-3.56	-7.46	278.671	289.792
3	-3.42	-10.88	279.080	289.778
4	-3.34	-14.22	279.322	289.766
5	-3.28	-17.50	279.495	289.758
6	-3.23	-20.73	279.636	289.751
7	-3.18	-23.92	279.783	289.746
8	-3.13	-27.05	279.950	289.743
9	-3.06	-30.11	280.165	289.742
10	-2.97	-33.09	280.441	289.744
11	-2.86	-35.95	280.797	289.749
12	-2.72	-38.67	281.238	289.758
13	-2.56	-41.23	281.770	289.770
14	-2.36	-43.59	282.396	289.788
15	-2.14	-45.73	283.114	289.809
16	-1.89	-47.62	283.921	289.835
17	-1.61	-49.24	284.817	289.866
18	-1.31	-50.55	285.792	289.900
19	-0.99	-51.54	286.844	289.939
20	-0.64	-52.18	287.967	289.982
21	-0.28	-52.46	289.156	290.029
22	0.10	-52.36	290.407	290.079
23	0.50	-51.85	291.711	290.133
24	0.92	-50.93	293.066	290.189
25	1.35	-49.59	294.465	290.249

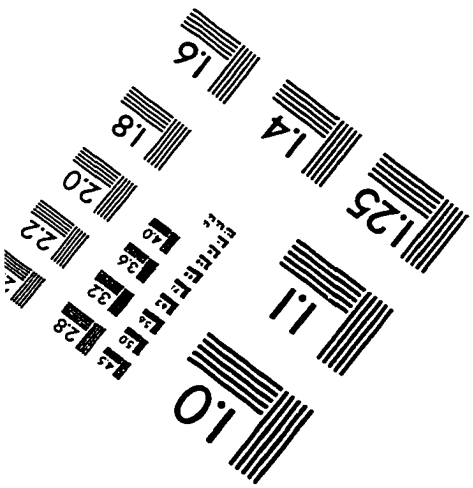
IMAGE EVALUATION TEST TARGET (QA-3)

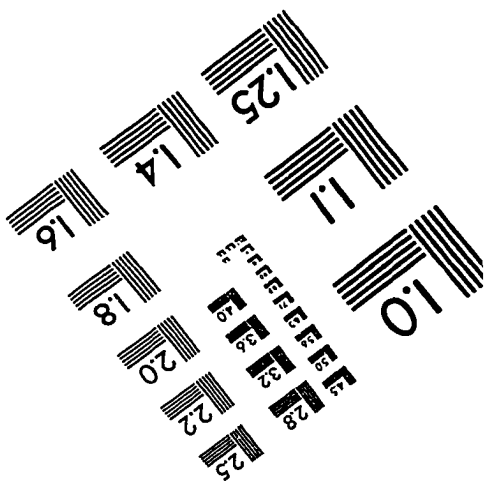












APPLIED IMAGE, Inc
1653 East Main Street
Rochester, NY 14609 USA
Phone: 716/482-0300
Fax: 716/288-5989

© 1993, Applied Image, Inc., All Rights Reserved